"OVIDIUS" UNIVERSITY OF CONSTANTZA
UNIVERSITATEA „OVIDIUS" CONSTANȚA

"OVIDIUS" UNIVERSITY ANNALS - CONSTANTZA

Year V
(2003)

Series: CIVIL ENGINEERING

ANALELE
UNIVERSITĂȚII „OVIDIUS"CONSTANȚA

ANUL V
(2003)

Seria: CONSTRUCȚII

Ovidius University Press
2003

"OVIDIUS" UNIVERSITY OF CONSTANTZA
UNIVERSITATEA „OVIDIUS" CONSTANȚA

"OVIDIUS" UNIVERSITY ANNALS - CONSTANTZA

Year V
(2003)

Series: CIVIL ENGINEERING

ANALELE
UNIVERSITĂȚII „OVIDIUS"CONSTANȚA

ANUL V
(2003)

Seria: CONSTRUCȚII

Ovidius University Press
2003

“OVIDIUS“ UNIVERSITY ANNALS - CONSTANTZA – SERIES: CIVIL ENGINEERING
ANALELE UNIVERSITĂȚII „OVIDIUS“ CONSTANȚA – SERIA: CONSTRUCȚII

ORDERING INFORMATION

The journal may be obtained by ordering at the “OVIDIUS” University, or on exchange basis with similar romanian or foreign institutions.
Revista poate fi procurată prin comandă la Universitatea „OVIDIUS“, sau prin schimb de publicații cu instituții similare din țară şi străinătate.
124, Mamaia Blvd., 900527, RO., Constantza, Romania

TABLE OF CONTENTS

SECTION I
Calculus and Structures Reliability

SECTION II
Hydraulics and Fluid Mechanics

ISSN-12223-7221

SECTION III
Water Resources Management
Environment Engineering
The Land Reclamation Systems Engineering

SECTION IV

Urban and Public Works
Materials, Technologies and Management in Civil Engineering

Graphical Study about the Generation of Some Surfaces Used in Civil Engineering

Delia DRĂGAN[a] Carmen MÂRZA[a]

[a]*Technical University of Cluj-Napoca, Cluj-Napoca, România*

Abstract: In this paper, using the blending (Coons) method, we generate some families of free-form surfaces feasible in civil engineering and in other theoretical or practical situations.

Keywords: Blending surfaces, Free-form surfaces, Computer Aided Geometric Design (CAGD).

1. Introduction

Classical surfaces as spheres, cylinders, cones, hyperboloids with one sheet, paraboloids, ruled surfaces and velaroidal surfaces are widely used in civil engineering as artistic coverings for large halls, stadiums and many other buildings. This is because their shapes are easily manufactured. On the other hand the possibility of designing free-form surfaces with the aid of computers has determined surfaces of the following types: Bezier [3], spline [3], Shepard [13], blending (Coons and Gordon) [8], [3] and others. In some situations the distribution of parabolic points on a surfaces is needed.

Recall that the points of a surfaces (S), represented by the equation:

$$z=F(x,y),\quad (x,y)\in D,\ D\subset \Re^2 \tag{1}$$

are parabolic points if

(PF)(x,y)=0, where

$$PF= F_{x^2}F_{y^2} - F_{xy}^2 . \tag{2}$$

The points for which (PF)(x,y) > 0, (PF(x,y) < 0, respectively) are called elliptic points of (S) (hyperbolic points of (S), respectively).

In this paper we will localize these points on a surface of blending type (Coons). The blending surface has been created by S.Coons [8].

2. Determination of a family of blending surfaces

Next we consider the space frame ABCD, where (AB),(CD),(DC) and (AD) are four given curves, see Figure 1. Let us assume that these curves are represented by the following equations:

$$(AB)\begin{cases} z=f_0(x)\\ y=0,\end{cases}\quad (DC)\begin{cases} z=f_1(x)\\ y=b,\end{cases}\quad x\in[0,a], \tag{3}$$

$$(AD)\begin{cases} z=g_0(y)\\ x=0,\end{cases}\quad (BC)\begin{cases} z=g_1(y)\\ x=a,\end{cases}\quad y\in[0,b], \tag{4}$$

see Fig. 1.

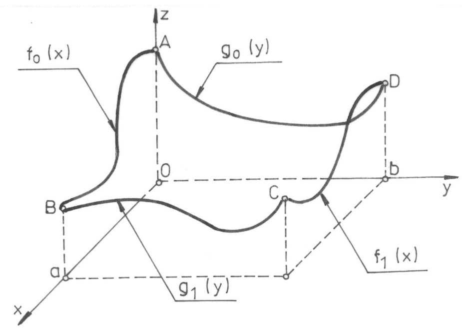

Fig. 1. A blending surface with supports the curves (AB), (BC), (CD) and (AD).

ISSN-12223-7221

The equation (1) represents the blending surface from Figure 1, if

$F(x,0)=f_0(x)$, $F(x,b)=f_1(x)$, $F(0,y) = g_0(y)$ and

$F(a,y)=g_1(y)$, (5)

$x\in[0,a]$, $y\in[0,b]$.

Further one considers the surfaces:

$$(S_1)\, z=(L^x F)(x,y),$$
$$(S_2)\, z=(L^y F)(x,y),$$
$$(S_3)\, z=(L^x L^y F)(x,y). \quad (6)$$

where $L^x F, L^y F$ are the Lagrange operators:

$$(L^x F)(x,y)=\frac{a-x}{a}F(0,y)+\frac{x}{a}F(a,y), \quad (7)$$

$$(L^y F)(x,y)=\frac{b-y}{b}F(x,0)+\frac{y}{b}F(x,b), \quad (8)$$

and (in matrix form):

$$(L^x L^y F)(x,y)=\begin{bmatrix}\frac{a-x}{a} & \frac{x}{a}\end{bmatrix}\begin{bmatrix}F(0,0) & F(0,b)\\ F(a,0) & F(a,b)\end{bmatrix}\begin{bmatrix}\frac{b-y}{b} & \frac{y}{b}\end{bmatrix}^T \quad (9)$$

One easily remarks that the first two surfaces from (6) are ruled surfaces; (S_1) interpolates to the curves (AD), (BC) and (S_2) interpolates to the curves (AB), (DC).

The surface (S_3) interpolates only to the points A, B, C and D.

By direct calculus one checks that the surface:

$$z=(L^x F+L^y F-L^x L^y F)(x,y), x\in[0,a], \quad y\in[0,b] \quad (10)$$

interpolates to the all above curves.

Denoting F(0,0) = h, F(a,0) = h_{10}, F(0,b) = h_{01} and F(a,b)=h_{11} and taking into account (5), (6), (7), (8) and (9), the final form of the equation (10) is

$$z=H(x,y;f_0,g_0,f_1,g_1), \quad (11)$$

where,

$$H(x,y;f_0,g_0,f_1,g_1)=$$
$$\frac{1}{a}[(a-x)g_0(y)+xg_1(y)]+\frac{1}{b}[(b-y)f_0(x)+yf_1(x)]-$$
$$\frac{1}{ab}[(a-x)(b-y)h+(a-x)yh_{01}+x(b-y)h_{10}+xyh_{11}]$$

$x\in[0,a]$, $y=[0,b]$.

This surface is of the blending (Coons) type.
Next we consider some particular cases:

- If $f_0(x)=\left(\alpha x-\frac{h}{a}\right)(x-a)$, $f_1(x)=0$,

$$g_0(y)=\left(\beta y-\frac{h}{b}\right)(y-b), \quad (12)$$

and $g_1(y)=0$, $\alpha\neq 0$, $\beta\neq 0$, then the equation (11) becomes

$$z=\frac{(a-x)(b-y)}{ab}(h-a\alpha x-b\beta y)$$
$(x,y)\in D$, $D\supset[0,a]\times[0,b]$. (13)

The parabolic points of this surface, taking into account equation (2), one projects onto ellipse:

$$\frac{4\alpha\beta}{ab}(a-x)(b-y)-\frac{1}{a^2b^2}(h+\alpha a^2+\beta b^2-2a\alpha x-2b\beta y)^2=0, \quad (14)$$

with the center $C(x_0,y_0)$, where:

$$x_0=\frac{h+2\alpha a^2-\beta b^2}{3a\alpha} \text{ and } y_0=\frac{h+2\beta b^2-\alpha a^2}{3b\beta} \quad (15)$$

In the special case a=b and α=β, the equations (13) and (14) and formulas (14) become:

$$z=\frac{(a-x)(a-y)}{a^2}[h-a\alpha(x+y)], \quad (16)$$

$$4a^2\alpha^2(a-x)(a-y)-[h-2a\alpha(a-x-y)]^2=0, \quad (17)$$

and $x_0=y_0=\dfrac{h+a^2\alpha}{3a\alpha}$. (18)

After the changes of coordinates:

$$x = x_0 + \frac{\sqrt{2}}{2}(X - Y) \text{ and } \quad y = y_0 + \frac{\sqrt{2}}{2}(X + Y),$$

the equation (17) becomes:

$$3X^2 + Y^2 = \left(\frac{h - 2a^2\alpha}{a\alpha\sqrt{6}}\right)^2, \tag{19}$$

which represents a family of ellipses, α - real. The interior (exterior) points of each ellipse are of hyperbolic (elliptic) type. For $\alpha = \frac{h}{2\alpha^2}$ the surface (16) becomes:

$$z = \frac{h}{2a^3}(a - x)(a - y)(2a - x - y) \tag{20}$$

and

$$P(x, y) \equiv (a - x)^2 + (a - y)^2 + (a - x)(a - y) = 0 \tag{21}$$

From here results the all points of surface (20) are of elliptic type excepting the parabolic point A(a,a).

The envelope of the family of ellipses (17) are the straight lines x=a and y=a,m see figure in [10]. From this figure one deduces that for $\alpha \in \left(-\infty, -\frac{h}{4a^2}\right) \cup \left(\frac{h}{2a^2}, \infty\right)$ the all points of blending surface (16) are of hyperbolic type.

In the special case α=0, β=0, from (12) results $f_0(x) = \frac{h}{a}(a - x)$ and $g_0(y) = \frac{h}{b}(b - y)$ and the corresponding blending surface has the equation

$$z = \frac{h}{ab}(a - x)(b - y), \tag{22}$$

which represents a hyperbolic paraboloid so, all its points are of hyperbolic type.

3. Extensions of the blending surface (11)

Extension (restriction) of the blending surface (11) by symmetry with respect to yOz plane is represented by the equation:

$$\begin{aligned} &z = H(|x|, y, f_o(|x|), g_0(y), f_1(|x|), g_1(y)) \\ &|x| \le a, \quad 0 \le y \le y_1(|x|) \end{aligned} \tag{23}$$

Analogously, extension (restriction) of the surface (11), by symmetry with respect to xOz plane is represented by the equation:

$$\begin{aligned} &z = H(x, |y|, f_o(x), g_0(|y|), f_1(x), g_1(|y|)) \\ &0 \le x \le a, \quad |y| \le y_1(x), \quad y_1(x) \ge 0 \end{aligned} \tag{24}$$

Finally, the extension (restriction) of the surface (11) with respect to both xOz and yOz planes has the equation:

$$\begin{aligned} &z = H(|x|, |y|, f_0(|x|), g_0(|y|), f_1(|x|), g_1(|y|)) \\ &|x| \le a, \quad |y| \le y_1(|x|), \quad y(|x|) \ge 0. \end{aligned} \tag{25}$$

Next we consider some particular case of the equation (11) extended in the form (26).

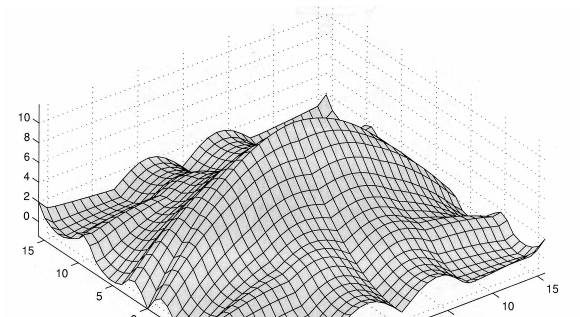

Fig.2 Blending surfaces corresponding to the curves (26), with α=-0.05, β=0.05, h=12, k_1=1, k_2=1/2, m=1, n=2, c_1=1, c_2=1, c_3=1, c_4=1, a=b=15.

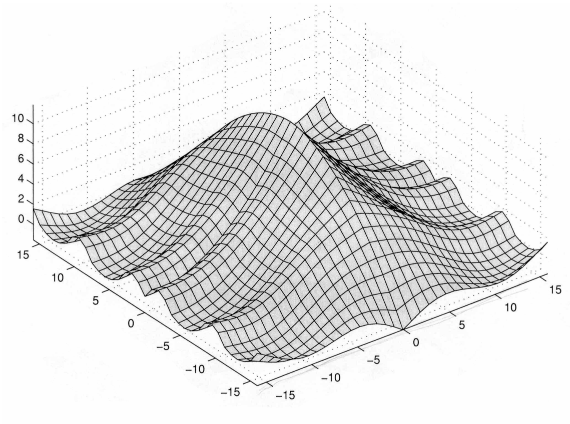

Fig.3 Blending surfaces corresponding to the curves (26), with α=0.05, β=-0.05, h=12, k_1=0, k_2=0, m=1, n=2, c_1=1, c_2=0, c_3=1/2, c_4=0, a=b=15.

In the Fig. 2 and 3 are represented the blending surfaces corresponding to the following set of functions:

$$\begin{aligned} f_1(x,a) &= k_1\left(c_1 \sin\frac{2m\pi x}{a} + c_2\left|\sin\frac{2m\pi x}{a}\right|\right) \\ g_1(a,y) &= k_2\left(c_3 \sin\frac{2m\pi y}{b} + c_4\left|\sin\frac{2n\pi y}{b}\right|\right) \end{aligned} \tag{26}$$

4. Conclusion

These types of surfaces can be used in civil engineering as artistic coverings for large halls, stadiums and many other buildings. Also one can use these surfaces in household products, car, plane, ship and other industries.

We mention geometric aspects of CAD/CAM, animation as well physical phenomena.

5. References

[1] Barnhill, R.E., (1975), *Blending Function Interpolation: A survey and some new results. Proceedings of the Conference on Numerical Methods in Approximation Theory*, Oberwolfach, Germany , ISNN 30, pag.43-90 and University of Dundee Numerical Analysis Report No.9.

[2] Barnhill, R.E., (1977), *Representation and Approximation of Surfaces, Mathematical Software III*, Academic press, Inc. New York , San Francisco, London, 1977, 69-120 pp.

[3] Farin, G., (1990) *Curves and Surfaces for Computer Aided Geometric Design*, Academic Press, Inc. Harcourt Brace Jovanovich, Publishers, Boston, San Diego, New York, London, Sydney, Tokyo, Toronto.

[4] Coman G., Gânscă I., (1983), *An applications of blending interpolation*. Itinerant Seminar of functional equations, approximation and convexity, Cluj-Napoca, Preprint nr.7, pp. 29-34.

[5] Coman G., Gânscă I., (1986), *Some practical applications of blending interpolation*. Itinerant Seminar of functional equations, approximation and convexity, Cluj-Napoca, Preprint nr.7, pp.75-82.

[6] Coman G., Gânscă I. and Ţâmbulea L., (1989), *Some practical applications of blending approximation III*, Itinerant Seminar of Functional Equations, Approximation and Convexity, Cluj-Napoca, Preprint nr.7, pp. 5-22.

[7] Coman G., Gânscă I. and Ţâmbulea L., (1991), *Some new roof-surfaces generated by blending interpolation technique*, STUDIA, Univ. "Babeş-Bolyai", Mathematica, XXXVI, 1, pp. 119-130.

[8] Coons S.A. (1964) *Surfaces for computer aided design of space forms*. Project MAC< Design Div. Department of Mechanical Engineering, MIT.

[9] Gânscă I. and Coman G., (1981*) Aproximare blending cu aplicatii in constructii*. Buletinul Stiintific al Institutului Politehnic Cluj-Napoca, 24, pp. 35-40.

[10] Gânscă I., Trâmbiţaş R., Drăgan D., *Parabolic points location on some blending surfaces*, Proceedings of the International Conference "Constructions 2003", May 2003, Cluj-Napoca.

[11] Gordon W.J. (1971), *Blending- function methods of bivariate and multivariate interpolation and approximation*. SIAM J.Numer.Anull.8, pp. 158-177.

[12] Hosaka M., (1992), *Modeling of Curves and Surfacesin CAD/CAM*. Springer-Verlag, Berlin, Heidelberg, New York.

[13] Mihailescu, M. and Horvath, I., (1977), *Velaroidal Shell for Covering Universal Industrial Halls*, Acta Technica Academiae Scientiarum Hungarical, 85, 1-2, pp.135-145.

[14] Schumaker L.L.,(1976), *Fitting surfaces to scattered data*. In Approximation Theory II (ed. By G.C. Lorenz, C.K.Chui and LL Schumaker), Academic Press Inc., pp.203-268.

Considerations on the Yielding Mechanism of Plane Rectangular Slabsunder Limit Distributed Loads

Mircea IEREMIA[a] Dan V. IORDACHE[a]

[a]*Technical University of Civil Engineering - Department of Strength of Materials, Bucharest, 020396 Bucharest, Romania*

Rezumat : În articol se propune o abordare statică pentru determinarea valorii încărcării ultime pentru plăci dreptunghiulare având diferite rezemări pe laturi sub actiunea unor încărcări uniform distribuite

Abstract: This paper proposes a static approach for the determination of the ultimate load value for rectangular slabs generally supported with distributed loads.

Keywords: Yield line, slab, limit load, flow law.

1. Introduction:

The determination of ultimate load always was a basic concern in the field of structure calculation, especially in the calculation of reinforced concrete slabs.

The determination of the intensity of the load related to the yielding capacity of an elasto-plastic construction can be done in two ways. One of these consists in following all process of the construction behaviour under the action of certain growing external factors, starting from the perfect-elastic state trough elasto-plastic states to the end of the load-carrying capacity (personal interpretation of the theories of elasto-plastic deformation).

The second method expressed by the theory of load-carrying capacity, deals exclusively with the transformation of a structure into a mechanism. The analysis is done here on the basis of a model of rigid-plastic deformation and the relations of the plastic flow theory are used. This method allows the relatively simply resolution of the load-carrying capacity, but cannot provide information about the construction behaviour during the previous stages to the end of the load-carrying capacity. Also she cannot answer to the question if the construction had loose or not its technical utility due to the arising of other phenomena, such as changes not allowed by its geometry.

The solution of the limit load-carrying capacity of a construction submitted to growing loads $\mu_G P_j$ consists in calculate the μ_G coefficient that defines the intensity of limit load. From these results that the complete solution of the limit load-carrying capacity (calculation of μ_G) has to satisfy:

a) The plasticity condition (condition of plastic state);

b) The equations of equilibrium (static conditions);

c) The relations of deformation and the flow law (cinematic conditions).

The complete solution of the problem of load-carrying capacity, hence the fulfilment of both conditions in tensions and cinematic conditions inside the construction and on its surface is practically possible only for certain types of constructions. On this account, the formulation of the criteria that make possible the assessment of limits to the range of limit real load intensity has a considerable importance for practical purposes.

Proximate solutions. These will be classified in two groups, as the possibility to not fulfil static and cinematic conditions is accepted or not. So, during the search of proximate values of the limit load there are used static and cinematic methods.

Due to the fact that the authors had developed a static method intended to solve the problem of ultimate

ISSN-12223-7221

load, we will expose only the conditions that must be fulfilled in this situation:

a) The equations of internal equilibrium and limit conditions in tensions (static conditions);

b) Hence the fulfilment of the condition of plasticity (condition of plastic yielding) is closely related to the static admitted fields of the generalized tensions. Only the static admitted multiplier of load can be defined trough static methods.

The static method do not give the possibility to determine the deformation mechanism of the construction in the moment of plastic yielding, so the displacement field related to the static approach is not necessary the real one.

2. Theory

Rectangular slab with different edges support.

Consider the case of a rectangular thin slab having the dimensions $a \times b \times h$, submitted to the action of a uniformly distributed force q. The von Mises criterion of plasticity can be applied to the material on which the slab is made to (see 2). The origin of the axes system of the slab is the slab centre (fig.1a), where by k_i(i =1÷4) is denoted the type of supports:

- $k_i = -1$ denote an encastrement
- $k_i = 0$ denote an sumply support

Considering the differential relations of static equilibrium, expressed as matrix: $\{\nabla\}[M] = \{T\}$,we introduce the expressions (1) of undimensional moments (fig.1b):

$$m_x = \frac{\sigma_x}{\sigma_c} = \frac{M_x}{M_p} \cdot \frac{W_p}{W_e} = 1{,}5 \cdot \frac{M_x}{M_p} = \frac{M_x}{M_e},$$

$$m_y = \frac{\sigma_y}{\sigma_c} = \frac{M_y}{M_p} \cdot \frac{W_p}{W_e} = 1{,}5 \cdot \frac{M_y}{M_p} = \frac{M_y}{M_e},$$

$$m_{xy} = \frac{\tau_{xy}}{\sigma_c} = \frac{M_{xy}}{M_p} \cdot \frac{W_p}{W_e} = 1{,}5 \cdot \frac{M_{xy}}{M_p} = \frac{M_{xx}}{M_e}, \qquad (1)$$

where:

$W_e = \dfrac{h^2}{6}$ (module of elastic resistance);

$W_p = \dfrac{h^2}{4}$ (module of plastic resistance);

$M_p = \dfrac{h^2}{4} \cdot \sigma_c$ (the plastifying bending moment of the rectangular section of unit width);

$M_e = \dfrac{h^2}{6} \cdot \sigma_c$ (elastic moment)

The equation related to the plane state of stresses, according to which the equivalent von Mises stress „σ_e" is equal, to the limit, with the flow resistance of the material, is:

$$\sigma_x^2 + \sigma_y^2 - \sigma_x \sigma_y + 3\tau_{xy}^2 = \sigma_c^2 \qquad (2)$$

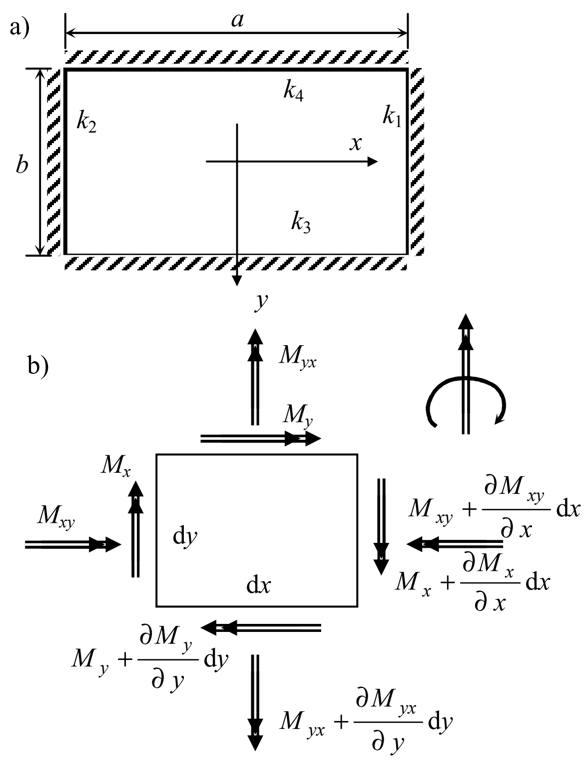

Fig.1 a)Slab axes system; b) Efforts

The expressions of the generalised bending moment function, respectively generalised torsion moment are considered as having parabolic variations, respectively equilateral hyperbole, having the form (3):

$m_x = 1 + Ax + Bx^2$,

$m_y = 1 + Cy + Dy^2$,

$m_{xy} = Exy \qquad (3)$

By writing below the synthesis equation of static study, we express its generalised form:

$$\frac{\partial^2 m_x}{\partial x^2}+2\frac{\partial^2 m_{xy}}{\partial x\partial y}+\frac{\partial^2 m_y}{\partial y^2}=-\frac{q}{M_e} \qquad (4)$$

and by replacing the moment functions m_x, m_y, m_{xy} by their expressions we obtain a relation between the constants:

$$2\cdot(B+D+E)=-q/M_e\,. \qquad (5)$$

3. Results and Discussions:

Conditions on edges: we will distinguish three cases of supporting – a, b, c treated below.

a)Rectangular built-in slab or simply supported on all edges.

In this case the contour conditions will be:

for $x = a$ there results $m_x = k_1$;
for $x = -a$ there results $m_x = k_2$;
for $y = b$ there results $m_y = k_3$;
for $y = -b$ there results $m_y = k_4$. (6)

Only the mode to obtain the A and B constants will be described, and the results obtained will be used for the other two constants.

$$\begin{cases}1+\dfrac{Aa}{2}+\dfrac{Ba^2}{4}=k_1\\[2mm] 1-\dfrac{Aa}{2}+\dfrac{Ba^2}{4}=k_2\end{cases}\rightarrow$$

$$A=\frac{k_1-k_2}{a},\quad B=2\cdot\frac{k_1+k_2-2}{a^2}. \qquad (7)$$

Respectively, for the other set of constants, there results:

$$C=\frac{k_3-k_4}{b},\quad D=2\cdot\frac{k_3+k_4-2}{b^2}, \qquad (8)$$

Concerning the E constant, this is deducted by using the relation (5).

$$E=-\left(\frac{q}{2M_e}+2\cdot\frac{k_1+k_2-2}{a^2}+2\cdot\frac{k_3+k_4-2}{b^2}\right). \qquad (9)$$

The fulfilment of von Mises plastic flow criteria, impose the observance of the relation (10).

$$\left(1+\frac{k_1-k_2}{a}\cdot x+2\frac{k_1+k_2-2}{a^2}\cdot x^2\right)^2+$$
$$+\left(1+\frac{k_3-k_4}{b}\cdot y+2\frac{k_3+k_4-2}{b^2}\cdot y^2\right)^2-$$
$$-\left(1+\frac{k_1-k_2}{a}\cdot x+2\frac{k_1+k_2-2}{a^2}\cdot x^2\right)\cdot$$
$$\cdot\left(1+\frac{k_3-k_4}{b}\cdot y+2\frac{k_3+k_4-2}{b^2}\cdot y^2\right)-$$
$$-3\cdot\left(\frac{q}{2M_e}+2\frac{k_1+k_2-2}{a^2}+2\frac{k_3+k_4-2}{b^2}\right)^2x^2y^2=1 \qquad (10)$$

We will note for $x = y = 0$ (for the slab centre), that the flow condition is identically fulfilled. Due to the fact that the yielding configuration is this shown in fig. 1a, the flow condition is expressed for all four corners of the rectangle as:

$$k_1^2-k_1\cdot k_3+k_2^2+\frac{3}{16}a^2b^2E^2=1$$
$$k_1^2-k_1\cdot k_4+k_4^2+\frac{3}{16}a^2b^2E^2=1$$
$$k_2^2-k_2\cdot k_3+k_3^2+\frac{3}{16}a^2b^2E^2=1$$
$$k_2^2-k_2\cdot k_4+k_4^2+\frac{3}{16}a^2b^2E^2=1 \qquad (11)$$

By adding the relations above and by replacing the value of constant E we will obtain the following expression, from which it will result the value of limit load value:

$$q=\frac{4M_e}{b^2}\left[\frac{\Phi_1}{\sqrt{3}\beta}-\frac{k_1+k_2-2}{\beta^2}-(k_3+k_4-2)\right], \qquad (12)$$

where:

$\beta = a/b$

$$\Phi_1=\sqrt{4-2\left(k_1^2+k_2^2+k_3^2+k_4^2\right)+(k_1+k_2)\cdot(k_1+k_2)}$$

If the slab is built-in on the edges ($k_1 = k_2 = k_3 = k_4 = -1$), the formula above becomes:

$$q=\frac{16M_e}{b^2}\left(\frac{1}{\beta^2}+1\right). \qquad (13)$$

For a slab simply supported on edges, the expression obtained is (14):

$$q=\frac{8M_e}{b^2}\left(1+\frac{1}{\sqrt{3}\cdot\beta}+\frac{1}{\beta^2}\right). \qquad (14)$$

Supposing now a square slab simply supported on its four edges ($\beta = 1$), for the ultimate load value we have:

$$q=\frac{8M_e}{b^2}\left(1+\frac{1}{\sqrt{3}\cdot\beta}+\frac{1}{\beta^2}\right)=$$

$$=\frac{8M_e}{a^2}\left(1+\frac{1}{\sqrt{3}}+1\right)=\frac{20,62}{a^2}M_e\approx\frac{13,746}{a^2}M_p\,. \quad (15)$$

We will note that the value obtained is placed under the limit inferior value with about 17%. Taking into account that practically the ultimate load is superior to the value o 16 M_p the result is that for square slab the using of de exposed mode of calculation is safe.

b)Rectangular three edges supported slab.

In this case two separated yielding configurations can be developed (fig2a, b), depending on the relation between the edges β. So, if we will assume the free edge having the dimensions a, b; $a<2b$ then we obtain the mode of yielding shown in fig.2a; but if $a>2b$, then there will be obtained the mode of yielding shown in fig.2b. Nearly the relation $\beta=a/b=1$, the calculations must be verified considering that both modes of yielding arise, and the final mode will be considered one for which the lowest value of ultimate force is obtained.

For the yielding mode shown in fig.2a a good approximation can be obtained considering that we have a rectangular slab supported on four edges, having the dimensions $2b\times a$. This fact allows the use of the relation (14), with the mentioned correction. For relations $a/b>2$ we can consider in calculations that the slab behaves in fact as a girder in consol, the ultimate load calculated for a unitary band can be assumed as ultimate load for the slab as well.

In first case of yielding, the problem can be approached as well trough the modification of the set of relations (6) by assuming that for $y=-b/2$ we have $k_4=0$.

In this situation constants will have the following values:

$$C=\frac{k_3}{b},\quad D=2\frac{k_3-2}{b^2},$$

$$E=-\left(\frac{q}{2M_e}+2\frac{k_1+k_2-2}{a^2}+2\frac{k_3-2}{b^2}\right), \quad (16)$$

the two constants A and B are unchanged.

The expression of the plasticity condition in corners defined by $x=\pm a/2$ and $y=b/2$ leads to the following system:

$$k_1^2-k_1\cdot k_3+k_2^2+\frac{3}{16}a^2b^2E^2=1$$

$$k_2^2-k_2\cdot k_3+k_3^2+\frac{3}{16}a^2b^2E^2=1 \quad (17)$$

Taking into account the relation (16) we obtain the value of limit load according to (18):

$$q=\frac{4M_e}{b^2}\left[\frac{\sqrt{2}\cdot\Phi_2}{\sqrt{3}\cdot\beta}-\frac{k_1+k_2-2}{\beta^2}-k_3+2\right] \quad (18)$$

where: $\Phi_2=\sqrt{2-\left(k_1^2+2k_2^2+k_3^2\right)+k_3\left(k_1+k_2\right)}$

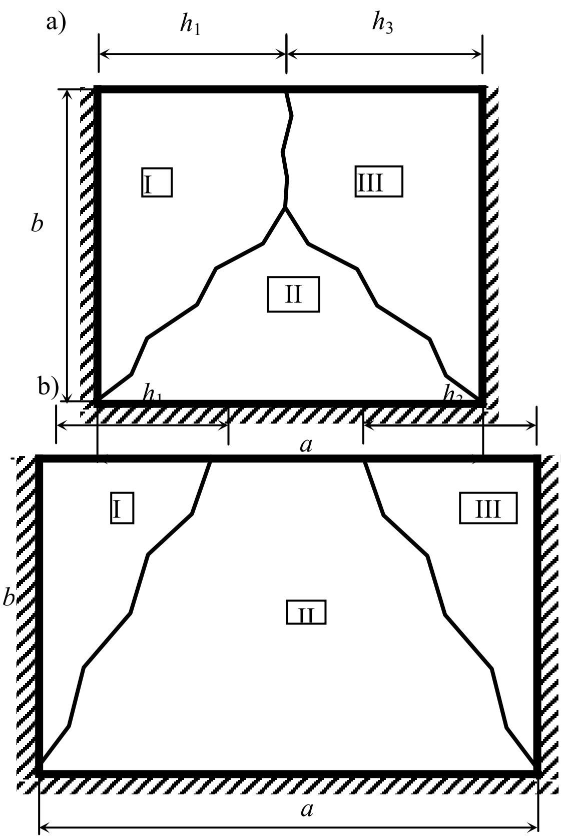

Fig.2 a,b Yield line mechanisms for a rectangular three edges supported slab
(I, II, III rigid portions of the slab)

In case of the slab ($k_1=k_2=k_3=-1$), the formula above becomes:

$$q=\frac{4M_e}{b^2}\left(\frac{4}{\beta^2}+3\right), \quad (19)$$

and for the slab simply supported on three edges

($k_1 = k_2 = k_3 = 0$):

$$q = \frac{4M_e}{b^2}\left(\frac{2}{\beta\sqrt{3}} + \frac{1}{\beta^2} + 1\right). \qquad (20)$$

Let's make a comparison between the results obtained using the approximation proposed in indent two of this paragraph and those given by using one of equation (19), respectively (20).

A slab simply supported on three edges will be assumed, for which there is the following relation between dimensions: $a = b$.

Its assumption as a rectangular slab supported one four edges, having the dimensions a and $b = 2a$ (β = 0,5) leads, by using (14), to the following value of the ultimate force:

$$q = \frac{8M_e}{(2a)^2}\left(1 + \frac{1}{\sqrt{3}\cdot\beta} + \frac{1}{\beta^2}\right) =$$

$$= \frac{12{,}309M_e}{a^2} = \frac{8{,}206M_p}{a^2},$$

instead the use of formula (20),in which β = 1, leads to:

$$q = \frac{4M_e}{a^2}\left(\frac{2}{\beta\sqrt{3}} + \frac{1}{\beta^2} + 1\right) =$$

$$= \frac{4M_e}{a^2}\left(\frac{2}{\sqrt{3}} + 1 + 1\right) = \frac{12{,}619M_e}{a^2} = \frac{8{,}413M_p}{a^2}$$

We can see that the difference between the results obtained is not significant (~ 2,52%), but taking into account the fact that there is a static approach, the value given by the formula (20) can be used.

c)Rectangular slab supported on two adjacent edges.

In this case as well we identify several modes of yielding (fig3a, b, c).

But the last manner leads to lower values of the ultimate load related to the others two modes, so only first two modes of yielding will remain in discussion.

Edge conditions are:

for $x = -a$ we have $m_x = k_2 = 0$

for $y = -b$ we have $m_y = k_4 = 0$ (21)

As follow, the values of integration constants will be:

$$A = \frac{k_1}{a}, \quad B = 2\frac{k_1 - 2}{a^2},$$

$$C = \frac{k_3}{b}, \quad D = 2\frac{k_3 - 2}{b^2},$$

$$E = -\left(\frac{q}{2M_e} + 2\frac{k_1 - 2}{a^2} + 2\frac{k_3 - 2}{b^2}\right), \qquad (22)$$

The expression of plasticity condition for the point having the coordinates $x = a/2$ and $y = -b/2$ leads to the expression:

$$k_1^2 - k_1 \cdot k_3 + k_2^2 + \frac{3}{16}a^2 b^2 E^2 = 1, \qquad (23)$$

The relation above will allow obtaining the ultimate load value. We will have, successively, taking into account the set (22):

$$E = \frac{4}{ab\sqrt{3}}\sqrt{1 - (k_1^2 + k_2^2) + k_1 k_3}$$

$$q' = \frac{4M_e}{b^2}\left[\frac{2\Phi_3}{\sqrt{3}\cdot\beta} - \frac{k_1 - 2}{\beta^2} - k_3 + 2\right] \qquad (24)$$

where:

$$\Phi_3 = \sqrt{1 - \left(k_1^2 + k_3^2\right) + k_1 k_3}$$

In the case of slab built-in on two edges ($k_1 = k_3 = -1$), the formula above becomes:

$$q' = \frac{4M_e}{b^2}\left(\frac{3}{\beta^2} + 3\right) = \frac{12M_e}{b^2}\left(\frac{1}{\beta^2} + 1\right), \qquad (25)$$

and for the slab simply supported on two edges ($k_1 = k_3 = 0$):

$$q' = \frac{8M_e}{b^2}\left(\frac{2}{\beta\sqrt{3}} + \frac{1}{\beta^2} + 1\right). \qquad (26)$$

This approach meets the mode of yielding shown in fig.3a.

If we refer to the yielding mode shown in 3b, we should repeat the calculations for points defined by the coordinates $= a/2$ and $y = -b/2$ and $x = -a/2$ and $y = b/2$, which will lead to the expressions:

$$k_1^2 + \frac{3}{16}a^2 b^2 E^2 = 1, \; k_3^2 + \frac{3}{16}a^2 b^2 E^2 = 1. \qquad (27)$$

By adding the two expressions above the result is the value of constant E:

$$E = \frac{2\sqrt{2}}{ab\sqrt{3}}\sqrt{2 - (k_1^2 + k_3^2)}. \qquad (28)$$

Due (22) the following limit load-carrying value will be obtained:

$$q'' = \frac{4M_e}{b^2}\left[\frac{1}{\beta}\sqrt{\frac{2}{3}\left(2 - k_1^2 - k_3^2\right)} - \frac{k_1 - 2}{\beta^2} - k_3 + 2\right] \qquad (29)$$

In case of slab built-on on two edges ($k_1 = k_3 = -1$), the formula above becomes:

$$q'' = \frac{12M_e}{b^2}\left(\frac{1}{\beta^2}+1\right), \tag{30}$$

and for the slab simply supported on two edges ($k_1 = k_3 = 0$), results:

$$q'' = \frac{8M_e}{b^2}\left(\frac{2}{\beta\sqrt{3}}+\frac{1}{\beta^2}+1\right). \tag{31}$$

Note that any of two modes of yielding discus-sed is critical when the supported edges is built-in or simply supported.

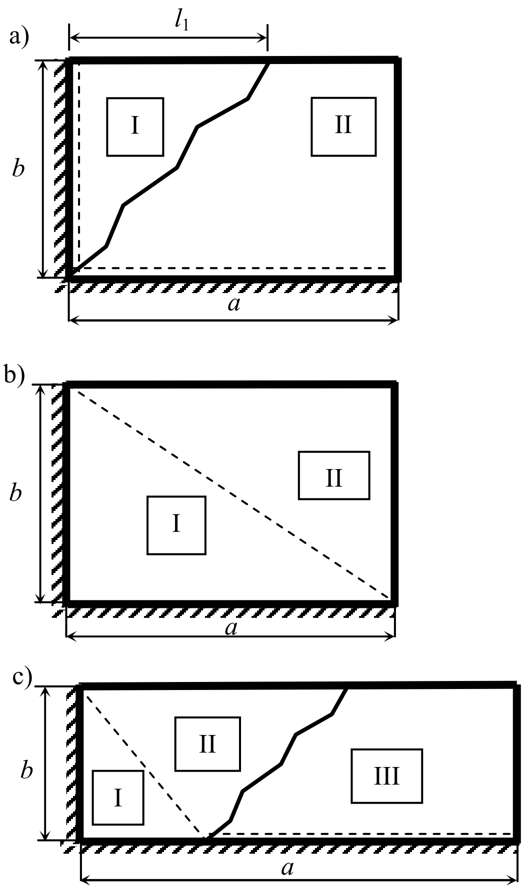

Fig.3a,b,c Yield line mechanisms for a rectangular slab supported on two adjacent edges (I, II, III rigid portions of the slab)

Let's study the situation of one edge simply supported and other built-in. In fact we have two situations:

$k_1 = -1$ and $k_3 = 0$ $\rightarrow$

$$q' = \frac{4M_e}{b^2}\left(\frac{3}{\beta^2}+2\right) < q'' = \frac{4M_e}{b^2}\left(\frac{1}{\beta}\cdot\sqrt{\frac{2}{3}}+\frac{3}{\beta^2}+2\right) \tag{32}$$

$k_1 = 0$ and $k_3 = 1$ $\rightarrow$

$$q' = \frac{4M_e}{b^2}\left(\frac{2}{\beta^2}+3\right) < q'' = \frac{4M_e}{b^2}\left(\frac{1}{\beta}\cdot\sqrt{\frac{2}{3}}+\frac{2}{\beta^2}+3\right) \tag{33}$$

Hence in these cases the second yielding mode is the critical one.

4) Conclusion:

The advantage of using the formulaes obtained is given by the fact that, being a proximate static solutions (bending moment functions are in fact function depending on both variables), the value obtained for the ultimate load is safe.

The limits of the approach of the calculation limit load value according to the above mentioned proposals are given by the fact that their use is possible only for rectangular metallic or concrete reinforced slabs with isotropic reinforcement.

5. References

* Ieremia M – mieremia@hidro.utcb.ro

[1] M.Ieremia – *Încărcarea transversală limită pentru o placă dreptunghiulară cu diferite rezemări pe contur*, St.Cerc.Mec.Apl.,Tom.44,Nr.6,1985,pp.569-573

[2] K.W.Johansen – *Yield-Line Formulae for Slabs*, Routledge,1998

[3] W.Olszag,P.Perzyna,A.Sawczuk – *Teoria plastic-ității*, Ed.Tehnică,Bucureşti,1970, p.582-586

[4] M.A.Save, C.E. Massonnet, G. de Saxce – *Plastic limit analysis of plates, shells and disks,* Elsevier, 1997,pp.238-246

[5] H.E.Shull, L.W.Hu "Load-carrying Capacities of Simply Suppported Rectangular Plates", J.Appl. Mech 30;617,december1963

Generalized Algorithm for Stiffness Degradation of Strength Concrete Bars

Mircea IEREMIA[a] Elena SIDORENCO[b]

[a]*Technical University of Civil Engineering, Bucharest, Romania*
[b]*Technical University of Moldavia, Chisinau, Rep.Moldova*

Rezumat: Algoritmul rezolvarii numerice incrementale a problemelor elastoplastice se construieste în baza teoriei curgerii plastice cu considerarea consolidarii (ecruisarii) izotropice si a modelului de calcul bazat pe determinarea modulului generalizat al deplasarii plastice. Din spectrul metodelor numerice compatibile cu MEF, în functie de metoda de calcul adoptata in rezolvarea problemei abordate, algoritmul se ramifica în doua directii: - calculul prin metoda tensiunilor initiale, denumita si metoda solutiilor elastice; - calculul prin intermediul metodei proiectarii analitice pe suprafata de curgere (metoda antigradientului de coborare a tensiunilor inadmisibile pe suprafata de curgere). De asemenea, se prezinta algoritmul procedeului de pronosticare al pasului optim de considerarea a încarcarii în faza de propagare a fisurii. Totodata se expune schema de utilizare a procedeului de regularizare.

Abstract: The algorithm of computational incremental solving of elasto-plastic problems is based on the plastic flow theory with the application of yield criterion and considering elastic kinematic/isotropic hardening behaviour and the computing model for determining the generalized modulus of plastic displacement. When solving the problem the algorithm diverges in two directions depending on the chosen computational method. This method is chosen from the familly of computational methods compatible with FEM. The two directions are: -calculus through initial stresses, also called the elastic solution method; -calculus through analytical design method on the yield surface (the antigradient lowering of inadmissible stresses on the yield surface method). The paper also deals with the algorithm of forseeing optimal step of considering the loading in the crack propagation stage and with the scheme of the adjustment process. At the same time the scheme of the regularization process utilization is presented.

Keywords: Algorithm, stiffness, degradation, concret, computational, plastic displacement.

1. Introduction

The nonlinear calculus of the structures now represents a necesity. This difficult calculus at structural ensemble level is, nowadays, possible because of the fast development of computational resources. In current practice of design of the reinforced concrete structures, the real nonlinear behaviour from the physical point of view of this composite material, can't be emphasized. This behaviour is reflected in the development of the cracks from the tensioned concrete, in the crash of the material in the compressed concrete area as well as in reinforcing yield. All these constitutive particularities determine the response of the material not to be produced as a single whole at some post – elastic loading levels. Consequently, a nonlinear analysis is approached, using the modern concept of stiffness degradation of the strength elements under the action of increasing/decreasing monotonous loading or cyclic.

The algorithm of computational incremental solving of elasto-plastic problems is based on the plastic flow theory with the application of von Mises yield criterion for concrete and reinforced concrete and considering elastic kinematic/isotropic hardening behaviour and the computing model for determining the generalized modulus of plastic displacement. The numerical integration of condition ecuations is made

ISSN-12223-7221

by the finite and boundary element computational method, considering the material yield theory adapted to this method. Computational iterative methods are used for the extension of the class of problems solved in case of body deformation according to the plastic limit with yield criterion.

At each iteration the objective in solving with displacement method is to observe the conditions of static eqiulibrium. When solving the problem the algorithm diverges in two directions depending on the chosen computational method. This method is chosen from the familly of computational methods compatible with finite element method. The two directions are:

-calculus through initial stresses, also called the elastic solution method;

-calculus through analytical design method on the yield surface (the antigradient lowering of inadmissible stresses on the yield surface method).

The paper also deals with the algorithm of forseeing optimal step of considering the loading in the crack propagation stage and with the scheme of the adjustment process. At the same time the scheme of the regularization process utilization is presented.

An often difficulty of the modelling process of the crack increase, appears and it is expressed by the next paradox: the boundary conditions depend on the variation crack parameter, which also depends on the control parameter. These conditions must be calculated before the crack increase, while they are determined in the final increase stage. This problem is motivated by the fact that this limit conditions are explicitly expressed in FEM. This difficulty can be avoided in two ways:

- the loading promoting with small steps;

- the extension of the eventual value of the caracteristic parameter, depending on the crack length.

The major contribution of this work is finishing a mathematics algorithm of the proposed methodology development.

2. Iterative Process of the Initial Deformation Method

The presentation of the computing algorithm will be done in solving stages, as follows:

1st stage: The incremental loading process is applied (step by step) in static /dynamic numerical compuational analysis. The initial action $\{P_0\}$ is applied according to the case of loading. The linear analysis with FEM is done and consequential stress and strain fields are obtained $\{\sigma_0\}$, $\{\varepsilon_0\}$. The initial loading is conditioned so that after its application all the points of the discreet model should displace (linearly or angularly) only elastically; the reach of the boundary state of yield in some points of the model should take place when applying the next loading step,which is incremented $\{\Delta P_1\}$. This can be done by using the scale coefficient method, taking into account the fact that the loading is proportional. The analysis of the distribution of plastic areas depends on the size of the loading step $\{\Delta P\}$.

2nd stage:

✓ The increase of the loading $\{\Delta P_i\}$ is applied. The linear computational calculus with FEM is done, consequential stress increase $\{d\sigma^*\}$ and strain increase $\{d\varepsilon^*\}$, are obtained. The values of the total current deformations are calculated by adding the plastic deformation increment $\{d\varepsilon^p_{ij}\}$ to the previously obtained value.

Further on the work presents the algorithm of checking the boundary areas corresponding to the functions of plastic potential, f_0, f, F (the potential function).

✓ The value of the yield function (the plastic potential function) is calculated depending on the adopted constitutive law and the stress function around that point is checked to see if it falls on the boundary aria frontier.

If $f_0(\{\sigma^*_i\})<0$, then the point corresponding to the given stress state is situated in the elastic behaviour domain (in the elastic deformation stage); but if $f_0(\{\sigma^*_i\})>0$ there results that at the considered point, a process of plastic flow of the material takes place, which corresponds to the potential function, f_0. This condition is verified for all the points from the considered descrete domain. The time history (for several steps of loading) for the deformation of the material around the point where the plastic flow condition is obtained, is examined.

If $f_0(\{\sigma^*_i\})=0$ and $f_0(\{\sigma^*_{I-1}\})>0$, then it is necessary that the inadmissible stress state should be corrected, so that one should obtain $f_0(\{\sigma_i\})=0$. This condition means that the point corresponding to the stress state falls on the limit just on the yield area.

✓ The split of the part corresponding to the increase of elastic deformation in proportion to the rate of the increase of plastic deformation is done through the r coefficient. The determination of this coefficient is done by putting the condition of observing the next ecuation (1), which has the meaning from the above mentioned point 2:

$$f_0(\{\sigma_{i-1}\}+r\{d\sigma^*\})=0 \qquad (1)$$

The linear interpolation is made and the first approximative value of r_1 coefficient is obtained through (2):

$$r_1=-\left(f_{i-1}/\left(f\left(\{\sigma_i^*\}\right)-f\left(\{\sigma_{i-1}\}\right)\right)\right) \qquad (2)$$

From several reasons (nonlinearity, nonmaintainance of the 1D loading condition,the convexity of the yield area) first approximation of the r_1 coefficient doesn't always satisfy the incremental development strain condition:

$$f=f_0\left(\{\sigma_{i-1}\}+r_1\{d\sigma^*\}\right)\neq 0 \qquad (3)$$

✓ Then, the following approximation for the determination of the r coefficient is done, considering the next (4) formula:

$$r=r_1-\frac{f}{\{\partial f_0/\partial\sigma\}^T\{d\sigma^*\}} \qquad (4)$$

The elastic part of the deformation is defined by the relation r{d σ^*} and the remaining part corresponds to the plastic deformation characteristic curve " σ-ε".

✓ That is why the influence of the loading step be decreased as much as possible while the elasto-plastic deformation interval is divided into m subintervals.

$$m=f_i^*/\Delta f \qquad (5)$$

6. Then calculus of the corresponding stresses for each subinterval m_I, is done as follows:

$$\{\sigma_1\}=\{\sigma_{i-1}\}+\{d\sigma^*\}-\lambda\{d\} \qquad (6)$$

$$\{\sigma_i\}=\{\sigma_1\}-\left\{\frac{\partial F}{\partial\sigma}\right\}\frac{F_1}{\{\partial F/\partial\sigma\}^T\cdot\{\partial F/\partial\sigma\}} \qquad (7)$$

where,

$$\lambda=\frac{\{d\}^T\{d\varepsilon\}}{A+\beta}, \qquad \{d\}=[D]\left\{\frac{\partial F}{\partial\sigma}\right\}, \qquad (8)$$

$$\beta=\left\{\frac{\partial F}{\partial\sigma}\right\}^T\{d\}, \qquad A=H',$$

H'- the slope of the curve of material deformation.The nominator from (5) depends on the size of the loading step ΔP. It is recommanded that the potential function variation should be calculated after the formula: $\Delta F=0.1\cdot\sigma_c$, where σ_y is the value of the yield stress.

[D] – is the constitutive matrix (stress – strain relationship) for a linear elastic, isotropic material and for plane strain/stress.

3rd stage: If the conditions for the current point situated in the considered discreete domain are furfilled:

$$f\left(\{\sigma_i^*\}\right)>0 \quad \text{si} \quad f\left(\{\sigma_{i-1}\}\right)=0, \qquad (9)$$

then the incremental increase of the stress {dσ^*} is the result of the plastic deformation of the body. In this case, the pursuit of the curve of the material deformation is done through the relations from 2nd stage; we then obtain the point where the value of the coefficientr is zero.

4th stage: We verify the eqiulibrium condition by previously determining the deviation value, which defines the difference between the state created by correcting the inadmissible stresses {σ^*_i} and the state corresponding to the current stresses {σ_I}:

$$\{d\sigma^{**}\}=\{\sigma_i^*\}-\{\sigma_i\} \qquad (10)$$

$$\{\Delta P\}=\int_V\{d\sigma^{**}\}[B]^T\,dV \qquad (11)$$

Next, the {ΔP} vector is applied as external loading (the right part of the equilibrium ecuation system) and the linear problem is solved. The incresaes of the displacements and those corresponding to $\{d\sigma^*_i\}$ stresses and to $\{d\varepsilon^*_i\}$ strains are obtained.

5^th^ stage: The process from 2nd and 3rd stages is repeated and the convergence criteria of the iterative process, defined by the next (12) relation, is verified:

$$\frac{\{dq_i\}\cdot\{dq_i\}^T}{\{q_i\}\cdot\{q_i\}^T} \le \varepsilon\,, \qquad (12)$$

where, ε - is the allowable variation of the accuracy.

6th stage: For verifying the accomplishment of the convergence criterion, the next loading step with exterior forces {ΔP} is activated. Linear analysis is accomplished. The observance of the boundary conditions is analized in the potential curve neighbourhood in every point of the discreete domain, according to the stages presented above. The iterative incremental analysis cotinues till the stipulate application of the exterior force is obtained (corresponding to the increase of the crack length) or the calculus steps in case the iterative proccess deosn't converge, which means that the convergence condition is not observed after (10-20) iterations. Phisically, this means that the pass of stable increase into an instable increase of the crack, therefor the breakage of the body; from the mathematic point of view this signifies the fact that the structure matrix degenerates.

Table 1

I	II		III		IV	
n	0 or 1	1, 2, ..	0 or 1	1, 2,..	0 or 1	1, 2, ..

The identification is introduced for the „n" point (n indicates the point's number). In table 1 above, number II - corresponds to the initial yield (f_0=0), number III - indicates the current loading surface (f=0), number IV - refers to the limit yield surface (F=0). In every cell two digits are indicated: 0 and 1. 1 - indicates that when loading, in that point, the initial fracture surface is achieved, and if the stress state around that point didn't achieve the initial fracture surface, 0 will be written. The rest of the are needed to reach the considered stress surface.

3.The Algorithm of the Elasto-Plastic Deformation Modelling by Analytical Projection on the Yield Surface

According to the arguments shown above, the application of the projection on the yield surface method simplifies the algorithm of elasto-plastic problem, essentially. The algorithm is made in stages, as follows:

I. The P_0 force is applied. The stress and the strain states components {σ},{ε} are calculated around current point.

II. The numerical value of the following yield function, F (the plastic potential function) is calculated for every discreete point of the domain and the next expressions are verified.

- If the value of the yield function, F≥0, we pass to IV.

- If F<0, an inadmissible stress/strain state takes place and we pass to III.

III. An element which has the discreete point of the domain is actioned by an unloading force (the unloading phenomena by which the return on the yield surface is made, takes place) through the mentioned analytical expressions, according to the next sequence:

- the α (anghe of open crack), f, d, γ parameters are calculated;

- the plasticity matrix components are calculated;

- the FEM computational process is pursuing the observance of the convergence condition.

IV. We verify the continuing criterion of the problem.

V. We action with the next loading step {ΔP}. The persistance of the loading is made by passing to II. The process described at II and III is repeated.

4.Conclusions

1. We made an analysis of the modern constitutive models which renders the concrete and reinforced concrete elements behaviour, elements solicited in any possible way (monotonous, increasingly /decreasingly, or certain solicitation). The models were elaborated by using computational simplifying theories and by proper mathematics for

2. continuous spectrum and deformated mechanics and for nonlinear breakage mechanics.

3. We promote an original computational model in which three functional areas are considered: - the initial yield of the material, the flowing area of the material and the damage surface of the body. With such mathematical - mechanical approaching the variables for each case are argued by experimental physical determinations; Uniaxial, bi-triaxial tests are used. We prefere those computational models in which experimental data are confirmed by analytical solutions or by some special elaborated tests according to the existent engineering compuational standards.

4. A nonlinear numerical incremental analysis was made by using the difference ecuations of mathematical physics until the reaching of the boundary flowing state of the reinforced and cracking/crushing of the concrete.We continued the analysis till the final state of the material damage around a point from the reach of degradation state on the section. The concept of damage development of material performance.

5. A generalized algorithm for determining the limit deterioration state of the construction element was done by making some constitutive models specific to the real state of loading, into an incremental analysis frame, for random iteration. We used the initial deformation method for this incremental analysis.

5. Bibliography

* Ieremia M. – mieremia@hidro.utcb.ro

[1] Craciun I., Nojoc G.V., Spinei N.T – *O sposobe resenia uravnenii dvijeniea metoda conecnih elementov*, Cislennie isledovania v mehaniche splasnih sred, Matematiceschie isledovaniea, Kisinev, Ed. Stiinta, stp. 26-32, 1987.

[2] Gerstle K. H. et al. - *Behaviour of concrete under multiaxial stress states*, Journal of Engineering Mechanics, ASCE, 106(6), 1980, pp. 1383-1403.

[3] Grama V. – *Despre modelarea numerica a fenomenului de crestere stabila a fisurii*, Conferinta Siguranta constructiilor în conditiile de teren si seismicitate specifice României si Rep. Moldova, Chisinau, 27-28.10.1999, pag. 279-282.

[4] Grama V. – *Analiza cvasi-statica neliniara pana la stadiul ultim de fisurare a elementelor de constructie cu comportare ductila*, teza de doctorat, Universitatea Tehnica a Moldovei, Chisinau, Rep. Moldova, 2000.

[5] *Ieremia M. – *Elasticitate. Plasticitate. Neliniaritate*, Ed. Printech, Bucuresti, 1998.

[6] *Ieremia M., Craciun I., Ginju S. – *The contact-impact analisys of two buldings during Vrancea earthquake*, 15th ASCE Engineering Mechanics Conference, Columbia University, New York, USA, 2-5.06.2002.

[7] Mazilu P., Topa N., *Ieremia M. – *Aplicarea teoriei elasticitatii si a placilor in calculul constructiilor*, Ed. Tehnica, Bucuresti, 1985.

Apendix

The algorithm of plastic strains calculus

The load at „i” time (iteration) $\{P\}_i = \{P\}_{i-1} + \{\Delta P\}_i$

The stresses and strains at „i” time (iteration)

$$\{\sigma\}_i = \{\sigma\}_{i-1} + \{d\sigma\}_i$$

$$\{\varepsilon\}_i = \{\varepsilon\}_{i-1} + \{d\varepsilon\}_i$$

Volumetric stress

$$\sigma_0 = \frac{1}{3}(\sigma_x + \sigma_y + \sigma_z)$$

$$[T_V] = \begin{bmatrix} \sigma_0 & 0 & 0 \\ 0 & \sigma_0 & 0 \\ 0 & 0 & \sigma_0 \end{bmatrix}$$

Deviatoric stress

$$[S] = [T_\sigma] - [T_V]$$

$$[S] = \begin{bmatrix} \sigma_x - \sigma_0 & \tau_{xy} & \tau_{xz} \\ \tau_{yx} & \sigma_y - \sigma_0 & \tau_{yz} \\ \tau_{zx} & \tau_{zy} & \sigma_z - \sigma_0 \end{bmatrix}$$

Von Mises equivalent stress (yield criterion)

$$\sigma_e = \frac{\sqrt{2}}{2}\sqrt{(\sigma_x - \sigma_y)^2 + (\sigma_y - \sigma_z)^2 + (\sigma_z - \sigma_x)^2 + 6(\tau_{xy}^2 + \tau_{yz}^2 + \tau_{zx}^2)}$$

Invariants stress state

$$I_1 = \sigma_x + \sigma_y + \sigma_z = \sigma_1 + \sigma_2 + \sigma_3$$

$$I_2 = \sigma_x\sigma_y + \sigma_y\sigma_z + \sigma_z\sigma_x - (\tau_{xy}^2 + \tau_{yz}^2 + \tau_{zx}^2$$

$$I_3 = \det|S|$$

Calculus of material modulus $H^p; k_1; \beta$

The incremental **plastic strains** $d\varepsilon_{ij}^p = \frac{S_{kl}}{3H^p\tau_0}\left(\frac{S_{ij}}{\tau_0} + \delta_{ij}\frac{\beta}{3}\right)d\sigma_{kl} + \delta_{ij}\frac{1}{9k_t}d\sigma_{kk}$

The algorithm of computational calculus of generalized modulus of plastic displacement H^p

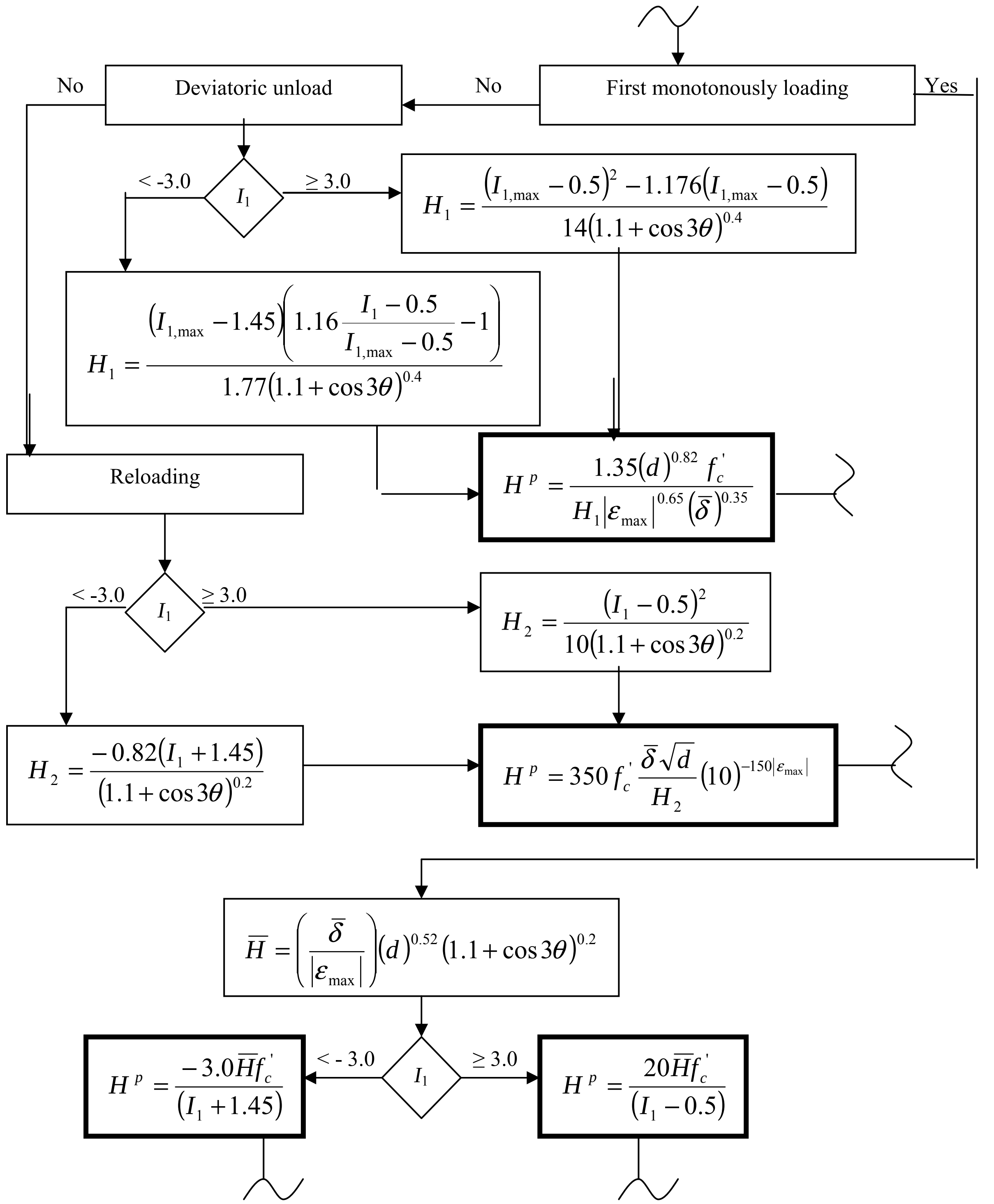

Algorithm calculus of modulus k_t

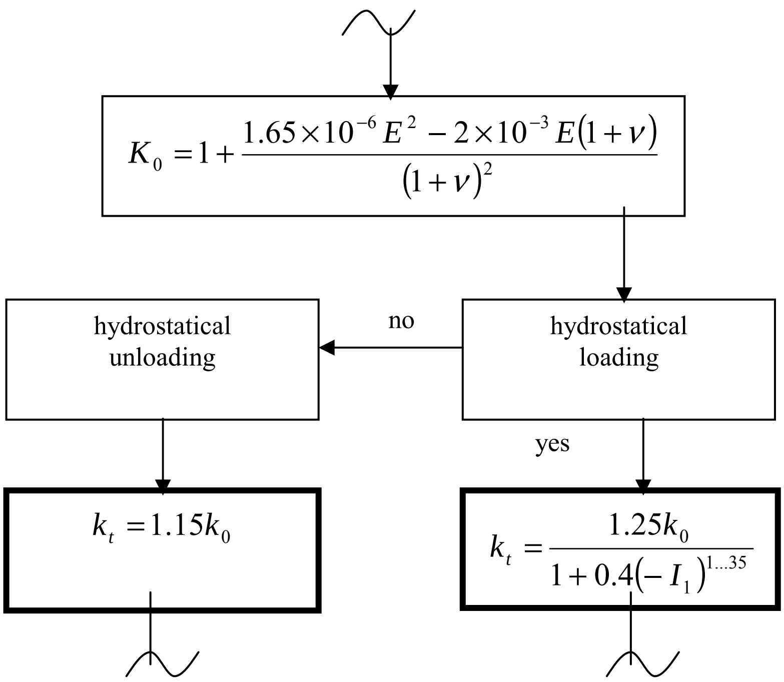

Algorithm calculus of contract - dilatation modulus

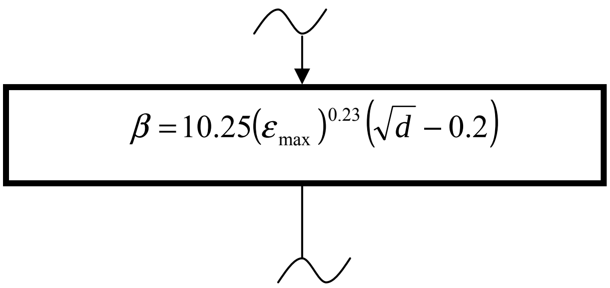

Buckling Resistance of the Compression Members With Open Cross – Section (Part I)

Petru MOGA[a] Traian ORGHIDAN[a] Ştefan GUŢIU[a]

[a]*Technical University of Cluj-Napoca, Cluj-Napoca, România*

Rezumat: În lucrare se prezintă bazele teoretice privind pierderea stabilităţii barei comprimate centric prin fenomenul de încovoiere – răsucire simultană şi metodologia de verificare la flambaj a barei comprimate centric în conformitate cu literatura tehnică şi cu normativele româneşti şi în conformitate cu EUROCODE 3.

Abstract: This paper presents the basis of the analysis regarding the compression members, combined flexural and torsional buckling and the checking methodology according to technical references and Romanian norms as well as to the EUROCODE 3 norm.

Keywords: Eurocode 3, flexural - torsional buckling, compression member.

1. Basis of flexural-torsional buckling

Taking into account the assumption made by V. Z. Vlasov (1940) and I. N. Goodier (1941) the system of differential equations, in *u, v* and φ parameters, is:

$$\begin{cases} EI_y \dfrac{d^2u}{dz^2} + P\cdot u + P\cdot y_c\cdot\varphi = 0 \\ EI_x \dfrac{d^2v}{dz^2} + P\cdot v - P\cdot x_c\cdot\varphi = 0 \\ EI_\omega \dfrac{d^4\varphi}{dz^4} - \left(GI_t - \dfrac{I_c}{A}P\right)\dfrac{d^2\varphi}{dz^2} - \\ - P\left(x_c\dfrac{d^2v}{dz^2} - y_c\dfrac{d^2u}{dz^2}\right) = 0 \end{cases} \qquad (1)$$

where (Fig. 1):

u, v – deflection of the shear centre with respect to the principal axes;

φ – angle of rotation of the cross section;

I_c – polar moment of inertia with respect to the shear centre.

$$I_c = I_x + I_y + A\left(x_c^2 + y_c^2\right) = i_c^2\cdot A$$

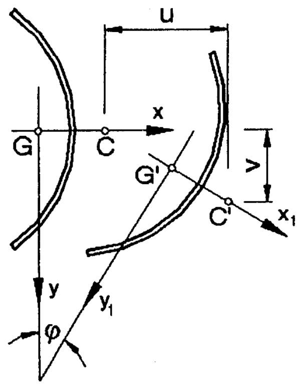

Fig. 1

In the particular case of the thin walled columns with two symmetry axis of the cross section (G ≡ C and $x_c = y_c = 0$), the system of equations becomes:

$$\begin{cases} EI_y \dfrac{d^2u}{dz^2} + P\cdot u = 0 \\ EI_x \dfrac{d^2v}{dz^2} + P\cdot v = 0 \\ EI_\omega \dfrac{d^4\varphi}{dz^4} - \left(GI_t - \dfrac{I_c}{A}P\right)\dfrac{d^2\varphi}{dz^2} = 0 \end{cases} \qquad (2)$$

ISSN-12223-7221

From the first two equations the Euler forces can be determined:

$$P_{x.cr} = \frac{\pi^2 EI_x}{l_{fx}^2}\ ; \quad P_{y.cr} = \frac{\pi^2 EI_y}{l_{fy}^2} \qquad (3.a, b)$$

and from the 3rd equation results:

$$P_\omega = \frac{1}{i_c^2}\left(\frac{\pi^2 EI_\omega}{l_{f\omega}^2} + GI_t\right) \qquad (3.c)$$

In the general case of the thin – walled open cross section, for $l_{fx} = l_{fy} = l_{f\omega} = l$, at the end of the member (for z=0 and z=l), the following conditions are fulfilled:

$$u = v = \varphi = 0\ ,\ \frac{d^2u}{dz^2} = \frac{d^2v}{dz^2} = \frac{d^2\varphi}{dz^2} = 0$$

The differential equations (1) admit general solutions (4):

$$u = C_1 \cdot \sin\frac{\pi \cdot z}{l}\ ; v = C_2 \cdot \sin\frac{\pi \cdot z}{l}\ ; \varphi = C_3 \cdot \sin\frac{\pi \cdot z}{l}$$

Replacing these solutions in the system of equations (1) it is obtained:

$$\begin{cases} \left(P - P_{y.cr}\right)\cdot C_1 + P \cdot y_c \cdot C_3 = 0 \\ \left(P - P_{x.cr}\right)C_2 - P \cdot x_c \cdot C_3 = 0 \\ P \cdot y_c \cdot C_1 - P \cdot x_c \cdot C_2 + i_c^2\left(P - P_\omega\right)\cdot C_3 = 0 \end{cases} \qquad (5)$$

In admitting solutions different from the banal solutions $C_1 = C_2 = C_3 = 0$, the following condition must be fulfilled:

$$\begin{vmatrix} \left(P - P_{y.cr}\right) & 0 & P \cdot y_c \\ 0 & \left(P - P_{x.cr}\right) & -P \cdot x_c \\ P \cdot y_c & -P \cdot x_c & i_c^2\left(P - P_\omega\right) \end{vmatrix} = 0 \qquad (6)$$

The following cubic equation it is obtained:

$$\begin{aligned} f(P) = i_c^2\left(P - P_{x.cr}\right)\left(P - P_{y.cr}\right)\left(P - P_\omega\right) - \\ - P^2 \cdot y_c^2\left(P - P_{x.cr}\right) - P^2 \cdot x_c^2\left(P - P_{y.cr}\right) = 0 \end{aligned} \qquad (7)$$

Equation $f(P) = 0$ has three real solutions and it can be demonstrated that one of these is smaller that $\min\left(P_{x.cr}; P_{y.cr}; P_\omega\right)$; this solution is the critical force P_{cr}.

In the case of the mono-symmetrical cross section (Fig. 2) the equation (6) becomes:

$$\begin{vmatrix} P - P_{x.cr} & -P \cdot x_c \\ -P \cdot x_c & i_c^2\left(P - P_\omega\right) \end{vmatrix} = 0 \qquad (8)$$

or:

$$i_c^2\left(P - P_{x.cr}\right)\left(P - P_\omega\right) - P^2 \cdot x_c^2 = 0 \qquad (9)$$

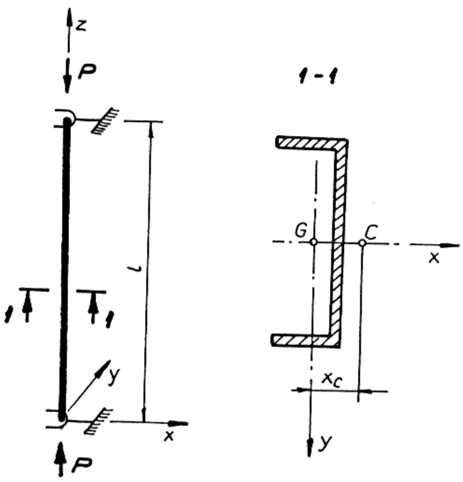

Fig. 2

2. Flexural – torsional buckling checking according to Romanian norms

Knowing the critical force P_{cr}, as being the minimum value of the solutions of equation (7) or (9), it results the critical buckling stress:

$$\sigma_{cr} = \frac{P_{cr}}{A} \qquad (10)$$

This stress can be put in the form:

$$\sigma_{cr} = \frac{\pi^2 \cdot E}{\lambda_{tr}^{\ 2}} \tag{11}$$

so it results $\lambda_{tr} = \pi \sqrt{\frac{E}{\sigma_{cr}}}$ and then the buckling coefficient $\varphi_{tr} = \varphi_{tr}(\lambda_{tr})$ - curve "b" from SR 1911-98.

The compression member carrying capacity will be:

$$N_{cap} = \varphi_{tr} \cdot A \cdot \sigma_a \tag{12}$$

The relation (11) can be applied only in the elastic domain. In the elasto-plastic domain ($\sigma_p < \sigma \le \sigma_c$) can be used a relation of the form:

$$\sigma^*_{cr} = \sigma_c \left(1 - 0{,}25 \frac{\sigma_c}{\sigma_{cr}}\right) \tag{13}$$

3. Buckling resistance of compression members according to EC 3

The design buckling resistance of a compression member shall be taken as:

$$N_{b.Rd} = \chi \cdot \beta_A \cdot A \cdot f_y \cdot \frac{1}{\gamma_{M1}} \tag{14}$$

where:

$$\beta_A = \begin{cases} 1 & \text{- for class 1, 2 or 3 cross sections;} \\ A_{eff} / A & \text{- for class 4 cross section.} \end{cases}$$

For constant axial compression in members of constant cross – section (uniform members), the value χ for the appropriate non-dimensional slenderness $\overline{\lambda}$, can be determined from:

$$\chi = \frac{1}{\phi + \sqrt{\phi^2 - \overline{\lambda}^2}} \; ; \; \chi \le 1 \tag{15}$$

where:

$$\phi = 0{,}5\left[1 + \alpha\left(\overline{\lambda} - 0{,}2\right) + \overline{\lambda}^2\right];$$

α - the imperfection factor, Table 1

$$\overline{\lambda} = \sqrt{\frac{\beta_A \cdot A \cdot f_y}{N_{cr}}}$$

Table 1

Buckling curve	a	b	c	d
The imperfection factor α	0,21	0,34	0,49	0,76

3.1. Flexural buckling

In the flexural buckling case, the non-dimensional slenderness ratio will be:

$$\overline{\lambda} = \sqrt{\frac{\beta_A \cdot A \cdot f_y}{N_{cr}}} = \sqrt{\frac{A \cdot f_y}{N_{cr}}} \cdot \sqrt{\beta_A}$$

where:

$$N_{cr} = \min\begin{bmatrix} P_{x.cr} = P_{Ex} = \dfrac{\pi^2 \cdot E \cdot I_x}{l_{fx}^{\ 2}}; \\ P_{y.cr} = P_{Ey} = \dfrac{\pi^2 \cdot E \cdot I_y}{l_{fy}^{\ 2}} \end{bmatrix}$$

or: $$\overline{\lambda} = \sqrt{\frac{\beta_A \cdot A \cdot f_y}{N_{cr}}} = \sqrt{\frac{f_y}{\sigma_k}} \cdot \sqrt{\beta_A};$$

$$\sigma_k = \sigma_{cr} = \min\left[\sigma_{Ex} = \frac{P_{Ex}}{A} \; ; \sigma_{Ey} = \frac{P_{Ey}}{A}\right]$$

The slenderness can be put also in the form:

$$\overline{\lambda} = \frac{\lambda}{\lambda_1}\sqrt{\beta_A} \; ; \; \lambda_1 = \pi\sqrt{\frac{E}{f_y}} = 93{,}9\varepsilon ,$$

where: $\varepsilon = \sqrt{\frac{235}{f_y}}$; $\lambda = \frac{L}{i_{\min}}$.

3.2. Flexural – torsional buckling

In this case the non-dimensional slenderness $\overline{\lambda}$ will be:

$$\overline{\lambda} = \sqrt{\frac{\beta_A \cdot A \cdot f_y}{N_{cr}}} = \sqrt{\frac{f_y}{\sigma_k}} \cdot \sqrt{\beta_A}$$

where:

$$\sigma_k = \sigma_{cr} = \frac{P_{cr}}{A}$$

in witch P_{cr} is determined according to point 1 of this paper.

4. Conclusions

The flexural-torsional buckling problem is a complex phenomenon, in calculation formulas being involved the cross - section properties (shear center, warping constant etc.).

This mode of buckling is generally characteristic for mono-symmetrical or non-symmetrical open cross sections, especially when warping constant I_ω (C_ω) is very small or zero.

According to EC 3 the load bearing capacity of the compression member is evaluated by taking into account the effective cross-section area and even more accurately considering the bending moment caused by the shift of effective cross-section neutral axis with respect to gross cross-section.

5. References

[1] Dalban, C., Juncan, N., *Construcţii metalice.* E.D.P.Bucureşti, 1983.
[2] Moga, P.: *Poduri metalice. Alcătuirea şi calculul elementelor.* U.T.C.-N., 2000.
[3] Moga, P., Guțiu, Şt.: *Poduri metalice. Probleme de stabilitate.* U.T.C.-N. 2003.
[4] *** SR 1911-98. *Poduri metalice de cale ferată. Prescripţii de proiectare.*
[5] *** STAS 10108 / 0 – 78. *Calculul elementelor din oţel.*
[6] *** EUROCODE 3. Part 1. *Design of Steel Structures.* CNCMET, Doc. No. 91/03.
[7] *** EUROCODE 3. *Exemple de calcul.* Tempus Phare Project 01198. 1997.

Proposal for a Roof Structure of Cluj-Napoca Municipal Stadium

Vasile PĂCURAR[a] Ştefan I. GUȚIU[a] Cătălin MOGA[a]

[a]*Technical University of Cluj-Napoca, Cluj-Napoca, România*

Rezumat: In lucrare se prezinta o propunere pentru structura de acoperire parțială a tribunelor stadionului municipal din Cluj-Napoca. Soluția a fost elaborată cu ocazia întocmirii studiului de fezabilitate privind reabilitarea şi modernizarea stadionului, astfel încât acesta să corespundă condițiilor impuse în cadrul Uniunii Europene.

Abstract: This paper presents a proposal of a roof structure for the partial covering of Cluj-Napoca Municipal Stadium tribune. The solution has been elaborated in the fezability study regarding the rehabilitation and modernization of the stadium, according to European Union norms.

Keywords: roof structure, seismic action, dynamic characteristics, structure stability

1. Introduction

The design procedure started with the documentation phase, taking into consideration other similar projects in our country and also abroad.

The models presented in Figure 1 have been selected as source (Goteborg Stadium– Sweden, Kingston Stadium – England, Vicente Calderon Stadium – Spain, Erastmus Bridge – Holland).

Goteborg Stadium – Sweden

Kingston Stadium – England

Vicente Calderon Stadium – Spain

Erastmus Bridge – Holland

Fig. 1

ISSN-12223-7221

On deciding the structural solution, for the partial roofing of the stadium tribune, the following criteria have been studied:

- choosing the optimal shape for the mechanical behavior of the structure, able to generate a minimal metallic consume (normal steel for constructions and high resistance steel for the cable stays);
- simple execution in the workshop, having selected plane elements obtained from laminate profiles and steel plates;
- subdividing the elements to obtain a minimum number of joints, at the building site;
- relatively simple joints, clearly organized on execution stages and without the risks of producing accidents on assembling the structure elements;
- safety during exploitation and easy maintenance, by avoiding the closed sections, inaccessible for cleaning and painting.

A special attention on choosing the structural solution has been paid to the aesthetic form of the building, taking into consideration that this structure besides the functional aspect– that of covering the tribune, also has an architectural function with respect to the area and the city.

2. Description of the selected structure

The structure selected for the covering system of the stadium tribune contains the following main elements:

- three transversal semiframes with the span of 31 m and the height of 17 m, which sustain the elements of the roof system;
- three pylons with the height of 30 m which sustain the transversal semiframes, each with one stay cable for suspension the end of the semiframe to the top of the pylon, the pylon being anchored with two inclined cables to the foundation blocks;
  - the roof system contains:
  - three longitudinal main steel plate girders, spaced on 12.5 m, made up as a succession of simply supported beams with cantilever;
  - six transversal steel plate girders, spaced on 10 m;
  - truss purlins, spaced on 2.5 m;
  - covering layer, made up by profiled steel sheet or polycarbonate;
- three individual foundations for the semiframes, 2x3 individual foundations for the pylons, 2x3 anchor blocks;

The assembly structure is presented in Figure 2 and Figure 3.

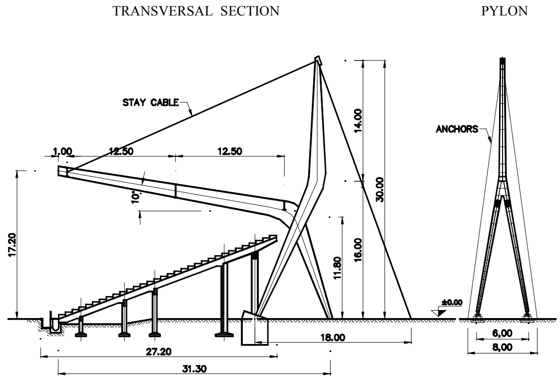

Fig.2

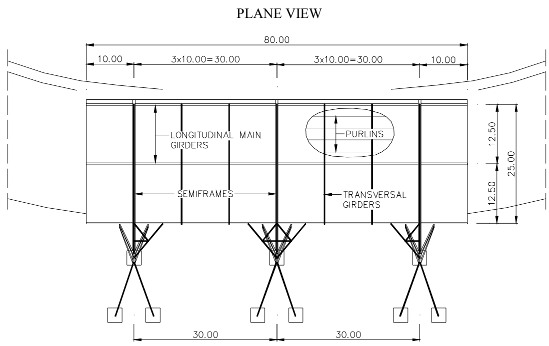

Fig.3

3. Aspects concerning the mechanic behaviour and the static calculation of the structure

The calculation of the structure has been done considering all the possible loads combinations. Taking into consideration the load combination cases the following aspects have been mainly analyzed:

- in the fundamental load combination case – the stability of the structure regarding the wind action, considering the dynamic structure characteristics;
- in the special load combination case – the structure response on seismic action.

Other considerations for the structure design are:

- the optimal shape for the semiframe, taking into account the bending moment distribution (the number and position for the stay cables), leading to the solution of a single stay cable, placed at the end of the semiframe;
- the shape of the sustaining pylon for an optimal mechanic behavior and to obtain minimum effort in the anchoring cables;
- the structure deformations have to be situate in the allowable limits;

As follows, are present some aspects concerning the pylon conformation and the structure response on seismic action.

The pylon

Two variants of pylon building have been studied:
- Variant 1: pylon fixed in foundation;
- Variant 2: pylon hinged in foundation.

Each of these versions presents certain advantages and disadvantages, as follows:

- pylon fixed in foundation:

Advantages:

- o the pylon has not to be sustained in the erection stage;
- o together with the anchoring cable, it results a system static undetermined (1 degree of static undetermination), which creates certain reserves of resistance, that can be emphasized through a calculus in elasto-plastic domain.

Disadvantages:

- o at the fixing level of the pylon into the foundation a bending moment appears, thus resulting a higher solicitation of the foundation and as a consequence larger dimensions of this;
- o the fixing of the pylon into the foundation has to be ensured for undertaking of the bending moment at the fixing level.

- pylon hinged in foundation:

Advantages:

- o at the level of the hinging the pylon into the foundation the bending moment is zero, thus the solicitation of the foundation is smaller and so are its dimensions;
- o the cross section dimensions of the pylon are smaller towards the hinge level.

Disadvantages:

- o the pylon has to be sustained in the erection stage;
- o it results a determined static system, which doesn't present reserves of resistance.

From the constructive point of view in both cases have been adopted the building of the pylon with the shape of a non rectangular bar, with a vertical section in the superior half and an inclined section in the inferior half.

This constructive solution presents the following technical and economical advantages:

- the adoption of this shape leads to important decrease of the tension efforts into the anchoring cables, with a favorable consequence on the dimensions of the anchoring blocks and implicitly to lower costs;
- the pylon foundations can be placed closer to the existing construction, reducing the space occupied by the new one;
- the adoption of such a shape has beneficial aesthetic effects on the construction.

The inferior section of the pylon, inclined, is made by using two branches, which creates stability for the pylon in the erection and exploitation stages and much more favorable overall mechanic behavior.

Taking into account the previously mentioned facts and the diagrams of the bending moment and axial force, it can be appreciate that the solution of the pylon hinged into the foundation (variant 2) is more advantageous than the one with the pylon fixed into the foundation.

In Figure 4 the diagrams of the bending moment (M) and axial force (N) are presented for the hinged pylon into the foundation.

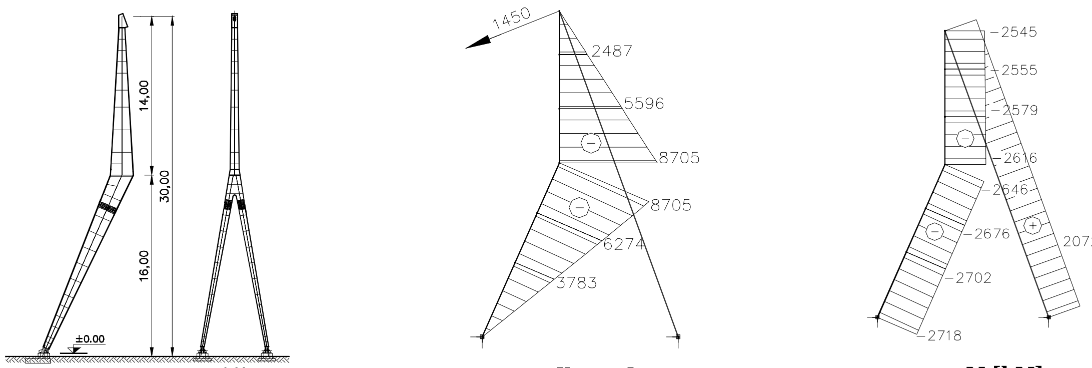

M [kN m] **N [kN]**

Fig.4

The structure analyze on seismic action

The design was carried out according to the Romanian Seismic Code P100-92, the design spectrum results from the following relation:

$$c_r(=S_d)=\alpha\cdot k_s\cdot\beta_r\cdot\psi\cdot\varepsilon_1$$

$\alpha=1.2$ - importance class II
$k_s=0.08$ - design ground acceleration (Cluj-Napoca – Zone F)
$\beta_r=2.5$ - spectral acceleration amplification factor, for $T_c=1.0\,\text{sec}$
$\psi=0.20$ - behavior factor
$\varepsilon_1=1.0$ - equivalence coefficient

The analysis based on A method

The seismic analysis of any structure is being made, according to the seismic code, in a simplificated way through A method, which replaces the dynamic action of the earthquake with a static load, determined with the relation:

$$S_r=c_r\cdot G$$

where:
G – in this case self weight plus snow load.

Taking into consideration the structural system (there is not a spatial cooperation between the semiframe and the pylon) the seismic load will be evaluated distinctively for the semiframe and pylon. The potential seismic loads, on semiframe and pylon, with opposite sign, are tested through load combinations.

The evaluation of seismic load for the semiframe

After evaluating the self weight (permanent action) and the snow load, it results:

$$G=\sum P_i^n+Z^n=3108\,\text{kN}$$
$$S_S=1{,}2\cdot 0{,}08\cdot 2{,}5\cdot 0{,}20\cdot 1\cdot G=0{,}048\cdot G=150\,\text{kN}$$

The evaluation of seismic load for the pylon

Self weight load of the pylon is:

$$G=G_{pylon}\cdot 3\approx 23000\cdot 3=69\,000\,\text{daN}=690\,\text{kN}$$

Seismic force:

$$S_P=0{,}048\cdot G=33{,}12\,\text{kN}$$

The load combination case

The calculus is made for the special load combination case:

$$\sum P_i+\sum n_i^d\cdot V_i+S$$

where:
P_i - self weight load (characteristic value);
V_i=96 daN/m^2 - variable load (here snow load – characteristic value);

$n_i^d = \gamma_1 = 0{,}35$ - long period coefficient;

S - seismic force.

For the static computation, it has been evaluated an equivalent load from the action of self weight and snow load, which is distributed to each semiframe:

$$g = \frac{\sum P_i^n + 0{,}35 \cdot Z^n}{3 \cdot L} = \frac{111080 + 0{,}35 \cdot 199680}{3 \cdot 26{,}4}$$
$$= 2285\, daN/m = 22{,}9 \text{ kN/m}$$

The distribution of seismic load

- Semiframe:

The seismic force is undertaken by the three semiframes. In the static calculus the force of each semiframe is considered acting at the intersection points of the semiframe with the longitudinal beams:

$$S_{1S} = \frac{S_S}{3} = \frac{150}{3} = 50 \text{ kN}$$

The seismic force is distributed proportionally with the self weight:

- the seismic force at the contact point of the semiframe with the longitudinal boundary beam:

$$S_{GLM} = 1 \cdot \frac{S_{1S}}{4} = 12{,}5 \text{ kN}$$

- the seismic force at the contact point of the semiframe with the longitudinal central beam

$$S_{GLM} = 2 \cdot \frac{S_{1S}}{4} = 25 \text{ kN}$$

- Pylon:

$$S_{1P} = \frac{S_P}{3} = \frac{33{,}12}{3} = 11{,}04 \text{ kN} \approx 11 \text{ kN}$$

$80\% \cdot S_{1P} = 8{,}8$ kN - for the bottom section;

$20\% \cdot S_{1P} = 2{,}2$ kN - for top section.

For the static calculations the following independent loads have been established:

- **1** – self weight + snow load;
- **2** – seism action on semiframe in longitudinal direction;
- **3** – seism action on semiframe in transversal direction;
- **4** – seism action on pylon in longitudinal direction;
- **5** – seism action on pylon in transversal direction.

The following load combinations resulted are presented in Table 1:

Table 1

Load Combination	Load Cases				
	1	2	3	4	5
CO1	1	1	0	1	0
CO2	1	-1	0	-1	0
CO3	1	-1	0	1	0
CO4	1	1	0	-1	0
CO5	1	0	1	0	1
CO6	1	0	-1	0	-1
CO7	1	0	1	0	-1
CO8	1	0	-1	0	1

As a consequence of the accurate structure modeling in finite elements and the application of corresponding static forces, the efforts and the displacements of the structure have been obtained; the values resulted are inferior to those resulted in the fundamental load combination case.

Calculus based on the modal analysis (Annex C)

The seismic loads are taken into account according to the Response Spectrum Analysis method. This method requires a previously calculated number of undamped free vibration frequencies and the corresponding mode shapes.

Based on these vibration mode shapes, the software generates equivalent static loads (for each vibration mode shape) which are then applied to the model in a static analysis. Then displacement and internal force results obtained for each mode shape are summed according to the equation below, in order to obtain the internal forces:

$$Y_k = \sqrt{\sum_i Y_{ki}^2}$$

where Y_k is a cross-sectional displacement or internal force component. If two consecutive vibration frequencies are closer than 10%, the corresponding values are summed as: $Y_{j,j+1} = |Y_j| + |Y_{j+1}|$, and used later in the equation above. Due to the exponents in the equation the results give positive values. Therefore, when generating the seismic type load cases, two are included. One "+" with values included as positives, and one "-" with values included as negatives. In addition the results corresponding to each vibration mode shape are provided (corresponding to load cases with 01, 02, ….n suffixes), that can be used in the generation of further combinations or of critical combinations.

It must be specifying in addition the following parameters:

Ve - seismic wave propagation speed (Ve=400 m/s);

Lc - the largest horizontal dimension of the structure (Lc=80m).

Based on the values of the frequencies, Axis determines the β_i factors as follows (Fig. 5):

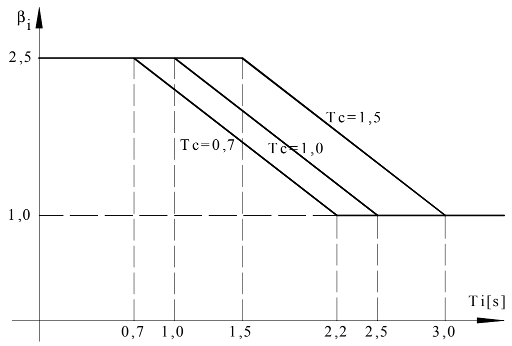

Fig.5

For each vibration mode shape, the program generates horizontal forces applying the formula below:

$$S_{k,r} = k_s \cdot \alpha \cdot \beta_r \cdot \psi \cdot \eta_{k,r} \cdot G_k$$

where: k - degree of freedom of the node;
r - index of the respective mode shape.

In case of Romanian design code a warning message is sent if the inequality below is not satisfied: $\frac{L_c}{V_e \cdot T_r} < \frac{1}{3}$.

Table 2 presents a comparison of the resulted values obtained in method A versus method C.

Table 2

Efforts and displacements		A	C	Differences [%]
Effort in the stay cable	[kN]	436	408	7
Effort in the anchoring cable	[kN]	263	290	9
Displacement in x direction	[cm]	6,8	6,06	12
Displacement in y direction	[cm]	11,4	9,32	22
Displacement in z direction	[cm]	21,1	20,3	4

4. Final remarks

It can be appreciated that the solution proposed for the roof structure of the municipal stadium tribunes complies with the requests of resistance, functional and aesthetical for this specific kind of construction. Thus the construction can be integrated within the structural type category used worldwide in this field.

In what the metal requirement for the execution of the structure is concerned, the steel specific consume resulted is of approx. 80 kg/m^2, considered as having a medium value for this type of structure. If the structure of the construction is being taken into consideration omitting the pylons, the steel consume resulted would be of approx. 50 kg/m^2, which is a usual consume for the metal industrial halls with high-medium span.

5. References

[1] Mateescu, D., Caraba, I.: *Construcții metalice. Calculul și proiectarea elementelor din oțel.* Ed. Tehnică, 1980.
[2] Bârsan, G.,M.: *Dinamica şi stabilitatea construcțiilor.* EDP Bucureşti, 1979.
[3] * * * STAS 10108/0-78: *Calculul elementelor din oțel.*
[4] * * * STAS 3300/2-85: *Calculul terenului de fundare.*
[5] * * * P100-92: *Normativ pentru proiectarea antiseismică a construcțiilor.*
[6] * * * EURODODE 3: *Design of steel structures*
[7] * * * EUROCODE 8: Design of structures in seismic zones

Implications of Available Instrumental Data on the Specification of Seismic Conditions of Romania

Horea SANDI[a] Ioan Sorin BORCIA[b]

[a] *Institute of Geodynamics "Sabba S. Ştefănescu" of the Romanian Academy, Bucharest, Romania*
[b] *INCERC (National Building Research Institute), Bucharest, Romania*

Abstract: The wealth of strong motion records obtained during the Vrancea earthquakes of 1977.03.04, 1986.08.30, 1990.05.30 and 1990.05.31 is at the origin of the paper. After presenting some methodological aspects, the main developments are related to attenuation (dealt with first irrespective of azimuthal orientation, but subsequently also in directional terms) and to the factors influencing the spectral contents of ground motion (features of source mechanisms versus local conditions). Some conclusions and needs of further research are finally pointed out.

An appendix is devoted to some data and estimates concerning the seismic conditions of Dobrogea.

Keywords: Strong ground motion, attenuation, local conditions, spectral characteristics.

1. Introduction

Romania ranks high in Europe from the viewpoint of the severity of seismic conditions. This is comparable with the severity of conditions of Turkey, Greece or Italy. The seismicity of Romania is dominated by the activity of the Vrancea seismogenic zone {*VSZ*}, which generates, in the average, per century, three events of Gutenberg - Richter magnitudes 7.0 or more.

Romania entered, during the destructive earthquake of 1977.03.04 (M_{GR} = 7.2), the era of accelerographic recording of strong ground motion. The considerable development of the accelerographic network (its bulk having been provided by the US post-disaster aid) that took place after that event made it possible to obtain numerous, particularly valuable, records during the strong earthquakes of 1986.08.30 (M_{GR} = 7.0), 1990.05.30 (M_{GR} = 6.7) and 1990.05.30 (M_{GR}=6.1).

The 150 strong motion records available made it possible to derive a comprehensive picture of the features of ground motion due to earthquakes originating in the {*VSZ*}, which contributed considerably, and is to contribute in future too, on the basis of further analyses, to a more in-depth understanding of the seismic conditions of Romania, particularly from the viewpoint of the zones affected mainly by the *VSZ* activity.

The paper presents some developments in following main directions: methodological aspects, references to the records available, references to the processing of records, references to some main results and conclusions obtained. The main directions in which results obtained are referred to are represented by the features of attenuation and by the remarks on the contributions of source mechanism and attenuation on one hand, and by the local conditions on the other hand, to the features of ground motion at various sites.

2. Methodological aspects

The main methodological aspects to be referred to at this place are related to the characterization of ground motion, to the techniques of processing of accelerographic records, as well as to the techniques of attenuation analysis.

The characterization of ground motion was made using several categories of parameters and functions. The parameters used were *PGA*, *PGV*, *PGD*¸ *EPA*„ *EPV* and I_S (while the sense of the first five parameters is quite well known, the parameter I_S represents the spectrum based intensity, as defined e.g. in [11], along with other parameters, like intensity based on Arias'

ISSN-12223-7221

definition, and with functions as intensities related to a frequency or averaged over a frequency interval, based on response spectra, $i_s*(\varphi', \varphi'')$, on destructiveness spectra, $i_d*(\varphi', \varphi'')$, and also on Fourier spectra, $i_f*(\varphi', \varphi'')$, where (φ', φ'') represent intervals of frequencies, Hz, while the asterisk represents averaging according to some specific rules).

The processing of accelerographic records included as a first step a primary processing (corrections, integration to obtain velocities and displacements, response spectra). The additional step of secondary processing included as a subsequent step determination of response spectra along twelve equidistant horizontal directions (as introduced first in [13]), as well as determination of various intensities for various frequency intervals, as e.g. in [9], [4], [12].

The attenuation analysis included first, for each of the earthquakes of 1986.08.30 (M_{GR} = 7.0), 1990.05.30 (M_{GR} = 6.7) and 1990.05.30 (M_{GR} = 6.1), a statistical analysis irrespective of directionality and, subsequently, an analysis of attenuation directionality performed in terms of Fourier expansion with respect to the azimuthal angle.

3. References to the records available

The most relevant records were related to the four events referred to in the introduction. These records were obtained by two different networks, managed respectively by the National Building Research Institute (INCERC) and by the National Institute of Earth Physics (INCDFP). Most of them were obtained by SMA-1 accelerographs, installed as a rule in basements of buildings.

The records available, obtained for successive events having originated in the same source zone, offer an extremely valuable information, since they make it possible to put to evidence, to a high extent, what is permanent and what is variable in the effects of earthquakes generated by the *VSZ* source zone.

4. References to the features of attenuation

The low attenuation rate of [*VSZ*] earthquakes (which is in good agreement with the source depths referred to) is known since long. Events with magnitudes $M \geq 7$. tend to affect with intensities $I \geq$ VII important parts of the Romanian territory. It is also known, [2], [7], that major earthquakes tend to generate isoseismals elongated in the NE-SW direction (this was the case of the events of 1940.11.10, 1977.03.04, 1986.08.39, but not that of the events of 1990.05.30, 1990.05.31).

The results presented at this place are based mainly on the analysis presented in [10].

A basic parameter used in the attenuation analysis was represented by a non-dimensional distance,

$$\rho = lg\,[(1 + r^2 / h^2)^{1/2}] \qquad (4.1)$$

This expression is suggested by Blake's attenuation law [3], subsequently generalized by Sandi [8]. The attenuation directionality was analyzed on the basis of a Fourier expansion with respect to the azimuthal angle,

$$I_S^* (\rho_i, \alpha_i) = I_{S0}^* (\rho_i) + \Sigma_n (a_n \cos n\alpha_i + b_n \sin n\alpha_i)$$

$$(n = 1, 2, 3 \ldots) \qquad (4.2)$$

where $I_{S0}*(\rho_i)$ represents the expected spectrum based intensity, irrespective of direction, while the left member $I_S*(\rho_i, \alpha_i)$ represents the expected spectrum based intensity, with account on directionality. A summary of the most relevant results is provided in Table 1.

The data presented make it possible to formulate following comments:

a) The gradient of attenuation was relatively high on 1986.08.30, but unexpectedly low on 1990.05.30. This is in contradiction with the expectation of influence of source depth (the source depth was 133 km for the first event, 89 km for the second and 79 km for the last one).

b) The scatter of results was high, even for events considered individually (especially on 1986.08.30). It tended to be lower for peak spectral values than for peak values of direct ground motion parameters, and to be lowest for the spectrum based intensity I_S.

c) The macroseismic epicentre was close to the instrumental epicentre for the first two events, but was considerably far for the last event (see values a_1, b_1).

Table 1. Results of statistical attenuation analysis

Parameters	Events		
	1986.08.30	1990.05.30	1991.05.31
$I_S = a - b\rho$	$7.7 - 7.6\,\rho$	$7.2 - 2.1\,\rho$	$5.9 - 2.6\,\rho$
	R.m.s. values of ground motion parameters		
$\log_2 PGA$	0.925	0.662	0.910
$\log_2 PGV$	0.999	0.790	0.916
$\log_2 PGD$	1.025	0.901	0.756
$\log_2 EPA$	0.836	0.653	0.883
$\log_2 EPV$	1.012	0.735	0/911
I_S	0.873	0.588	0.584
	Fourier coefficients for the azimuthal distribution of intensities I_S		
a_1	- 0.09	-0.03	0.01
b_1	-0.01	0.09	0.63
a_2	0.14	0.24	- 0.16
b_2	0.23	-0.08	- 0.47
	Dominant azimuthal angles of seismic radiation for intensities I_S		
$N\alpha°E$	$N58°E$	$N161°E$	$N71°E$

d) The radiation directionality was quite strong in all cases (see values a_2, b_2), while the main radiation directions were considerably different from one event to the other (see values a_1, b_1). While for the first event the main direction was approximately *NE-SW*, as for the strong earthquakes of 1940.11.10 and 1977.03.04, it was considerably different for the events of 1990. The general picture of radiation for the event of 1990.05.30 may have been similar to that of the destructive earthquake of 1471.08.29 which, according to sources of literature affected severely the North of Moldova (Neamţ Monastery, Moldoviţa Monastery, Suceava citadel).

5. Data and considerations on response spectra

Response spectra for absolute accelerations were determined for all records available. A more in-depth analysis could be performed on the basis of determining, for part of the stations, of spectra along twelve azimuthally equidistant horizontal directions, according to techniques introduced first in [13]. The histories of spectra for successive events offer a particularly useful insight into the features of seismic phenomena. In order to illustrate some features of successive motions at specific sites, histories of twelve-directions spectra (for 5% critical damping) are presented in Figures 1 and 2 for following stations: Bucharest-INCERC (44.44 N, 26.16 E), Bucharest-Carlton (44.44 N, 26.10 E), Focşani (45.69 N, 27.18 E), Râmnicul Sărat 2 (45.38 N, 27.04 E), Oneşti (46.25 N, 26.76 E), Vaslui (46.64 N, 27.73 E), Baia-Dobrogea (44.72 N, 28.68 E) and Cernavodă 1 (44.34 N, 28.03 E).

The data provided by the response spectra were analyzed and commented in detail for the 9 stations of Bucharest in [9], and for the 14 stations located in the zones *A* and *B* (the most severe ones in Romania, as defined by the earthquake resistant design code, in [14]). The primary processing (response spectra) was followed by secondary processing: determination of I_S, T_C (velocity / acceleration corner period) and T_D (displacement / velocity corner period) for both recording directions and for their ensemble, determination of averaged frequency dependent intensities $i_s*(\varphi', \varphi'')$, as defined in [11], for various frequency intervals (φ', φ''), again for both recording directions and for their ensemble. This secondary database made it possible to develop plots on the dependence of intensities (of various kinds, as referred to) and of corner periods on earthquake magnitude and to summarize the outcome in some relevant tables. Some main findings were as follows:

- the examination of 12-direction spectra shows that there are important differences between spectral ordinates for different directions (in several cases, ordinate ratios even around 1:3);

- the comparison of spectra at a same station shows, for different events, important differences of spectral contents for several stations, where deep, relatively soft, upper layers exist (considerable modification of predominant periods, as e.g. at Bucharest (both stations presented), Focşani, Râmnicul Sărat); there are also stations where the predominant periods are quite stable (Cernavodă, Baia-Dobrogea), while there exist relatively thin soft superficial layers, supported by quite hard rock (strong contrast of *S*-wave propagation velocities);

- a systematic positive correlation of velocity / acceleration corner periods with magnitude (as shown in [6] too) is observed at the nine stations of Bucharest [9], while for the stations of Cernavodă and Baia-Dobrogea, referred to above, there is a positive correlation with intensity, as put to evidence by Figures 1 and 2;

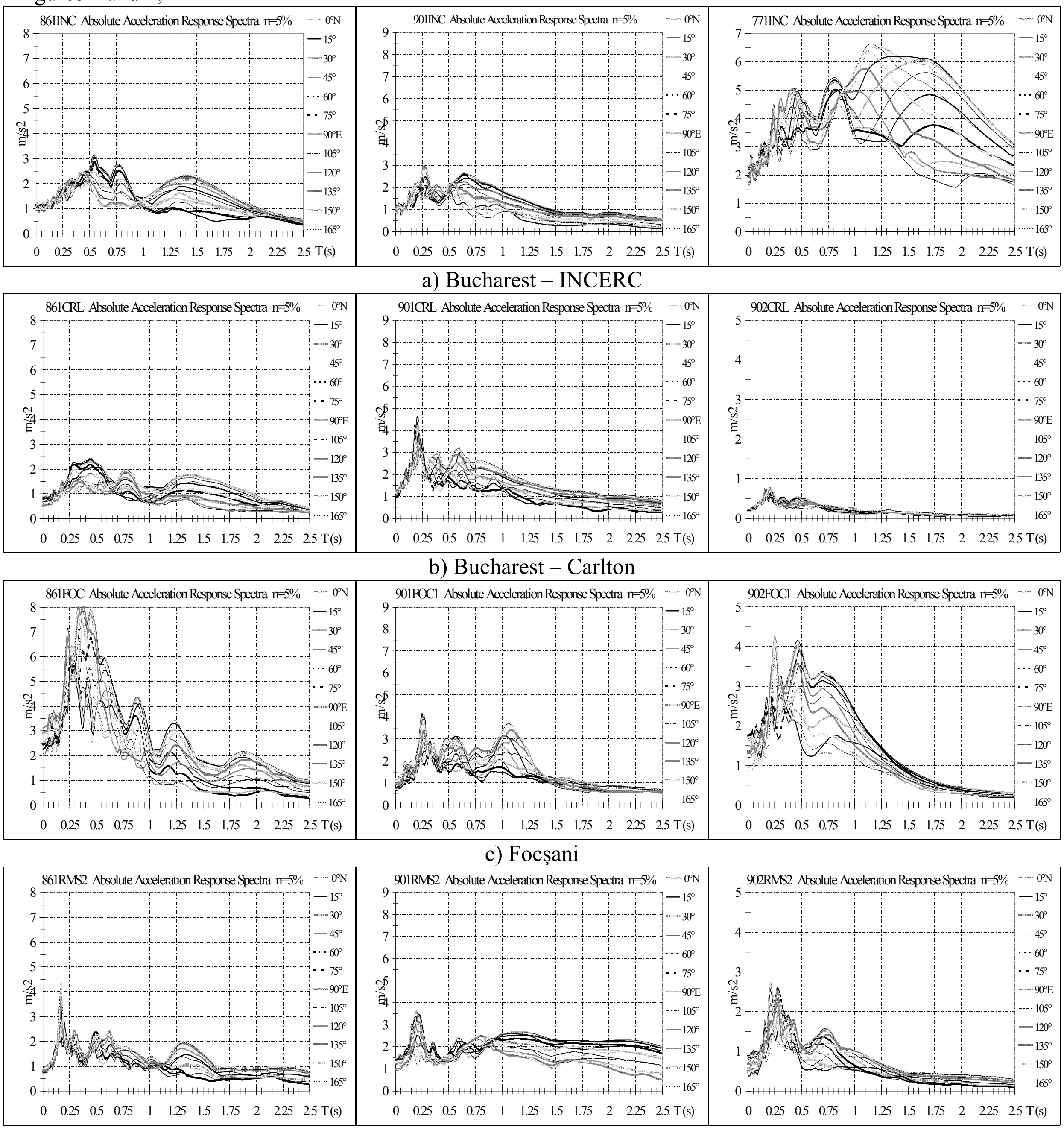

a) Bucharest – INCERC

b) Bucharest – Carlton

c) Focşani

d) Rm. Sărat 2

Fig. 1. Response spectra (12 horizontal directions) for Bucharest – INCERC, Bucharest – Carlton, Focşani, Rm. Sărat

- the variation of predominant and corner periods differs at different places; while in Bucharest the situation was as shown, on the contrary, in Focşani and Râmnicul Sărat these periods became much longer on 1990.05.30 than on 1986.08.30.

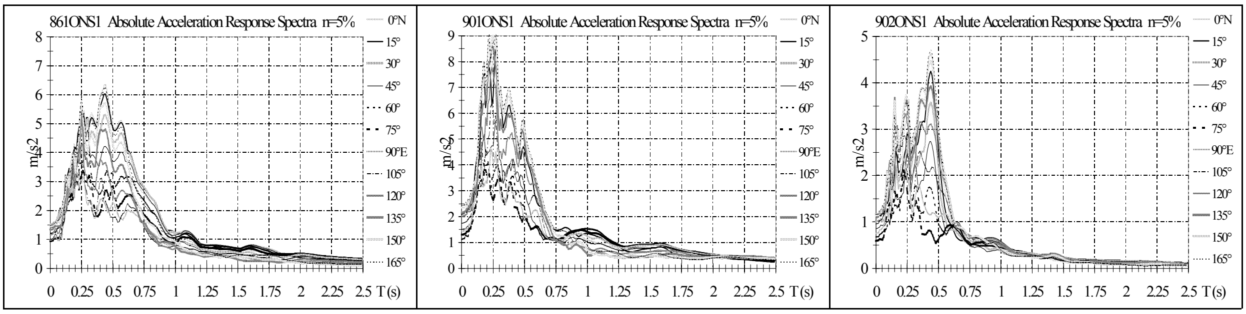

a) Oneşti

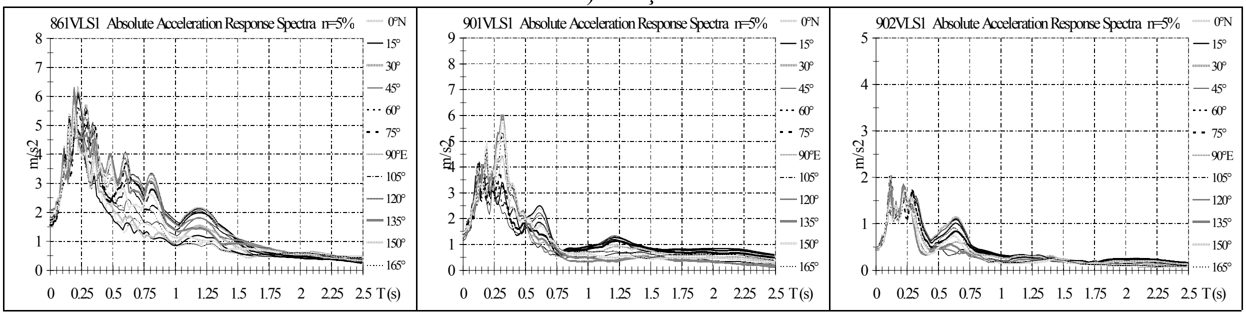

b) Vaslui

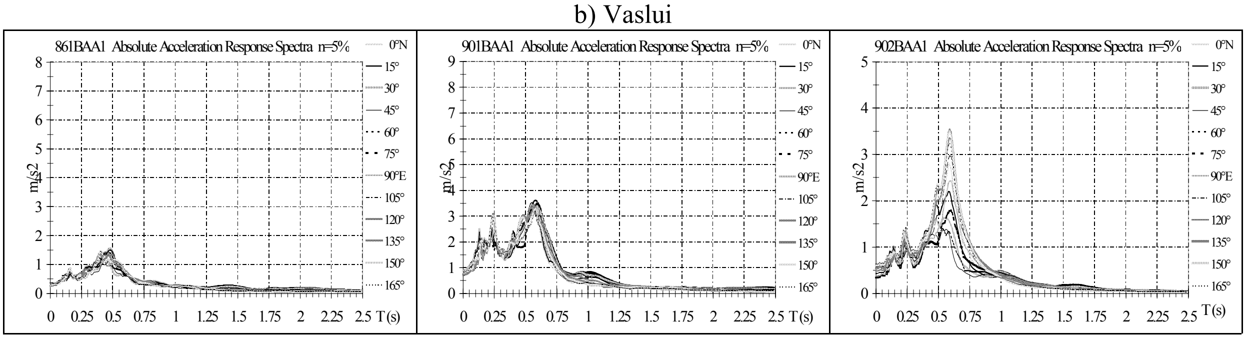

c) Baia - Dobrogea

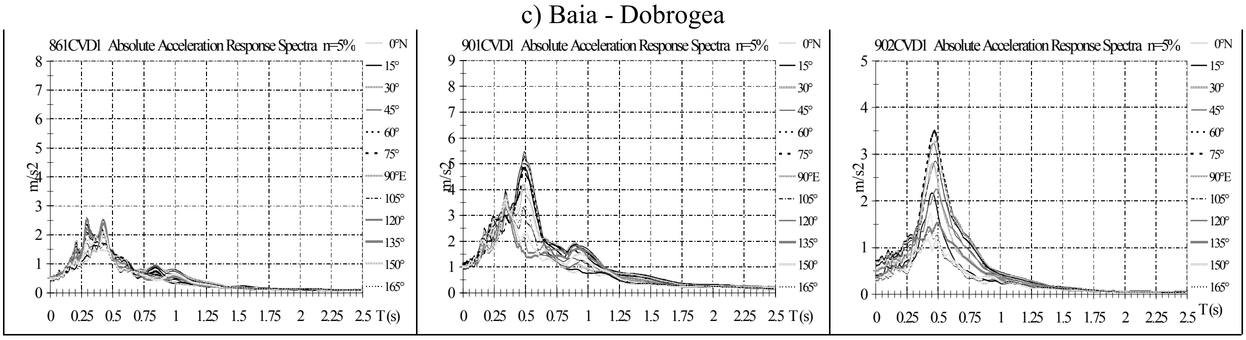

d) Cernavodă 1

Fig. 2. Response spectra (12 horizontal directions) for Oneşti, Vaslui, Baia - Dobrogea, Cernavodă 1

Former remarks, together with those of [9], [4], make it possible to conclude that:

- the effect of local conditions is obvious and stable at places where there are relatively thin (thickness: a few tens of meters) relatively soft superficial layers, in strong contrast with a hard base rock (in those cases, local amplification corresponds well to the fundamental periods of the upper package), while
- in case of deep, relatively soft, upper layers the variation of spectral content is strong and random, being apparently influenced to a major extent by the features of source mechanisms (in those cases, the fundamental periods of upper packages are long, of several seconds, while dynamic amplification appears to occur alternatively for some higher natural frequencies of the geological package);
- the comparison of variation of spectral contents at different stations in cases where the influence of local conditions appears to be surpassed by that of focal mechanisms (e.g.: Bucharest-INCERC vs. Focşani or Râmnicul Sărat) shows that the directionality of radiation is highly different for different frequency bands; this means that in-depth analysis of attenuation requires an approach to jointly consider directionality and various spectral bands;
- the use of the system of parameters and functions defined in [11] in order to characterize the features of ground motion appears to be efficient and consistent.

6. Final remarks

The developments presented in the paper are based on methodological approaches which proved to be satisfactory throughout a period of sustained research activity.

The outcome of analyses put to evidence the need of research directed towards several main topics:

- more detailed representation of hazard at source, with reconciliation of knowledge on various categories of source mechanisms and of probabilistic approach to hazard (desirable outcome: pluri-dimensional hazard representation, considering also some other relevant parameters besides magnitude);
- more detailed statistical attenuation analysis, combining the consideration of radiation directionality and of spectral content of ground motion;
- gathering of more detailed data concerning the local conditions, in order to conduct analyses of correlation with the features of ground motion;
- additional diversification of parametric hazard analyses, considering a wider spectrum of basic assumptions.

7. Appendix: Some data and considerations on the seismic conditions of Dobrogea

The territory of Dobrogea is affected to a lesser extent by earthquakes originating in $\{VSZ\}$. Yet, its southern part may be affected seriously by earthquakes originating in the Shabla – Caliacra seismogenic zone. Following data and considerations are based on the outcome of some hazard analyses related to the effects of the $\{VSZ\}$ activity, to instrumental data at hand (out of which some most relevant ones were presented in Figure 2) and on some data related to the Shabla – Caliacra earthquakes.

The outcome of probabilistic hazard analyses performed for several localities potentially affected by Vrancea earthquakes led [4] to the results summarized in Table 2.

Table 2. Intensities with various return periods due to Vrancea earthquakes, determined for some localities of Romania

Return periods (years)	Localities		
	Buzău, Câmpina, Focşani, Oneşti, Ploieşti, Văleni	Bucharest, Vaslui	Constanța
50	8.4…8.6	7.9…8.0	6.4
100	8.9…9.1	8.3…8.4	6.8…6.9
200	9.1…9.4	8.6…8.7	7.1…7.2
300	9.3…9.5	8.8…8.9	7.3…7.4
500	9.5…9.7	9.0…9.1	7.6

These values correspond to the assumption that a limiting magnitude for the $\{VSZ\}$ is M_{GR} =7.8 and that there is a tendency of dominant radiation direction NE-SW for the $\{VSZ\}$ events (for more details, see [4]) The data of this table make it possible to compare seismic hazard and show that Constanța is affected to a considerably lesser extent than localities referred to in the previous two columns. This is in agreement with the zonation maps given in [14].

As mentioned before, the instrumental information on strong motion in Constanța is limited.

There has been obtained in Constanța just one record, on 1990.05.30. The response spectra, in log-log representation, are given for the three directions of motion in Figure 3.

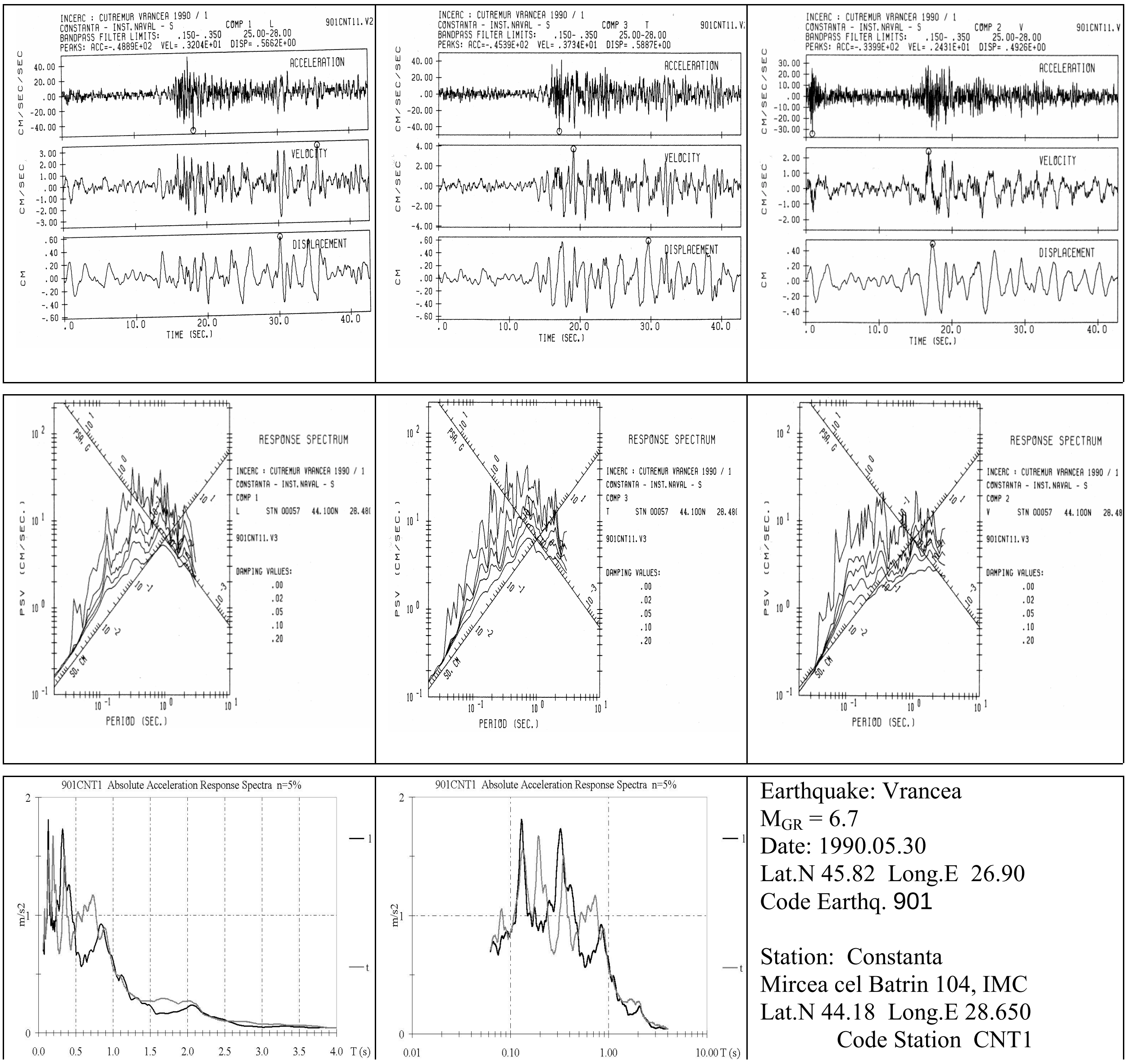

Fig. 3. Accelerographic record in Constanta, on 1990.05.30 and spectra derived

It may be remarked that there exist some similarities with the spectra determined for Baia – Dobrogea and for Cernavodă, even if dominant periods are not as evident. The main spectral accelerations for the horizontal directions correspond to periods around 0.3 s. Spectral ordinates of absolute acceleration for periods in the range of 1.0 s or more are quite low. In case one uses concepts like those developed in [11] and used in [9] and [4], it turns out that the spectrum based intensity I_S was of about 5.5, while the highest (averaged) frequency dependent intensities were of almost 6.0 in the interval (1.0 Hz, 4.0 Hz).

Coming now to the effects of the Shabla – Caliacra seismogenic zone, the major earthquake of 1901.03.31 (M_{GR} = 7.2, geographical coordinates 43.4°N and 28.7° E, depth 14 km) must be mentioned. Taking into account the attenuation law used for hazard analyses, it turns out that the *MSK* or *EMS* intensities should have been in the range of VIII in Mangalia and VII in Constanța. Such intensities exceed, of course, the provisions of the code in force [14] and raise the question of revision of the zonation map. It is not easy to take a justified decision in this connection, since this maximum observed event does not correspond to a history of frequently occurring strong earthquakes. On the contrary, catalogues at hand mention a cluster of earthquakes in 1901 (the second to the previously mentioned one having had a magnitude of 6.0) and just a moderate earthquake of magnitude 4.5 in 1904. This information does not justify the use of a Poissonian recurrence model and of the concept of return period, so revision of zonation in southern Dobrogea is bound to be based rather on expert judgement.

8. References

[1] Athanasiu I. *Cutremurele de pământ din România*, 1961. Editura Academiei, Bucharest.

[2] Bălan, Şt., Cristescu, V., Cornea I. (editors): *Cutremurul de pământ din România de la 4 martie 1977*, 1982. Editura Academiei, Bucharest.

[3] Blake A. *On the estimation o focal depth from macroseismic data*, 1941. Bull. SSA, Vol. 31.

[4] Borcia I.S., Sandi H., Stancu O.: *Condițiile seismice din zonele A şi B definite de normativul P.100-92. Constatări pe marginea datelor instrumentale şi analize de hazard seismic*, 2000. Gazeta AICR No. 43-44.

[5] Godefroy P., Levret A. : *Nature et définition de l'aléa sismique.* In Génie parasismique (ed.: V. Davidovici), 1985. Presse de l'Ecole Nationale des Ponts et des Chaussées.

[6] Marcellini A. *Probabilistic hazard evaluation in terms of response spectra*, 1995. Proc. Turkish National Conf. on Earthquake Engineering, Istanbul.

[7] Radu C., Rădulescu D., Sandi H.: *Some data and considerations on recent earthquakes of Romania*, 1990. Cahier Technique No. 3, AFPS, 1990.

[8] Sandi H. *Use of instrumental data for evaluation of ground motion and for specification of seismic conditions*, 1992. Proc. International Symp. on Earthquake Disaster Prevention. CENAPRED – JICA, Mexico City.

[9] Sandi, H.., Borcia, I.S.: *Instrumental data versus prospects of microzonation in Bucharest*, 2000. Proc. 3rd Japan-Turkey on Earthquake Engineering, Istanbul.

[10] Sandi H., Floricel I.: *Analysis of attenuation for recent intermediate depth earthquakes of Romania,* 1995. Proc. 6-th International Conf. on Seismic Zonation, Nice.

[11] Sandi H., Floricel I.: *Some alternative instrumental measures of ground motion severityI* 1998. Proc. 11-th ECEE, Paris.

[12] Sandi H., Stancu O., Borcia, I.S.: *Some features of seismic conditions of Romania, as derived from instrumental data and from hazard analyses,* 2002. Paper no. 674, Proc. 12-th ECEE, London.

[13] Stancu M., Borcia I.S.: *Studies concerning the directionality of seismic action for Vrancea earthquakes,* 1999. Proc. International Workshop for Vrancea earthquakes, Kluwer, Dordrecht.

[14] MLPAT: *Normativ pentru proiectarea antiseismică a construcțiilor de locuințe, social-culturale, agrozootehnice şi industriale, P.100-92,* 1992. Buletinul Construcțiilor, No. 11.

Identification of Vibration Sources from a Turbogenerator Foundation

Doina ŞTEFAN[a]

[a]*Technical University "Gh.Asachi" Iassy, Iassy, Romania*

Rezumat: În timpul funcţionarii orice maşină produce zgomote şi vibraţii caracteristice. Spectrul de frecvenţă al semnalelor complexe astfel generate este specific fiecărei maşini în parte constituind „amprenta" maşinii. Analiza „amprentei" facilitează localizarea surselor de vibraţie iar observarea evoluţiei ei permite aprecierea stării mecanice a maşinii. Pentru identificarea surselor de zgomot şi vibraţii se face o corelare a frecvenţelor corespunzătoare maximelor din spectrele măsurate experimental cu parametrii funcţionali şi constructivi ai maşinii.

Prin urmărirea variaţiei în timp a spectrelor de frecvenţă se poate constata creşterea amplitudinilor anumitor componente şi prin corelarea cu parametrii de lucru ai maşinii se pot detecta uzuri, fisurări, slăbiri sau modificări locale.

Ansamblul turbogeneratorului electric pentru care s-a urmărit identificarea acţiunii este amplasat în cadrul centralei termice a unei întreprinderi şi a fost pus în funcţiune în anul 1970.

Abstract: During the working, any device yields specific noise and vibrations. The complex signal frequency spectrum thus generated is specific to every device, constituting the "stamp" of the engine. The "stamp" analysis allows the localisation of the vibration sources and its evolution enable the estimation of the mechanical state of the engine.

In order to identify the noise and the vibration sources, a correlation of the frequencies corresponding to the maximum experimentally measured spectre with the function and constructive parameters of the machine is made.

Following the time variation of the frequency spectra one can state ascertain the amplitude increase of some components and by correlating with service parameters of the device, one can detect wear cracks weakening or local modification.

The electric turbo-generator ensemble for which it was monitored the action identification is located in the thermal power of an enterprise and has been putting function before 1970.

Keywords: vibration, dynamic identification, frequency.

1. Introduction:

Any device produces characteristic noise and vibration during functioning. The frequency spectrum of the generated complex signals is specific to each machine and mark it's "stamp". The analysis of this "stamp" facilitate the localization of the vibration sources and the observation of it's evolution permits the technical state identification of the machine.

Applying "stamp" analysis methods permits to pass from one simple identification of some defects to predict appearance and evolution of them.

By watching time variation of frequency spectrums it can be seen the growing of some components and by associating with machine working parameters it can be detected wears, weaknesses or local modifications.

2. Experimental testing

The measurements have been done in a lot places situated on the foundation floor and also on the turbo generator ensemble casings.

The measurements have been done in three directions:

V – vertical

ISSN-12223-7221

L – horizontal, longitudinal to the machine primary axis

O – horizontal, crossing the machine primary axis

The turbine ensemble dynamic characteristics in the repose state have been determinate by applying a shock using a hammer.

The plan view with the generator and turbine position are represented in figure 1.

Figure 2 and 3 represents the Fourier spectrums obtained in the points 1 and 3, when the shock had been applied nearing the point 2.

Figure 4 and 5 represents the Fourier spectrums obtained in the points 1 and 3 when the shock had been applied on the opposite extremity of point 1.

The resulted frequencies have the following values:

- 10 - 12 Hz
- 40 - 42 Hz
- 52 Hz

With the machine running, at normal turn, on the foundation floor it have been obtained the following Fourier spectrums:

All this spectrums indicated the normal frequency when then machine is working at 50 Hz.

In point 2 on the V axis have been obtained values around 40-42 Hz, that can be correspond to cantilever floor vibration.

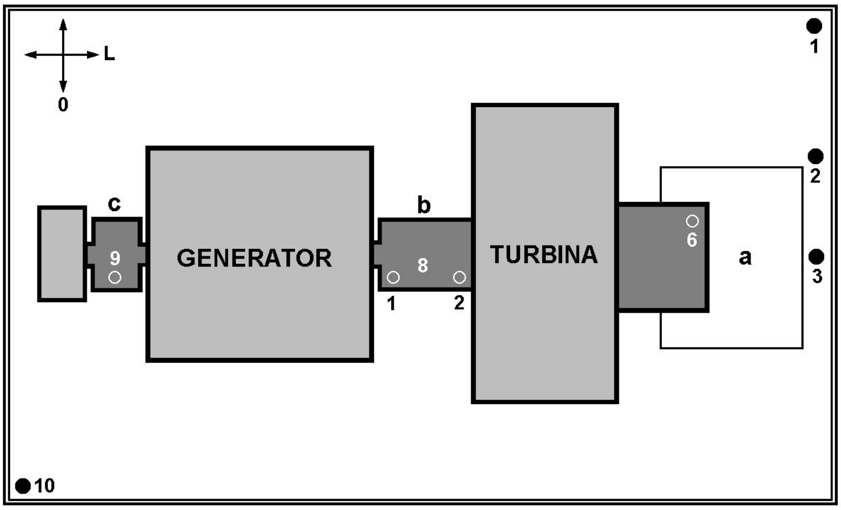

Fig.1 Plan view. Turbine emplacement

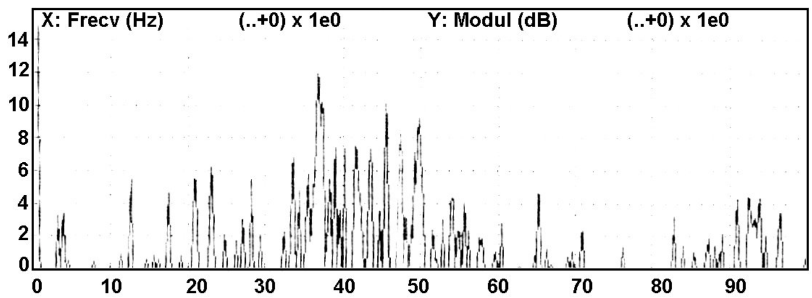

Fig.2 The Fourier spectrum obtained in the point 1 of the O axis.

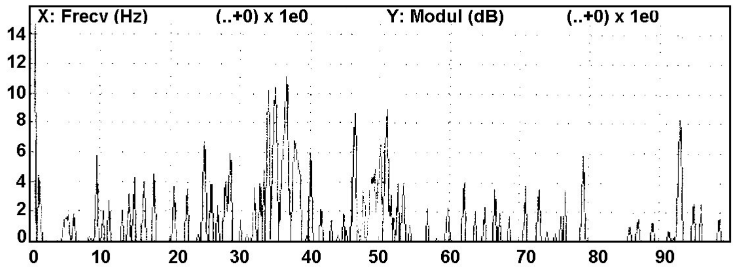

Fig.3 The Fourier spectrum obtained in the point 3 of the O axis

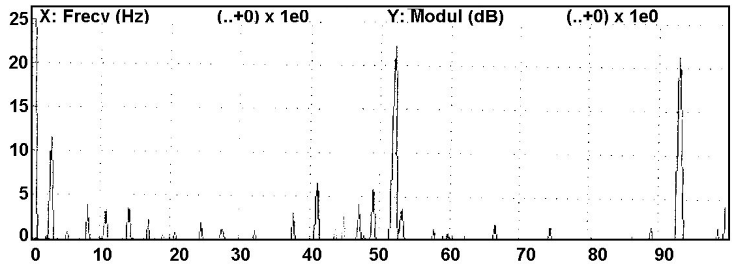

Fig.4 The Fourier spectrum obtained in the point 1 of the O axis

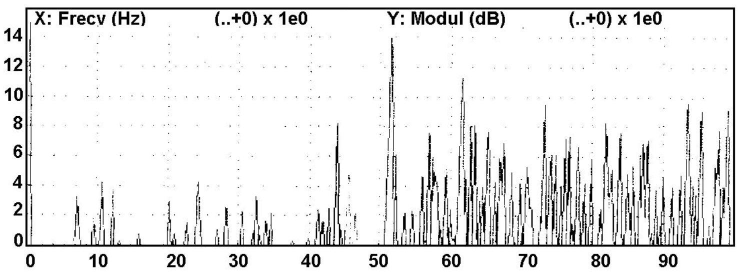

Fig.5 The Fourier spectrum obtained in the point 3 of the O axis

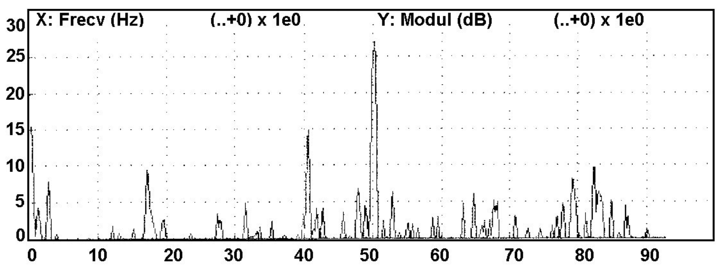

Fig.6 The Fourier spectrum obtained in the point 2 of the V axis.

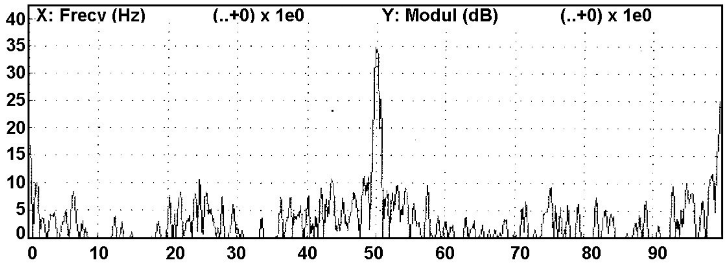

Fig.7 The Fourier spectrum obtained in the point 10 of the L axis

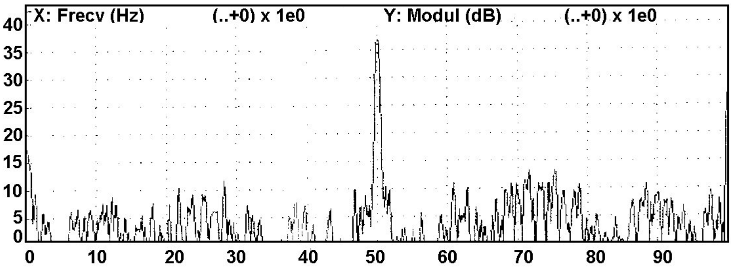

Fig.8 The Fourier spectrum obtained in the point 10 of the V axis.

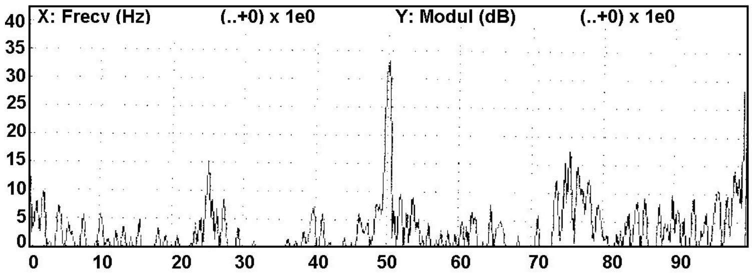

Fig.9 The Fourier spectrum obtained in the point 10 of the O axis

Nearest point 10, where the vibrations have less intensity it can be seen that the perturbations correspond especially to the 50Hz frequency because of the machine running state.

On the machine bearing, during running state have been obtained the following Fourier spectrums:

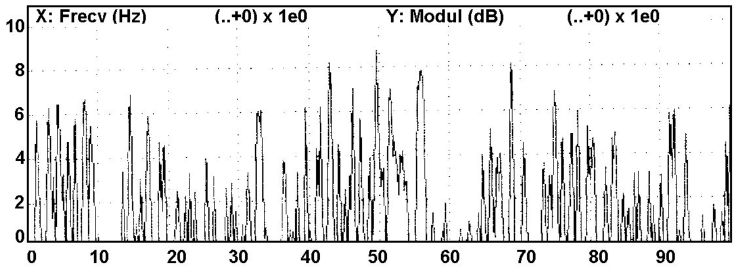

Fig.10 The Fourier spectrum obtained in the point 6 of the O axis.

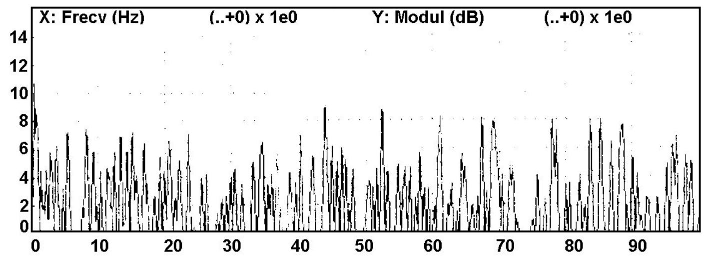

Fig.11 The Fourier spectrum obtained in the point 6 of the L axis

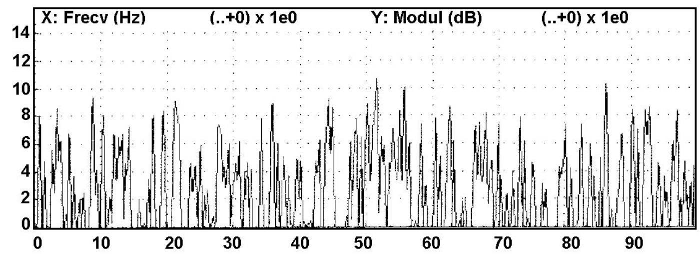

Fig.12 The Fourier spectrum obtained in the point 6 of the V axis

From the analysis of the bearing "a" spectrums (point 6) we are able to see the existence of a white noise type powerful perturbation, which can be considerate, the primary perturbation source. This is confirmed by the appearance in bearing "b" (point 8) and bearing "c" (point 9) of the machine normal frequency.

Analyzing these spectrums on the longitudinal axis from bearing "b" it can be observe the existence of some similitude components of white noise which are transmitted from the perturbation central zone – the bearing "a" placed previous the turbine.

The effective values of the speed and acceleration in the three bearing zones of the machine demonstrate the observations made on the Fourier spectrum, table 3.

Table no. 3

Measure point {PRIVATE}	Speed mm/s			Acceleration m/s^2		
	V	**O**	**L**	**V**	**O**	**L**
6	24.0	7.0	4.2	10.5	6.0	15.0
8-2	-	4.8	-	-	3.2	-
8-1	4.5	5.8	1.7	2.8	3.2	5.2
9	2.0	2.5	1.4	2.4	1.2	2.0

3. Conclusions

Finally, it had been identificated the perturbation source as being placed in the bearing "a" which is situated previous the turbine, around measure point 6 where the acceleration are being bigger than the gravitational ones.

The accelerations in the others bearings of the machine are lower, signify that they are transmitted from the source, and it's also demonstrate the white noise characteristic of the spectrum from the longitudinal axis around bearing “a” and “b”.

The Fourier spectrum around bearing “a” with a white noise characteristic is explain by the existence of some moving gearing in advanced state of wear and with a oiling defect system.

The foundation itself is not affected by the resonance phenomenon because the first proper frequencies of 10-12 Hz are much below 50Hz (normal machine frequency) and cannot be excited with sufficient intensity. The next proper frequencies above 50Hz are situated after the normal machine frequency, the amplification factor being

The 40-42 Hz frequencies corresponding to the vertical vibrations of the cantilever floor are below the normal machine frequency, the moving amplitudes being direct proportional with the perturbation intensity force.

References:

[1] Bertalanfly L.V. - *"Theorie generale des systemes"* Ed. Dunod, Paris, 1973

[2] Buzdugan Gh., Radeş M. - *"Măsurarea vibrațiilor"* Ed. Academiei RSR ,1979

[3]. Buzdugan Gh., Radeş M. - *"Vibrații mecanice"* Ed. Didactică şi pedagogică Bucureşti, 1982

[4] Buzdugan Gh. – *“Asupra metodelor de calcul pentru determinarea frecvențelor şi amplitudinilor fundațiilor de maşini”*, Buletin Inst. Pol. Bucureşti, 1957

[5] Eykhoff Peter - *"Identificarea sistemelor"* (traducere din limba engleza) Ed. Tehnică Bucureşti, 1977

[6] Goyder H.G.D. - *"Methods and aplication of structural modelling from measured structural frequency response data "*, 1980

[7] Harris C.M., Crede Ch.E. - *"Şocuri şi vibrații"* Ed. Tehnică, Bucureşti , 1988

[8] Doina Ştefan – “*Elemente de dinamică şi identificarea dinamică a structurilor de construcții”,* Editura Vesper, 2001

[9] Doina Ştefan, Ciongradi I. *“Aplicații ale identificării dinamice la structuri şi echipamente”,* Revista Construcțiilor, nr.4/1997

About the Causes of Wrench Out of the Compensator of a Large Diameter Air Pipe

Ovidiu ALEXANDRESCU[a] Ion TOMA[b]

[a]*Technical University "Gh. Asachi" Iassy, Iassy, Romania*
[b]*R.A.J.A.C. Iassy,Romania*

Rezumat: Lucrarea prezintă rezultatele studiului prilejuit de smulgerea din compensator şi deplasarea axială a unei conducte de aer de mare diametru, dintr-o stație de epurare a apelor uzate, eveniment produs după mai mulți ani de funcționare normală. Utilitatea acestora este cu atât mai importantă, cu cât personalul tehnic al stației considera - datorită temperaturii relativ ridicate a aerului transportat - că incidentul s-a datorat unor variații mari de temperatură, apreciere care s-a dovedit a fi falsă.

Abstract: This article presents the results of a study, which has been triggered by a technological incident: the wrench out of the compensator and its axial shifting of a large diameter air pipe in a wastewater treatment plant, event that occurred after many years of normal operating. The study is also very valuable because all plant's personnel was believed that the accident has been caused by the relatively high temperature of transported air in the pipe and hence by large temperature variations. Subsequently these theories have been proven to be false.

Keywords: Air pipe, axial shifting, compensator.

1. Background

The behavior in time of fluid pipes is determined by numerous quantifiable factors took into account by corresponding values of a quasi-normal operating in specific conditions of locations.

During operation may occur situations which, due to unusual combinations of factors, lead to serious loss of balance which impacts on the structures' stability and eventually leads to serious or less serious incidents. Assessing such events and identifying their causes bring useful information, which can optimize models, and criteria used in design process, and, furthermore, may lead to enhancing of safety and efficiency of respective systems.

This article shows the results of such a study, which has been triggered by a technological incident: the wrench out of the compensator and its axial shifting of a large diameter air pipe in a wastewater treatment plant, event that occurred after many years of normal operating. The study is also very valuable because all plant's personnel was believed that the accident has been caused by the relatively high temperature of transported air in the pipe and hence by large temperature variations. Subsequently these theories have been proven to be false.

The most probable causes have been identified through a *study of the structure's mechanical behavior*, under the complex stresses that impacted it *at the existing conditions of the accident* and considering also *the way of how these have evaluated*. The proof of veridicality of identified causes is made by the fact that, in the system's evolution, all corresponding circumstances have occurred only in the moment when the incident took place.

2. Fundamental data

The *physical and mechanical characteristics* of the air pipe are provided by: the topographic measurements and the current pipe route, constructive details of materials, $d_e \times s$, the compensators' features, flanges and bolts, the mounting temperature (t_m=15^{o}C) and certain specific

ISSN-12223-7221

properties of the fixings which support the pipe, are in Fig. 1 shown.

The *operating* conditions are represented by:

-The *parameters of operational ratings for the air plant*: flow: Q = 9.500…21.000 Nm^3/h per blower; 1…3 active blowers; pressure: p = 0,6 … 0,8 bar; fluid's operating temperature: t = 50 … 70^oC; maximal variation of pipe's temperature: Δt < 100^oC.

-The *climatic features of geographical area*: minimal recorded temperature –30,6^oC; maximal recorded temperature: +40,0^oC; annual average number of snowy days: 134 d/yr; average thickness of snow layer: 310 mm - in December and January ; main winds blowing on North-West direction (22,8 %) and on East direction (14,5 %); NW wind monthly average velocity: 4,9 ÷ 6,7 m/s; 1/10 frequency maximal wind velocity: 27 m/s;

Circumstances in which the incident occurred: last week of year 2001; frosty weather and sleet; plant operating on auto mode, by night.

3. Incident description

Incident consisted of a detachment of the air pipe from the C2 compensator which is located in the aeration tank area (Fig. 1 - *section 18*) and the shifting of the upstream pipe sector on 60 cm distance, with a subsequent deformation of the perpendicular pipe sector (*12 – 14*).

After replacing the pipe on position, with hydraulic jacks, the coupling with the compensator has been re-mounted with o-shaped seals. Stability of the pipe sector has been provided by blocking the axial motion with a metallic shaft supported against the secondary clarifier's structure present nearby the pipe, section *14*.

According to personnel's' statements the phenomenon started with air leaks on the compensator's o-shaped seal. These leaks slowly developed, while pipe sector *12-14* was getting deformed and while pipe sector *18-14* was axially shifting. The acute phase (detachment from compensator and shifting) occurred by night when the blower plant was on auto mode. The air leaks being heavier and heavier, the air flow need growed on till the second blower automatically has been started up by the system. The two blowers, parallel operating, led to a serious rise of air pressure which eventually triggered the start up of the third blower. All these conditions led to the acute phase above described.

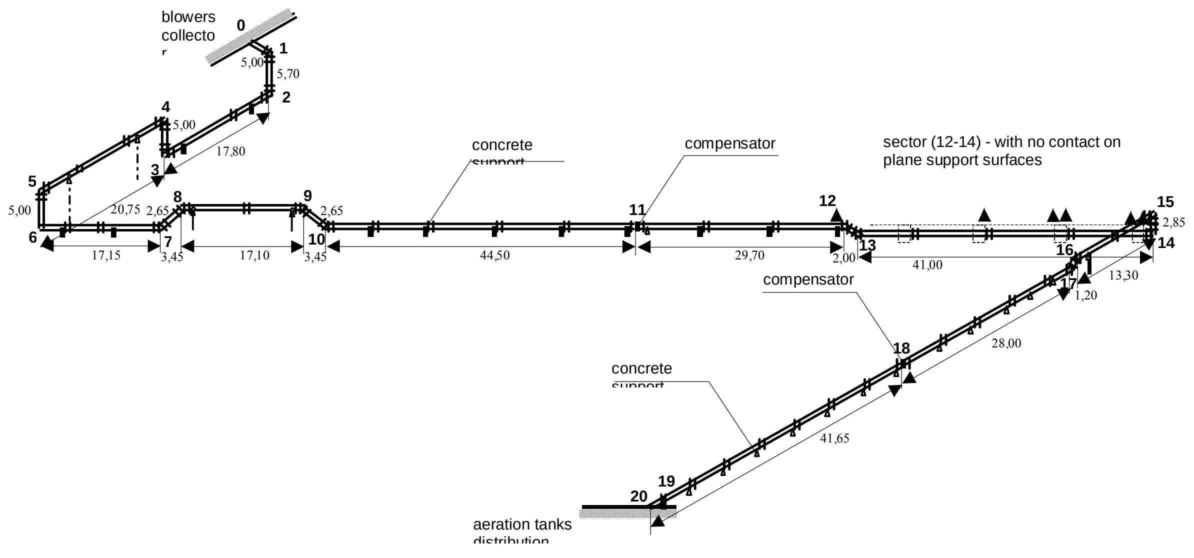

Fig. 1 Isometrical diagram of air main Dn 1200 mm

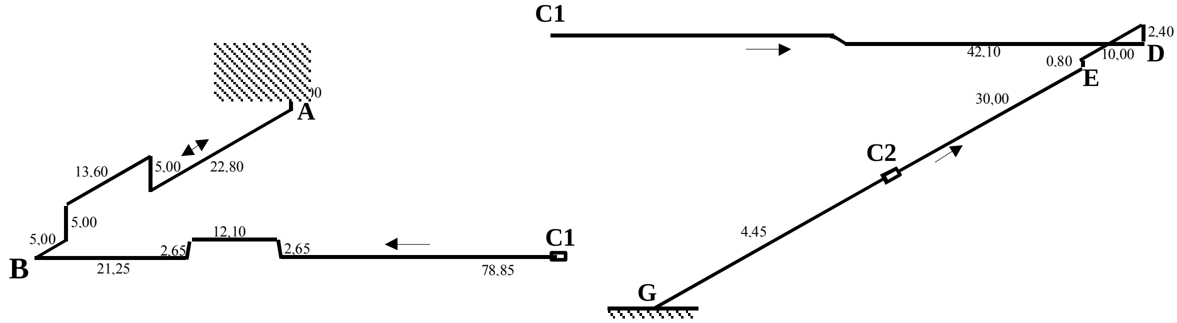

Fig. 2 Diagram of study relevant pipe sectors

4. Assumptions and work methods

Given the extent of pipe's shifting (~ 60 cm) and the circumstances of the event (frost, sleet, snow) this cannot be directly declared to be caused by temperature variation because, even at Δt = 100^{o}C, the main's length variation (on the aeration tank) would never exceed ΔL = 10 cm.

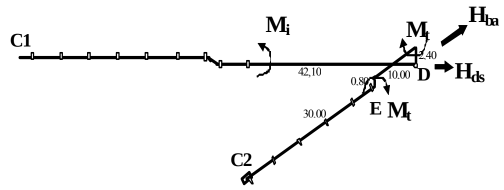

Fig. 3. Stresses that might induce axial shifting of air main's C2-D sector

The phenomenon can only be explained as a result of action of axial stresses, in the conditions when axial shifting of rectilinear pipes is not impeded by any stopping device but only by the friction of the main against its supports (on axial direction) and by the resisting torque developed (on the supports of perpendicular pipe sectors) by the pipes' own weights (Fig. 4).

So that the phenomenon to be explained it has to be stated that, because the presence of the two compensators, the air pipe in question can be illustrated in terms of mechanical behavior as it is shown in Fig. 2.

Therefore the next items can be identified:

- three pipe sectors that operate quasi-independently such as three beams (having annular sections) and having different spatial shapes and different connecting points: ABC1, C1DC2 and C2G;
- three pipe sectors relevant for the calculation of length variation induced by temperature variation : AB, BD and DG.

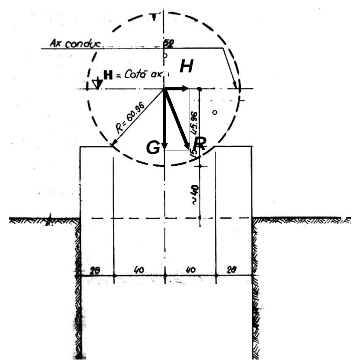

Fig. 4. Transverse forces on supports

Considering the air main configuration, the axial forces occurring in bends are balancing themselves two by two, their result being null on each of the system's pipe sectors.

Presence of compensators C1 and C2 may lead to axial unbalanced forces that might induce shifting of rectilinear pipe sectors; this may occur in (Fig. 1 and Fig. 2):

- bend *6* (pipe sector *B*, Fig. 2), action towards the exterior, on direction *11-6*;
- bend *14* (pipe sector *D*, Fig. 2), action towards the exterior, on direction *11-14*;

- bend *15* – force transferred through the adjacent vertical pipe sector *14,* on which acts towards the exterior, on direction *18-14;*

When system is operated balance of axial horizontal forces is provided by (Fig. 3 and Fig. 4):

- friction force between pipe and pipe sector's supports on which direction it occurs ;

- horizontal reactions in supports of the perpendicular pipe sector, on which it acts ;
- resilience of consoled pipe sectors, between the applying point and first active support.

The consoled pipe sector (12-14), which limits axial shifting of sector 18-14, will be deformed by bending stresses, according to its length and its resilience modulus of the pipe's transverse section, depending on the force that act upon the free end. This deformation of the consoled sector will allow an axial shifting of the perpendicular pipe sector, which will be equal to the arrow of the free end (*f*).

Considering the items above the study of the main's mechanical stability included the following:

- calculation of main loads that act upon studied system: weight forces (*G*), pressure forces (*P*), hydrodynamic forces in bends (*Fx*) and friction forces in supports (*Qf*);
- calculation of axial horizontal forces in unbalanced bends;
- calculation of vertical and horizontal forces that occur in supports;
- checking the stability to rolling of the pipe, on its support;
- calculation of unitary efforts and calculation of sectors' deformation in console;
- assessing axial shifting of perpendicular pipe sector;
- checking distance between supports;
- calculation of maximal variation of rectilinear sectors' lengths when temperature vary during operation;
- establishing the number of compensators needed to prevent the main's loss of tightness and their type.

Calculations have been made for each pipe sector separately considering the specific features of supports and the actual position of the pipe compared to these. It has to be stressed that the study accorded special interest to deteriorated sector C1DC2, but also checking the existing situation on sector ABC1.

- on pipe sector ABC1 the air main is stayed on supports made of low grade reinforced concrete that is roller-supports mounted on poles, in high areas where walkways are over-crossed.
- on pipe sector C1DC2, the air main is supported as it follows:

. on low grade concrete supports between sectors *11* and *12* (Fig. 1);

. on metallic surfaces that cover manholes of the secondary clarifier between sectors *13* and *14*;

. on the metallic supports of the aeration tank's trestle bridge.

The console sector which is the weak link that impacts on the system's stability is located in the pipe sector stayed on the metallic manholes of the clarifier, area in which some 30 m of pipe is literally suspended (with no contact with supports).

Study has been developed on *MathCAD* software, with classic methods of the field.

5. Results interpretation

The even distributed load of main's weight during operating period (kN/m) corresponds to the pipe's diameter and to its wall thickness, respectively to the air density (kg/m^3), depending on pressure:

air density	1,0	1,1	1,2	1,3	1,4
air weight	0,011	0,012	0,013	0,014	0,015
Pipe weight	3,059	3,060	3,061	3,062	3,063

In calculation the average value is adopted*:* Gc = 3,061 kN/m;

Weight of a flanged coupling: Gf = 2,326 kN/piece;

Pressure force in bend (A = 1,128 m^2) varies depending on air pressure in main, between P = 56,379 kN, at p = 0,5 bar and P = 90,207 kN, at p = 0,8 bar:

air pressure p (bar)	0,5	0,6	0,7	0,8
pressure force P (kN)	56,379	67,655	78,931	90,207

Hydro dynamical force in the 90^o bend varies very little compared to air density and flow in the main, depending, as the pressure force does, on the operating pressure:

air flow (m^3/s)	Pressure (bar)		
	0,6	0,7	0,8
5	67,686	78,962	90,238
10	67,779	79,055	90,331
15	67,934	79,210	90,486
20	68,152	79,427	90,703

For an air density ρ_{aer} = 1,4 kg/m^3, when an average 10 m^3/s flow is transported, hydrodynamic force takes values between Fx = 67,779 kN, at p = 0,6 bar and Fx = 90,331 kN, at p = 0,8 bar:

Friction forces on supports correspond to the total weight of the studied pipe (length and number of flanged couplings) and to the friction factor between pipes and supports. For friction factors having values μ = 0,1…0,4 the friction force that impedes the axial shifting takes different values from a sector to another as it follows below:

μ	sector **14- 18** L=45,35 m; n_{fl}=11; n_r=5		sector **11- 14** L=72,70 m; n_{fl}=10; n_r=5		sector **1- 11** L=139,9 m; n_{fl}=30; n_r=14	
	Q_f	F_r	Q_f	F_r	Q_f	F_r
0,1	16,44	3,288	24,58	4,916	49,80	3,557
0,2	32,88	6,576	49,16	9,832	99,60	7,114
0,3	49,32	9,864	73,74	14,748	149,40	10,672
0,4	65,76	13,152	98,32	19,663	199,21	14,229

Horizontal axial forces in vertical bends 14 and 6.

Axial forces that act upon bends (kN) correspond to the action's direction and is sensibly depending of friction factor between mains and supports. Assuming the values: ρ_{air}=1,4 kg/m^3, Q=10 m^3/s, α = 90^o and μ = 0,1…0,4 , axial forces in bends *14* and *6* take the values shown in the table below:

μ	***18-14:*** L=86,35 m; n_{fl}=11; n_r=5			***11- 14:*** L=118,05 m; n_{fl}=10; n_r=5			***11- 6:*** L=139,9 m; n_{fl}=30; n_r=14		
	p (bar)			p (bar)			p (bar)		
	0,6	0,7	0,8	0,6	0,7	0,8	0,6	0,7	0,8
0,1	39	51	61	29	41	52	18	29	41
0,2	10	22	32	-	2	13	-	-	-
0,3	-	-	-	-	-	-	-	-	-

When monitoring the variation of the active axial force in bends, which depends on the air pressure within the pipe, for different values of the friction factor, we may observe the following:

- in case of bend *6*, when friction factor drops down to μ = 0,2 , the force will have values which will not exceed 10...15 kN, even if air pressure boosts to 0,9...1 bar; in the exceptional situation when friction factor drops down to μ = 0,15, the values are not exceeded at air pressures of 0,7 ... 0,8 bar;
- in case of bend *14*, active axial force will take values sensibly superior compared to those above soon as μ < 0,25 (on direction *11-14*) and even if μ = 0,30 (on direction *18-14*), and this at lower pressures within the main (0,65...0,85 bar, on direction *11-14*, respectively 0,5...0,8 bar, on direction *18-14*).

Vertical force on supports corresponds to the quasi-even distribution of the total weight of the free shifting sector, on the n_r supports that exist on its route:

$$V(L,n_f,n_r)=\frac{L\cdot G_c+n_f\cdot G_f}{n_r}$$

pipe sector	length L (m)	flange silver n_f	support no. n_r	vertical force on support $V(L,n_f,n_r)$ (kN)
1-11	139,90	30	14	35,6
11-18	118,50	21	11	37,40

Horizontal axis-normal force, in supports

Generated by the active axial force applied by the perpendicular sector, the horizontal force that acts upon supports, in a direction normal to axis, results from:

$$H(p,\mu,L,n_f,n_r)=\frac{F_{a1}(p,\mu,L,n_f)}{n_r}$$

μ	***11-13:*** L=86,35 m; n_f=11; n_r=4			***15-18:*** L=118,05 m; n_f=10; n_r=5			***2-5:*** L=139,90 m; n_f=30; n_r=4		
	p (bar)			p (bar)			p (bar)		
	0,6	0,7	0,8	0,6	0,7	0,8	0,6	0,7	0,8
0,1	9,7	12	15	5,8	8,1	10	4,5	7,3	10
0,2	2,4	5,2	8,1	-	0,4	2,7	-	-	-
0,3	-	-	0,8	-	-	-	-	-	-

Pipe roll-over stability on supports is provided by over-unitary values for the safety coefficient:

$$c(p,\mu,L,n_f,n_r)=\frac{V\cdot a}{H(p,\mu,L,n_f,n_r)\cdot b}$$

μ	***11-13:*** L=86,35 m; n_f=11; n_r=4 V = 35,57 a=0,4; b=0,46			***15-18:*** L=118,05 m; n_f=10; n_r=5 V=37,42; a=0,9; b =1,24			***2-5:*** L=139,90 m; n_f=30; n_r=4 V=35,57; a=0,4; b= 0,46		
	p (bar)			p (bar)			p (bar)		
	0,6	0,7	0,8	0,6	0,7	0,8	0,6	0,7	0,8
0,1	3,2	2,5	2,0	4,7	3,4	2,6	6,9	4,3	3,1
0,2	13	5,9	3,8	-	68	10	-	-	-
0,3	-	-	38	-	-	-	-	-	-

Bend stresses on sector 12–14

In the existing situation, when the pipe sector between sector 12 and bend 14 do not have any support area, this pipe operates such as an annular beam having diameters D_e, D_i and length L, being embedded at one end (12), and stressed at the other end by a concentrated force which corresponds to the active axial force (F_{a1}), applied to the perpendicular sector (18-14).

The inertia momentum and the resilience modulus of the annular section having d = Di/De = 0,983, being:

$$I_x = \pi \cdot \frac{D_e^4}{64}\left(1-d^4\right) = 7{,}177 \cdot 10^5 \ \text{cm}^4,$$

respectively:

$$W_x = \pi \cdot \frac{D_e^3}{32}\left(1-d^4\right) = 1{,}177 \cdot 10^4 \ \text{cm}^3,$$

corresponding to the axial load with which acts the perpendicular pipe sector (*18-14*), within the embedding (*12*), will generate a bending momentum:

$$M_i = 10^{-1} \cdot F_{a1} \cdot L \quad \text{(MN.cm)}$$

which will next generate an unitary effort:

$$\sigma_x = 10^2 \frac{M_i}{W_x} \qquad (\text{N/mm}^2),$$

maximal arrow (in *14*):

$$f = \frac{10^9 \cdot F_{a1} \cdot L^3}{3 \cdot E \cdot I_x} \qquad \text{(cm)}$$

and the angle of the deformed:

$$\varphi = \tan^1\left[\frac{10^7 \cdot F_{a1} \cdot L^2}{2 \cdot E \cdot I_x}\right] \qquad \text{(rad)}$$

If we accept an elastic modulus E=2,02.10^7 N/cm^2, for sector *12-14*, having a length L=43 m, the main characteristics of the bending stress occurring in section *12*, under the active axial forces in range from 0 to 60 kN, are shown below.

Variation of the arrow function of the axial active load in node *14* (Fig. 5), correlated with its dependence on air pressure and support friction factor, leads to the conclusion that when the axial shifting on direction *18-14* is not impeded, section 14 will sensibly shift as soon as the air pressure exceeds 0,8 bar, even in normal conditions of support friction.

F_{a1}	kN	0	10	20	30	40	50	60
M_{i12}	MN.cm	0	43	86	129	172	215	258
σ_{x12}	N/mm^2	0	36,5	73,0	110	146	183	219
f_{14}	cm	0	18,3	36,6	54,8	73,1	91,4	109
φ	Grd.	0	0,37	0,73	1,07	1,5	1,8	2,2

Subsequently the phenomenon occurs at lesser and lesser pressures even when the friction factor takes values below μ = 0,25.

Bend stresses on sector 17 – 14

The pipe sector comprised between section *17* and bend *14* also do not have any supporting point. Therefore this sector works such as a annular beam of diameters D_e, D_i and a length L, embedded at one end (*17*), and stressed at the other end by a concentrated active force corresponding to the active axial force (F_{a1}), applied by the perpendicular sector (*12-14*). The inertia momentum and the resilience modulus of the annular section having $d = D_i/D_e$ = 0,983, being the same as in the previous case (I_x=7.177.10^5 cm^5, respectively W_x=1,177.10^4 cm^3), corresponding to the axial load with which the perpendicular sector (*12-14*) acts, in the embedding (*17*) will occur a bending momentum (M_{i17}), which generates: the unitary effort σ_{x17} (N/mm^2), the maximal arrow - in *14* - f_{14} (cm) and the deformation angle φ_{17} (rad), which, accepting an elastic modulus E=2,02.10^7 N/cm^2 and a length for sector *17-14*, L=15 m, for active axial forces in the range of 0 to 60 kN, takes the values shown in the table below.

F_{a1}	kN	0	10	20	30	40	50	60
M_{i17}	MN.cm	0	15	30	45	60	75	90
σ_{x17}	N/mm^2	0	12,7	25,5	38,2	51,0	63,7	76,4
f_{14}	cm	0	0,8	1,6	2,3	3,10	3,9	4,7
φ_{17}	grd.	0	0	0,1	0,1	0,2	0,2	0,3

Variation of arrow under the active axial load in node *14* (Fig. 6), correlated to its dependence of the air pressure and the support friction factor leads to the conclusion that the axial shifting of section 14 on direction *12-14* will not reach intensities impossible to be undertaken by the compensation devices, even when air pressure exceeds 0,8...1 bar, and the friction factor in supports drops down to $\mu = 0{,}15$.

6. Conclusions

The phenomenon that occurred can be justified only as a result of action of some axial forces, taking into account that axial shifting of rectilinear pipe sectors is not impeded by any special blocking device, but only by the friction of the pipe on its supports (axially) and by the resistance torque generated by its own weight (in the supports of the perpendicular sectors) (see Fig. 3).

Presence of compensators C1 and C2 may lead to axial unbalanced forces that might induce shifting of rectilinear pipe sectors; this may occur in (Fig. 1 and 2):

- bend *6* (pipe sector *B*, Fig. 2), action towards the exterior, on direction *11-6*;
- bend *14* (pipe sector *D*, Fig. 2), action towards the exterior, on direction *11-14*;
- bend *15* – force transferred through the adjacent vertical pipe sector *14,* on which acts towards the exterior, on direction *18-14;*

When system is operated, balance of axial horizontal forces is provided by (Fig. 3 and 4) :

- friction force between pipe and pipe sector's supports on which direction it occurs ;
- horizontal reactions in supports of the perpendicular pipe sector, on which it acts;
- resilience of consoled pipe sectors, between the applying point and first active support which will bear deformation corresponding to their length and the resilience modulus of the pipe's transverse section, depending on the value of the axial force that acts on the free end.

Deformation occurring in the console pipe sector allows an axial shifting of the perpendicular sector, corresponding to the arrow in its free end (*f*).

Pressure force in bend (corresponds to transversal section area A=1,128 m^2), increases sensibly together with the air pressure in the main, from P = 56,379 kN, at p = 0,5 bar to P = 90,207 kN, at p = 0,8 bar:

Hydrodynamical force in the 90^o bend vary very little compared to air density and flow in the main, depending, as the pressure force does, on the operating pressure. For an air density ρ_{air} =1,4 kg/m^3, when an average 10 m^3/s flow is transported, hydrodynamic force takes values between Fx=67,779 kN, at p= 0,6 bar and Fx = 90,331 kN, at p = 0,8 bar:

Friction forces on supports correspond to the total weight of the studied pipe (length and number of flanged couplings) and to the friction factor between pipes and supports. Forces take different values from one sector to another decreasing 4 times as the factor decreases from μ = 0,4 to μ = 0,1. In normal conditions the friction force that opposes to the axial load takes values Q_f =65,76 kN - on sector 14- 18; Q_f =98,32 kN – on sector 11- 14 and Q_f =199,21 kN – on sector 1-11.

Horizontal axial forces in vertical bends 14 and 6:

Axial forces that act upon bends correspond to the action's direction and are sensibly depending of friction factor between mains and supports. Monitoring the variation of the active axial force in bends which depends on the air pressure within the pipe, for different values of the friction factor, we may observe the following:

- in case of bend 6, when friction factor drops down to μ = 0,2 , the force will have values which will not exceed 10...15 kN, even if air pressure boosts to 0,9...1 bar; in the exceptional situation when friction factor drops down to μ = 0,15, the values are not exceeded at air pressures of 0,7 ... 0,8 bar;
- in case of bend *14*, active axial force will take values sensibly superior compared to those above soon as μ < 0,25 (on direction *11-14*) and even if μ = 0,30 (on direction *18-14*), and this at lower pressures within the main (0,65...0,85 bar, on direction *11-14*, respectively 0,5...0,8 bar, on direction *18-14*).

Vertical force on supports corresponds to the quasi-even distribution of the total weight of the free shifting sector, on the n_r supports that exist on its route; it takes the values V = 35,572 KN on sector 1-11, respectively 37,415 KN on sector 11-18.

Horizontal axis-normal force, in supports: Generated by the active axial force applied by the perpendicular sector, the horizontal force that acts upon supports, in a direction normal to axis, and depends on the air pressure in the mains and their friction factor on supports. On relevant sectors for the study, considering the worst scenario (μ = 0,1), this force takes values which increase directly with the air pressure in the pipe: H=6,847...15,304 kN - on sector

11-14; H=3,584...10,349 kN - on sector 15-18; H=1,645...10,101 kN - on sector 2-5.

Stability to roll-over of main on supports, guaranteed even when the safety factor M_{rez}/M_{rast} is over-unitary seems to be ensured - at pressures of 0,5 ... 0,8 bar - even when the friction factor in supports drops down to μ=0,1. In these conditions, axial shifting of a main is allowed only by bending deformation of the perpendicular sector and will correspond to the arrow generated in their free end (*f*).

Bending stresses on sector 12–14, **which do not have any support point between section *12* and bend *14*,** therefore working as an annular beam with diameters D_e, D_i **and having a considerable length** - L=43 m, practically - embedded at one end (*12*) and stresses at the other end by the concentrated force applied by the perpendicular sector (*18-14*), features the characteristics σ_{x12} (N/mm^2), f_{14} (cm) and φ (^{o}) with values that grow proportionally with the active axial force in bend *14* - F_{a1} = 0 ... 60 kN. Variation of arrow f_{14} together with the active axial load F_{a1} (fig. 3), correlated with its dependence of the air pressure and the friction factor in supports lead to conclusion that, when axial shifting on direction *18-14* is not impeded, *section 14 will sensibly shift soon as the air pressure exceeds 0,8 bar, even in normal conditions of support friction*, the phenomenon becoming present even at lesser and lesser pressions when the friction factor drops down and even below μ = 0,25.

Bending stresses on sector 17-14: The pipe sector comprised between section *17* and bend elbow *14* also do not have any supporting point. Therefore this sector works such as a annular beam of diameters D_e, D_i and a length L, embedded at one end (*17*), and stressed at the other end by a concentrated active force corresponding to the active axial force (F_{a1}), applied by the perpendicular sector (*12-14*). The inertia momentum and the resilience modulus of the annular section having $d = D_i/D_e$ = 0,983, being the same as in the previous case (I_x=7.177.10^5 cm^5, respectively W_x=1,177.10^4 cm^3), corresponding to the axial load with which the perpendicular sector (*12-14*) acts, in the embedding (*17*) will occur a bending momentum (M_{i17}), which generates: the unitary effort σ_{x17} (N/mm^2), the maximal arrow - in *14* - f_{14} (cm) and the deformation angle φ_{17} (rad), which, accepting an elastic modulus E=2,02.10^7 N/cm^2 and a length for sector *17-14*, L=15 m, for active axial forces in the range of 0 to 60 kN, takes the values shown in the table below. Variation of arrow under the active axial load in node *14*, correlated to its dependence of the air pressure and the support friction factor leads to the conclusion that the axial shifting of section 14 on direction *12-14 will not reach intensities impossible to be undertaken by the compensation devices*, even when air pressure exceeds 0,8...1 bar, and the friction factor in supports drops down to μ = 0,15.

Admissible distance between supports is conditioned by:

- calculation distributed load, generated by the own operating pipe's weight, including the weight of flanges
- the resilience modulus of the annular main section
- the admissible tension for wind and weight generated loads of the material of which the main is made (for OLT35 K, σ = 145,8 N/mm^2 [1]), is respected in the case of the air main having D_e=121,9 cm, and D_i=119,83 cm, even on sector *12-14* - which is not supported on the plane supports existing nearby on the clarifier (L=*43+13*m, l_{ad}=61,39m$\Rightarrow L<l_{ad}$).

The necessary number of compensators matches the maximal temperature variation which occurs during operating (ΔT), the length of straight main on which they are mounted (L) and the compensation capacity stated by the supplier (ΔL), respectively the linear thermal dilatation factor for steel (α = 11.10^{-6} m/m.^{o}C).

Keeping the same number of compensators on the two long sectors of the air main it results that at a maximal temperature variation ΔT=*100* ^{o}C, the main must undertake a length variation of ΔL=95...120mm.

Bibliography

1./ A. Leca, I. Prisecaru, H. M. Tanase, L .Lupescu, C. Raica – *Conducte pentru agenti termici*, Ed.Tehnica, Bucuresti, 1986

2./ D. Mateescu, M. Ivan – *Conducte metalice circulare cu diametru mare*, Ed. Tehnica, Bucuresti, 1985.

Determination of Operational Parameters in a Pump Complex Water Supply System

Ovidiu ALEXANDRESCU [a] Ion TOMA [b]

[a]*Tehnical University "Gh. Asachi" Iassy , Iassy , România*
[b]*R.A.J.A.C. Iassy , România*

Rezumat: Articolul prezintă o metodologie de stabilire a caracteristicilor de sarcină corespunzătoare diferitelor configurații de exploatare ale unor aducțiuni complexe - pe care pompele aspiră, direct sau printr-un colector de aspirație, dintr-o conductă de aducțiune sub presiune ce transportă la stație, apa prelevată din mai multe rezervoare, şi refulează, în final, pe mai multe rezervoare -, respectiv a regimurilor de referință pentru alegerea pompelor, împreună cu rezultatele aplicării acesteia în cazul aducțiunii prin pompare Păcurari – Aurora / fir 2, din sistemul de alimentare cu apă a municipiului Iaşi.

Abstract: This work presents a methodology used for establishing the head characteristics in pump complex supply systems, respectively the reference ratings which are to be used for the pump choosing process, together with the results gained when this method has been implemented in the case of the Pacurari-Aurora stream 2 water supply (belonging to the Iasi City's water supply system).

Keywords: Complex supply systems, head characteristics, reference ratings for pump choosing process.

1. Background

Operational efficiency for a pumping supply system is strictly determined by the type of pump used. Best performances are obtained when, so that user's needs to be met, pumps are set to operate at ratings located in the neighborhood of their maximal efficiency which at its turn must have optimal values for the best machines located in the respective class. As to reach that goal the process of pump choice has to be based on a thorough acknowledge of all operating parameters of such supply, that is the relations between flow (Q) and specific hydraulic energy that has to be released towards this flow by the pumps (H), in all different possible operational configurations.

In case of machines that draw water directly from tanks, through the pump's suction pipe, data are relatively easy to gather, determining the classic *network parameters*, associated to different static loads, specific for each user's operational rating and approximating some reasonable head losses on each pump's suction and delivery mains.

When pumps are drawing (directly or through a suction collector) from a pressurized supply main that carry water to the station, or from a number of tanks, the delivery being done towards other several tanks, the issue becomes more complex. Hence, to provide the most realistic data in this situation means to determine the head parameter for the pressurized supply, corresponding to different operating configurations and then assessing the representative operational ratings for the pumps in discussion.

Further on will be described a methodology used for establishing such head characteristics in pump complex supply systems, respectively the reference ratings which are to be used for the pump choosing process, together with the results gained when this method has been implemented in the case of the Pacurari-Aurora stream 2 water supply (belonging to the Iasi City's water supply system).

2. Theoretic - fundamental concepts

Let us consider the general case of a pump supply system that carries water between two ore several tanks located at inferior level and two or several tanks located at superior level through a pressurized line composed of the *supply towards the*

ISSN-12223-7221

pumping station and *its delivery main*, which is equipped with *two or several pumps*.

So that things to be simplified, without weakening the generality of the study, we will consider a system composed of two tanks on each of its two characteristic levels, a supply, the delivery main and a pumping station provided with two identical pumps. (Fig. 1).

Tanks are featuring parameters such as: the *elevation of the free water surface level* (Z_{I1} , Z_{I2} – at inferior level, respectively Z_{S1} , Z_{S2} – at superior level) and the *supply connection hydraulic resistance modulus* which - within the study - can be considered *fully open* (M_{rI1}, M_{rI2}, respectively M_{rS1}, M_{rS2}) or *fully closed* ($M_{rij}=\infty$; $i\in\{I,S\}$, $j\in\{1,2\}$). Operational efficiency for the system is provided when, at a normal operational rating, the water level is the same in both tanks, at each of characteristic levels ($Z_{I1} = Z_{I2} = Z_I$ – variable between $Z_{I\,min} \dots Z_{I\,max}$, respectively $Z_{S1} = Z_{S2} = Z_S$ – also variable between $Z_{S\,min} \dots Z_{S\,max}$), and connections have practically the same hydraulic resistance ($M_{rI1} = M_{rI2} = M_{rI}$, respectively $M_{rS1} = M_{rS2} = M_{rS}$).

The *supply towards the pumping station* and the *delivery main* are characterized by their *hydraulic resistance module* corresponding to the situation when the system is operated with stream valves fully opened (M_{rA}, respectively M_{rR}).

The *connection between the supply towards the PS and its delivery main* is achieved at one time by the active pumps, respectively by the associated *suction and delivery communications*, canal-like systems which, each, are featuring hydraulic resistance module, respectively: M_{rs}, M_{rr}, and $M_{rp}= M_{rs} + M_{rr}$.

The *supply operational configuration* corresponds to the combinations of the components' condition (activated/disabled). At nominal capacity, in the studied situation, water drawn from both inferior tanks is pumped towards the two superior tanks, by operating two pumps within the PS. Depending on events that may occur during operation at each level can be active, at one time, only one tank, the PS being able to operate only one pump. Obviously to each situation will correspond a certain resulting hydraulic resistance modulus of the supply (M_{rijk}; $i\in\{1,2\}$, $j\in\{1,2\}$, $k\in\{1,2\}$ this being in fact the number of active tanks/connections at lowest level, at highest level and the number of active pumps within the PS. Hence, each element being able to operate on a *all or nothing* basis the considered supply may take the shape of 8 operational configurations, each being characterized by a corresponding hydraulic resistance modulus(Table1).

Tabel 1

Supply hydraulic resistance modulus

Operating configuration		Pacurari 2 PS	
		1 Pump	2 Pump
Tanks	2I & 2S	M_{r221}	M_{r222}
	2I &1S	M_{r211}	M_{r212}
	1I & 2S	M_{r121}	M_{r122}
	1I &1S	M_{r111}	M_{r112}

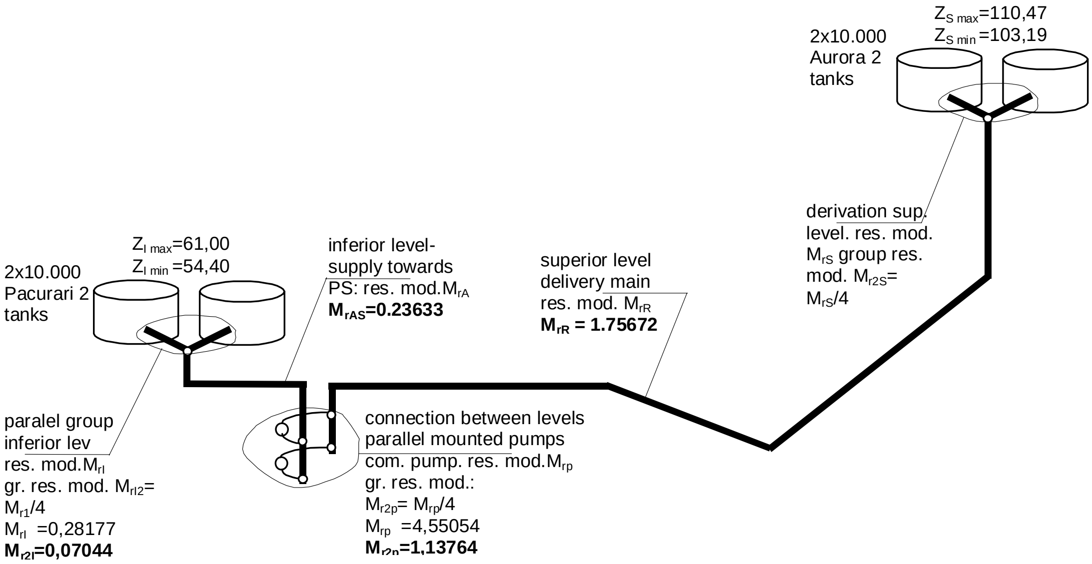

Reference parameters for pump choosing process (Q_P, H_P) must match the needs of the supply.

Within a rating for PS sizing process, the group made of the ν_p active pumps must carry the nominal supply's flow (Q_A), under a head corresponding to the static load:

$$H_o = H_g = Z_S - Z_I$$

and at the head losses incurred by its transportation through the mains in the normal operational configuration:

$h_{rA} = M_{r222} \cdot Q_A^2$,

so that each pump is set to provide (at an efficiency close to its maximal efficiency) the flow:

$Q_P = Q_A / \nu_p$,

providing on the pump's delivery a head:

$$H_P = H_o + M_{r222} \cdot Q_A^2 \qquad (1)$$

In each operational configuration (i,j,k), $(i,j,k) \in \{(1,1,1), (1,1,2), (1,2,1), (1,2,2), (2,1,1), (2,1,2), (2,2,1), (2,2,2)\}$, the specific hydraulic energy (H) which has to be delivered by the pumps (on their delivery pipe) to the flow carried in the supply (Q), will match the static load determined by the relative position of the water level at the two specific levels $H_o = H_g(Z_s, Z_I)$, and the associated supply hydraulic resistance modulus:

$$H(Q) = H_g(Z_S, Z_I) + M_{rijk} \cdot Q^2 \qquad (2)$$

To determine the load characteristics for this pump supply means to determine its hydraulic resistance moduli in different possible operational configurations. These can be calculated relatively easy if we consider that, hydraulically, the supply in its whole is made of three communication groups coupled in parallel/derivation:

– grouped tank connections, inferior level, with hydraulic resistance modulus M_{rgI} ;

– grouped tank connections, superior level, with hydraulic resistance modulus M_{rgS};

– grouped pumps communications, parallel coupled in the PS, with hydraulic resistance modulus M_{rgP},

serial connected through the supply towards the PS having the hydraulic resistance modulus (M_{rAS}) and its delivery pipe having hydraulic resistance modulus (M_{rR}):

$$M_{rijk} = M_{rgI} + M_{rAS} + M_{rgP} + M_{rR} + M_{rgS} \qquad (3)$$

The hydraulic resistance modulus of each communication (single streamed hydraulic system) is determined by its structure and by the geometrical and hydraulical features of the composing elements - lengths (L_i), diameters (D_i), equivalent absolute roughness (k_i), and by the singularities met - the local head loss factor ζ_{ij} (entrance/exit from pipes, direction changes, diameter changes, closing valves, retention valves, branches):

$$M_{r\,com} = \frac{8}{\pi^2 g}\sum_{i=1}^{n}\frac{1}{D_i^4}\left[\lambda_i \frac{L_i}{D_i} + \sum_j \zeta_{ij}\right], \qquad (4)$$

The Darcy-Weisbach factor (λ_i) must be calculated according to the sector's relative rugosity (k_i/D_i) and the type of flow corresponding to carried water volumes ($Re = 4.Q/\pi.D.\nu$), using the *Colebrook-White formula* or the *Moody diagram*.

The local head losses factors (ζ_{ij}) are to be calculated by classic methods depending on the nature of singularities (j) met on each sector and on their geometrical features (shape, diameters ratio, angles...). Special attention must be payed in the case of ramifications and confluences in which, depending of the case, the type of factor must be correctly assessed (ζ_{lt} sau ζ_{col}) and also the conditions of the calculations: areas/diameters ratios, respectively flow ratios (when communication operates alone $Q_{lt}/Q_{col} = 1$; when communications work in group $Q_{lt}/Q_{col} = 1/\nu_{com}$; ν_{com} being the number of active communications in the parallel group).

Lengths of the two sectors of the supply (L_{AS} and L_R) are determined by the relative location of the PS compared to the two tank groups; these are given, as for their connection lengths (L_{racI} , L_{racS}), by the *problem's formulation* which may provide the nominal diameters of the the respective communications (D_{racI}, D_{AS}, D_R, D_{racS}).

If nominal diameter of the supply is not provided, using classic methods, this diameter is to be established as an optimal energetic and economical diameter, corresponding to the supply's flow (Q_A).

Geometrical features of pumps' delivery and suction communications, usually *a priori* unknown, are established so that all lengths to be decreased to reasonable figures compared to the pumps' sizes, depending on their nominal flow, parameter which also provides their reference nominal diameter. These hydraulic systems belong to the class of *short pipes systems* (in which head losses are mainly generated by local resistances), hence errors made during the assessment of reference sectors' lengths (sectors having reference diameters) do not fatally affect the accuracy of the calculations.

Table2

Hydraulic resistance module of the supply in several operating configurations (3)

M_{rijk}	parallel group inf. level M_{rgI}	parallel group sup. level M_{rgS}	pumps parallel group M_{rgP}	supply's hydraulic resistance modulus
M_{r111}	M_{rI}	M_{rS}	M_{rP}	$M_{rijk} =$ $M_{rgI} + M_{rAS} + M_{rgP} + M_{rR} + M_{rgS}$
M_{r112}	M_{rI}	M_{rS}	$M_{rP}/4$	
M_{r121}	M_{rI}	$M_{rS}/4$	M_{rP}	
M_{r122}	M_{rI}	$M_{rS}/4$	$M_{rP}/4$	
M_{r211}	$M_{rI}/4$	M_{rS}	M_{rP}	
M_{r212}	$M_{rI}/4$	M_{rS}	$M_{rP}/4$	
M_{r221}	$M_{rI}/4$	$M_{rS}/4$	M_{rP}	

Considering this the procedures may include the following:

-the *pump's delivery communication* will have a nominal reference diameter (Dn_{cr}) which will carry the nominal pump flow (Q_P) at an average velocity close to the average velocity provided in the supply's flow (Q_A), on the delivery main of the PS, having the diameter D_R,: $Dn_{cr} \cong D_R / \sqrt{\nu_P}$.

Translation from this diameter to the pump's delivery connection diameter must be staged, the nominal diameter of the retention valve (Dn_{rr}) being recommended to be with a class lesser than the reference diameter resulted as above (Dn_{cr}). So that to be accomplished on the pump's exit must be mounted a diffuser Dn_{rP}/Dn_{rr}, followed by one or two direction changes having a diameter Dn_{rr}, a retention valve Dn_{rr}, a diffuser Dn_{rr}/Dn_{cr} and closing valve $Dn_{rî}$, together with the ancillary pipe sectors.

- the *pump's suction communication* will have a reference nominal diameter (Dn_{cs}) so that transportation of the pump's nominal flow to be made at a velocity able to be considered reasonable compared to the admitted head losses (so that cavitation to be avoided):

v_s = 0,8 … 1,2 m/s – for pumps with positive suction head (and no suction retention valve is to be mounted);

$v_s < 0{,}4\sqrt{H}$ m/s – for counter-pression pumps, on which suctions are usually mounted closing valves; if the respective condition is satisfied in this case can be adopted the same reference nominal diameter as for the delivery communication ($Dn_{cs}= Dn_{cr}$).

Because, usually, the suction main of the pump may have the nominal diameter (Dn_{sP}) with 2 classes lesser than the reference diameter resulted for the suction main (Dn_{cs}), on the pump inlet must be mounted a Dn_{cs}/Dn_{sP} reduction (assymetrical for positive suctions), streamwise preceded by one or two direction changes, if the case a closing valve, all items having diameters Dn_{cs}, together with all ancillary connecting pipes.

For each communication the length of sectors having diameters lesser than the reference one must be decreased to a strict minimum (singularities' lengths, at which must be added the length of necessary connecting sectors with the same diameter. The gap, up to the estimated length of the communication (L_{cs} sau $L_{cr} \cong 6\ldots15$ m), will be alloted to the corresponding diameter sector (Dn_{cs}, Dn_{cs}).

The relative absolute rugosity (k_i) depends on the mains' material and in this case will be adopted for *old pipes having operated for many years in average work conditions*.

For each *parallel group* there will be a different hydraulic resistance modulus, depending of the considered operating configuration in whcih one or more communications may work. In case of parallel/derivation groups constitued of (ν_c) identical communications (of modulus $M_{r\ c}$), the hydraulic resistance modulus for the group with $\nu_{=}1\ldots\nu_c$ active communications will be:

$$M_{rgc} = M_{rc} / \nu^2 \qquad (5)$$

Hydraulic resistance moduli of the supply in several operating configurations (3)

In the studied case, next to the calculations for the hydraulic resistance modulus of the composing items (M_{rI}, M_{rS} ; M_{rs}, M_{rr}, şi M_{rp} ; respectively M_{rAS} and M_{rR}), corresponding to those shown above, the hydraulic resistance module of the pump supply, in different operational configurations are given by Table number 2.

Table 3

Characteristics of communications for pumps of Pacurari 2 PS (project)

Sector	Length (m)	Diam. (m)	Rugosity k (m)	Headloss factor λ	Singula-rities	Local headloss Σζ	Hydr. rez. modulus Mr ($m^{-5}.s^2$)
1	5,10	0,700	0,0003	0,0170	Rf, Ct	1,58	0,58638
2	1,20	0,600	0,0003	0,0174	Re, Vf, Ct	1,13	0,74265
3	1,20	0,500	0,0003	0,0179	Ct, Ct, Df	0,70	0,98226
4	2,10	0,600	0,0003	0,0174	Rc, Df	2,64	1,72204
5	3,00	0,700	0,0003	0,0170	Vf, Cf	1,43	0,51721

Geometrical lift-up height (H_g), during operation, takes values between:

$$H_{g\min} = Z_{S\min} - Z_{I\max} \quad \text{and}$$

$$H_{g\max} = Z_{S\max} - Z_{I\min}\,, \qquad (6)$$

and will be represented, within this study, by its average value:

$$H_{g\,\mathrm{med}} = (H_{g\,\mathrm{min}} + H_{g\,\mathrm{max}})/2 \ , \qquad (7)$$

which, together with the hydraulic resistance modulus which corresponds to the supply normal operational configuration at its installed capacity (M_{r222}), determines the determină *reference load for pump choosing* (Fig. 2):

$$H_P = H_{g\,\mathrm{med}} + M_{r222} \cdot Q_A^2 \qquad (8)$$

3. A case study: the Pacurari–Aurora/ stream 2 water supply

The supply's layout is shown together with relevant elevations of free water surfaces in tanks in Fig. 1.

The pump delivery and suction commu-nications have the geometrical features, the singularities, and the hydraulic characteristics, showed in Table 3. Transportation of nominal flow on the pump communication generates head losses which are shown together with their corresponding hydraulic resistance module in Table 4.

Table 4

Head losses on pump communications

Communi-	Sector	Hydr. rez.mod		Q_P	hr
		symb.	value	(m^3/s)	(m)
Suction	1-2	Mr_s	1,329	0,85	0,96
Delivery	3-5	Mr_r	3,222	0,85	2,33
Comm. pump	1-5	Mr_{cp}	4,551	0,85	3,29

Supply towards PS and its delivery main have the geometrical features and singularities are shown together with their corresponding hydraulic characteristics in Table 5.

Table 5

Geometrical features and singularities of Pacurari Tanks PS2 supply and delivery main PS2-Aurora Tanks

sector	length (m)	diameter (m)	rugosity k (m)	headloss factor λ	singularities	local headloss $\Sigma\zeta$	hydr. res. modulus Mr ($m^{-5}.s^2$)
1	13,00	1,000	0,001	0,0200	Ic, Ct, Vf, T	3,15	0,28177
2	55,00	1,000	0,001	0,0200	Ct, Ct, Rf	1,76	0,23633
3	939,00	1,000	0,001	0,0200	Rf,Vf,Ct,Ct,Ct	2,48	1,75672
4	15,00	1,000	0,001	0,0200	T, Vf, Ct,Oc	3,15	0,28545

In normal operational configuration (at installed capacity of supply, the hydraulic resis-tance module of derivation groups being:

$M_{r21}=M_{r1}/4$ = 0,07044 and $M_{r24}=M_{r4}/4$ = 0,07136 ,

for the supply's hydraulic resistance modulus results the value:

$M_{rAd} = M_{r21}+M_{r2}+M_{r3}+Mr_{24} =$
M_{rAd} = 0,07044+0,23633+1,75672+0,07136 = 2,13485.

Transportation of installed flow along the supply is made with head losses:

$$h_{rAd} = M_{rAd} .Q_A^2 = 2{,}13485 \text{ x } 1{,}7^2 = 6{,}17 \text{ m} ,$$

therefore, also considering the losses on the connection provided by the communications of the active pumps group: $h_{rc\,p}$ = 3,29 m, the global head loss would be: h_{rtotal}=6,17+3,29=9,66 m ,

Geodesic lift-up height takes significant values:

$H_{g\,max}$ = 110,47 – 54,40 =56,07 m;

$H_{g\,min}$ = 104,05 – 61,00 = 43,05 m ;

$H_{g\,med}$ = ($H_{g\,max}$ + $H_{g\,min}$)/2 = 49,56 m , hence the reference value for the total pumping head is:

$H_p = H_{g\,med} + h_{rtotal} = 49{,}56 + 9{,}66 = 59{,}22$ m

Therefore the reference parameters for the pump choosing will be:

$Q_P = 0{,}850$ m^3/s; $H_P = 59{,}00$ m

The assessment of operational ratings of PS provided with pumps able to ensure the basic parameters above, with the best efficiency, shows that these pumps will efficiently operate on the whole operating domain determined by the particularities of the corresponding supply system - Fig. 3.

Bibliography

[1].Alexandrescu O., Toma I., Anastasoaei M., *Analytical Method for the Evaluation of the Functioning of the Battery of Wells Equipped with Submerged Pumps functioning in Different exploiting Configurations,* Ovidius University Annals of Constructions Volume 1, Number 3, 4, 2002
[2].Toma I.,Alexandrescu O.,Profire M., *Energetical Criteria in the Analysis of The Requests for Upgrading the Water Supplying*, Ovidius University Annals of Constructions Volume 1, Number 3, 4, April 2002
[3].*Optimizarea functional energetica a aductiunii prin pompare Pacurari-Aurora-Mijlociu-Breazu din sistemul de alimentare cu apa a municipiului Iasi*, Contract cercetare U. T. Iasi, 1999

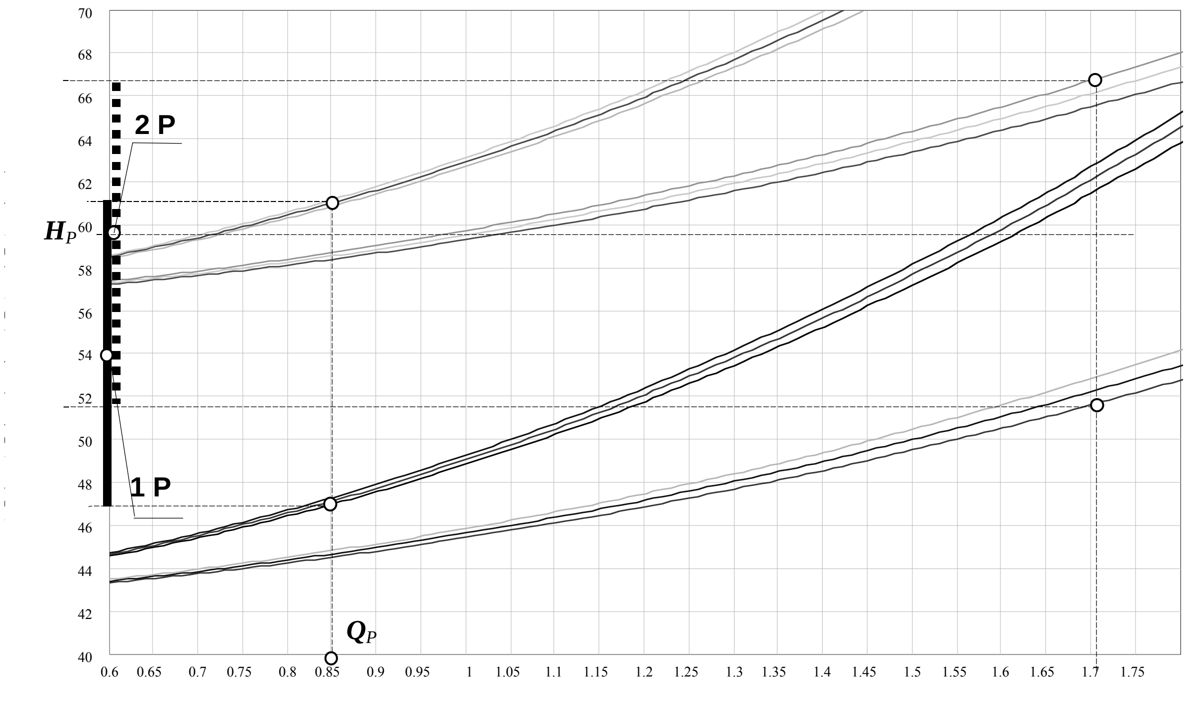

Fig. 2 Supply head features on several operating configurations and extreme static head conditions $H_{g\,min}$, $H_{g\,max}$. Ref. parameters for pump choosing (Q_P, H_P)

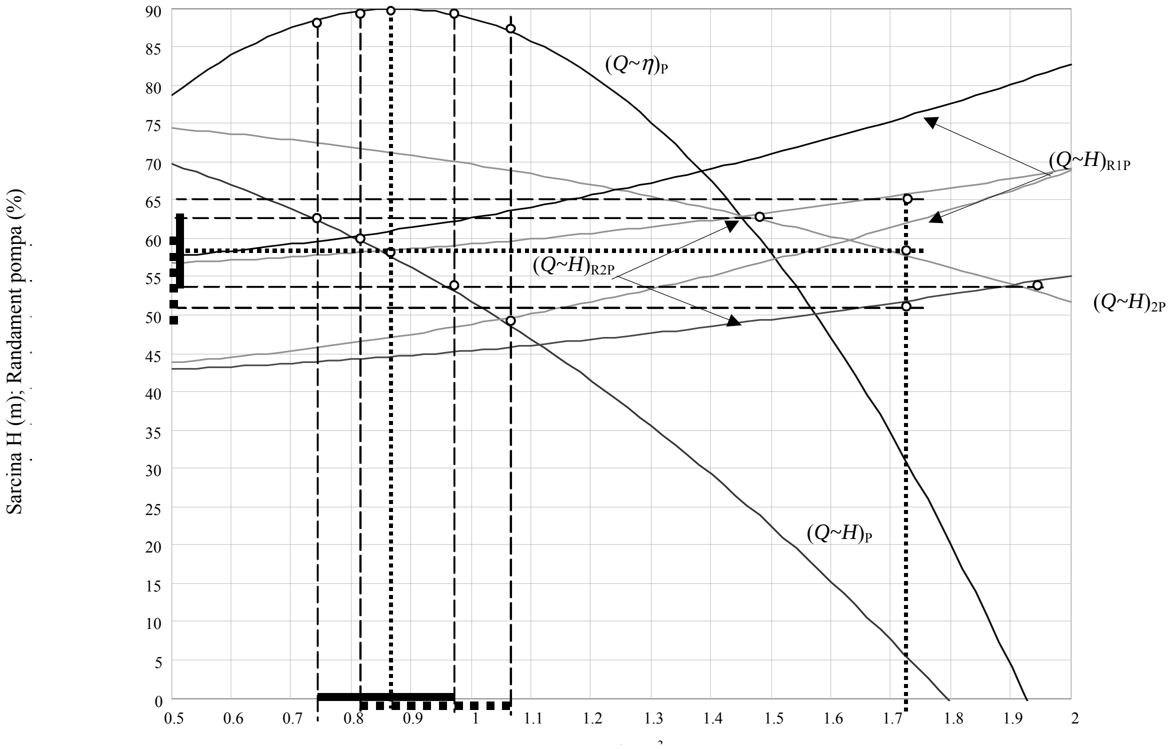

Fig.3 Assessment of operational ratings for a PS equipped with pumps selected according to calculated basic parameters: Q_p=0.850m^3/s ;H_p=59.00m.

A Cinematical Particularity Concerning the Helicoidal Movement of the Fluid Particle Along the Current Line

Dumitru Ion ARSENIE [a] Ichinur OMER [a]

[a] *University "Ovidius" Constantza , Constantza, România*

Rezumat: În lucrare se demonstrează existența mişcărilor elicoidale, adică a mişcărilor la care vectorul vitezei unghiulare de rotație a particulei fluide este paralel cu vectorul viteză în orice punct din domeniul mişcării. Se demonstrează că într-o astfel de mişcare, componentele vitezei trebuie să satisfacă ecuația diferențială de ordinul doi cu derivate parțiale a oscilatorilor armonici. De asemenea se demonstrează că nu există mişcare rotațională la care rotorul vitezei să fie gradientul unei funcții scalare. Se face şi o aplicație concretă, determinându-se câmpul de viteze într-un caz particular.

Abstract: In this paper we demonstrate the existence of the helicoidal movements, that the velocity components must satisfy the second-degree differential equation with partial derivates of the harmonious oscillations and that not exist a rotational movement, which has the velocity rotor equal with the gradient of one scalar function. In the end of the paper, we present a numerical example, where we determinate the velocity field in one particularly case.

Keywords: helicoidal movement, fluid particle, current line.

1. Mathematical model

In the elicoidal movement, which is mentioned in the title, the velocity vector (linear) and angular velocity vector are parallel (Fig. 1), that is exprimed by the following relations:

$$rot\,\vec{u} = 2\vec{\omega} = \vec{\nabla}\times\vec{u} = \vec{i}\left(\frac{\partial u_z}{\partial y} - \frac{\partial u_y}{\partial x}\right) + \vec{j}\left(\frac{\partial u_x}{\partial z} - \frac{\partial u_z}{\partial x}\right) + \vec{k}\left(\frac{\partial u_y}{\partial x} - \frac{\partial u_x}{\partial_y}\right) \quad \ldots \quad .(1)$$

$$\vec{u}\,\|\,rot\,\vec{u} \Rightarrow \begin{cases} \dfrac{\partial u_z}{\partial y} - \dfrac{\partial u_y}{\partial z} = ku_x \\ \dfrac{\partial u_x}{\partial z} - \dfrac{\partial u_z}{\partial x} = ku_y \\ \dfrac{\partial u_y}{\partial x} - \dfrac{\partial u_x}{\partial y} = ku_z \end{cases} \qquad (2)$$

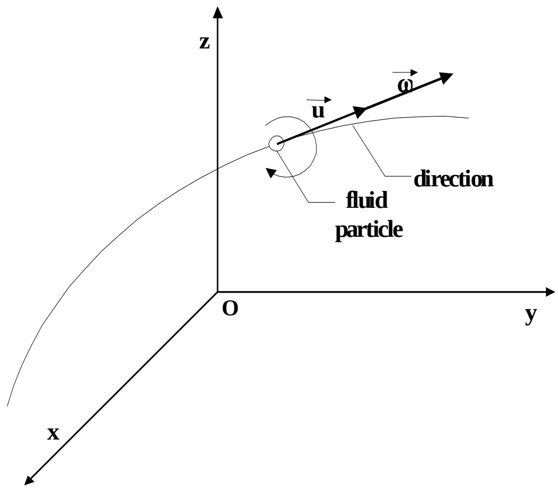

Fig. 1

Supplementary, the velocity must satisfy the continuity equation too:

$$div\,\vec{u} = \vec{\nabla}\vec{u} = \frac{\partial u_x}{\partial x} + \frac{\partial u_y}{\partial y} + \frac{\partial u_z}{\partial z} = 0 \qquad (3)$$

ISSN-12223-7221

The notations used in this relation has the following signification's:
$\vec{u}$ -the velocity (linear); u_x, u_y, u_z -the velocity components, k -a constant; $\vec{\nabla}$ -the Hamilton operator (nabla) ; rot - the rotor operator ; div - the divergence operator.

The system composed by the equations (2) şi (3) contains 4 equations with 3 functions. The first problem is that the system is compatible or not. We will demonstrate that the system is compatible because one of the equations is a result of the other three equations of the system.

We eliminate the unknown function u_z derivating the third equation of the system (2) successively by x and y:

$$k\frac{\partial u_z}{\partial x} = \frac{\partial^2 u_y}{\partial x^2} - \frac{\partial^2 u_x}{\partial x \partial y};\qquad k\frac{\partial u_z}{\partial y} = \frac{\partial^2 u_y}{\partial y \partial x} - \frac{\partial^2 u_x}{\partial y^2} \tag{4}$$

We introduce these expressions in the first and second equations of the system (2) after the multiplication by k:

$$\begin{cases} \dfrac{\partial^2 u_y}{\partial y \partial x} - \dfrac{\partial^2 u_x}{\partial y^2} - k\dfrac{\partial u_y}{\partial z} = k^2 u_x \\ k\dfrac{\partial u_x}{\partial z} - \dfrac{\partial^2 u_y}{\partial x^2} + \dfrac{\partial^2 u_x}{\partial x \partial y} = k^2 u_y \end{cases} \tag{5}$$

Also derivating the third equation of the system (2) by z on eliminate the function u_z and from the continuity equation after the multiplication by k:

$$k\frac{\partial u_z}{\partial z} = \frac{\partial^2 u_y}{\partial z \partial x} - \frac{\partial^2 u_x}{\partial z \partial y} \rightarrow k\frac{\partial u_x}{\partial x} + k\frac{\partial u_y}{\partial y} + \frac{\partial^2 u_y}{\partial z \partial x} - \frac{\partial^2 u_x}{\partial z \partial y} = 0 \tag{6}$$

We obtained a new system composed by three equations (5) şi (6) with two unknown functions (u_x şi u_y), system which has the following form:

$$\begin{cases} \dfrac{\partial}{\partial y}\left(\dfrac{\partial u_y}{\partial x} - \dfrac{\partial u_x}{\partial y}\right) = k^2 u_x + k\dfrac{\partial u_y}{\partial z} \\ \dfrac{\partial}{\partial x}\left(\dfrac{\partial u_x}{\partial y} - \dfrac{\partial u_y}{\partial z}\right) = k^2 u_y - \dfrac{\partial u_x}{\partial z} \\ \dfrac{\partial}{\partial z}\left(\dfrac{\partial u_y}{\partial x} - \dfrac{\partial u_x}{\partial y}\right) = k\left(\dfrac{\partial u_x}{\partial x} + \dfrac{\partial u_y}{\partial y}\right) \end{cases} \tag{7}$$

Derivating again the first equation from (7) by x and the second equation by y and making the sum of these equation, results the third equation of the system:

$$k^2\left(\frac{\partial u_x}{\partial x} + \frac{\partial u_y}{\partial y}\right) - \frac{\partial}{\partial z}\left(\frac{\partial u_y}{\partial x} - \frac{\partial u_x}{\partial y}\right) = 0 \tag{8}$$

It results that the system is compatible, so its exists such helicoidal movements. For distinguishing a particularity of movement, we derivate the first equation of the system (2) by y, the second one by x and we substract the two obtained equations:

$$\begin{cases} \dfrac{\partial^2 u_z}{\partial y^2} - \dfrac{\partial^2 u_y}{\partial y \partial z} = k\dfrac{\partial u_x}{\partial y} \\ \dfrac{\partial^2 u_x}{\partial x \partial z} - \dfrac{\partial^2 u_z}{\partial x^2} = k\dfrac{\partial u_y}{\partial x} \end{cases} \Rightarrow$$
$$\frac{\partial^2 u_z}{\partial x^2} + \frac{\partial^2 u_z}{\partial y^2} - \frac{\partial}{\partial z}\left(\frac{\partial u_x}{\partial x} + \frac{\partial u_y}{\partial y}\right) = -k\left(\frac{\partial u_y}{\partial x} - \frac{\partial u_x}{\partial y}\right) \tag{9}$$

Using now the third equation of the system and the continuity equation, the equation (9) has the following form, which is a known equation describing harmonious oscillations:

$$\frac{\partial^2 u_z}{\partial x^2} + \frac{\partial^2 u_z}{\partial y^2} + \frac{\partial^2 u_z}{\partial z^2} + k^2 u_z = \Delta u_z + k^2 u_z = 0 \tag{10}$$

Δ - Laplace operator.

Proceeding analogue with the components u_x and u_y we obtain the relations:

$$\Delta u_x + k^2 u_x = 0;\qquad \Delta u_y + k^2 u_y = 0 \tag{11}$$

The relations (10) şi (11) can have a single vectorial form:

$$\Delta\vec{u} + k^2\vec{u} = 0 \tag{12}$$

In the case k=0, when the rotor is null (rot $\vec{u}$ =0) we recover the known conclusion that, in the irotational (potential) movement, the velocity is an harmonique function.

Starting from the rotor's expression (1), we analyse the conditions where the velocity's rotor is the gradient of one scalar function. These conditions consist of three equalities of the mixte derivates:

$$\begin{aligned}
&\frac{\partial^2 (rot\vec{u})_x}{\partial x \partial y} = \frac{\partial^2 (rot\vec{u})_y}{\partial y \partial x};\\
&\frac{\partial^2 (rot\vec{u})_y}{\partial z \partial y} = \frac{\partial^2 (rot\vec{u})_z}{\partial z \partial y};\\
&\frac{\partial^2 (rot\vec{u})_z}{\partial x \partial z} = \frac{\partial^2 (rot\vec{u})_x}{\partial z \partial x};
\end{aligned} \tag{13}$$

We analyse the first equality, with the others proceeding in the same way:

$$\frac{\partial^2 u_z}{\partial y^2} - \frac{\partial^2 u_y}{\partial y \partial z} = \frac{\partial^2 u_x}{\partial x \partial z} - \frac{\partial^2 u_z}{\partial x^2} \tag{14}$$

Because by derivating the continuity equation with z results:

$$\frac{\partial^2 u_z}{\partial z^2} = -\frac{\partial^2 u_x}{\partial z \partial x} - \frac{\partial^2 u_y}{\partial z \partial y} \tag{15}$$

we obtain the same conclusion previously mentioned, a necessary and sufficient condition: the velocity's rotor is a gradient only when the movement is irotational (potential), respective the velocity is an harmonious function.

$$\Delta u_x = 0;\ \Delta u_x = 0;\ \Delta u_x = 0 \Rightarrow \Delta\vec{u} = 0 \tag{16}$$

From the relation (16), we can deduce that it not exists rotational movement which has the velocity's rotor a gradient of one scalar function of point.

2. Numerical example

In this estimation we develop one application, determinating the velocity's field for a particularity case concerning the equation of continuity. That we consider:

$$\begin{cases} u_x = u_x(y,z) = f(y) + g(z) \\ u_y = u_y(x,z) = h(x) + l(z) \\ u_z = u_z(x,y) = m(x) + n(y) \end{cases} \Rightarrow$$

$$\begin{cases} \dfrac{\partial u_x}{\partial y} = \dfrac{df}{dy};\ \dfrac{\partial u_x}{\partial z} = \dfrac{dg}{dz} \\ \dfrac{\partial u_y}{\partial y} = \dfrac{dh}{dx};\ \dfrac{\partial u_y}{\partial z} = \dfrac{dl}{dz} \\ \dfrac{\partial u_z}{\partial x} = \dfrac{dm}{dx};\ \dfrac{\partial u_z}{\partial y} = \dfrac{dn}{dy} \end{cases} \tag{17}$$

From the condition to satisfy the system (2) we obtain the following relations:

$$\begin{cases} \dfrac{dn(x)}{dy} - \dfrac{dl(z)}{dz} = k[f(y) + g(z)] \\ \dfrac{dg(z)}{dz} - \dfrac{dm(x)}{dx} = k[h(x) + l(z)] \\ \dfrac{dh(x)}{dx} - \dfrac{df(y)}{dy} = k[m(x) + n(y)] \end{cases} \Rightarrow$$

$$\begin{cases} \dfrac{dh(x)}{dx} = km(x); \dfrac{dm(x)}{dx} = -kh(x) \\ \dfrac{dn(y)}{dy} = kf(y); \dfrac{df(y)}{dy} = -kn(y) \\ \dfrac{dg(z)}{dz} = kl(z); \dfrac{dl(z)}{dz} = -kg(z) \end{cases} \tag{18}$$

By adequate derivates we obtain the conclusion that all these functions satisfy the equations on type harmonious oscillation's equation:

$$\frac{d^2 y}{dx^2} + \omega^2 y = 0 \Rightarrow y = C_1 \cos x + C_2 \sin x \tag{19}$$

In this way, we obtained the following field of velocities, containing six integration constants:

$$\begin{cases} u_x = C_1 \cos y + C_2 \sin y + C_3 \cos z + C_4 \sin z \\ u_y = C_5 \cos x + C_6 \sin x + C_7 \cos z + C_8 \sin z \\ u_z = C_9 \cos x + C_{10} \sin x + C_{11} \cos y + C_{12} \sin y \end{cases} \tag{20}$$

Using now the condition that these expressions verify the system (2) we obtain the relations (21):

$$-C_{11} \sin y + C_{12} \cos y + C_7 \sin z - C_8 \cos z =$$
$$= k\left(C_1 \cos y + C_2 \sin y + C_3 \cos z + C_4 \sin z\right)$$
$$\Rightarrow -C_{11} = kC_2;\ C_{12} = kC_1;\ C_7 = kC_4;\ -C_8 = kC_3$$

$$-C_3 \sin z + C_4 \cos z + C_9 \sin x - C_{10} \cos x =$$
$$= k\left(C_5 \cos x + C_6 \sin x + C_7 \cos z + C_8 \sin z\right)$$

$$\Rightarrow -C_3 = kC_8;\ C_4 = kC_7;\ C_9 = kC_6;\ -C_{10} = kC_5$$
$$-C_5 \sin x + C_6 \cos x + C_1 \sin y - C_2 \cos y =$$
$$= k\left(C_5 \cos x + C_{10} \sin x + C_{11} \cos y + C_{12} \sin y\right)$$

$$\Rightarrow -C_5 = kC_{10};\ C_6 = kC_9;\ C_1 = kC_{12};\ -C_2 = kC_{11}$$

Between these constants exist the next relations:

$$k = 1;\ C_7 = C_4;\ C_8 = -C_3;\ C_9 = C_6;$$
$$C_{10} = -C_5;\ C_{11} = -C_2;\ C_{12} = C_1$$

and we obtained only six independent constants: C_1, C_2, C_3, C_4, C_5, C_6.

$$\begin{cases} u_x = C_1 \cos y + C_2 \sin y + C_3 \cos z + C_4 \sin z \\ u_y = C_5 \cos x + C_6 \sin x + C_4 \cos z - C_3 \sin z \\ u_z = C_6 \cos x - C_5 \sin x - C_2 \cos y + C_1 \sin y \end{cases} \tag{22}$$

3. Conclusions

In this paper we demonstrate the existence of the helicoidal movements. In this case, the rotation angular velocity vector of the fluid particle is parallel with the velocity vector in any point of the movement domain.

We demonstrate too that the velocity components must satisfy the second-degree differential equation with partial derivates of the harmonious oscillations and that not exist a rotational movement, which has the velocity rotor equal with the gradient of one scalar function.

In the end of the paper, we present a numerical example, where we determinated the velocity field in one particularly field.

4. References

[1] Mateescu C., *Hidraulică*, 1963, Ed.Did. şi Ped., Bucureşti.

[2]. Cioc D., *Hidraulică*, 1975, Ed.Did. şi Ped., Bucureşti.

[3] Florea J., Panaitescu V., *Mecanica fluidelor,* 1979, Ed.Did. şi Ped., Bucureşti

Ovidius University Annals Series: Civil Engineering Volume 1, Number 5, 2003

A Method for Determination of the Hydraulic Conductivity in Soils of Middle Textural Type

Cornel GHERGHINA[a] Cristina GHERGHINA[a] LucicaROŞU[a]

[a]*University "Ovidius" Constantza , Constantza, România*

Rezumat: Conductivitatea hidraulică, *k,* reprezintă un parametru important în practica irigației, deoarece intra în calculele elementrlor tehnice ale udării: norma de udare, timpul de udare, indicii de calitate ai udării, etc. Pentru determinarea ei, literatura de specialitate recomandă utilizarea unor metode bazate pe măsurători făcute direct în câmp sau pe eşantioane pregătite în laborator, sau cu relații empirice de calcul. Această lucrare prezintă o metodă pentru calculul conductivității hidraulice, pe solurile cu textură medie, în intervalul umidității active, în care plantele cresc şi se dezvoltă în mod normal.

Abstract: The hydraulic conductivity, *k*, represents an important parameter in to irrigation practice, because it intervenes in the calculus of the watering technique elements: the watering rate, the watering timing, the watering quality indexes, etc. For its determination, the specialty literature recommends whether methods based on measurements made directly into the field or on samples purposefully prepared in labs, or empirical relations of calculus. This paper presents a method for the calculus of the hydraulic conductivity, in terms of a soil with medium texture, on the domain of the active moisture, in which the plants grow and develop in a normal way.

Keywords: hydraulic conductivity, unsaturated porous media, soils of middle textural type.

1. Introduction

In the case of water movement through the porous soil, the main mathematical relation used is the one given by the Darcy's law:

$$v = k \cdot J \qquad (1)$$

where:
v[cm/min]=the speed of the water;
J[cm/cm]=the slope of the piezometrical line;
k[cm/min]=the conductivity, a parameter which characterizes the possibility of water movement through the porous soil, introduced into relation no. (1) in 1931.

This parameter has a constant value in time in the saturated soil, and depends solely of the considered soil nature. In the technical literature it is known as "the filtration coefficient" or " the permeability coefficient", and is noted as *ksat*.

However, in the case of unsaturated soil, this parameter value depends also of the degree of the soil moisture - its humidity, and is known as "the hydraulic conductivity" or "the hydroconductivity coefficient", noted as $k_{w.}$

2. Theoretical considerations

The movement of the water through a porous soil takes place under the action of the resultant of the forces that act upon it: the gravitational force, respectively, the adsorption force and the capillary force**.** In the case of the saturated porous soil, the main force that acts over the water particles is the gravitational force, the effect of the other two being negligible. So, the water speed is called "speed of filtration" and Darcy's relation becomes:

$$v_f = k_{sat} J \qquad (2)$$

The water movement in this case is on vertical, from up to down, and the term J represents the difference of the piezometrical level, Δh, that exists between two points of the porous soil located on the same stream line with a distance of l between them:

ISSN-12223-7221

$$J = \Delta h / l \qquad (3)$$

In the case of water vertical filtration under the action of the gravitational force: $\Delta h=l$ and $J=1$, so the relation no. (2) becomes:

$$v_f = k_{sat} \qquad (4)$$

The effect of the adsorption and capillary forces has been measured using a tensiometer during these experiments, and it has been noted as h_T.

The calculus of the water speed in unsaturated porous media can be made using a relation similar to the Darcy's formula, in which the effect of the gravitational force (which doesn't depend of the soil humidity) appears apart from the effect of the other two forces, which depends of the humidity (5):

$$v= k_w (C-\Delta h_T / l) \qquad (5)$$

where:
k_w = coefficient of hydroconductivity,
C=constant which shows the effect of gravitation; its value is obtained by imposing that relation no. 5 be equivalent to the Darcy's formula in the case of saturated porous soil, when $\Delta h_T=0$ and $k_w= k_{sat}$.

Having relations no. (4) and (5), we obtain:

$$k_{sat}\, C=k_{sat} \Leftrightarrow C=1 \qquad (6)$$

From the dimensional point of view, the parameter k has the same dimension, hence the same measurement unit as the speed has: $[k]=[v]=L/T$. It may be noted:

$$k = (l / t)\chi \qquad (7)$$

where l and t are reference measures having the dimensions L, respectively T, and χ is the dimensionless value of the parameter k.

If we choose the two reference measures l and t so that they both satisfy the relation $l/t=v_f=k_{sat}$, relation no. (7) becomes:

- In the case of saturated porous soil:

$$k_{sat}=(l / t)\, \chi_{sat} \Leftrightarrow \chi_{sat} = 1 \qquad (8)$$

- In the case of unsaturated porous soil:

$$k_w=(l /t)\, \chi_w \Leftrightarrow k_w= k_{sat}\, \chi_w \,;\, \chi_w \in [0,1) \qquad (9)$$

the parameter χ_w will keep its dependence of the momentary unsaturated porous soil, $\chi_w=\chi(w)$, as the hydroconductivity coefficient, k_w , does. Under these circumstances, relation no. (9) becomes:

$$k_w = k_{sat}\, \chi(w) \qquad (10)$$

The general form of the relation of the hydraulic conductivity calculus in unsaturated soil, is:

$$k_w = k_{sat} (\alpha w^2 - \beta w + \gamma) \qquad (11)$$

3. The experimental research method and its results

In order to conduct this experiment, I chose a sample of porous soil with a medium textural type (A=24,9 %, N=43 %, P=32,9 %).

The probe was put into a recipient which dimensions were rather big, and the amount of water required to raise the humidity was supplied through an artificial rain with a intensity of i=4.0mm/h. The humidity of the soil was measured using a BWK LANZE moisturemeter, and the suction - with a SDEC tensiometer. A scheme of this installation is shown in Fig. 1.

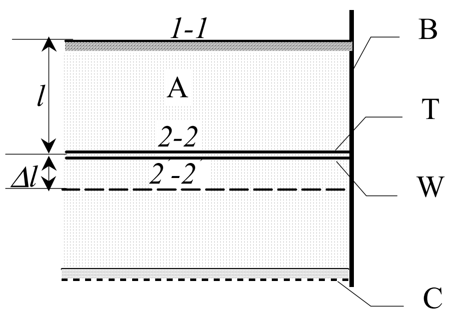

Fig. 1: The experimental installation

A=a sample of soil; B= a metallic recipient;
T=the tensiometer; C=a reversed filter;
W=moisture meter;
1-1=the section from the surface of the sample;
2-2=the section where the measurements take place;
2'-2'=the section where the humidity front is when the humidity in section 2-2 reaches its saturation point.

The experimental results are presented synthetically in Table no.1. The meaning of the terms is:

w_i [%] = the humidity the soil had when experiment no. *i* was conducted

t_0 =the moment when I started the wetting in the section 1-1

t_1 = the moment when the humidity front reaches section 2-2

t_2 = the moment when the soil humidity from the section 2-2 reaches its maximum (close to the saturation point)

l = the distance between sections 1-1 and 2-2

$h_{s\ i}$ = the initial suction of the soil (the same in the whole sample)

$h_{s\,f}$ = the soil suction in section 2-2 at the moment t_2

v_F = the speed by which the humidity front advances

Table no.1

No.	w_I [%]	t_0	t_1	t_2	l [cm]	$-h_{si}$ [mbar]	$-h_{sf}$ [mbar]	v_F [cm/mi]	Δl [cm]	k_{wi} [cm/min]	k_{ws} [cm/min]	χ_i
1	10	9^{33}	12^{37}	13^{14}	25	1100	60	0,135	5,02	$0{,}74 \cdot 10^{-3}$	$440{,}63 \cdot 10^{-3}$	$1{,}65 \cdot 10^{-3}$
2	20	15^{45}	17^{59}	18^{31}	25	650	60	0.186	5,97	$1{,}86 \cdot 10^{-3}$		$4{,}22 \cdot 10^{-3}$
3	40	10^{20}	12^{00}	12^{27}	25	400	60	0,250	6,75	$4{,}76 \cdot 10^{-3}$		$10{,}80 \cdot 10^{-3}$
4	50	8^{33}	9^{59}	10^{24}	25	330	60	0,297	7,44	$7{,}98 \cdot 10^{-3}$		$17{,}90 \cdot 10^{-3}$

$$v_F = l / (t_1 - t_0) \tag{12}$$

Δl = the distance the humidity front has covered during the two moments in time t2, respectively t1

$$\Delta l = v_F \,(t_2 - t_1) \tag{13}$$

$k_{w\,i}$ = the conductivity coefficient corresponding to the humidity wi:

$$k_{w\,i} = \frac{v_F \cdot \Delta l}{\Delta l - \left(h_{s\,f} - h_{s\,i}\right)} \tag{14}$$

k_{sat} = the filtration coefficient which is determined according to the experimental parameters values.

$$k_{sat} = v_{f\,=}\, V / A \cdot t \tag{15}$$

where:

V [cm^3] = the water volume supplied to the saturated sample soil

A[cm^2] = the aria of the sample soil transversal section

T [min] = the duration of the supplying process

The experimental data (Table no. 1) has been processed using the least square method, into the following expression of the function $\chi_w = \chi\,(w)$ from the no. (11) equation:

$$\chi = 0.105 w^2 - 0.029\, w + 0.0058 \tag{15}$$

The graphical form of the function $\chi_w = \chi\,(w)$ is shown in Figure no. 2:

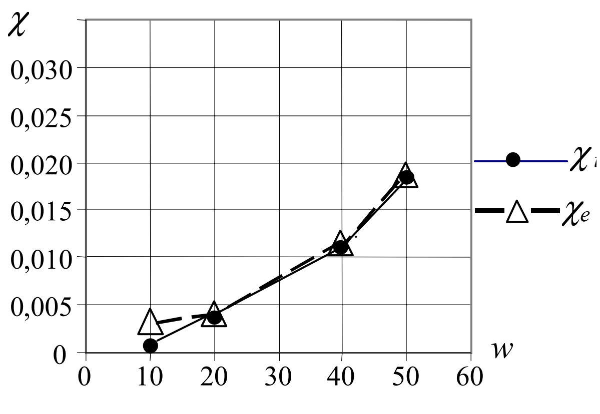

Fig. 2 The variation of the function χ_w related to the humidity

In order to estimate the calculation errors, I used the absolute medium deviation, which value is MAD = 0.000133 (Table no.2).

Table no.2

No.	w[%]	k [cm/min]	k_{sat} [cm/min]	χ_i	χ-e	e	e - abs
1	10	$0{,}74\cdot10^{-3}$	$440{,}63\cdot10^{-3}$	$1{,}65\cdot10^{-3}$	0,00395	-0,0023	0,00232
2	20	$1{,}86\cdot10^{-3}$	$440{,}63\cdot10^{-3}$	$4{,}22\cdot10^{-3}$	0,00419	0,001346	0,001346
3	40	$4{,}76\cdot10^{-3}$	$440{,}63\cdot10^{-3}$	$10{,}80\cdot10^{-3}$	0,0109	-0,00177	0,00177
4	50	$7{,}98\cdot10^{-3}$	$440{,}63\cdot10^{-3}$	$17{,}90\cdot10^{-3}$	0,0175	0,000722	0,000722
Σ	130	$15{,}34\cdot10^{-3}$			1,23821	6,86E-05	0,006158

The relation proposed in this paper to calculate the hydroconductivity coefficient of a soil with some humidity, when the filtration coefficient value is known, is:

$$k_w = k_{sat}\,(105\,w^2 - 29\,w + 5{,}8)\,10^{-3} \tag{16}$$

The values of coefficients α, β *and* γ *experimentally* determined for the case we have studied here, are the following: $\alpha=105\ 10^{-3}$; $\beta=29\ 10^{-3}$; $\gamma=5{,}8\ 10^{-3}$.

4. Conclusions

- The experiments have been conducted in conditions similar to those natural ones, the amount of water required in order to raise the humidity was supplied using an artificial rain, in the range of active humidity, because this is the range where the plants normally grow and evolve, and the production is maximum.
- The relation used in the hydroconductivity coefficient calculus allows the determination of its value based upon only the measured values of the momentary soil humidity, this operation being simpler and cost worthy.
- The rapid determination of the hydroconductivity coefficient is a great advantage especially for the setting of the wetting through leaking on the surface, where the technical elements of the wetting changes from one irrigation season to another and from one wetting, to another, during the same season.

5. Bibliography

[1]. Andrei, S. - *The water in unsaturated soil*, Publishing house. Tehnică - 1967

[2]. Gherghina, C., Arsenie, D. I., Roşu, L - *Considerations regarding a semi-empirical solution of the equation of the water vertical movement in unsaturated porous soil*. - The Papers of the Scientific Session of Homage, FIFIM Bucharest, Publishing house. BREN, Bucharest, 2002, pag. 117-122

[3]. Constantin Chiriță, *Ecopedologia cu baze de pedologie generală, E. D. P.,* Bucharest, 1970

[4]. Green R.E., Corey I.C., *Calculation of hydraulic conductivity*, Soil Sci. Soc. Amer., 35, 3-8, 1971

[5].Gherghina Cornel, Bărbulescu Alina, Roşu Lucica, *Considerations regarding the method of the soil hydraulic conductivity determination, in the range of active humidity*,Academic Timis' Days, Edition no. VII,The Symposium with international participation “Landed improvements between the present and the future", May 25th-26th 2001”, Publishing house Politehnica, Timişoara, 2001, pag. 24-29.

Aspects on Water Losses in Water Supply Systems

Paula IANCU[a] Adriana PIENARU[a]

[a]*University of Agronomic Sciences and Veterinary Medicine,Bucharest, România*

Rezumat: Pierderile de apa din sistemul de alimentare cu apa sunt importante pentru operatorul care furnizeaza acest serviciu catre consumatori, deoarece aceste pierderi influenteaza performantele economice ale companiei. Este important pentru furnizorul de servicii sa inteleaga mecanismul prin care se produc pierderile de apa, influenta acestora asupra indicatorilor de performanta, indicatori care servesc pentru comparatie in calculele care se fac in strategia de dezvoltare a relatiilor cu clientii (utilizatorii de servicii). In acest material se face o prezentare a tipurilor de pierderi de apa in alimentarea cu apa si o analiza a pierderilor de apa in retelele de distributie, in care pierderile de apa au ponderea cea mai mare.

Abstract: The leakages in the water supply system are important for the operator that performs this service to the consumers, because these water losses are influencing the economical performances of the company. For the services supplier it is important to understand the mechanism through which the leakages occur, the influences on the performance rates that serve for comparison within the calculation made in the customer's relations development strategy. In this paper a presentation of the leakage types in the water supply is made, as well as an analysis of the distribution networks water losses, losses that have the biggest weight in the water system.

Keywords: Water supply, water losses, water demand, distribution network.

1. General

Water supply works lead automatically to wasting a part of the water introduced in the system. The problem of maintaining the water losses from the water supply system beyond reasonable limits is important for both the water supplier because it influences the economical performance and the relations with the consumers, and also for the consumer because he pays the performance lack of the system and supports the problems of water lack or even low quality of water.

2. Water losses in a water supply system

The physical water loss is the quantity of water that leaves the system without being used for the purpose it was meant.

Water loss means also the quantity of water that cannot be recovered in the payment bill.

There are two distinct causes that lead to water leakages:

a) The works' design and execution manner
b) The operating manner of the component objects of the water supply system.

In a water supply system, the water losses take place in all component objects of this, thus:

- At the catchment and especially at surface catchments, in case of wrong selection of the water catchment location, at underground catchments water losses can appear due to irrational operation
- At storage water leakages appear due to incorrect execution of tanks or to their aging
- At Treatment Station the water loss may me caused by using reagents with impurities or by inefficiency of settling tanks leading to more often washings of rapid filters
- In the distribution network the water losses have the highest rate. The distribution network is the most developed and dynamic body of the water supply system (in 1998 in Romania the average was

ISSN-12223-7221

2.6 m network/inhabitant). It functions under the heaviest technological and constructive conditions because the values of flow and pressure in a section may vary continuously (fig. 1), and the pipes are usually posed under the traffic part of the road.

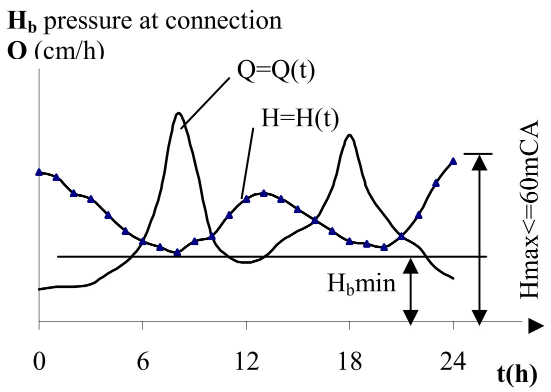

Fig. 1. Variation of pressure and flow in a section of the distribution network

The considerable length and the work conditions make the network the object with the highest water losses. The pipes operate at internal pressure of 1-6 bar, are permanently stressed by mechanical and dynamic loads, and the valves fixed on them represent the weak part in network's functioning.

The water losses are usually produced in the distribution networks because the leakages of joints and of valves that are not tight, through breakings, cracking, or pores in the pipes, and also through the leakages of the installations inside the buildings of the consumers.

3. Technically admitted water losses in the water supply system

Technically admitted water losses in the water supply system can be considered a water demand. They are expressed as a supplementary flow to the general water demand (k_p).

For new designed systems according to STAS 1343/1-95 it is estimated that the water losses would not be higher than (12-15)% with k_p=1.12-1.15.

For development or upgrading works by replacing, the losses are greater, depending on condition, age and material of distribution network. In this case, the losses are considered to be (25-30)% with k_p=1.25-1.30.

For rates over 30% the losses are considered abnormal and reducing measures must be taken.

4. Evaluation of water losses in a distribution network

The networks that transport drinking water may suffer bigger or smaller damages. In case of great damages called breakdowns that are indicated by breakings of pipes, elbows, branches, or valves, some parts of the water supply system are practically out of function.

The small, hardly to observe damages, excepting the visible ones, appear as fissures, small holes or pores, then the system's functioning is practically possible, and the stops of operation are partial and take place only during the period of repairing. These types of damages may produce in time the highest consequences for the consumers.

4.1. Methods for estimation of water losses in pipes

Estimation of water loss and of the manner this is produced, is important because depending on a series of influencing factors one can establish the reducing method.

Evaluation of initial water losses in a pipe can be made with a relation accepted by European norms, when the pressure test is done:

$$\Delta V_{\max} = 1{,}5V\Delta p\left(\frac{1}{E_W} + \frac{D}{e^* E_R}\right) \tag{1}$$

where:

$\Delta V_{\max}$ –maximum volume of water to be lost, in liters

V – volume of water, for the full section of the tested pipe part, in liters

Δp – pressure difference, in kPascal

E_W – incompressibility modulus of water, in kPascal

D – interior diameter of the pipe, in meters
e^* – wall thickness of pipe, in meters
E_R – elastic modulus of pipe, in kPascal
1.5 – factor that takes into consideration that not all the air can be evacuated from pipe before test.

For appreciating the leakages in case of small damages, caused by fissures, these can be assimilated with small orifices in the wall, with sharp edges. This type of losses depends on the pressure as the essential element influencing their value:

$$Q_p = \mu \sum S \sqrt{2g} \sqrt{p} \qquad (2)$$

where:

Q_p – lost water flow,
μ – average coefficient of flow by flowing through the multitude of diverse shapes and sizes of holes,
$\sum S$ – sum of the surfaces of the orifices through which the water is lost,
g –gravity acceleration,
p – difference of pressure between inside and outside of pipe.

Because in the distribution network the pressure varies during the hours of a day (fig. 1), the water loss also varies and presents maximum values during the night, when the pressure in the pipes grows because of the low flow demand.

4.2. Estimation of quantity of water wasted in water supply

In a distribution network the quantities of water wasted because the improper operation of the internal network to consumers has also to be taken into consideration.

Table 1 presents the lost, in fact wasted, water quantities, expressed in equivalent inhabitants, considering a consumption norm of 200 l/person.day.

Table 1. Lost water quantities in inside installations

No.	Source			Lost water quantity (m^3/day)	Equivalent inhabitants
1	Leaking tap		1 drop/min	0.144	0.70
			1 drop/sec	8.640	43.20
2	Orifice in the pipe		D= 1 mm P= 2 bar	0.540	2.70
			D= 10 mm P= 4 bar	73.100	366.0
3	Drinking fountain functioning continuously		q=0.01 l/s	0.860	4.30
4	WC	without float	0.8 l/s	6.910	34.60
		with defective float and self-discharge	8 l/10 min	1.152	5.80
5	Tap with continuous flow for not freezing in the winter		- 1" pipe - v_{min}=0.1 m/s	4.320	21.60
6	Shaving with open tap		q=0.01 l/s	0.864	4.30
7	Car washing		q= 0.5 l/s t=30 min	0.900	4.50

5. Influence of water losses on water supply system's functioning

The water loss in the water supply system can have technological consequences upon the system's functioning i.e:

- the high water loss increases the consumption and the consumption graph is changing (fig. 2). Consequently, the same equipment must ensure more water. That is why the pressure line will decrease and the pressure in the network will be not any more ensured at the connection for all the consumers (figure 3).

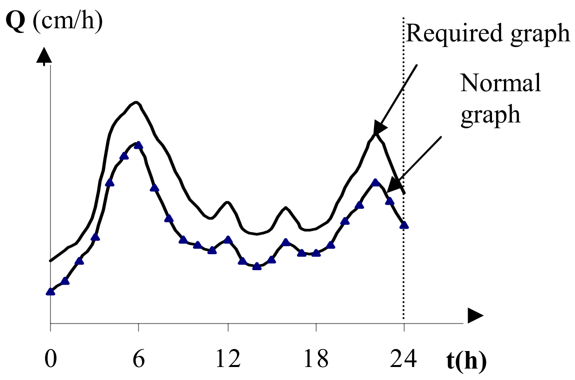

Fig. 2. Modification of consumption graph because of the water losses

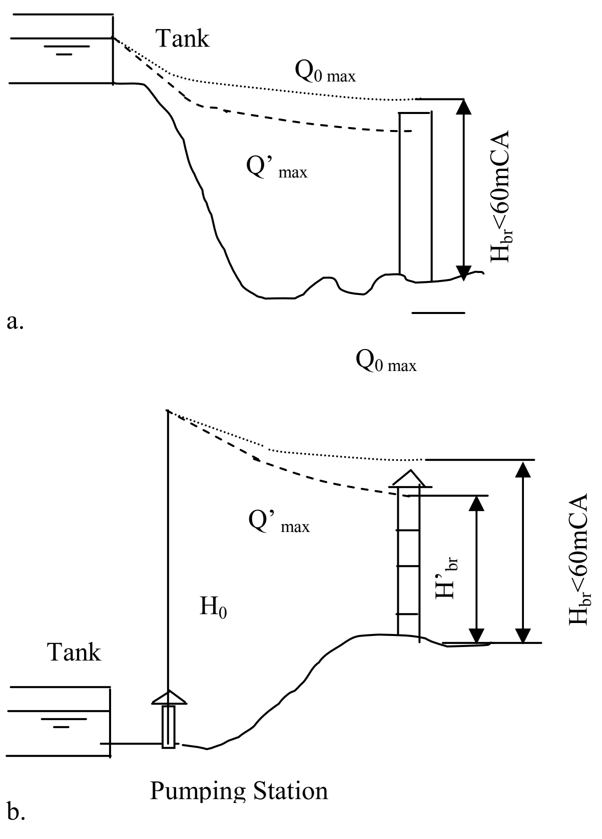

Fig. 3. Modification of pressure line because of the water loss in the distribution network
a. network functioning by gravity
b. network functioning by pumping

In this case the situation can be solved by:

a. discontinuous water supply and a consumption graph as in fig. 4.

b. covering the loss and wasting of water by adding some booster pumping stations or variable speed pumps (fig. 5), resulting a supplementary power consumption.

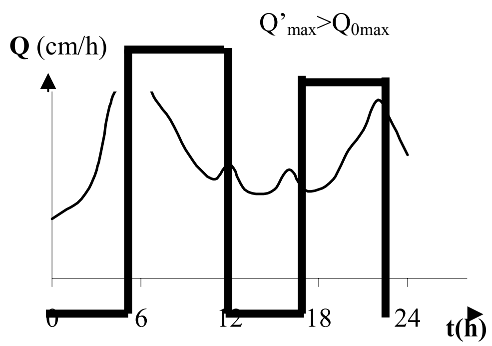

Fig. 4. Graph of discontinuous functioning

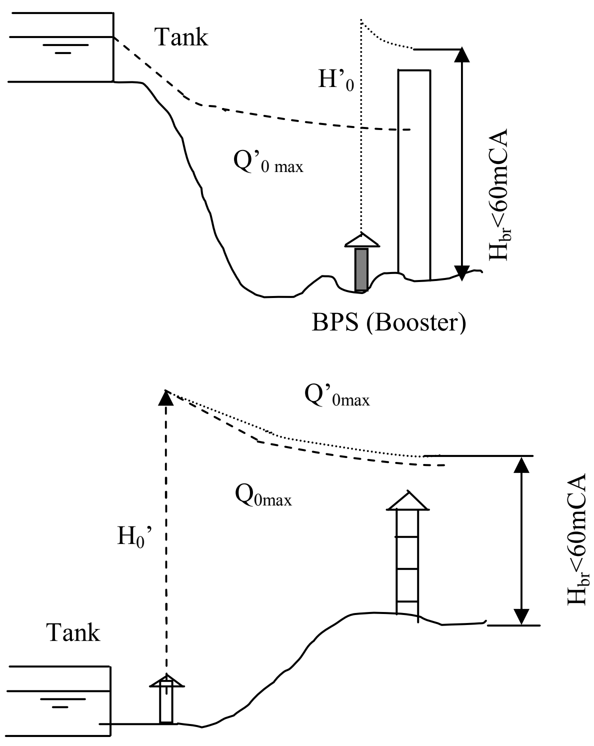

Fig. 5. Increasing pressure due to a supplementary pumping station

- the tank's volume is not sufficient so this gets in a situation of difficulty, needing a bigger compensation reserve. In this case it can use the damage reserve or part of that. That way the system's security decreases because it functions with stops, it is limited by the time of restoring the reserve and by the sufficiency of this time till the next stop.

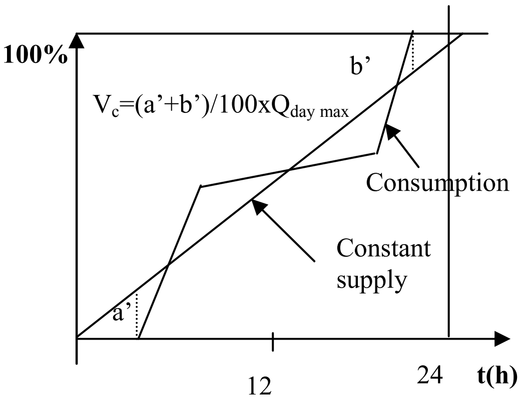

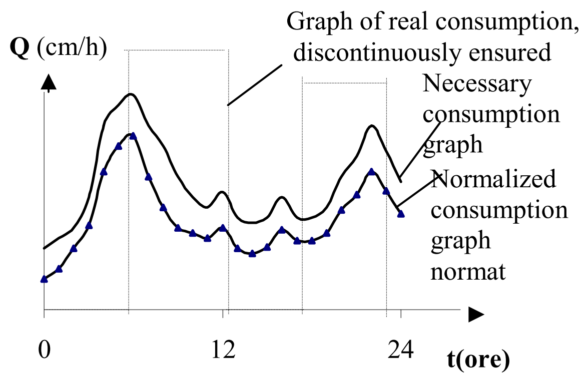

Fig. 6. Graph of tank's functioning with limited compensation volume

- deterioration of water quality due to variable values of speed in distribution network's functioning;
- hot water heating and pumping system has difficulties due to discontinuous supply of cold water.

6. Level of water losses

6.1. Level of water losses worldwide

According to the data published at the IWSA Durban Congress 1995, the level of water losses in diverse areas of the world is that presented in Table2.

Table 2 – Water losses worldwide

	Zone	Water losses m3/h km
1	North Europe	0.5
2	West Europe	0.5
3	South Europe	0.6
4	East Europe	1.9
5	Far East	3.8
6	South Africa	0.7
7	New Zeeland	0.7

6.2. Level of water losses in Romania

Statistics Bulletin is the only official document that presents a situation about the functioning of water systems from Romania.

The values from 1999 lead to the conclusion that per assemble the water loss are 35.2% and there are difficulties in reporting these water losses.

From the answers of a questionnaire realized by Romanian Water Association at the local Water Companies it resulted that:

- 90% of the networks are made from three materials: cast iron, steel and asbestos cement (table 3)
- the networks are very old, most pipes being older than 20 years (table 4)
- a non-uniform equipment with valves, hydrants and connections (table 5)
- water losses' value varies from 26.0% to 47%.

Town	L (km)	Cast iron	Steel	Asbestos cement	Reinforced concrete	PVC	HDPE	Ductile cast iron
Sibiu	312	65.5	18.6	2.4	9.8	0.06	3.6	
Cluj N.	562	31.1	14.4	24	25.1		5.3	
Oradea	529	39.7	11.0	45.3	2.2		0.1	0.7
Buzău	175	11.5	61.7	20.0			6.7	
Tg. Mureş	236	34.7	52.9	4.2	2.7	1.00	3.3	1.3
Constanța	550	23.6	44.7	28	2.3		0.8	0.2
Târgovişte	70	35.5	36.8	23.7	3.6			
Botoşani	286	21.0	34.0	40.2			4.9	
Roman	105	18.1	67.6	14.3				
Ploieşti	601	21.5	60.0	17.6	0.8			
Giurgiu	102	21.9	61.8	15.9		0.16		
Bistrița	235	12.8	74.3	5.8	0.3		6.8	
TOTAL	3763	29.4	39.0	23.1	5.6	0.07	2.5	0.2

Table 3. Water networks by materials

Town	L (km)	<10	10-20	20-30	30-40	40-50	>50
Sibiu	312	2.2	19.8	21.8	26.6	3.2	26.4
Cluj N.	562	5.3		29.5	42.9	4.5	17.8
Oradea	529	15.8	34.4	19.4	8.4	22.0	
Buzău	174	14.6	41.6	16.8	7.3	3.8	15.9
Tg. Mureş	236	8.4	26.1	13.5	52.0		
Constanța	550	10.3	15.8	20.7	30.5	10.1	12.6
Târgovişte	70	1.0	14.4	32.7	28.5	12.2	11.2
Botoşani	286	4.8		34.2	30.8	9.1	21.1
Roman	105	9.3	17.1	39.0	21.9	3.8	8.9
Ploieşti	601	48.4	17.0	4.6	4.0	3.7	22.3
Giurgiu	102	5.1	32.6	21.3	5.5	9.9	25.6
Bistrița	235	6.8	65.0	-	15.0	12.9	
TOTAL	3762= =100%	14.8	20.8	19.2	23.1	8.4	13.7

Table 4. Age of distribution network's pipes (% of total length)

Town	Damages/year				Water loss	
	Network	Valves	Hydrants	Connections	Mil. m^3/an	%
Sibiu	391	-	-	735	10.94	32
Cluj Napoca	1018	-	-	-	25.04	27
Oradea	300	-	-	560	20.90	38
Buzău	1776	-	-	-	9.06	45
Cernavodă	160	-	-	-	4.00	40
Tg. Mureş	4200	-	-	-	12.30	26
Constanța	339	-	-	-	46.90	45
Târgovişte	81	-	-	32	8.20	43
Botoşani	445	130	25	-	8.90	47
Roman	758	-	-	-	7.60	45
Ploieşti	1423	-	-	-	18.90	36

Table 5. Number of damages and volume of unaccounted water

7. Conclusions

Taking into consideration the actual (cumulative) amount of the water losses of 26 - 48% from the caught water (about 100 m^3/s at the level of the country) the physical dimensions are appreciable.

From the total quantity of caught water 20 - 50 m^3/s are losses, this quantity being equivalent to ensuring the water demand for 8.6 - 21.6 million inhabitants. This leads to an impressive energy loss of 0.7 - 1.7 x 10^6 kWh/day, and the corresponding value of that is about 400 - 920 million Lei/day.

These water losses result from the fact that in most networks there is a permanent damage condition leading to these losses.

The replacement and upgrading rate of the distribution networks that benefited from Municipal Utilities Development Programme (MUDP) rehabilitation programs is reaching maximum values of 3 - 4%/year, when worldwide it reaches only 1.0 - 1.2% from the total length.

It is necessary to fulfill the conditions that are leading to optimal operation of the distribution networks i.e. maintaining the pressure at practical constant values and replacing the pipes older than 30 years.

8. Bibliography

[1] Mănescu A., *Situation of estimated water losses for Romania*, International Conference Quality of drinking water in distribution networks, Bucharest, 5-7 Sept. 2000;

[2] Mănescu A., *Water losses' management,* C.N.P.D.A.R., Bucharest, 1997;

[3] Mănescu A., *Water losses' control in distribution network,* Guide-handbook ARA, Bucharest, 2000;

[4] Mirel I., a/o, *New technologies and equipments in water losses detection,* International

Conference Quality of drinking water in distribution networks, Bucharest, 5-7 Sept. 2000;

[5] Sandu M., *Point of view about evaluating water losses in distribution networks*, Rom Aqua no. 4/2002;

[6] xxx Statistics Bulletin, Bucharest, 1998.

About the Induced Voltage by the Cavitation Bubble

Vasile MÂRZA[a] Dumitru Ion ARSENIE[a] Georgeta MÂNDRESCU[a] Alina BĂRBULESCU[a]

[a]*University "Ovidius" Constantza , Constantza, România*

Rezumat: În lucrare este determinata expresia tensiunii electrice induse de cavitația ultraacustică, în apă (caz particular). S-a determinat, în mod experimental, apariția diferențelor de potențial alternativ, în care sunt cuprinse atât armonice cât şi subarmonice. Acestă concluzie este confirmată şi de analiza Fourier a semnalului electric captat în lichid.

Abstract: The aim of this paper is to determine the expression of the induced voltage by the ultrasonic cavitation bubbles, in the exterior of the cavitation bubbles, particularly, in the water. Experimentally, it was determinate that appears an alternative potential difference, which contain both the frequency of the ultrasound and the inherent harmonics and subharmonics. This conclusion is also determined by Fourier analysis of the electrical signal intercepted by the two air gaps inlaid in the liquid.

Keywords: cavitation bubbles, induced voltage.

1. Introduction

The alternative potential difference, which appears when an ultrasonic field convey through the liquid, is distinct from the metal- liquid boundary potential. The potential difference induced by the ultrasonic cavitation bubbles is an alternative one as the metal- liquid (metal- liquid-metal) boundary potential is continue.

Experimentally, it was determinate that appears an alternative potential difference, which contain both the frequency of the ultrasound and the inherent harmonics and subharmonics.

2. The expression of the induced voltage by the ultrasonic cavitation bubbles

In order to determine the induced voltage by the ultrasonic cavitation bubbles, we apply the Lorentz-Lorenz equation [5] considering the liquids.

$$\frac{M}{\rho}\frac{(\varepsilon_r - 1)}{(\varepsilon_r + 2)} = \frac{\alpha \cdot N_A}{3\varepsilon_0} \quad (1)$$

From (1) relationship results:

$$\alpha = \frac{3\,\varepsilon_0 M(\varepsilon_r - 1)}{N_A \rho(\varepsilon_r + 2)} \quad (2)$$

where: ε_0 - void dielectric permittivity; ε_r- liquid dielectric permittivity; ρ- liquid density; N_A- Avogadro number; α- liquid polarizability.

Replacing in (2) relation, the values of the quantities which intervene, results the value for water polarizability:

$$\alpha = 76 \cdot 10^{-38}\left[\frac{Cm^2}{V}\right] \quad (3)$$

The expression of the atomic polarization [3], for a solid, is the following one:

$$P = qa = \alpha\, N_0\, \vec{E} = \frac{\alpha U}{D} N_A \quad (4)$$

Considering the (4) relation, where q=ne results the induced voltage:

$$U = \frac{n \cdot e \cdot a \cdot D}{\alpha \cdot N_A} \quad (5)$$

where: n-number of electrons;
N_A- Avogadro number;
a-the atom dimension in the crystal network;

ISSN-12223-7221

D- the points distance between is measured the induced voltage U. The coefficient K=100 indicate how many times is more compressible the liquid than the solid. Results the relationship:

$$U = K \cdot \frac{n \cdot e \cdot r \cdot D}{\alpha \cdot N_A} \tag{6}$$

where: *r* is the ray of the cavitation bubble.

It is necesarly to know the electron number which can be included in the bubble with given ray. For this, we consider the density of the superficial electric load σ, for a certain ray of the cavitation bubble, which was experimental determined [6] $\alpha = 76 \cdot 10^{-38}\, Cm^2/V$. The ray of the bubble is $r_1 = 7{,}3 \cdot 10^{-4m}$. The relationship for density of the superficial electric load σ is:

$$\sigma = \frac{q}{A} = \frac{n \cdot e}{4\pi r_1^2} \tag{7}$$

Results:

$$n = \frac{4\pi \sigma r^2}{e} \tag{8}$$

Finally results the following value for *n*:

$$n \cong 10^{10} \text{ electrons} \tag{9}$$

Replacing the relation (9) in (6) we determine the value of the induced voltage by the bubble with given ray *r*, not only for water but also for other liquids, when are calculated α şi σ. The values calculated for the induced voltage *U* coincide with those experimental determinated[4].

3. Ultrasonic unit I.U.S.-150 used for the experimental study

This installation (as shown in figure 1 and figure 2) is monoblock type composed of:

- -transducer- core tank;
- -highfrequency generator;
- -active network transformer;
- -aluminium radiator;
- -power transistors;
- -carcas.

The transducer- core tank assembly is formed of two piezoceramic type transducers. The transducers are fixed on the bottom of the core tank, on the exterior, by adhesion with tin argent alloy. The electronic highfrequency generator is autodyne type, realised with power commutation transducers and with current supply from the network doughnut-type transformer. The carcas is metallic and on its frontal side are disposed the control switch gear. In the back side of the carcas is the attachment network cable and the alarm fuse.

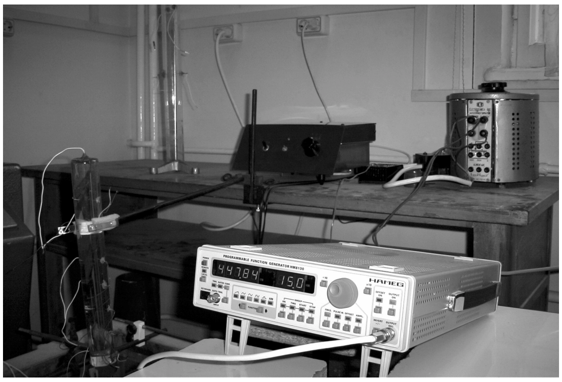

Fig.1- Ultrasonic unit I.U.S.-150

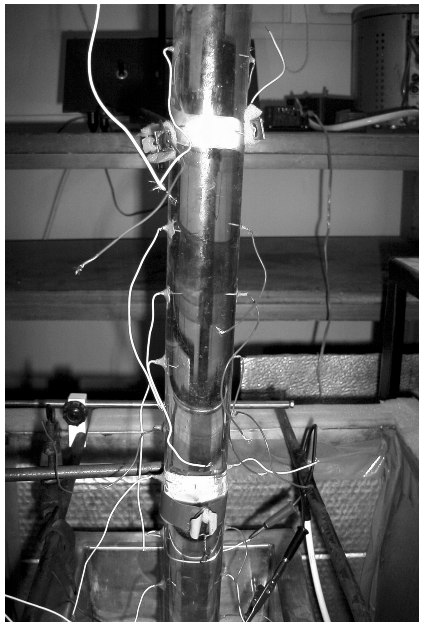

Fig.2- Detail of the experimental unit

The ultrasonic unit functionate based on the principle of phenomenon acoustic cavitation or super-audible cavitation generation, due to ultrasonic waves.

The cavitation effect is the film of rust, fine mechanical impurities, grease ablation from the immersed object in the respective liquid. The ultrasonic waves amplify the cleaning capacity of the solvents.

Also the cavitation effect allow the cleaning of the fine details which are not accesible to mechanical cleaning, such as: the holes, the canals, the fine mechanism bearings.

The climate environmental for the accurate efficiency impose those values:

-temperature +5°C÷+35°C
-relative humidity max.80%
-atmosphere pressure (0,86÷1,06)x10^5 N/m^2.

4. Data acquisition processing

CompuScope LITE belongs to a class of Gage boards called CompuScope ISA.

All these boards are supported by a common driver and Software Development Kit (SDK).

In single-channel mode, the maximum number of sample points is equal to the memory depth of the CompuScope LITE model being used, whereas in dual-channel mode the maximum number of sample points per channel is equal to half the memory depth.

The data stored in the CompuScope LITE memory can be transferred to the PC memory or hard disk for post-processing without any interface bus. The CompuScope LITE memory is mapped into the memory map of the IBM PC, so it can be accessed just as easily and quickly as the PC's own memory. The fast data transfer rate to the PC's memory allows CompuScope LITE to be used in applications which have a high Pulse Repeat Frequency (PRF).

The CompuScope LITE is accompanied by GageScope software, which allows CompuScope LITE to be used as a digital oscilloscope. GageScope to ASCII conversion utility converts GageScope binary files in to ASCII files.

Each line in the resulting ASCII file contains the running time of the sampled data in seconds and the data that was digitized, in volts, at that time.

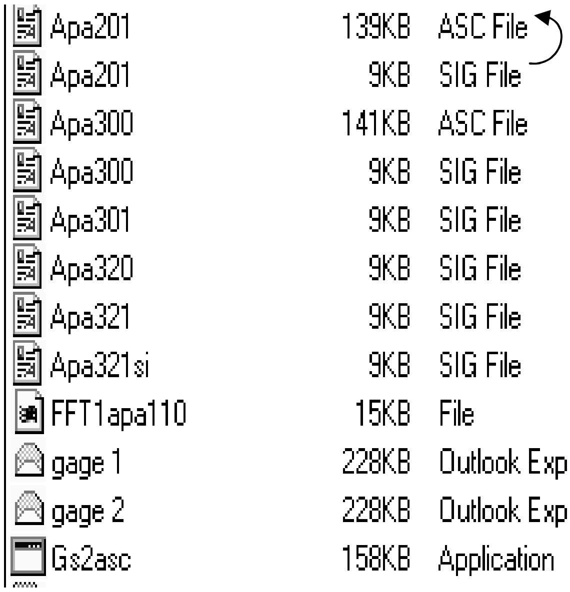

Fig.3- 'Gs2asc.exe' application and SIG file (binary file) converted in ASCII file

The set of recordings (in ASCII files) is organized in two fields separated by a tab, with a carriage return separating each line , as shown in figure number 4.

first field	second field
-0.001839000	+0.992187500000
-0.001838500	+0.992187500000
-0.001838000	+0.835937500000
-0.001837500	+0.726562500000
-0.001837000	+0.726562500000
-0.001836500	+0.804687500000
-0.001836000	+0.898437500000
-0.001835500	+0.968750000000
-0.001835000	+0.968750000000

Fig.4 – Sampled data in the two fields

Those recordings are submitted to discrete Fourier transform, finaly obtaining specific charts, as shown in figure 5.

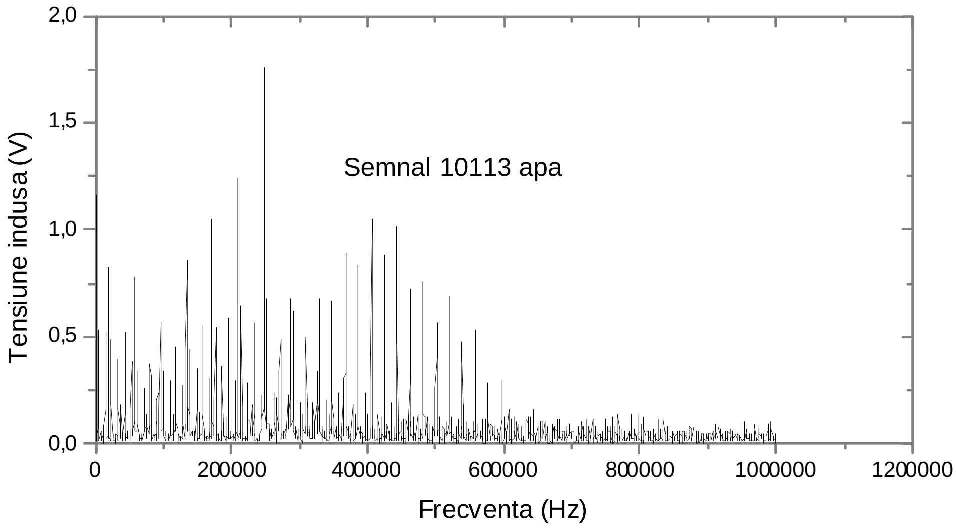

Fig.5 - Spectrum Fourier transform representation

5. Conclusions

The study conclude that this apparance of the electrical potential is due to the following factors:

-the water and oil are polar liquids and under the acoustic variable pressure the active dipoles displace inducing this electrical potential with many frequency components;

-the fundamental frequency corresponds to the acoustic one and is the maximum one.

The size of the electrical potential induced by the cavitation depends on: liquid density, the surface of the plates that measure d.d.p., the power bench of the ultrasounds generator,the air gap.

6. References

[1] V.Dolocan*, Fizica stării solide. Proprietăţi dielectrice şi optice,* Ed. Universităţii Bucureşti 2002.
[2] V.Dolocan*, Fizica dispozitivelor cu corp solid.* Ed. Academiei, Bucureşti 1978
[3]E.Luca, *Elemente de fizică modernă,* vol.II, Ed. Junimea Iaşi, 1978.
[4] V.Mârza, *Contribuţii la studiul cavitaţiei ultraacustice şi a unor fenomene electrice şi chimice indue de aceasta,* Teza de doctorat, Constanţa 2003.
[5] A.Necula, Ghe, Cristea, S.Simion, *Electricitate şi magnetism,* Ed. Did. şi Pedagogică, Bucureşti 1982.
[6] Whybrew,W.E., Kinzer,G.,D., and Gunn, R. (1952) *J.Geographys. Research,* 57, 459.

On the Study of Currents in the Black Sea with the Assistence of Limnology

Angela MUNTEAN [a]

[a] *Naval Academy "Marea Neagra", Constanța, România*

Rezumat: Se face o trecere în revistă a caracteristicilor Mării Negre şi se enumără câteva argumente în favoarea studierii curenților marini din Marea Neagră, cu ajutorul metodelor specifice limnologiei. Se prezintă, în continuare, o metodă de analiză obiectivă, folosită pentru studiul curenților în lacuri, metodă ce ar putea fi utilizată şi în cazul Mării Negre. Sunt prezentate, pentru comparaţie,câteva hărți ale curenților în lacul Ontario respectiv în Marea Neagră.

Abstract: : A review of the characteristic features of Black Sea is done and some of the arguments in favour of the study of marine currents in the Black Sea, with the assistence of the methods specific of limnology, are enumarated. Further on, a method of objective analysis, used in the study of currents in lakes is presented, method which could also be used in the case of Black Sea. For comparison, some maps of the currents in the lake Ontario, respectively in the Black Sea, are presented.

Keywords: marine circulation, limnology, numerical methods, marine currents.

1. Introduction

The Black Sea is a continental sea, semi-closed, whose characteristics are very close to those of a lake. The characteristic due to which it is not considered a lake is the connection with the Mediterranean Sea, by means of Bosphorus Straits. As the matter interesting us is marine currents, we consider that in the study of such a problem, the Black Sea is closer to an ocean. The penetration of the Mediterranean Sea water into Black Sea could be assimilated to a large salted spring, which influences the latter's volume of water and salt. Taking into account the fact that in othe regions of the globe there are larg lakes, which, in their turn, communicate with other oceans and which are much studied within limnology, we believe that good results may be obtained by using some of these studies in the investigation of the Black Sea. The present paper tries to motivate the integration of the Black Sea, for the study of currents, on the category of lakes and presents a method used for the study of the Ontario Lake that could be adaptated for the case of the Black Sea.

2. Characteristics of the Black Sea. Results regarding the circulation in the Black Sea

The Black Sea is a continental sea, having a surface of 413 490 skm. The maximus depth is of 2 245m and the average depth of 1 288m.

The Carspian Sea, which is included in the category of lakes, has a surface of 371 000 skm, and the Tanganika Lake has a maximum depth of 1 435m. The hydrological basin of the Black Sea overpasses 2 400 000 skm. From this drainage surface, the Danube occupies 34%, after which it follows the Niper, Don, Kizil Irmak, etc [1].

The Black Sea is a semi-closed sea, having a restricted water exchange with the Mediterranean Sea. The rivers flowing into the Black Sea, together with the Mediterranean Sea waters, have an influence on the volume of water and salt. As Soljankin has shown, the volume of water that fills into the Black Sea from the Mediterranean Sea, of about 180 m^3 per year, has a value closed to the volume of water that evaporated on the surface of Black Sea [2].

The large rivers flows, in the majority, through the North-West part (according to Altman and Kumish

ISSN-12223-7221

in a percentage of 79%). In the works dealing with the study of the circulation in the Black Sea, for instance, the work of Stanev, the function by which introduced the water flow from the Danube Delta in introduced, differs very little from that which approximates the below surface current which flows through Bosphorus Straits.

The average is of 22 units. There is a strong halocline that separates the surface stratum , with the average salinity of 18 units, form the buttom waters, where the salinity is about 23 units.

Even if the physical processes which take place in this sea are commun with those in the planetary ocean, the strong vertical stratification that exists in every season, poses extremely interesting problems to oceanographers and make the Black Sea unique sea.

The evolution of the physical and chemical processes in the Black Sea, in the different geological periods, was strongly controlled by the exchanges with the Mediterranean Sea through the Bosphorus Straits. The were periods of thousands of years when the connection with the Mediterranean Sea was suspended, the Black Sea becoming a lake. In these periods the sea was isolated and oligosaline [2].

A very long period of time the waters were strongly aerated and life existed close to the water bottom too. But due to the morphobarometric configuratin of the basin as against the Marmara Sea and respectively the Mediterranean Sea, even about 7 000 years ago, a process of accumulation of sulphuretted hydrogen began. This harmful gas, formed at the bottom, as a consequence of the decomposition of organic substances, increased in volume, raising to the superior strata, to the detriment of the dissolvated oxygen [5].

So, the stratum was created, starting from the bottom of the sea, which expanded during the time and reached today up to a depth of 200 m, sometimes even higher. The Black Sea reached the sad performance to be the sea with the biggest percentage of anoxic water, its volume being estimated at about 90% of the total volume [1].

The water located at above 300 meters, besides the fact that they contain sulphuretted hydrogen, are characterized by the fact that the temperature and salinity are strongly homogeneous in the horizontal direction. As regards the increase of the temperature and salinity by the depth, this proves to be very small. Not even the seasonal variations of the density are felt in the deep strata. It is supposed that the circulation in the Black Sea at depths over 300 m is much less intense and not many hydrological measurements were made, generally for the strata situated down to 300 m of depth. Therefore it would be sufficient to know the processes that take place beyond this depth.Then the simulation for a sea (lake) with a depth of 200-300 m can be made.

The hydric evaluation is the quantitative estimation, at a given moment or over a certain period of time, of all components that contribute to the supply or the loss a water volume from a lake, by the surface leakage into the lake and from the lake and the underground supply and leakage. The hydric evaluation is transposed quantitatively in the hydric evaluation [1]. It can be adapted to the conditions of the Black Sea including the entries from the Mediterranean Sea and the outlets to same sea, in terms of supplies and losses of volume at the water surface or bottom.

The Black Sea could be studied together with the salted lakes, especially that among these there are some in which important changes in the profile of the temperature and salinity are produced, due to the presence of some strongly salted springs within the lacustrine tub.

3. A Method of Objective Analysis of the Currents in a Lake

a) The general presentation of the method:

Starting from the models of the tropical circulation in the meteorology and taking into account the effects of the field of wind over the average circulation, Schwab (1977) developed a relatively simple scheme for the study of the currents in the Ontario Lake [3]. It is the case of an iterative method, which is not completely objective, because its results depend on the choice of some parameters used for the initiation of the interpolated fields of the currents. Schwab and Desidaju applied this method, by using some orthogonal functions which are characteristic of certain basins and allow an objective analysis of the field of current.

These orthogonal functions correspond to the streamfunctions, determined by the topography of the basin. The set of streamfunctions is orthogonal, for a network of irregular points is preferred, sets of orthogonal functions may be generated by the Gram-Schmidt method.

Considering the mesoscale circulation, the horizontal currents in a lake may be assimilated to a non-divergent motion (stationary). Under these circumstances, the equation of continuity leads to the existence of a function of current φ, so that the horizontal components of the speed are expressed by the relation:

$$\bar{v} = H^{-1}\bar{k} \times \nabla \psi \qquad (1)$$

that is

$$u = -H^{-1}\frac{\partial \psi}{\partial y}, \quad v = H^{-1}\frac{\partial \psi}{\partial x} \qquad (1')$$

where Δ is the horizontal gradient operator, $H = H(x, y)$ is the depth of the lake in equilibrium conditions, and $\bar{k}$ is the unit vector. The vertical component of the vorticity is given by

$$\zeta = \bar{k} \cdot \nabla \times \bar{v} \quad , \quad \zeta = \frac{\partial v}{\partial x} - \frac{\partial u}{\partial y}$$

Then it is written, using the relation (1),

$$\zeta = \bar{k} \cdot \nabla \times \bar{v} = \nabla \cdot H^{-1}\nabla \psi \qquad (2)$$

If the field of vorticity $\zeta(x, y)$ is known, the relation (2) represents an elliptical non homogenous equation, to which boundary conditions are associated. In the case of Ontario lake, these were conditions of Dirichlet type on the borders of the field. We propose to replace in the future the above condition speeds on the border of the field.

$$H^{-1}\psi = 0 \qquad (3)$$

Generally, the vertical field of the vorticity may be calculated from the data obtained from the observations made in several points of the stidied basin. From the equation (2) the function of current is determinated, and from (1) the components of the horizontal field of the velocity may be calculated.

The procedure proposed by schwab starts with the construction of the orthogonal functions, specific fo the considered basin.

These functions are that is the characteristic solutions associated to the elliptical operator in the equation (2) that is the solutions of the problem on the border of the field.

$$\begin{aligned} &\nabla \cdot H^{-1}\nabla \psi_\alpha = -\mu_\alpha \psi_\alpha \\ &H^{-1}\psi_\alpha = 0 \end{aligned} \qquad (4)$$

The solution of the equation (4) is an auxiliary matter, which requires the determination of the own values and vectors. The characteristic functions from a complete set of orthogonal functions. The streamfunction may be expressed by the set of characteristic functions above described, by

$$\psi = \sum_\alpha a_\alpha \psi_\alpha \qquad (5)$$

where the coefficients are calculated subject of proper values and the characteristic functions in the problem (4) after the relation:

$$a_\alpha = \mu_\alpha \int \psi \psi_\alpha dA \qquad (6)$$

b) The spectral model of the stationary motion:

By the introduction of the mass transport vector $\overline{M}$ [4],with the expression given by the relation below

$$\overline{M} = \int_{-H}^{0} \bar{v} dz \;,$$

the equations of the stationary motion may be put under the form

$$f\bar{k} \times \overline{M} = -gH\nabla\eta - \lambda H^{-1}\overline{M} + \rho^{-1}\bar{\tau} \qquad (7)$$

where the function of the height of the sea surface above a level surface was marked with η, with coefficient and f- the Coriolis coefficient and with $\bar{\tau}$ the wind driving force. The hypothesis is made that tha friction from the bottom of the basin is directly proportional to the mass transport and inversely proportional to the depth. Also g and f are considered as constant.

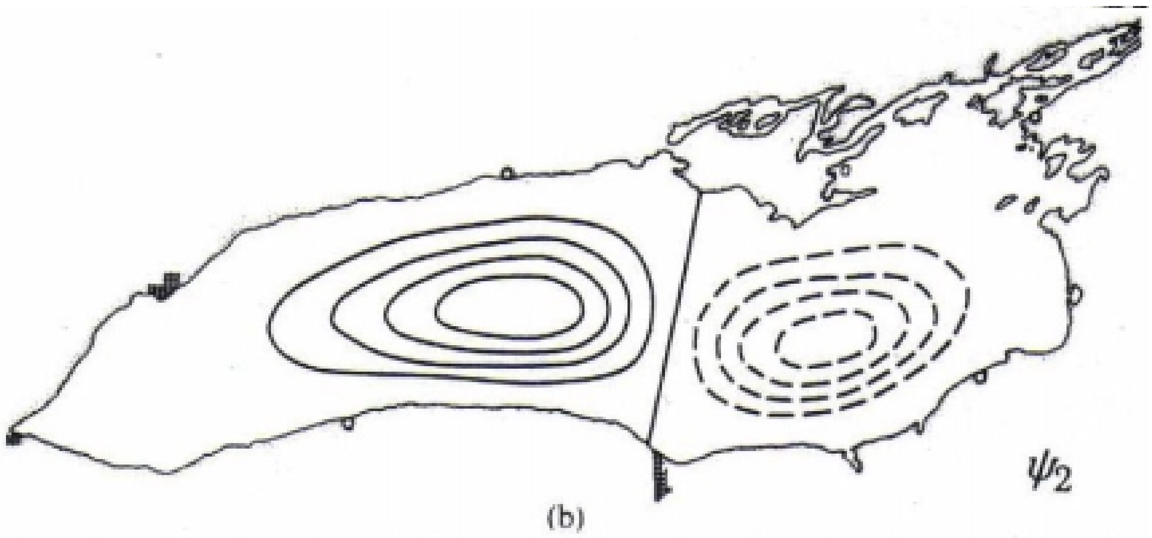

Figure 1. A scheme of the currents in Ontario lake for a particular streamfunction (from [3])

By the vertical integration of the equation of the equation of continuity and by the expression of the horizontal components of the velocity with the assistence of the streamfunction, the mass transport is expressed by

$$\overline{M} = \bar{k} \times \nabla \psi$$

Replacing in the relation (7) it is obtained

$$\begin{aligned} &\nabla \cdot H^{-1} \nabla \psi - H^{-2} \nabla H \cdot \nabla \psi + \\ &f(\lambda H)^{-1} J(H, \psi) = \lambda^{-1} \\ &\left(\bar{k} \cdot \nabla \times \rho^{-1} \bar{\tau} - H^{-1} \rho^{-1} \tau \cdot .\bar{k} \times \nabla H\right) \end{aligned} \tag{8}$$

where J represents the Jacobian [3].
Further on, in the relation (8) the expression given by the development (6) is replaced and the orthogonality condition of the functions is used. The result obtained is

$$a_\varepsilon + \sum_\beta b_{\alpha\beta} a_\beta = p_\alpha \tag{9}$$

$$\begin{aligned} p_\alpha = \lambda^{-1} \cdot \int (\bar{k} \cdot \nabla \times \rho^{-1} \bar{\tau} - \\ - H^{-1} \cdot \rho^{-1} \cdot \bar{\tau} \cdot \bar{k} \times \nabla H) \cdot \psi_\alpha dA \end{aligned} \tag{10}$$

and

$$b_{\alpha\beta} = \int H^{-1} \psi_\alpha \begin{bmatrix} \lambda^{-1} f J(H, \psi_\beta) - \\ - H^{-1} \nabla H \cdot \nabla \psi_\beta \end{bmatrix} dA \tag{11}$$

if the two functions that give the wind driving force and the depth of the basin are known, the B matrix can be obtained, formed of the coefficient $b_{\alpha\beta}$, given by the relation (10) and the column matrix **p**, formed of the components p_α, calculated with (11).
Then, the equation (9) may be written under matrix form

$$(I + B) a = p \tag{12}$$

where a is the column matrix formed of the coefficients a_α, which must be determined, because they allow the writing of the streamfunction by means of the set of the orthogonal functions.

The calculation of the matrixes B and p is made from the relations (10) and (11) approximating the differential operators which appear in these formulas, by finite differences, starting from the values obtained from observations. For the solution of the matrix equation (12) one of the standard methods for the calculation of the inverse matrix I+B is used.

For the determination of the solutions of the equations (4) the so called Lanczos procedure was used, which consists of the development of the functions subject of another set of functions, which satisfy, in their turn, the boundary conditions. An iterative method is applied for the construction of this set of functions. It is started with the choice of the first function from this set, choice that is mad with the fulfillment of the boundary conditions after which the other values of the set of functions are calculated. The proper values ψ_{α} are determinated and the spectral functions are built.

The methods requires a large number of data, obtained by observations and their processing with the assistence of the finite element method

The lake is considered as homogenous, and the barotrop currents (the same at any depth). For the real case of baroclin currents the spectral currents may be calculated for several strata, then a vertical mediation is made.

We further present the scheme of the currents in the Ontario lake (figure 1) for one of the streamfunctions obtained by above method and the map with the lines of the total currents in Black Sea (figure 2). For the Black Sea, the map was drawn up on the basis the calculations made by Roventza [6] using the theory of the drift currentd in closed basins, under the influence of the homogenous and nonhomogenous fields of winds, theory issues by Ekman. A sufficiently good correlation between the two configurationsis noticed, although the boundary conditions from the two basins are completely different.

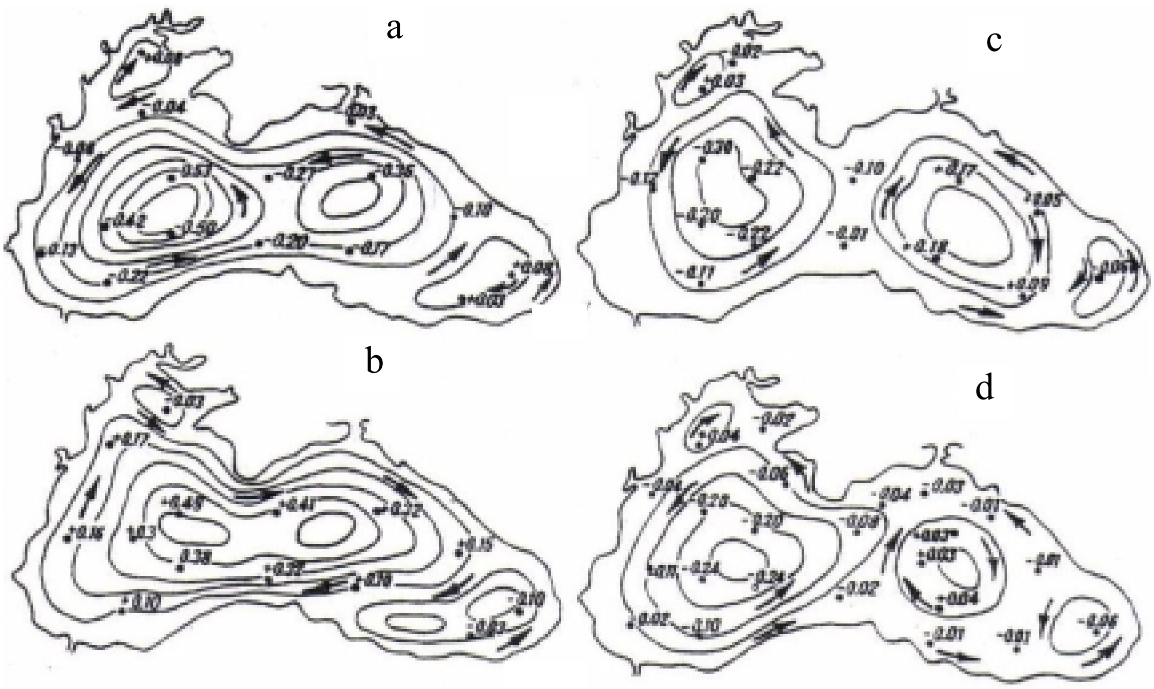

Figure 2. The maps of the total currents in the Black Sea obtained by Roventza

4. Conclusions

We wish to point in the present paper the arguments for the studies of marine currents in the Black Sea, considering it like a lake. A method which was used for the study of Ontario lake is presented and two maps for the currents in Ontario lake and in Black Sea.

Bibliografie

[1] Gâştescu P., *Limnology and Oceanography*, Publishers *H*G*A*, Bucharest 1998

[2] Stanev E., *On the mechanisms of the Black Sea circulation*, Earth- Science Reviews, 28 (1990) Elsevier Science Publishers B. V., Amsterdam

[3] Desiraju R., Schwab D., *A Method of Objective Analysis for Curents in a lake with Application to Lake Ontario*, Journal of Physical Oceangraphy, 1981

[4] Stewart R., *Introduction To Physical Oceanographiy*, Ed. Texas A&M University, 2000

[5] ***, *The Black Sea in the Roumanian Seaside Zone*, Hydrological Monograph , IMH, Bucharest, 1973

[6] Roventza, V., *Contribution to the Total currents in the Black Sea*. Studies of Hydrology , Tome XIX Bucharest, 1967

Studies Regarding the Evaluation of the Environmental Impact of the Gilău Storage Lake (Cluj County)

Roxana BOLBA[a]

[a]*Tehnical University "Gh.Asachi" Iassy , Iassy, România*

Rezumat: Lacul de acumulare Gilău (Județul Cluj) este situat lângă Orașul Cluj-Napoca. El este folosit pentru aprovizionarea cu apă şi alte folosințe.
Acesstă lucrare îşi propune estimarea echilibrului natural pentru acest lac de acumulare folosind cei mai importanți indicatori fizici, chimici şi biologici.

Abstract: The Gilău Storage lake (Cluj county) is situated near Cluj-Napoca city being used for water supply and other uses.

This paper proposes the estimation of the environmental balance for this storage lake using the most important physical, chemical and biological indicators.

Keywords: storage lake, physical, chemical and biological indicators, environmental impact.

1. Introduction

The Gilău river it is placed on Someşul Mic river, at 2 km of confluence between Someşul Cald river and Someşul Rece river.

Of administrative territorial point of view, the Gilău dam and retention are placed in Gilău village area and at 19 km upstream of Cluj-Napoca city.

About block of retention point of view, the Gilău retention it is in downstream of hydroelectrically falls retentions, at Someşul Cald river (Fântânele, Tarnița and Someşul Cald) and the second captations (Iara- Someşul Rece I – Rătăcău –Fântânele and Someşul ReceII–Tarnița)(Figure 1).

The Gilău retention it is in 2nd class of importance, conformable with STAS 4273-83.

The functions of the retention are many: the utilization of the water; the generation of electrical power; the protection against flooding; the assurance of the uses capacity in downstream at dam; other uses [3].

2. Some aspects regarding the environment impact

At the other retentions, the Gilau retention has a normal influence on some Environment components, as: the surface and under ground water, aquatic and land ecosystem and the socio- humanities components without arise distinct problems.

The generation of power function is realized without problems regarding the river pollution.

In the dam exploitation are used some toxic substances as: diesel fuel, driving oil, essential oil, acids and antifreeze solution. The storage and the management of the toxic substance is does in accordance with books and normative used in this area.

Because this activity, which is developed, is not pollution, the Gilău retention is not representing one danger for the environment and for the healthy of the populations [3].

3. The analysis a water quality factors of the Gilău retention

The main aim of the Gilău retention was planned for discharge regulation in Someşul Mic hydrographic

ISSN-12223-7221

basin, for completion with water in the contiguous soils and for the growth of the fish.

For the following the water quality and the eutrophical rate, in 2002 had been effect 4 campaign of harvest in April, May, August and September. The water tests has elected by 10 points of collection at the surface water and at varied depth. In the Table 1 are presented the physical and chemical indicators with the water in

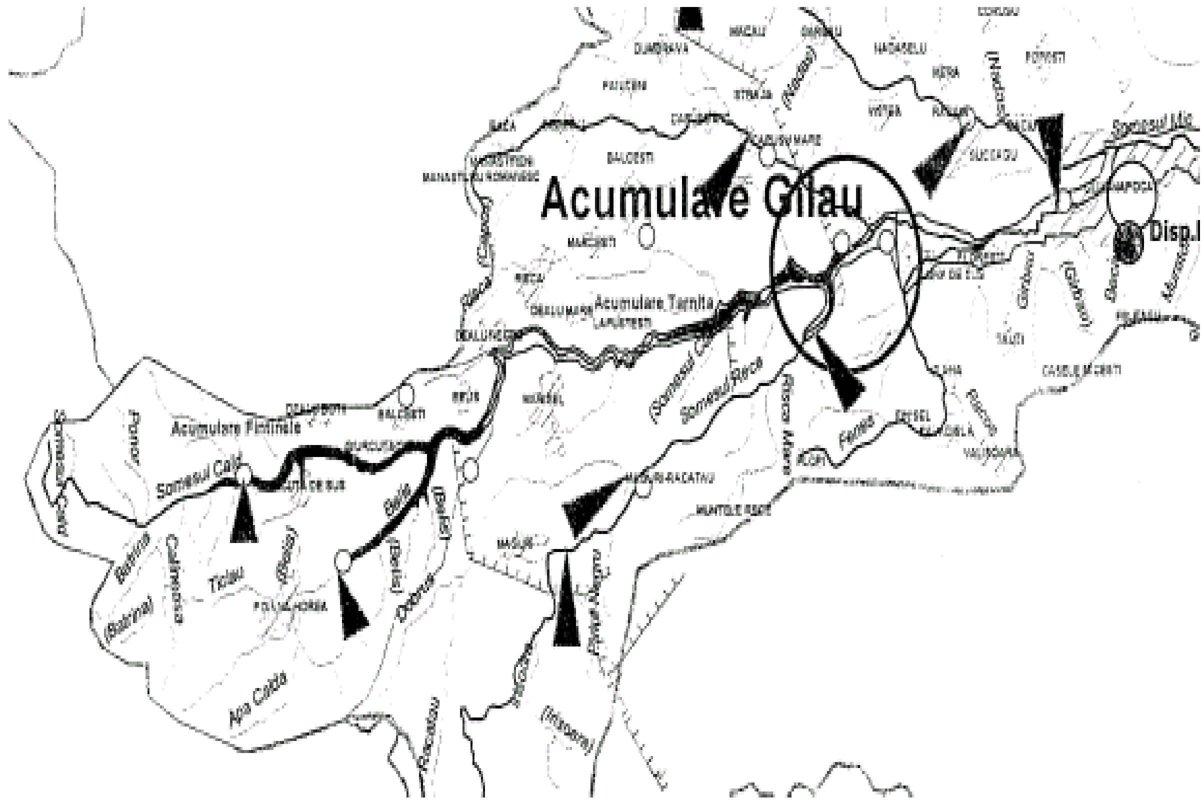

Figure 1. The Gilau storage lake

quality categories about the STAS 4706/88 and in the Table 2 the values of the biological quality indicators, determined after 2001 and 2002 campaign.

After the physical-chemical, biological and bacterial analysis are done, in concordance with STAS 4706/88, are formulated some conclusions regarding the trophic evolution of artificial lake:

- the water transparency, measured with Secchy disk was differed values between 1 m and 3.5 m;
- regarding the water temperature, was registered a remission of temperature from the surface to the depth of lake;
- reaction of the water was slightly alkaline, the pH values was varied between 7.11-7.98;
- the water color was gray – greenish and is not preset distinct odor;
- oxygen regimen : the dissolved oxygen was varied between 7.3 mg/l and 12.01 mg/l; this means that the lake water had a good dissolved: oxygen saturation is not more low that 70%, the lake water is farmed in oligotroph lakes; the organic substances show that the values of indicators CBO_5 and CCO-Mn;
- the nutritive rate; it is one important indicator in eutrophic process, the main indicators are N and P: the total N put the water lake in eutroph lake category; the total P is no varied; the water lake is put in the

oligotroph category; the phytoplankton, the minimal values are obtain at the surface and in the lower depths. The maximal values are registered in the high depths. The values put the water of lake in oligotroph category; the zooplankton was oscillated between 0.0005 mg/l and 6.1454 mg/l; the zooplankton numbers was presented trough gender groups: Keratella Polyarthra remata, Cyclops strennus, Daphnia sp., Vorticella sp., Stentor. cochearis, Trichocerca stylata [1].

Table 1. The physical and chemical indicators determined after the 2001 campaign in the Gilău storage lake

Quality indicators	Values	Quality categories
Oxygen regime		
Oxygen dissolved [mg/l]	8.20	I
DBO5 [mg/l]	2.60	II
CCO-Mn [mg/l]	6.40	II
CCO-Cr [mg/l]		
Nutrients regime		
Saprobe index (Pantle-Buck) [mg/l]	1.74	I
NH_4^+ [mg/l]	1.33	IV
NO_2^- [mg/l]	0.009	I
NO_3^- [mg/l]	0.6	I
PO_4^{3-} [mg/l]	0.47	I
Basic chemical indicators		
Temperature [^oC]	5.0	
pH	8.5	
Suspensions [mg/l]	21.5	I
Rezid. Fixe [mg/l]	130.8	I
Durity [^oG]	5.8	I
HCO_3^- [mg/l]	85.4	I
Ca [mg/l]	30.5	I
SO_4^{2-} [mg/l]	30.8	I
Mg [mg/l]	9.7	I
Fe [mg/l]	0.2	I
Cl^- [mg/l]	5.0	I

Source: C.N. Apele Romane, Cluj-Napoca

Framing the lake water in quality category based on saprod index, encoding the water of lake in β-mezasopod area in Somesul Rece section, upstream retention and in the other section the lake water was put in α- mezasoprob category.

The hygienic- sanitary status at lake water is good, the possible numbers of totals coliform bacterial/dm^3 is more low that is in STAS 4706-88; the lake water is encoded in first category of quality [2,4].

Table 2. The quality biological indicators determined after the 2002 campaign in the Gilău storage lake

Biological indicators	Minimal	Averagge	Maximal
Phytoplankton [mg/l]	0.195	3.077	9.328
Zooplankton [mg/l]	0.000	0.932	6.145
Zoobentos [Nb./m^2]	42.0	347.0	952.0
Bacilli [Nb.dm^3]	2200	28332	92000
Streptocoques [Nb./dm^3]	0.000	5148.5	39000

Source: C.N. Apele Romane, Cluj-Napoca

4. Conclusions

1. True to the physical – chemical analysis, the lake water in the throughout the year was good dissolved and the biochemical oxygen consuming (CBO_5) was registered characteristic values for oligotroph lakes.

Regarding the capacity of aerobe mineralization of organic materials, the values put the water of lake in oligotroph category. The nutritive rate put the lake water in oligo-mezotroph category. Because of the short time of retention it was not signalized permanent and massive blooming.

2. True the biological analysis; the phytoplankton registered some values, which put the lake water in oligotroph category.
3. True the bacterial analysis; the water of lake is placed in first category of quality.
4. The water of Gilău artificial lake is in oligo-mezatrophe category with eutrophic trend.

5. Acknowledgements

I want to tank at C.N. "Apele Române" - Cluj-Napoca for the offer data base.

6. Bibliography

[1] Brezeanu Gh., *Ecosisteme acvatice din România. Caracteristici hidrogeografice şi limnologice*, Rev. Mediul Înconjurător, vol. VI, nr.2, Bucureşti, 1996

[2] Crăciun I., ş.a. *Mathematical Modeling of the Same Physical, Chemical and Biological Parameters of the Bahlui Catchement Retention*, Ovidius University Annals of Construction, Vol. 1, Nb. 3,4, Constanța, April 2002, 675-678

[3] Dumitraş R., *Situația actuală a cercetărilor în domeniul impactului acumulărilor asupra mediului. Metode de cercetare,* Referat Doctorat nr.1, Fac. de Hidrotehnică, U.T. Iaşi

[4] Ioniță V., *Lacurile de acumulare-ecosisteme supuse proceselor de eutrofizare*, Rev. Hidrotehnica nr.9, Bucureşti, Vol. 42, 1997

Black Sea Level Rising and Coastal Erosion

Glicherie CARAIVAN[a] Daniela POPESCU[b] George PADURARU[a] Cosmin PANTELIMON[d]

[a] *"Ovidius" University Constantza , Constantza, Romania*
[b] *Romanian Water National Administration, Dobrogea – Litoral Water Branch, Constantza, Romania*
[d] *S.C. Building, Constantza, Romania*

Rezumat: Creşterea nivelului Marii Negre si eroziune costiera**.** Pe parcursul ultimei transgresiuni marine (Würm), nivelul Mării Negre a crescut continuu, de la cca –130 m în urmă cu 12 – 15 000 ani, către poziţia actuala. În perioadele de relativă stabilitate a nivelului mării, s-au format structuri acumulative costiere, sau ţărmuri cu faleză activă, configuraţii relicte, care au fost înregistrate pe şelf.
Creşterea nivelului mării fiind un proces eustatic, global, tendinţă care se manifestă şi în prezent, se prognozează o retragere continuă a liniei ţărmului.
În consecinţă, se recomandă strategii de protecţie costieră adecvate, cu structuri hidrotehnice uşoare, adaptabile unor situaţii noi.

Abstract: Following the continuous sea level rising curve from approximately 130 m below the present one, about 12 – 15 000 y.B.P.) there were moments of relative stability, when accumulative and erosional coastlines developed. These relict fisiographical features are recorded on the modern shelf surface. Their age was estimated by C^{14} determination from mollusk shells.
The modern coastline erosion processes, respectively the landward passage of the shores, was to be expected, taking into account the rising trend of the World Ocean level.
The heavy structures are gradually abandoned, and new geotextile submerged groins and breakwaters are projected. The last ones make possible rapid modifications and adjustment, requested by the induced effects upon the coastal dynamics.

Keywords: *Black Sea, coastal erosion, sea level rising*

1 Introduction

From the north to the south of the Dobrogea region, one can distinguish three major geological units: the Predobrogean Depression, the North Dobrogean Orogenous, and the Moesian Platform. Two major fault lines separate these units: the St. George fault, and the Peceneaga-Camena fault. The Capidava-Ovidius fault is also, very important.

The bathymetrical, seismo-acustical and sedimentological studies of the Romanian shelf permit us to divide it into three distinct units: the littoral zone, the inner shelf and the outer shelf. On this background, one can separate a very distinct unit: the Danube Delta (fig. 1).

Littoral zone

The Romanian coast is 240 km long. From a genetical and geomorfological point of view, there are two types of shores:

- **primary coasts,** respectively the northern shore, corresponding to the Danube Delta, and the Razelm-Sinoe lagunar complex, and
- **secondary coasts,** respectively the southern zone, between Cape Midia and Vama Veche, prevailing the erosional cliff shores, with two sub-units:
  - Cape Midia-Cape Singol zone, having a transition character, with large barrier beaches, connecting a series of active head-lands, and
  - Cape Singol-Vama Veche zone, in which, clearly prevail the active erosion shores, interrupted only, in front of lagunas, by barrier beaches.

ISSN-12223-7221

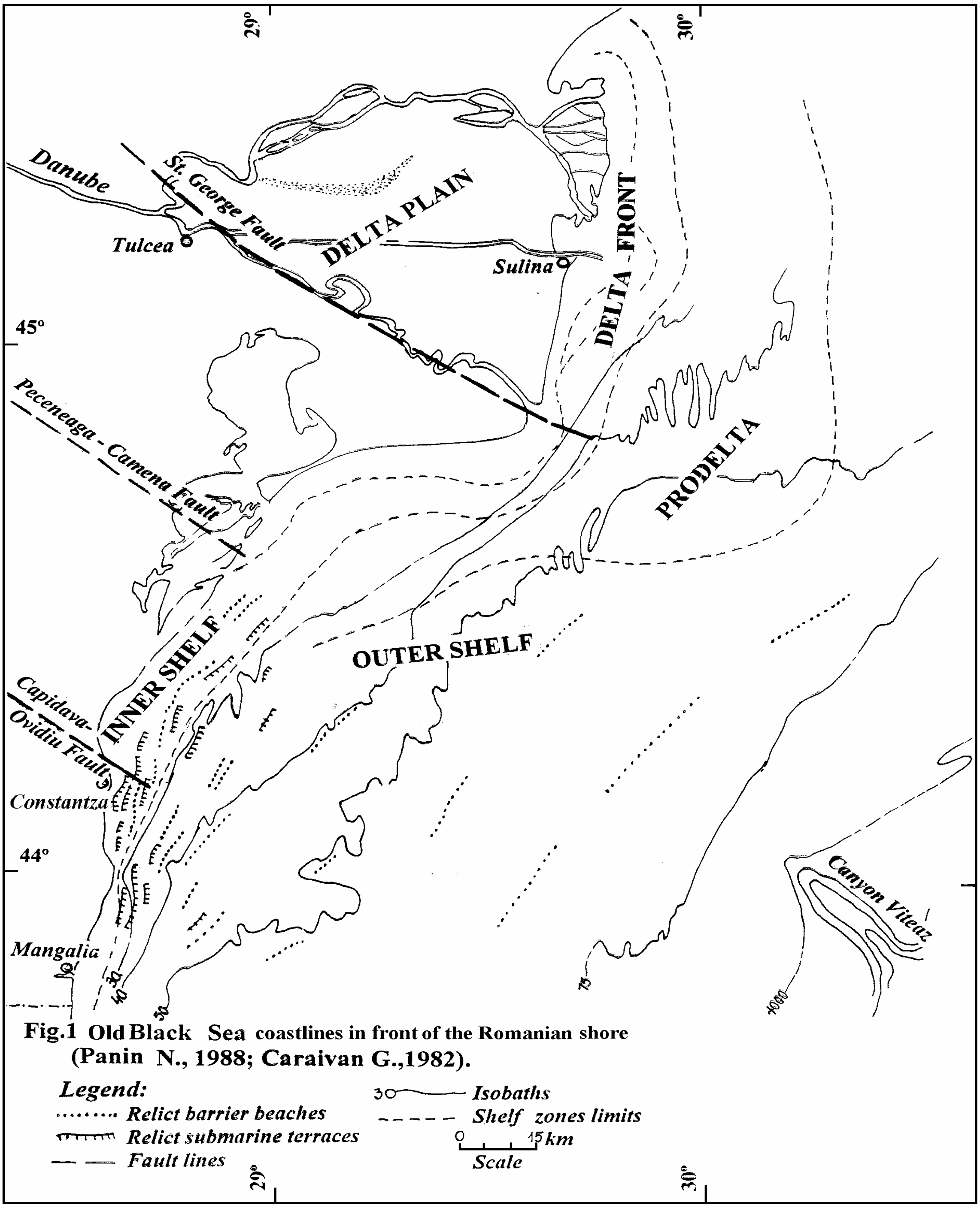

Fig.1 Old Black Sea coastlines in front of the Romanian shore (Panin N. 1988; Caraivan G. 1982)

The littoral zone is dominated energeticaly by the action of the waves (0-6 m deep) and of the coastal currents (6-12m deep) against the sea floor. This zone extends offshore up to 1000-3000m far for the coast, with a slope of 2,3-6‰ north of Constantza, and 8,4-22‰ in the southern part.

The coastal geomorphological features are the result of the combined action of several factors (from the geological to the hydrodynamical and antropogenical ones).

The littoral zone between Mussura branch and Cape Midia comprises the Danube Delta coast, including the deltaic front and its submarine slope, until 5-12m depth. It is also notable the presence of the Sahalin barrier island southward from the St.George branch's mouth.

Inner shelf

The Romanian Black Sea inner shelf is very well defined, having 10-15 km width in the northern zone, and cca 1-5 km, southward of Constantza (fig.1). The modern sediments mask locally, the relict geomorphological features. Northward of Cap Midia, the bottom slope varies between 1,1 ‰ and 4‰, while to the south of Constantza, the relict features are better preserved, especially the submarine terraces; the slope is higher (1,6-6‰).

To the east, the inner shelf border is marked by the isobathes of 27-30m.

The inner shelf sedimentary processes are dominated by the alternation of fear weather (fine sediments) and storms, during which typical "sandy sheets" are deposited.

The relative high hydrodynamic regime of the inner shelf blurred the relict accumulative features (old barrier beaches), their previous existence being marked only by the relict mineralogical and faunistic components found in the superficial sediments.

Across the inner shelf, there are many positive relief features, which are considered to be relict barrier beaches. These are disposed at the critical depths of 25m, 27m, 32m, 35m, pointing the former position of the accumulative shores. Other type of slope breaks have been interpreted to be traces of submarine terraces, disposed at the depths of 10m, 17m, 23m, 27m, 35m, indicating the position of older erosion coasts.

From a hydrodynamical and sedimentological point of view, the Danube Delta front is the equivalent of the inner shelf unit (fig.1).

Outer shelf

From its western limit, along the izobathes of 27-30m to the east, the outer shelf is developing, having a very gentle slope (below 1‰), and extending eastward until its offshore limit (about 200m depth).

The sedimentation rates are very reduced on the surface of the outer shelf so, one can find a lot of relict geomorphological features: submarine terraces, barrier beaches, and submarine valleys in the extension of the modern land rivers. The most spectacular feature is the canyon Viteaz, genetically connected with the Danube arm. St.George.

The Danube Prodelta (fig. 1), respectively the outer shelf, display all the known types of deformation processes of non-consolidated sediments (Panin N., 1988).

Romanian Black Sea shelf reveals the presence of several positive and negative geomorphological features, witnesses of the older coastal and land environments, such as: submarine terraces, barrier beaches, submarine valleys etc. (fig. 1).

2.Upper quaternary sea level changes:

The lithostratigraphycal studies of the Mamaia barrier beach drillings (Caraivan G., 1982; Caraivan G., Hertz N. and Noakes J., 1986), corroborated with the geomorphological data of the Black Sea Romanian shelf make possible the reconstruction of paleogeographic and sedimentation environment in the studied area, during the Upper Quaternary times.

The oldest strata intercepted in the Mamaia drillings are continental deposits, formed in the conditions of a very low sea level (fig. 2; fig. 3 – zones A-D3).

The 26-22m level, with marine fauna (fig. 2 – zones D4-E), surely of marine type represents the first level. According to the radiocarbon data (26.925±690 y.B.P.), this level belongs to the Middle Würm interstadial (Arcy-Stillfried B interstadial), which corresponds to the Surojskian Beds (Scerbakov F.A. et al., 1978).

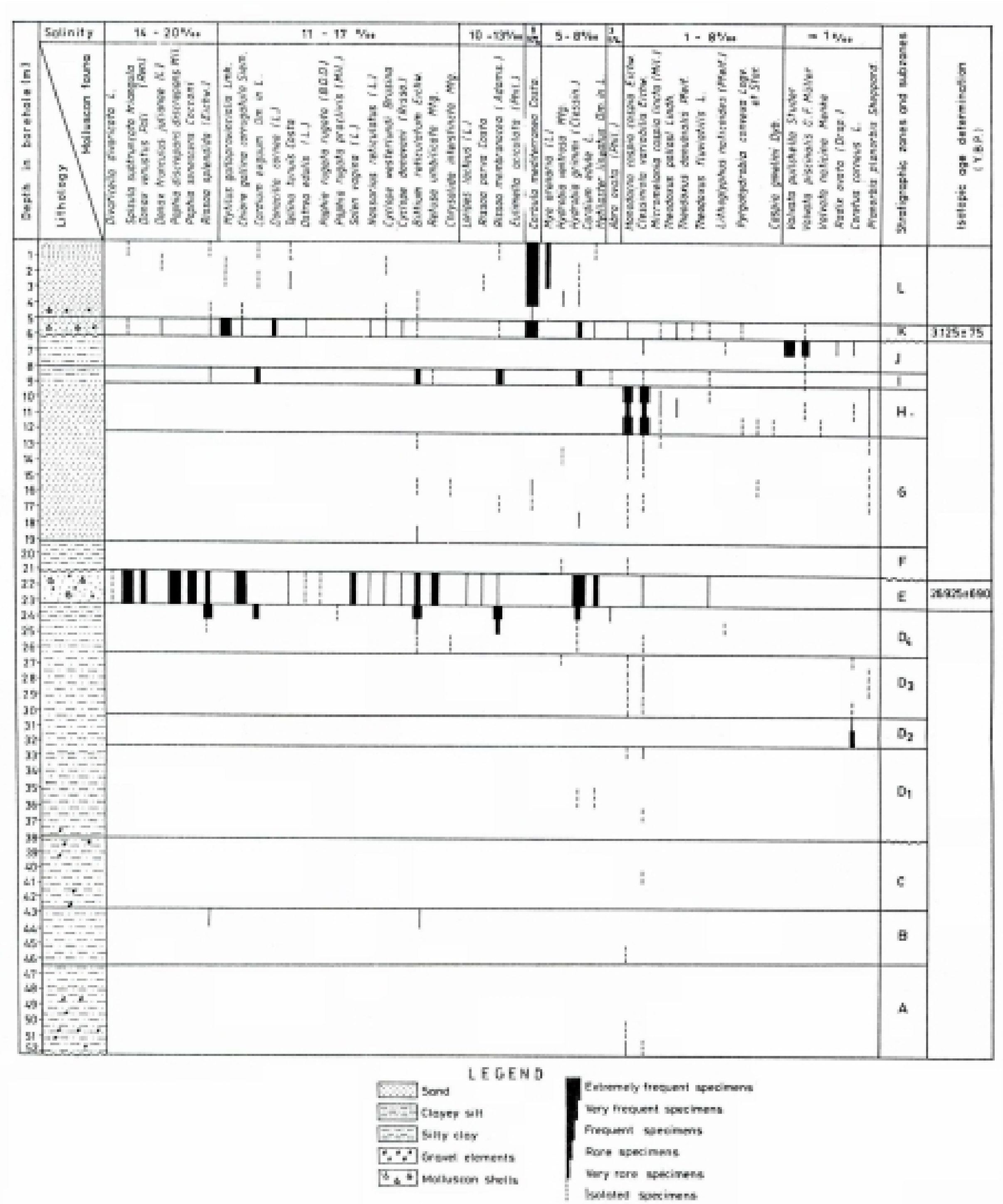

Fig.2 Mamaia North Quaternary sequence (Caraivan Gl., et al., 1986)

The Upper Würmian glaciation entails the regression of the sea level to about 100-130m below to the present day one (Ross D.A., 1978). The lowermost level is reached about 18.000-12.000 years B.P., followed than by the continuous sea level rise toward the present one. Durring this stage, the beach deposits of the zone "E" (23-22m level) from the studied borehole (Upper Surojskian Beds) are cemented under continental conditions.

The relict barrier beaches lying on the shelf at the depths of 23m and 27m are marked by the presence of red shells ("Red Coquina" – Caraivan G., 1982). Red Coquina is a bulk of coastal marine molluska shells, intensively polished and colored in red-brown. This physical state is due to a longtime reworking of the molluska shells under subaerian oxidant conditions.

We assume that the age of the relict coastal traces (terraces and barrier beaches), lying at the depths of 23m and 27m is about the same to the "beach rock" deposits about the same to the "beach rock" deposits (fig. 2; fig. 3 – zone E) from the Mamaia drilling. Both of them have been formed according to the gradual sea level retreat, during the last wurmian regression (18.000-12.000 years B.P.).

The submarine relict terraces, cut in the seaward side of the relict barrier beaches have been formed during the last rise of the sea level.

The prelude of the "Black Sea" stage (fig. 2; fig. 3 – zones F, G, H, I, J, K, L) is represented in the Mamaia zone by continental deposits, containing brackish water fauna, synchronous with the "Bugazian Beds", at the depth of 21m (fig. 2; fig. 3. – zone F).

In the same time, on the inner shelf surface appear the terraces cut in the seaward side of the barrier beaches, at the depths of 23m and 27m, containing "Red Coquina".

During the stage subsequent to the Holocene transgression, in the Mamaia zone "Viteazian Beds" have been deposited (fig. 2; fig. 3 – zone G).

In the same time, in front of the head-lands (Cape Singol, Cape Constantza, Cape Agigea), the 17m depth terraces have formed. Between these promontories long and width barrier beaches have been developed.

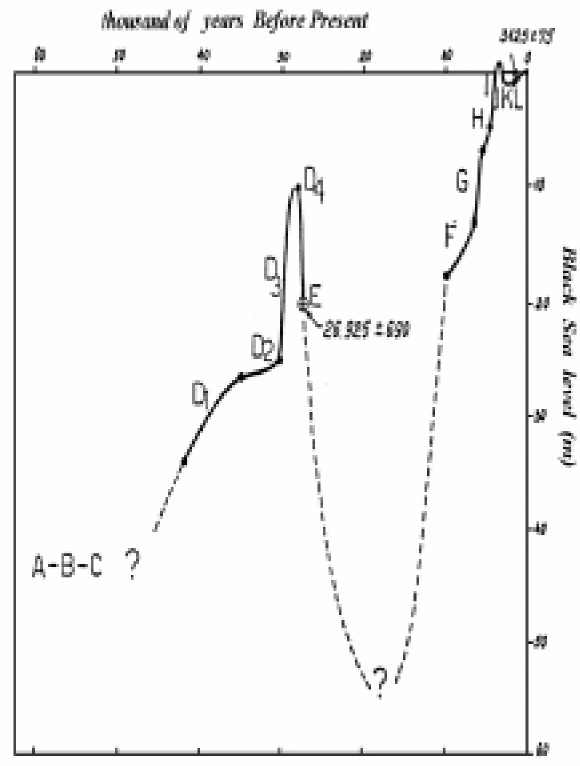

The next stage marked a continuous rise of the sea level. In the beginning of this stage ("Lover Kalamitian Beds"), the littoral waters, populated by brackish water molluska fauna, are influenced by fresh water supply. Later on, ("Upper Kalamitian Beds"), the influence of Mediterranean water becomes general. The sea level rises, being 1-2m higher than the present day one; the western cliff shores of the Siutghiol and Agigea Lakes are generated by wave abrasion.

During the next stage: Phanagorian Regression (fig. 2; fig. 3 – zone J), in the Mamaia region a widespread lagoon appeared, with characteristic peat deposits. The sea level is, probably, about 2m lower than the present day one, the witness being the relict abrasion submarine terrace, found at that depth.

The absolute age of molluska shells, taken from this bed, is 3.125±75 years B.P. The morphologic study of these shells points to their resedimentation from a lower level deposit (possible the zone I).

The last stage – The Nymphean Transgression – generalized the present – day marine conditions (fig.2; fig. 3 the zones K, L).

We emphasize the importance of the Upper Quaternary sea level changes (mainly the last 30.000 years), that determined the repeated passage of the coastline across the western Black Sea shelf.

3.Coastal erosion

Following this continuous sea level curve, from about – 130 m below the present one, about 12 – 15 000 y. B.P.) there were moments of relative stability, when accumulative and erosion coastlines have been developed. These relict physiographical features are recorded on the modern shelf surface. Their age was estimated by C^{14} determination made on molluska shells.

The modern coastline erosion processes, respectively the landward passage of the shores, was to be expected, taking into account the rising trend of the World Ocean level.

Besides, the reduction of sediment river input, especially from the Danube mouths, as well as the obstacles to longshore transport given by harbours, have induced severe erosion downward.

Previously, the shore protection was based on heavy structures (groins and breakwaters), which effect was partially positive.

Nowadays, coastal engineers realized the global character of the sea level rising, reviewing drastically the coastal protection strategies.

The heavy structures are gradually abandoned, and new geotextile submerged groins and breakwaters are projected. The last ones make possible rapid modifications and adjustment, requested by the induced effects upon the coastal dynamics.

The beach monitoring becomes more and more important.

4.Bibliography

[1] Caraivan, G. 1982 – *The sedimentological study of the beach and inner shelf deposits in front of the Romanian coast between Portitza*. Thesis.

[2] Caraivan, G. 1982 – *Upper Quaternary evolution of the Mamaia zone.* – Pontica, 15, p. 15-32

[3] Caraivan, G. and Selariu, O. 1985 – *Quaternary environmental changes of the Black Sea* – Rev. Roum. Geol., Geophys., Geogr. Geographie,Tome 29, p.13-19

[4] Caraivan, G., Hertz, N. and Noakes, J. 1986 – *New proofs of the Black Sea rise during the Middle Wurm interstadial.* – D.S. Inst. Geol. Geofiz., vol. 70-71/5, p. 57-62

[5] Panin, N. 1983 - *Black Sea coastline changes in the last 10.000 years. A new attempt of identifying the Danube mouths as described by the ancient*.– Dacia, N.S. 27, 1-2, p. 175-184

[6] Panin, N. 1988 – *Danube Delta: genesis, evolution, sedimentology,* - Rev. Roum Geol. Geophys., Geogr. Geographie, 33, p. 25-36

[7] Ross, D.A. 1978 – *Summary of results of Black Sea drillings, in: Initial Reports of the Deep Sea* Drilling Project, XLII, 2

[8] Scerbakov, F.A. et al. 1978 - *Osadkonakoplenie na kontinentalinoi okraine Cernogo Moria, Izd. Nauka*, Moskva, 210 p.

[9] Wong, H.K. et al. 1994 – *Morphology and post Chaudian (Late Pleistocene) evolution of the submarine Danube fan complex*. – Terra Nova, 6.

Studies Regarding the Evaluation of the Impact of the Industrial Area on the Soil and Ground Water

Ioan CRĂCIUN[a] Roxana BOLBA[a] Petru CERCEL[a]

[a]*Tehnical University "Gh.Asachi" Iassy , Iassy, Romania*

Abstract: The ground water quality management is very important for the drinking water supply and the evaluation of the ground water contamination risk. Using the mathematical modeling we can realize an image about the risk zone and for the elaboration of the preventive steps.

Keywords: environment, industrial activity, pollutants, soil, ground water, mathematics modeling, risk evaluation, water quality management

1. Introduction

For underground water quality management and soil and for determining the tolerance level of the environment regarding the pollutants we can to effectuate risk analysis. We can to determine if the aquifer water used for water supply can be utilized for drinking water supply, the risk for contamination of the resource and the impact of the human activity regarding these resources.

This analysis can be effectuated using adequate mathematical models on the make: creating a reference data base in correlation with legislation, to avoid different analysis which guide at divers results, using the same calculus methods for the basic parameters, guaranteed an active control of the authorities.

The results can be utilized for risk analysis regarding the human health and environment, the connection of the database at a cartographic support for analysis of the sire risk [1].

2. The analysis of the data

The models contain a database with limit concentrations of the principal pollutants which can be in the soil and ground water, being confronted with the observed and monitories drawing data.

This admissible concentration can be actualized depending with the legislation.

Another analysis can be the hazard studies:

- the analysis of the potential exposed receptors (the people and ground water resources) at the contamination risk;
- the accomplishment for each substance of the toxicological studies for defining of the admissible limits for cancerous and non-cancerous substance;
- the analyze of the admissible levels of the proposed risk depending of the legislation [3].

3. Input data

The collected data from the site used are: the concentration of the each contaminant in soil [mg/kg]; the concentration of the each contaminant in ground water [mg/l].

If we have detected the hydrocarbons in the soil we can divide this in two groups: light hydrocarbons with C<12 and high hydrocarbons with C>12.

3.1. Levels analysis

In the first level are visualized the detected contaminants in the analyzed site and the accepted limits of the normative. For the soil we can analyze two types of the limits in term of utilities: residential and public; industrial and commercial.

The model makes a comparison for the admissible limits of these utilities for soil contaminants and ground water.

In the second level we can analyze the contaminants which passed the admissible level; the concentration from superficial and profound soil; the

ISSN-12223-7221

way by we can produce the contamination; the establishment of the risk level of the site [5].

3.2. The conceptual model

The analyzed site should be defined in term of utilities.

The characteristics of the site should be analyzed for all contamination possibilities of the aquifer: the covered type of the soil; the existence of the access zone protected by the pavement concrete; the existence of an aquifer in the studied site.

For the people we can define the possibilities of the contacting with the contaminants: derma contact; dust inhalation in the enclosure; the dust inhalation in the open area; the vapors inhaled from enclosure by the superficial soil; the vapors inhaled from open area by the superficial soil; the vapors inhaled from enclosure by the profound soil; the vapors inhaled from open area by the profound soil; the migration of the contaminants from soil on the surface [3].

The migration of the contaminants from the site may be: the vapors from enclosure, from open area and the migration of the dissolved phase in aquifer.

The results of this analysis based by any site observation can be:

-risk analysis for cancerous substances; for this substances the risk represent the probability to developed of any cancerous formed during the life an we can calculate this by the formula:

$$\text{Risk} = CDD \cdot S_f \tag{1}$$

where:
CDD is the daily critical dose accumulated by the human receptor, which is finding in the site;
S_f, is the toxicological parameter for cancerous substances $[mg/kg/day]^{-1}$.

For an industrial area CDI is calculate in function by a maximal daily critical quantity MCD using the formula:

$$CDD = \frac{MCD \cdot TE}{D} \tag{2}$$

where:
TE is the time of exposition [years];
D, is the average duration of the life [years].

In the case of a scenario for residential public utilities we can calculate CDD from an average between MCD calculated for children and the adults

$$CDD = MCD_{ch} \cdot ED_{ch} + \frac{MCD_{ad} \cdot ED_{ad}}{L} \tag{3}$$

The formula used for CDI and DMI appreciation can be detailed:

MDI by the contaminants accumulation in the soil [3]

$$MDI = \frac{Cs \cdot IS \cdot 0{,}000001 \cdot EF}{BW \cdot 365} \tag{4}$$

where:
Cs is the concentration from soil [mg/kg];
IS, the accumulated quantity in the soil [mg/day];
EF, the exposition frequency [day];
BW, the weight [kg].

MDI from the vapors exhalation from the contaminated superficial soil

$$MDI = \frac{V_{so} \cdot B_0 \cdot EF}{BW \cdot 365} \tag{5}$$

where:
V_{so} is the vapor concentration exhalation by the contaminated soil [mg/m^3];
B_o, is the inhalation rate [m^3/day];
EF, is the exposition frequency [day];
BW, the weight [kg].

$$V_{so} = \frac{1000 \cdot E_i}{U_{air} \cdot W \cdot \delta_{air}} \tag{6}$$

where:
U_{air} is the velocity of the wind about the soil in the mix zone of the contaminants [m/s];
W, the breadth of the pollutants sources by the wind direction [m];
E_i, the emission rate of the vapors [g/s]; δ_{air}, the height of the mix zone [cm] [2].

$$E_i = \frac{Cs \cdot \rho_s \cdot H}{1 \cdot 10^6 \cdot ((\theta_{as} \cdot H) + \theta_{ws} + (\rho_s \cdot K_d))} W \cdot D_s^{eff} \cdot \frac{1}{Ls} \quad (7)$$

where:
θ_{as} is the fraction of the air from soil;
θ_{ws}, is the water fraction from soil;
ρ_s, the dry density of the soil [g/cm^3];
D_s^{eff}, the diffusion coefficients of the vapors from air [cm^2/s];
L_s, the deep of the contaminated zones [cm];
H, the Henry constant;
K_d, the rapport water/soil [l/kg].

MDI due by the below ground vapors [4]

$$MDI = \frac{V_{gi} \cdot B_i \cdot EF}{BW \cdot 365} \quad (8)$$

where:
V_{gi} is the vapor concentration by the below ground [mg/m^3];
B_i, the inhalation rate [m^3/day];

$$V_{gi} = \frac{H\left[\dfrac{D_{ws}^{eff} / L_{gw}}{ER \cdot L_B}\right]}{1 + \left[\dfrac{D_{ws}^{eff} / L_{gw}}{ER \cdot L_B}\right] + \left[\dfrac{D_{ws}^{eff} / L_{gw}}{(D_{fr}^{eff} L_{fr})\eta}\right]} 10^3 C_{gw} \quad (9)$$

where:
D_{ws}^{eff} is the diffusion effective coefficient between the aquifer and the surface;
L_{gw}, the deep of the aquifer [cm];
ER, the change rate of the air in the enclosure [1/s];
D_{fr}^{eff}, the diffusion effective coefficient of the fissured soil;
L_{fr} the depth of the building foundation [cm];
η, the fraction of the existed fracture in foundation;
C_{gw}, the concentration in the aquifer.

$$D_{ws}^{eff} = (h_{cap} + h_v)\left[\frac{h_{cap}}{D_{cap}^{eff}} + \frac{h_v}{D_v^{eff}}\right]^{-1} \quad (10)$$

where:
h_{cap} is the depth of the capillary band [cm];
h_v, the depth of the unsaturated zone [cm];
D_{cap}^{eff}, the effective diffusion coefficient in the capillary band;
D_s^{eff}, the effective diffusion coefficient of the soil in function of the concentration of the gaseous phase.

- Risk analysis for no cancerous substance

For this substance the risk can be calculated with the formula:

$$HI = MDI/TDI \quad (11)$$

where:
MDI is the maximal daily dose of the no cancerous substances receipted by a human subject in the site;
TDI, the toxicological parameter for no cancerous substances (tolerable daily dose) [7].

- Risk analysis for the site

In the analysis of the risk for the site should make a confrontation between the concentration of the each contaminant and the acceptation limits in the reference point. This point can be: near by the source, at an intermediary distance by the source and the limit of the study zone (down stream by the source), at a distance by the source at the middle between zone study and an intake point of the ground water.

- Residual admissible concentration (CRA)

The saturated concentration for a contaminant can be calculated by the following formula:

$$C_{sat} = \frac{S}{\rho}(K_d \cdot \rho + \theta_w + \theta_a \cdot H) \quad (12)$$

where:
C_{sat} is the saturation concentration of the soil [mg/kg];
S, the solubility [mg/l];
K_d, the rapport water/soil [l/kg];
ρ, the dry density of the soil [kg/l];
θ_w, the fraction of the water in the soil;
θ_a, the fraction of the air in the soil;
H, the Henry constant.

4. Application for hydrographic basin Bahlui

In the hydrographic basin Bahlui a sensible zone is the site of the medicament factory S.C. Antibiotice

Iaşi. In a geological drilling are effectuated a study regarding the risk of contamination of the soil and ground water for the finding contaminants (Table 1) [1].

Table 1 - The contaminants values for
S.C. Antibiotice S.A. Iaşi geological drilling

Zinc mg/l	Iron mg/l	Manganese mg/l
2.34	2.30	70.0

Source: C.N. Apele Române, Filiala Iaşi

4. Conclusion

The analysis makes by the model we find that two contaminants passed the admissible limits: the iron with 2.1 mg/l and the manganese with 69.95 mg/l [1].

Basing these values and the characteristics of the study zone we draw the conclusions:

- is not a risk contamination for the workers of the factory;
- the existence of a risk contamination (no cancerous) for water resources by the existence of the iron (CR=11.5) and manganese (CR=1,400) [6].

5. References

[1] Crăciun I., *Modele matematice de gospodărirea calităţii apelor*, Referat nr. 2, 2001, U.T.C. Bucureşti
[2] Giurma I., Crăciun I., Giurma C.-R., *Hidrologie şi hidrogeologie-aplicaţii*, Ed. "Gh. Asachi" Iaşi, 2001
[3] *** *Drinking Water Guidelines,* O.M.S., 1989
[4] *** *Risk Based Corrective Action Applied at Petroleum Release Sites*, ASTM, 1995
[5] *** *Supplementary Risk assessment Guidance for Superfund,* USEPA, 1989
[6] *** *Limitele de încărcare cu poluanţi a apelor uzate evacuate în resursele de apă* (c., HG 730/1997), Colecţia de STAS-uri
[7] *** *Health Effects Assessment Summary Tables,* USEPA, 1989

The Validation of the Mike 11 - N.A.M. Hydrological Model on the Hydrographic Basin Bahlueț

Ioan CRĂCIUN[a]
[a]*Technical University "Gh.Asachi" Iassy, Iassy, Romania*

Abstract: The mathematical modeling can be an instrument for the quantitative management of the water surface. The measurements makes for the limiting of the negative effects depends to the mathematical model used and our performances.

In this paper we present the validation procedure of the Mike11 model, using the hydrological data from the Bahluet hydrographical basin, in the section Târgu Frumos (Iaşi county) using the land phase and underground parameters of the hydrological cycle.

Keywords: hydrographical basin, hydrological cycle, mathematical modeling, water surface management

1. Introduction

The Mike 11 model was elaborated by Danish Hydraulic Institute and the hydrological module (NAM-Nedbor Afstromning Modele) can be is used for the procedure of validation. The input data are the elements of the hydrological cycle of the land phase [4].

2. The presentation of the hydrographical basin Bahluet

The hydrographical basin Bahlueț is placed in the N-V of the Iasi country in the Moldova Plateau, between Jijiei Plain and Barlad Plateau.

The surface in the cross section Targu Frumos is 77.5 km^2. In this basin not exist storage lakes, which can make any influence to the flow by the attenuation of the flood. The period analyzed is three years long covering 1994,1995 and 1996 [1].

The hydrological characteristics of this period are presented in the Table 1.

Table 1

Characteristics	1994-1995	1995-1996
Rain [mm/year]	381.8	561.3
Evaporation [mm/year]	267.8	305.9

3. The structure of the Mike 11-NAM model

The structure of the model Mike 11–NAM are presented in the figure 1 [2,3].

The parameters of the schema showed in the figure 1 are:

S.T. snow stock;
V.T. Vegetation stock tank;
S.S. surface stock tank;
P rain;
Ep, evapo-transpiration;
Ea, evaporation to the surface soil;
U, humidity of the vegetation;
Pn, net rain;
Q_{IF}, runoff flow;
L/L_{max} linear variation of the water stock in the soil;
CKi, time of the hypodermic flow;
PN the excess rain which flow to the hydrographical network or is infiltrate in soil;
Q_{OF}, the part of PN which go to the surface flow;
G, percolation;
GWLBFo, the distance between the superior level of the aquifer GWL and the water level in the river;
BF, base flow;
CAFLUX, capillary flux [4,5].

ISSN-12223-7221

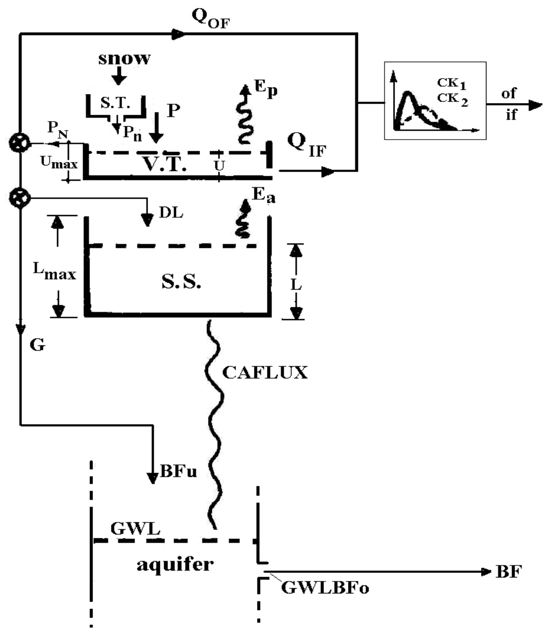

Fig. 1. The tank structure of the model Mike11- NAM

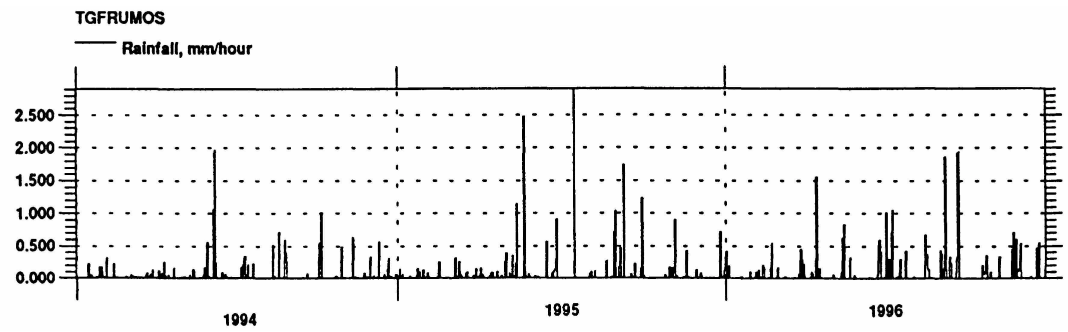

Fig. 2. The rain series between 1994-1996

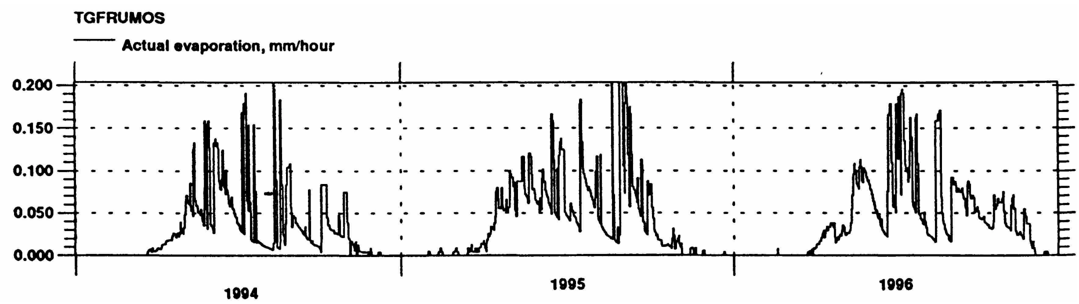

Fig. 3. The evaporation series between 1994-1996

The necessary data for the validation of the model are:

- meteorological data: rainfall series with daily values (fig.2), actual evaporation series calculated in function of the potential evaporation and by the soil humidity (fig.3) and temperature like average daily values (fig.4);

- supplementary data appreciate to the scale of the basin: hypodermic flow (depending by the water stock variation of the soil), surface flow, data regarding the infiltration and percolation to the aquifer, the stocking in the aquifer, the value of the base flow and the capillary flux [3,4].

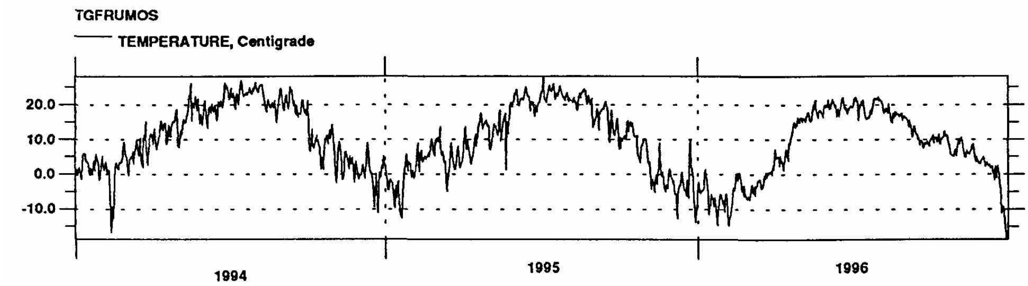

Fig. 4. The temperature series between 1994-1996

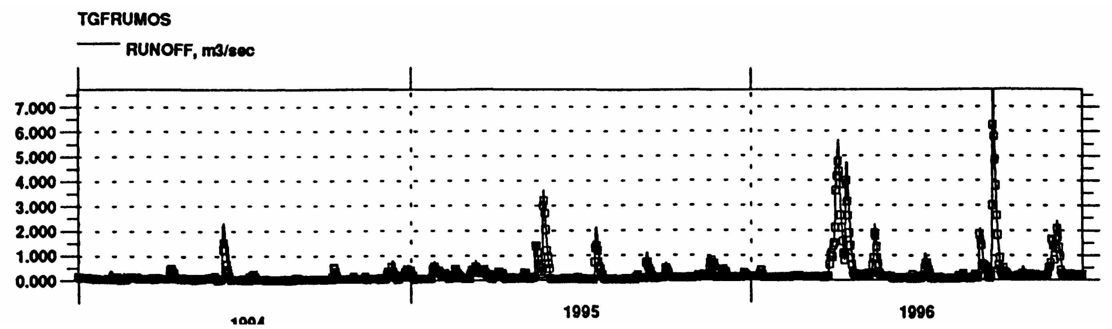

Fig. 5. The measured and simulated runoff on the cross section Târgu Frumos

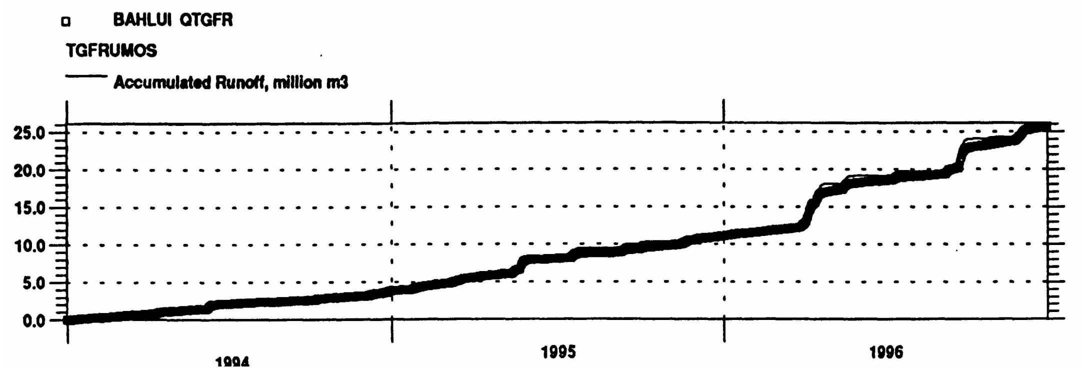

Fig. 6. The measured and simulated accumulated runoff on the cross section Târgu Frumos

4. Conclusions

The results of the validation using the Mike11-NAM model are presented in the figure 5 (the runoff measured and simulated) and figure 6 (the accumulated runoff) on the cross section Târgu Frumos.

We can observe a good correlation between the simulated and measured runoff. In the case of the higher values corresponding with the overflow the correlation isn't very good but this hydrological phenomena is very complex.

The accumulated runoff is enough good simulated being in the 1996-year any non-concordances.

5. References

[1] Crăciun I., *Modele matematice de gospodărirea calității apelor*, Referat nr. 2, 2001, U.T.C. Bucuresti

[2] Crăciun I., *Gestion des eaux de surface su bassin versant Bahlui, utilisant de modélage mathématique*, Buletin I.P.Iasi, Tom XLIII(XLVII), Fasc. 1-4, Sectia VII, Hidrotehnica, 75-84, 1997

[3] Giurma I., Crăciun I., Giurma C.-R., *Hidrologie şi hidrogeologie-aplicații*, Ed. "Gh.Asachi" Iaşi, 2001

[4] *** Mike 11, Version 3.01, *NAM Reference Manuel*, Danish Hydraulic Institute, 1992

[5] *** Mike 11, Version 3.01, *User Manuel*, Danish Hydraulic Institute, 1992.

A Study on Waves and Beaches Protection

Mihai FLOREA[a] Corneliu Dan HÂNCU[a] Ichinur OMER[a]

[a]*University "Ovidius" Constantza , Constantza, România*

Rezumat:În această lucrare sunt prezentate câteva soluții tehnice pentru protecția plajelor. Lucrările propuse ar trebui să fie executate sub nivelul apei pentru a nu schimba peisajul natural. Au fost realizate cercetări hidraulice pentru a hotărâ dimensiunile minime ale prefabricatelor din beton care să aibă eficiență în atenuarea efectului distructiv al valurilor asupra plajei. Se propune amplasarea acestor prefabricate pe curba batimetrică de –3m. Soluția propusă duce la un consum mai mic de beton pe 1m de construcție în comparație cu soluția clasică cu stabilopozi realizând şi o protecție mai bună a plajei.

Abstract: : In this paper are presented some technical solutions for beaches protection executed under water level, so as not to be visible from the coast. At last, making some hydraulic researches, minimal dimensions of the concrete prefabs to be used was established. This prefabs have to be located approximate parallel with the coast, on 3m bathymetric contour. These prefabs were calculated on floating. They can be make up on the beach, on the prefab platforms. Then they have to be transported by floating and placed on their site. For approach evaluations of the costs per meter of protection, the concrete volume was determined. Also, to execute these works the equipments and transportation means capabilities were determined. To finalise the designing of these works are necessary strength and tiredness calculus. We appreciate that by the studied solutions we can execute a higher protection of the beach as compare with classical protection which exceed water level.

Keywords: beaches protection; precast units; under water protections.

1. Introduction

The present paper is structured in two parts, noted by A and B.

In the first part we make some general commentaries concerning the problems which must be studied and some constructive solutions. In the second part we present two protection solutions studied in the hydrotechnical laboratory of the Civil Engineering Faculty Constantza.

2. The analysed solutions

2.1. In the region near the beaches, where the water level is relative small, the most part of the waves' energy is dissipated, respective one part of these energies are transmitted to the solid foundation bed and they produce the movement of the sand.

This phenomenon is very complex because is influenced by local topographical, hydrometeorological and geological factors. So, in present, we don't know efficient solutions valuable to all cases.

To the erosive actions of the waves, it is necessary to add the marine current effect, which transport the sediments dislocated by the water waves actions, especially in the breaker moment.

About the complexity of this phenomenon we must take count that it possible to adopt different solutions with some typical of restrictions: for example in the touristic zone where the protection works do not debase the landscape.

The problems that our team considers necessary to be solved are:

– a greater attention about the solid foundation bed in the zone in front of the beach zone (avanshore), because from this zone begins the erosive process

ISSN-12223-7221

– the protection position to a bigger or smaller distance from the shore line

– the optimal water depth where must be placed the protection work

– most of the executed works were destroyed by the creep of the foundation ground.

– We must study thoroughly the interaction between water wave and foundation ground.

Concerning the constructive solutions, we consider that the protection solutions with concrete dam stopping which exceed the hydrostatic level, ripraps and stabilopods are not the best solutions because they present the following disadvantages relative to the interaction water wave - foundation ground:

– local bearings on the solid foundation bed, which lead to uneven pressure on the foundation ground

– a good water wave's energy dissipation. This dissipation has also negative effects through concentrations of the local courents in the foundation zone. We obtain an intense carrying away of the light fractions.

– the most of the construction materials is posed in the smallest strain forces produced by the water waves.

For executed the protections, the designer must have accurate elements concerning:

a) under water protections or the protections which exceed the hydrostatic level

b) massive protections from heavy elements (stone blocks, concrete precast units with or without shell from stabilopods) or protections from cellular concrete precast units.

c) protections placed near or farther the coast

d) protections extended until the solid foundation bed or limited protections only to the top of the section

e) fixed protections, which work all the time or a protection which functions only the cold period of the year when the most of storms are taking place. For the second type of protection there are possible many constructive variants with partial or complete mobile protections.

f) rigid or flexible protections.

What conclusion can we formulate? It is very difficult to justify and design a cheep and safe beach protections because:

– the complex character of the beach erosion phenomenon

– many possible solutions

– absence of the systematic national laboratory researches or through pilot stations

Maybe in this stage a logical solution will be one similarly to those used in historical monument protection: international contest to choose the best protection solution for every beach sector.

2.2. The research team of the Civil Engineering Faculty from Constantza is interested in some problems of coastal engineering aspects. For example we mention the educational master form "Coastal and harbour engineering" which was established in 1998. In our faculty also exists the PhD activity in this speciality.

Along the time, in our hydraulic research laboratory we made some theoretical and experimental studies. In the following paragraphs we present some of the these researches.

The protection efficaciously was appreciated by a mitigation coefficient of the water wave height define by the next relation:

$$c_{at} = \frac{\Delta H}{H_{am}} = \frac{H_{am} - H_{av}}{H_{am}} = 1 - \frac{H_{av}}{H_{am}} \tag{1}$$

H_{av} - water wave height behind the obstacle
H_{am} - water wave height in front of the obstacle

Hydraulic modelling, using Newton and Froude similarity criteria made the research. The lengths scale, adopted function the laboratory possibilities was 1:10. The height of the water waves considered was H = 2m. The natural considered depth of water was 3 m, which in laboratory is corresponding to 30 cm.

The studied models can be surrounded in two types:

A. Protections executed from under water grates posed: horizontally, vertically, oblique or combinations of these. We appreciate that these grates don't realise individually an efficient protection, obtaining an attenuation coefficient until 25%.

B. Protections from cellular concrete precast units like the water basins used for the energy dissipation to the waterfalls. In the end we recommended this variant because it presents advantages concerning the foundation: small pressures on the foundation ground, uniform allotment and more difficult carrying away of the light fractions from the foundation ground.

3. Recommended variant:

Out off technical and economical reasons the optimal variant resulted were those, which was executed a cellular concrete precast unit of 7 meters length. In this case, the energy dissipation is made about 50%. This dissipation by the water from cellular concrete precast unit is materialised in the same mode as in hydroelectric plants dissipation basin.

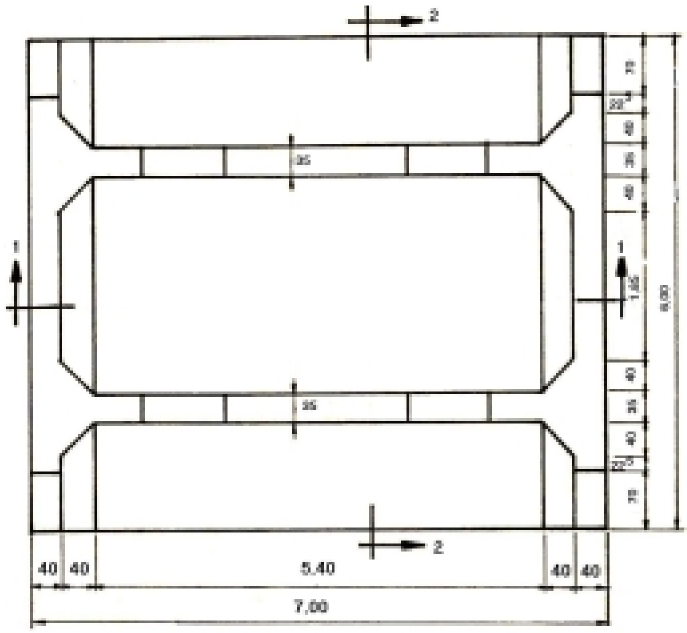

a)

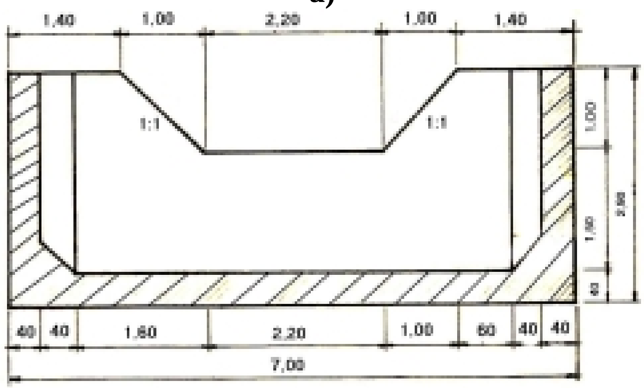

b)

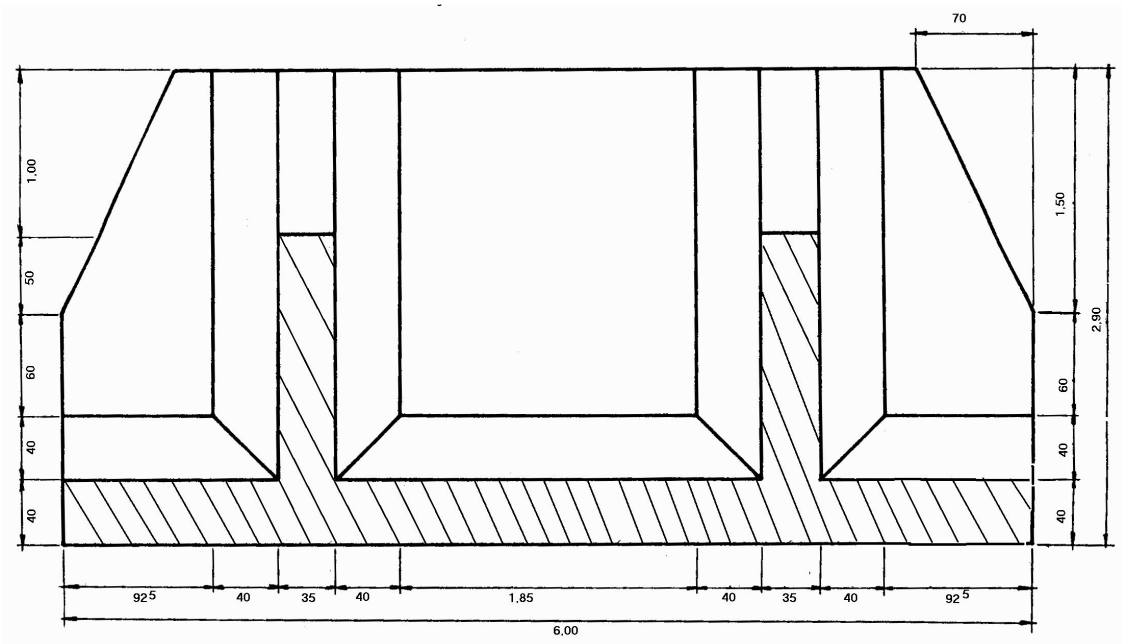

c)

Fig. 1Cellular concrete precast units type I:
a) Plan**; b)** Section 1-1**; c)** Section 2-2

This is why we considered two types of cellular concrete precast units numbered I and II. Precast unit number I consists of 38,75 mc of hydrotechnical concrete, that means about 93 tones. It assures protection for 6 meters of beach. (Fig.1)

Precast unit number II consists of 22,61 m^3 of hydrotechnical concrete, that means about 54,27 tones. It assures protection for 3,5 meters of beach. (Fig. 2).

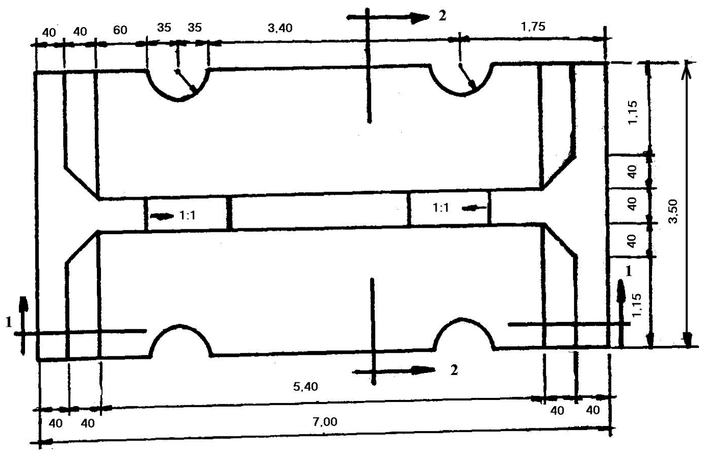

a)

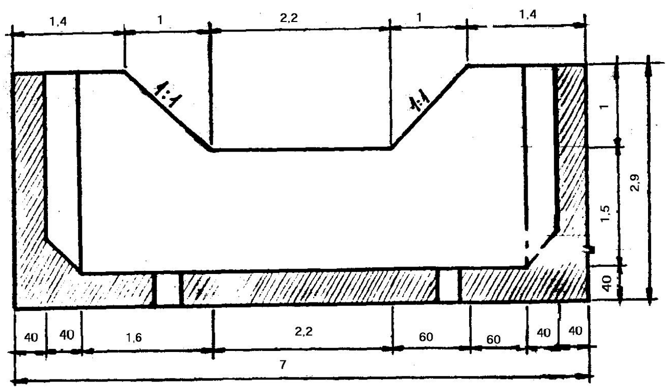

b)

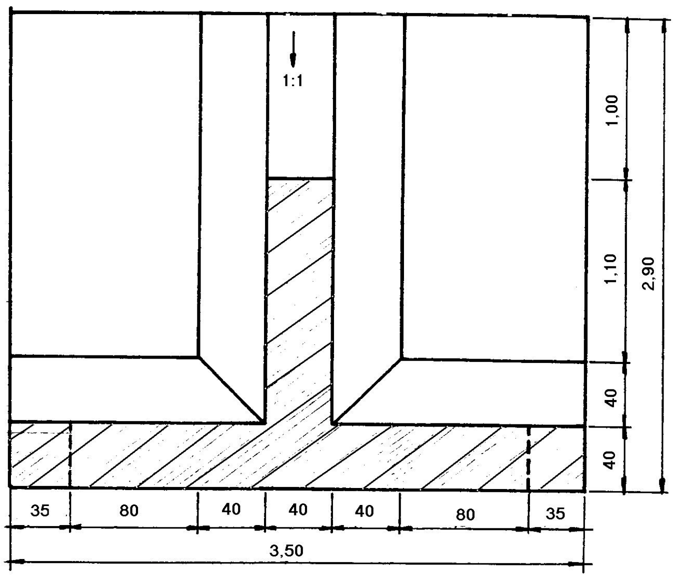

c)

Fig. 2 Cellular concrete precast units type II:
a)Plan **; b)**Section 1-1 ; **c)**Section 2-2

Concerning the researches with these types of protections we found:

- the attenuation degree decreases with model length diminishing
- for length between 10 and 7 meters attenuation degree decrease is relative reduced
- for length between 6 and 5 meters the decrease become appreciably.

5. Conclusions

In this paper we present some problems concerning the beaches protections solution choosing. This solution must be analysed in larger background than usual one. It has to be verifying by experimental researches.

We present main possible variants. We detailed and recommended one solution by cellular concrete precast unit. The experimental researches were made in the Civil Engineering Faculty of Constantza laboratory.

References

[1].Shore *Protection manual*, CERC, Washington, 1984;

[2].David A. Ross - *Intorducere în oceanografie*, Ed. Ştiinţifică şi encicopedică, Bucureşti, 1976;

[3].R. Craig - *Marine Phisics*, Academic London Press, 1975;

[4].A. Spătaru - *Construcţii costiere şi acvatorii*, Ed. Tehnică, 1990;

[5]*Studii de Hidraulică XXXII*, ICIM, Bucureşti, 1991;

[6].Leo C. van Rijn - *Principle of Fluid Flow and Surface wave in rivers, estuaries, seas and oceans,* Aqua Publications, 1994.

Close Downstream Control Algorithm for Irrigation Canals

Nicolae MARCOE [a] Adrian PRICOP[a]

[a]*Tehnical University"Gh. Asachi" Iassy, Iassy, România*

Rezumat: Se propune un model matematic pentru controlul local aval al canalelor de irigații echipate cu regulatoare de nivel. Algoritmul de control se bazează pe soluționarea pe cale numerică a ecuațiilor Saint Venant printr-o schemă în diferențe finite de tip explicit. Testarea algoritmului s-a realizat pe un canal format din trei biefuri separate de două stavile plane verticale.

Abstract: In this work is proposed a mathematical model for close downstream control of irrigation canal systems. The control algorithm is based on numerical solution of Saint Venant equation using a finite difference scheme by explicit type. Algorithm testing is done on an irrigation canal with three pools separated by two vertical rectangular gates.

Keywords: Automation, canal irrigation system, unsteady flow, explicit method.

1. Introduction

Different types of control method have been developed for the operation of irrigation canals. The advantages and disadvantages of many schemes have been discussed by a number of authors [Buyalski et al. 1991; Goussard 1993]. Control schemes are generally divided into upstream control and downstream control. In a system operated with upstream control, water is released from the intake according to the prediction of water demand in the system, and the adjustment of each gate is based on the information upstream from it. Due to the difficulty of predicting precisely the actual water demand, the water users at the downstream end of the system often receive either excessive or insufficient water. Water release and demand, however, is better matched in a system operated with downstream control, in which water is released in response to the actual water withdrawal from the system, and the adjustment of each gate is based of the information downstream from it. Another advantage of this type of control is that users can take water whenever they need it. In a system operated with close downstream control, a target water level is maintained immediately downstream from each gate (at the upstream end of each pool), or at the downstream end of the pool.

A close downstream control algorithm implemented with a finite difference method (explicit method) is discussed in present paper. A constant water level is maintained at the downstream from each gate. Since it is able to take into account all physical parameters of the system and the dynamics of flow transients, this algorithm can be applied to different canal systems ant it provides an effective control of abrupt disturbances.

2. Basic equations

2.1. Channel equations:

The Saint Venant equations are the governing equations describing one-dimensional unsteady flow in open channels. They consist of the continuity and the dynamic equation. After Popa (1997):

$$\frac{\partial h}{\partial t}+\frac{A}{B}\cdot\frac{\partial U}{\partial x}+U\cdot\frac{\partial h}{\partial x}+\frac{U}{B}\left(\frac{\partial A}{\partial x}\right)_{h=const}=0 \qquad (1)$$

$$\frac{\partial U}{\partial t}+U\frac{\partial U}{\partial x}+g\cdot\frac{\partial h}{\partial x}+g\cdot\left(S_f-J_f\right)=0 \qquad (2)$$

where A – wetted cross sectional area; t – time, Q – discharge; x – horizontal co-ordinate in the flow

ISSN-12223-7221

direction; g – gravitational acceleration; h – water depth; J_f – bottom slope of the channel; S_f – friction slope; and U – constant cross sectional mean velocity.

2.2. Gate equations

The flow through a rectangular vertical gate under free and submerged flow conditions can be described as (Kiselev, 1988):

$$Q = \varphi \frac{b \cdot \varepsilon \cdot a}{\sqrt{1 + \varepsilon \frac{a}{H}}} \cdot \sqrt{2gH_{up}} \qquad (3)$$

$$Q = \mu \cdot a \cdot b \cdot \sqrt{2g\left(H_{up} - H_{dw}\right)} \qquad (4)$$

where φ – head loss coefficient ($\varphi = f(Fr)$; Fr – Froude number); ε – contraction coefficient ($\varepsilon = f(a/H_{up})$); a – opening gate; H_{up} – upstream depth; H_{dw} – downstream gate; b - gate width; and μ – discharge coefficient.

3. Explicit method

The governing equations (1) and (2) cannot be solved analytically, but must be solved by a numerical approximation method. The most directly method for solution of equations (1) and (2), is *explicit method* (based on Euler method by first order) which use an explicit scheme with finite differences at fixed temporal steps (Graf, 1993).

Schematic definition is done in Fig. 1: there is a grid points with point P, projected on plan, x and t; Δx being distance interval and Δt – time interval between the grid points.

The known conditions, U_L, h_L and U_R, h_R, at temps $t = t$, are used for explicit express of unknown conditions, U_P, h_P, after temporal step Δt, which mean at the time $t = t + \Delta t$.

Partial derivates of Saint Venant equations are approximated using finite differences as:

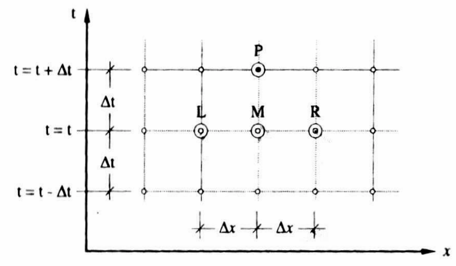

Fig. 1. Finite differences scheme used in explicit method

$$\left.\frac{\partial U}{\partial x}\right|_M = \frac{U_R - U_L}{2\Delta x} \qquad \left.\frac{\partial h}{\partial x}\right|_M = \frac{h_R - h_L}{2\Delta x}$$

$$\left.\frac{\partial U}{\partial x}\right|_P = \frac{U_P - U_M}{\Delta t} \qquad \left.\frac{\partial h}{\partial t}\right|_P = \frac{h_P - h_M}{\Delta t} \qquad (5)$$

For a rectangular canal, replacing these relations (5), into the continuity equation (1) leads to:

$$h_P = h_M + \frac{\Delta t}{2\Delta x}\left[U_M\left(h_L - h_R\right) + h_M\left(U_L - U_R\right)\right] \qquad (6)$$

Replacing relation (5) into the dynamic equation (2) leads to:

$$\frac{U_P - U_M}{\Delta t} + U_M \frac{\left(U_R - U_L\right)}{2\Delta x} + g\frac{\left(h_R - h_L\right)}{2\Delta x} = g\left(J_f - J_e\right) \qquad (7)$$

where J_e is energetic slope. It can express:

$$J_e = \frac{\left|U_P\right| U_P}{R_{h_P}^{4/3}} n^2 \text{ and } \Gamma = \frac{R_{h_P}^{4/3}}{n^2} g\Delta t \qquad (8)$$

where R_{hP} – hydraulic radius in section corresponding of point P; and n- Manning coefficient.

Simplified, it can be written:

$$U_P^2 + \Gamma U_P - \Gamma\beta = 0 \tag{9}$$

where:

$$\beta = \left[U_M + \frac{\Delta t}{2\Delta x} U_M \left(U_L - U_R\right) + \frac{g\Delta t}{2\Delta x}\left(h_L - h_R\right) + g\Delta t J_f\right] \tag{10}$$

Equation (9) is quadratic, and results U_P:

$$U_P = \frac{1}{2}\left[-\Gamma + \left(\Gamma^2 + 4\Gamma\beta\right)^{1/2}\right] \tag{11}$$

This method make possible calculus of water depth, h_P, at a temp fix, Δt, by mean of continuity equations written previously, then is determined the velocity U_p, at the point P.

Numbers and the type of boundary conditions are described in the control algorithm.

For solution stability is always necessary the Courant condition:

$$\Delta t \le \frac{\Delta x}{\left(|U| + c\right)} \tag{12}$$

where c is the celerity.

4. The control algorithm

The objective of this control algorithm is to determine the gates operating way, in order to maintain target levels (imposed), immediately downstream of its.

Figure 2 shows a canal system with a series of pools separates by gates. The number of pools is ($m+1$) and the number of gates is (m). The control gates are manipulated in order to maintain a target water level at the upstream end of each pool (at the downstream end of each gate).

The flow within the canal pools is described by Saint Venant equation (1, 2). The flow rate under free and submerged flow conditions is

described by the equations (3, 4). The discharge coefficient for submerged flow conditions (Kiselev, 1988):

$$\mu\mu = \frac{\varepsilon\varepsilon}{\sqrt{2\varepsilon m^2 - \varepsilon^2 n^2 + \zeta_0 + 1 - 2\varepsilon m}} \tag{13}$$

where n – ratio between orifice cross sectional area and stream cross sectional area upstream by gate; m - ratio between orifice cross sectional area and stream cross sectional area downstream by gate; ζ – resistance coefficient ($\zeta \approx 0{,}06$); ε - contraction coefficient.

The system is in non-disturbed condition when the flow in the whole system remains steady and the water level at the downstream by gates is at its target value. Otherwise, the system is in disturbed state. The disturbance may be caused by any increasing or decreasing of water withdrawal, from the system, or incorrect setting of control gates. If the system is disturbed, the control gates have to be adjusted in order to have the water level downstream by the gates to return to its target value.

To avoid instability of the canal system, the gates will not respond to any small disturbances - it must be a dead band for which the gates are not operated, or a filter. Also the gates will not respond instantly to disturbances - the velocity of gates operating it must be into an acceptable range as a compromise between time response and stability.

The canal system could be supplied by a reservoir with constant level or from pumping station – in this case it must be known the inflow hydrograph. At the downstream end of the canal system could be free flow ($Q(x,t) = A(x,t)\ U(x,t)$), or other way (weir, reservoir, pumping station etc.).

At the initial moment ($t=0$) the flow in entire canal is steady gradually varied flow, the water level downstream of each gate is normal depth; $Q\ (t=0)$.

The boundary conditions for extremely pools of canal system depend by type of supplying or evacuation. In pools bounded by gates, the boundary conditions are done by the discharge through gates.

The water levels, velocities and discharges are computed in specified nodes, at successive time steps, along the canal from upstream end to downstream end.

The size of time and distance steps, it must be established in such way to respect Courant stability conditions.

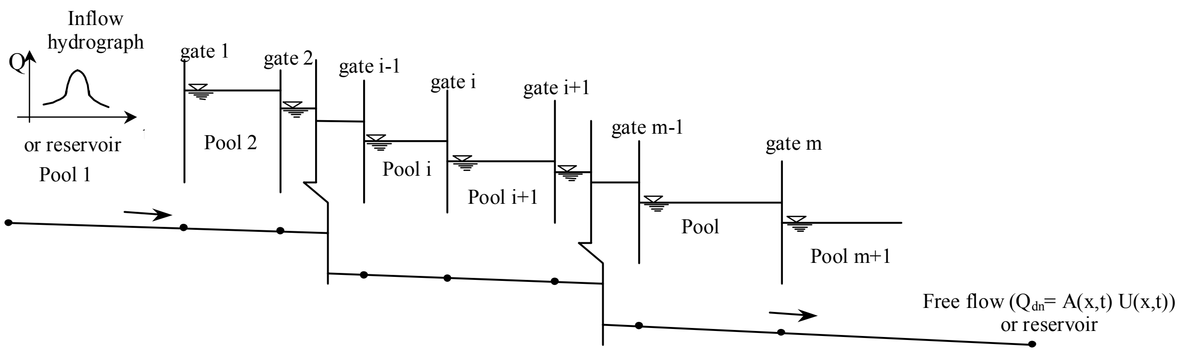

Fig. 2. A general canal system

5. Calculus example

A simple but realistic canal system is used to implement the proposed control algorithm. It has 3 pools, separated by 2 identical gates; first pool supplied by pumping (inflow hydrograph) and last pool having free flow downstream of it (Fig. 3). Cross sectional form is trapezoidal. Physical parameters of the system are specified as:

- canal length = 9000 m ($pool_1$ = 2000 m; $pool_2$ = 5000 m; $pool_3$ = 2000 m);
- bottom width = 2 m;
- bottom slope = 0.0005;
- side slope = 1:1.5;
- Manning's coefficient = 0.018;
- rectangular gate width = 2 m;

There are no lateral inflows and outflows in canal. The parameters involved in control algorithm are specified as:

- target level downstream of gate 1: H1 = 0.8 m;
- target level downstream of gate 1: H2 = 0.5 m;
- step interval: Δt = 0.01 s;
- step distance: Δx = 10 m; number of calculus nodes = 903;
- velocity of operating gates = $0.05 \times \Delta t$;
- dead band width = 0.04 m (± 2 cm);
- initial conditions: Q (t = 0) = 1.2 m^3/s;
- total calculus temp = 7000 s.

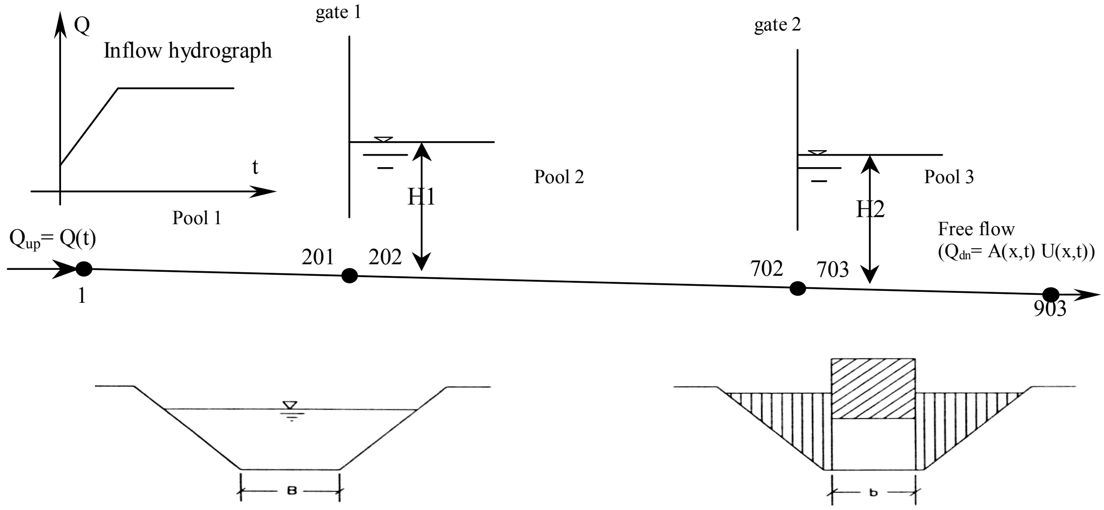

Fig. 3. Close downstream controlled canal

The inflow hydrograph at upstream end of the canal system is presented in Fig. 4.

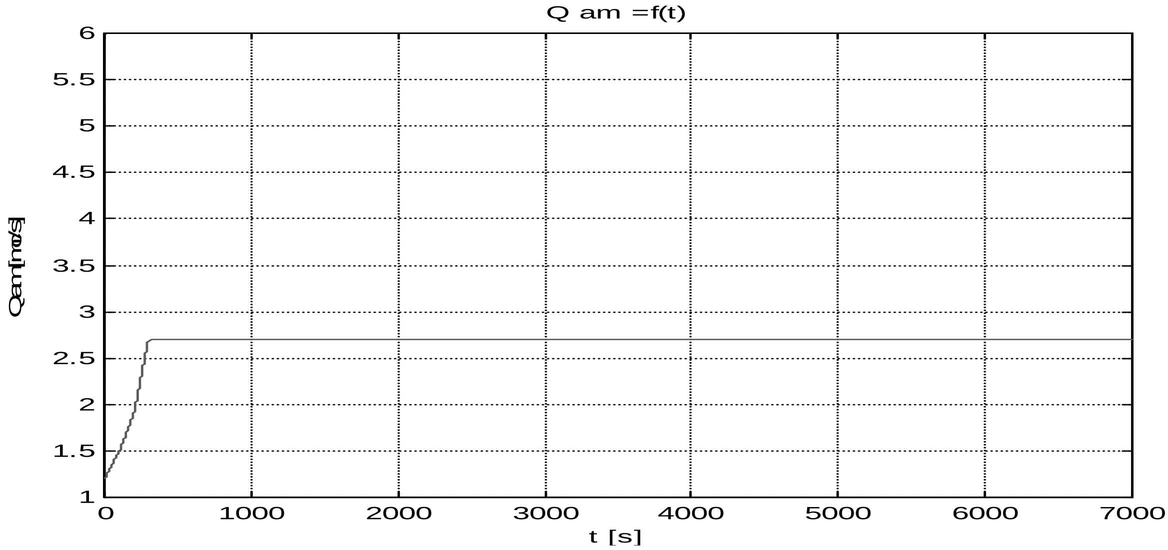

Fig. 4. Inflow hydrograph at upstream end of the canal system

With boundary conditions previously mentioned, we realised a mathemathical model and a PC software program in Matlab code for analyzing of entire behaviour of canal system.

5.1. Results

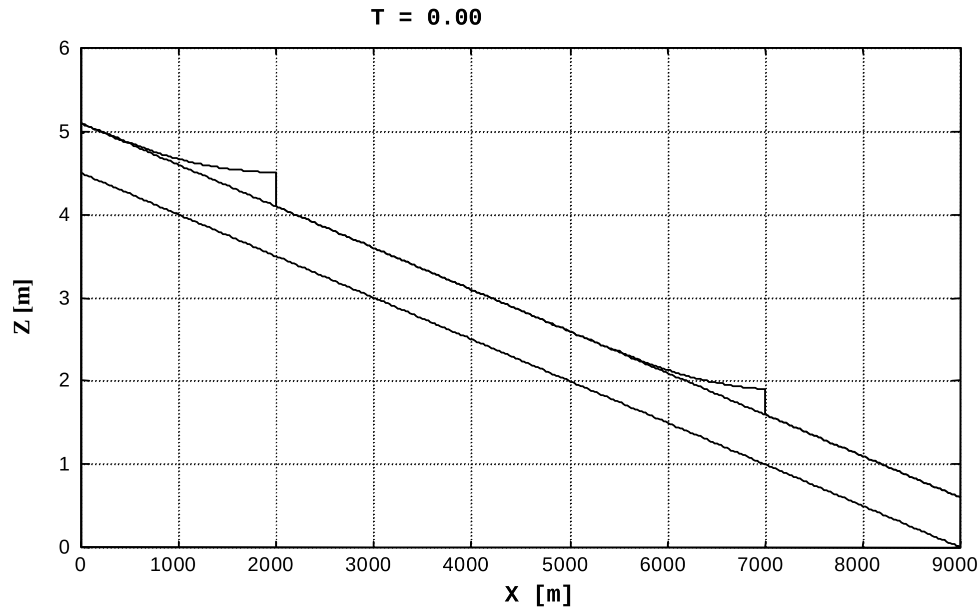

Fig. 5. Initial conditions – steady gradually varied flow: free surface flow at (t = 0)

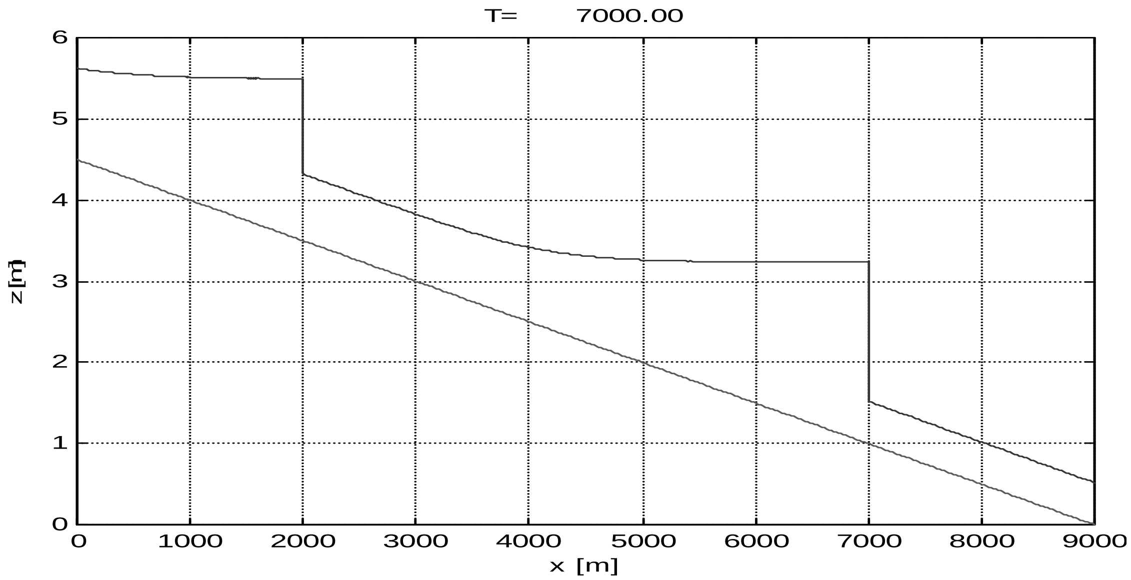

Fig. 6. Surface water level at t = 7000 s

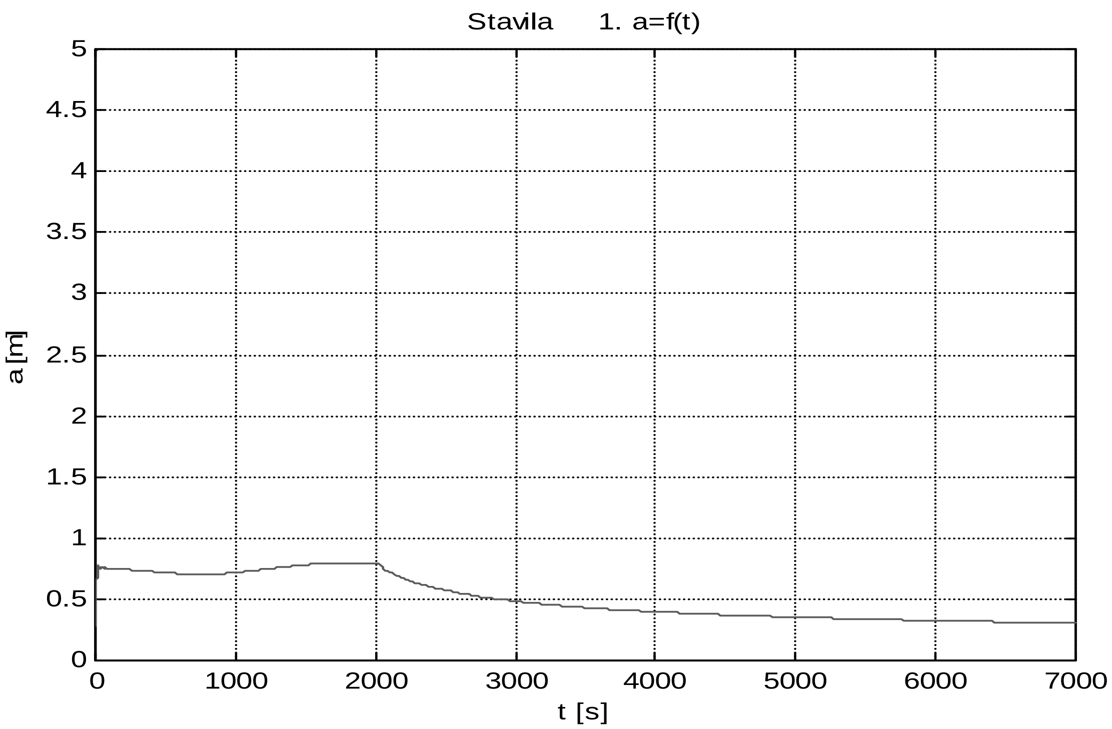

Fig. 7. The adjusting way of gate 1

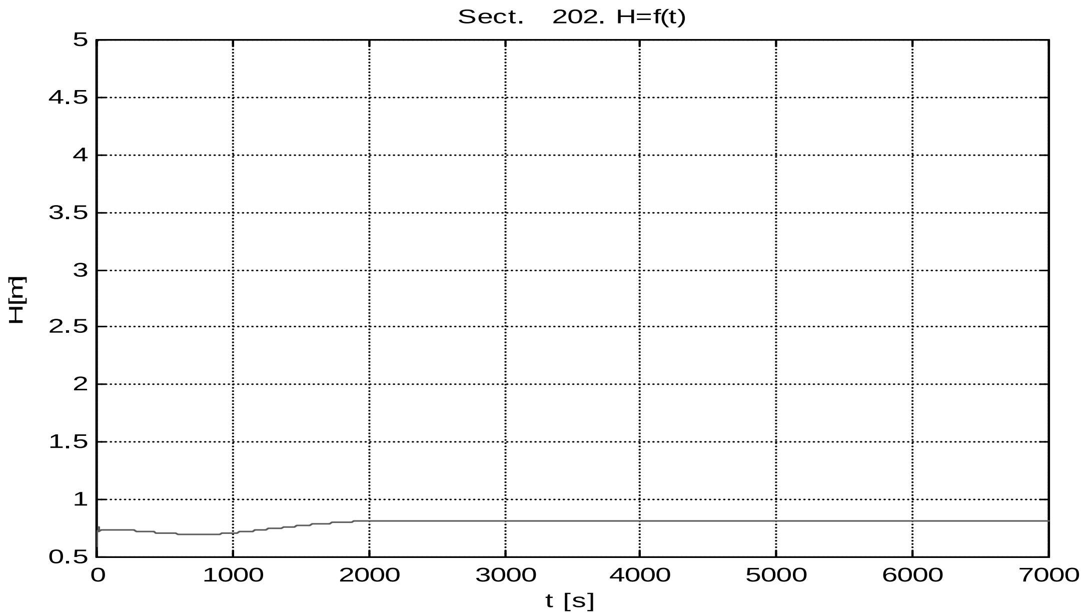

Fig. 8. Target water level downstream of gate 1

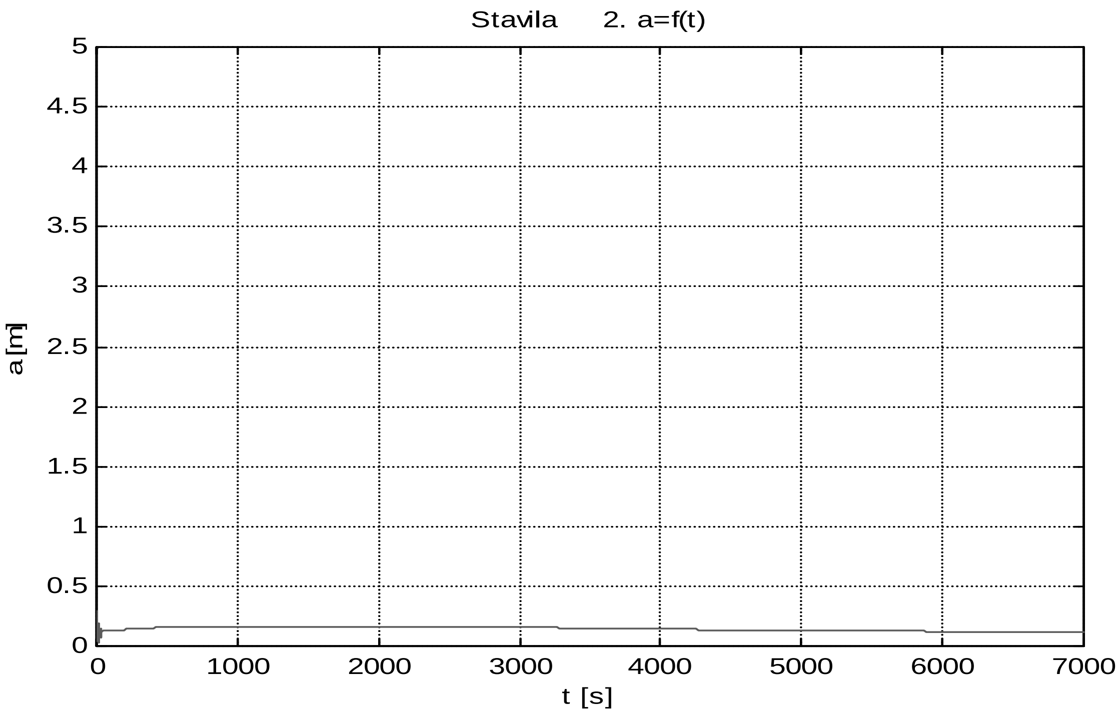

Fig. 9. The adjusting way of gate 2

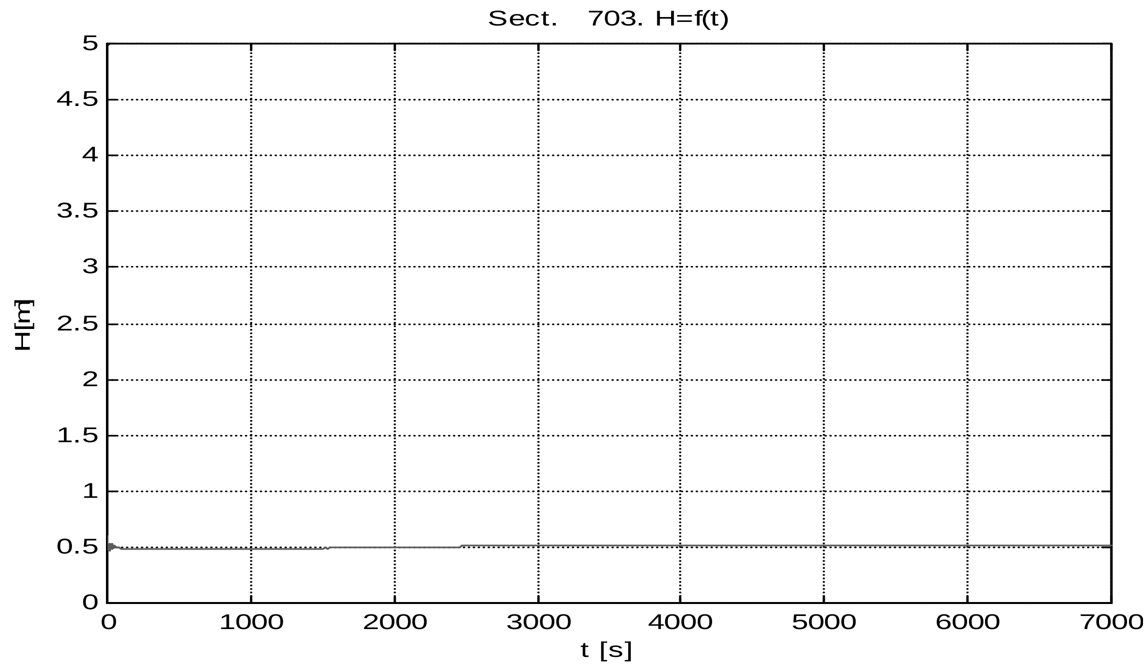

Fig. 10. Target water level downstream of gate 2

6. Conclusions

A close downstream control algorithm for on-demand operation of irrigation canal system has been proposed. Since it takes into account all the physical parameters of the system, the control algorithm can be applied to different canal systes without extensive tuning, also it can be extended to a canal network.

With this algorithm, a target water level is maintained at the downstream of each gate, by adjusting the gate at the upstream end of each pool. Adjustment of each gate is based on the water level at node downstream of the gate. Large distant between the information nodes and incorrect estimation of some of the physical parameters on the system can result in an offset of the maintained water level from its target value.

For the convenience of ilustration, it was assumed that the example canal system had 3 identical pools and 2 identical gates. However, it is obvius that there is no limitation of applying the control method to canmal systems with pools and gates of various sisez and physical parameters.

7. References

[1] Buyalski, C. P., Ehler, D. G., Falvey, H. T., Rogers , D. C. and Serfozo, E. A., *Canal systems automation manual.* 1991, Vol. I. U.S. Bureau of Reclamation, Denver, Colorado.

[2] Goussard, J., *Automation of canal irrigation systems*. 1993, ISBN 81-85068-44-5.

[3] Graf, W., H., Altinakar, M., S. (1993) *Hidraulique fluviale;* Tome I. Press Polytechniques et Universitairea de Romandes, Laussane, ISBN: 2-88074-261-7.

[4] Kiselev P. G, *Îndreptar pentru calcule hidraulice*. 1988, Editura Tehnică, Bucuresti.

[5] Marcoie, N., Pricop, A., Cismaru, C., *Model şi program în Matlab pentru analiza hidraulică a canalelor de irigații echipate cu regulatoare de nivel.* 2002, Lucrările Sesiunii Ştiințifice Omagiale, 17-18 mai, U.S.A.M.V. Bucureşti, Editura BREN, ISBN973-648-020-8, p. 403-414.

[6] Popa, R., *Elemente de hidrodinamica râurilor*. 1997, EDP, Bucuresti, 1997, ISBN: 973-30-5705-3.

Ovidius University Annals Series: Civil Engineering Volume 1, Number 5, 2003

Mamaia Beach Coastal Dynamics

Daniela POPESCU[a] Glicherie CARAIVAN[b]

[a] *Romanian Water National Administration, Dobrogea – Litoral Water Branch, Constantza, Romania*
[b] *"Ovidius" University Constantza , Constantza, Romania*

Rezumat: Dinamica plajei Mamaia. În ani '75 devenise evidentă dezechilibrarea balanței proceselor sedimentare litorale.
În anul 1989, sectorul sudic al plajei Mamaia a fost atificial înnisipat cu sedimente dragate din lacul Siutghiol.
În paralel ,a fost edificat un sistem hidrotehnic construit din 5 diguri "sparge val". Acesta a determinat formarea mai multor celule de circulație litorală cu structuri de tip "tombolo" în umbra lor delimitate prin canalele curenților de "rip".
Comparand ridicările batimetrice actuale cu cele anterioare portului Midia, rezultă un deficit de 10 – 12 mil. mc de sedimente. Acesta poate fi atenuat prin "by pass" de sedimente blocate la nord de portul Midia şi printr-un sistem adecvat de structuri hidrotehnice uşoare.

Abstract: In the years '75, it was clearly proved the continuously unbalance of the coastal sedimentary processes.
In 1989 the southern part of Mamaia beach was artificially nourished with sediments dredged from the adjacent Siutghiol Lake. In the same time, a system of 5 several breakwaters was built, which induced the setting up of several littoral circulation cells, with "tombolo" type accretionary features behind the breakwaters, and "rip channels" between.
Comparing pre-Midia harbour topography with the modern one, a sedimentary deficit of approximately 10 – 12 mil.m^3 is obtained for the entire area of Mamaia bay until the 6 – 7 m depth.

Keywords: *Black Sea, Mamaia beach, coastal erosion*

1.Introduction:

Mamaia beach belongs to the "complex barrier beach" shoreline type, being delimited by the Midia harbour to the north and Cape Singol to the south (fig. 1). It was built by waves and currents during the last transgressive stage of the Black Sea, isolating behind the Siutghiol laguna. The continuos rising of the sea induced a deep unbalance of the coastal sedimentary processes.

2.Coastal sedimentary budget:

Before 1975 the Midia harbour extended seaward up to 6m depth only. In 1975, the northern breakwater was prolonget offshore up to 12m depth. Consequently, the southward drift of sediments was bared, braking the Danubian sands to reach the dawnward nearshore area and a severe erosion of the beach was remarked.

With a view to protect the coastal buildings a "Y" shape groin was placed in front of the Hotel Parc and additional sand was dredget from the Lake Tabacarie to nourish artificially the new created beach area. The local currents dispersed the sediments to the north.

Afterwards, during the next years, the erosion was moved northward, between Dacia and Perla hotels (fig.2; fig. 3).

In 1984 a new goin was in built in of Cape Singol aiming to diminish the erosion.

The hydrotechnical engineers planned all these protection scheems based on the action of the wellknown southward littoral current. They have ignored however the effects induced by the extension of Midia harbour. So, according as this new groin

ISSN-12223-7221

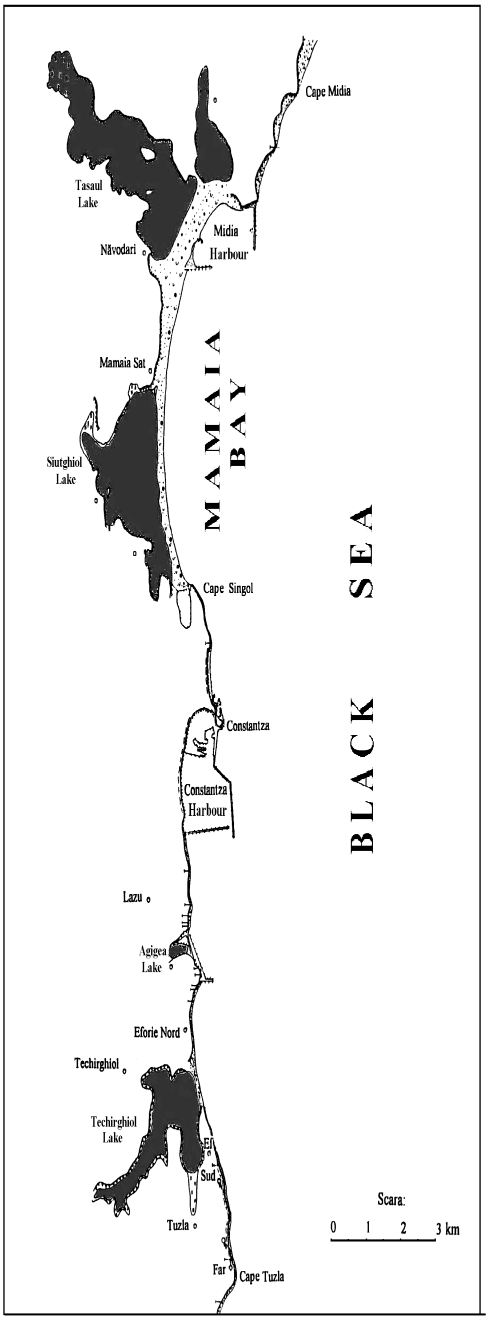

Fig.1 Mamaia barrier beach location

Black Sea	Cape Midia	Techirghiol Lake
Siutghiol Lake	Cape Singol	Cape Tuzla
Midia Harbour	Constantza	Mamaia Bay

advanced seaward the eroded coastal segment shifted to the north.

At that time, we warned to the changes induced on the coastal dynamics. A new circulation cell was developed, but its orientation was opposite to the general coastal current, namely northward.

An evaluation of the bottom physiographical changes was made, confronting the bathymetrical maps of the Mamaia Bay from 1961 and 1978; a deficit of 8.350.000m3 was revealed.

During the period 1974-1984 the loss of sediments was much greater (about 10-12 mil.m^3).

The erosion was progressively developed, affecting a submarine area extended up to 10-m depth seaward, according the advancing rate of the Midia harbour.

3.Coastal engineering solutions:

Because the erosion became dangerous, in the period of 1989-1990, the southern part of Mamaia beach was artificially nourished with sandy sediments dredged from the adjacent Siutghiol Lake. In the same time, a system of 5 breakwaters was started to be built, which induced the setting up of several littoral circulation cells, with "*tombolo*" type accretionary features behind the breakwaters and "rip channels" between (fig. 2; fig.3).

The dredging operation was made without a previous study concerning the lithologic sequence of the sub-bottom lake sediments.

Consequently, a great amount of silt and silty clay was added in the coastal circulation, worsening the beach quality, and the hydrogeological safety of the lake was affected, as well.

In fig. 2 is shown the effect of breakwaters system upon the shoreline configuration and bottom physiography from 1988 since 1994.

If, in the southern extremity of the beach a net gain of 14.200 m^2 was obtained, immediately to the north, the shoreline have been retreated about 5 m, excepting the "*tombolo*" *type* structure developed behind the breakwaters.

Generally, for the entire zone considered in fig. 2, a loss of 27.300 m^2 was obtained.

The bottom morphology became more complicated: shallower surfaces behind the breakwaters and deeper rip channels between.

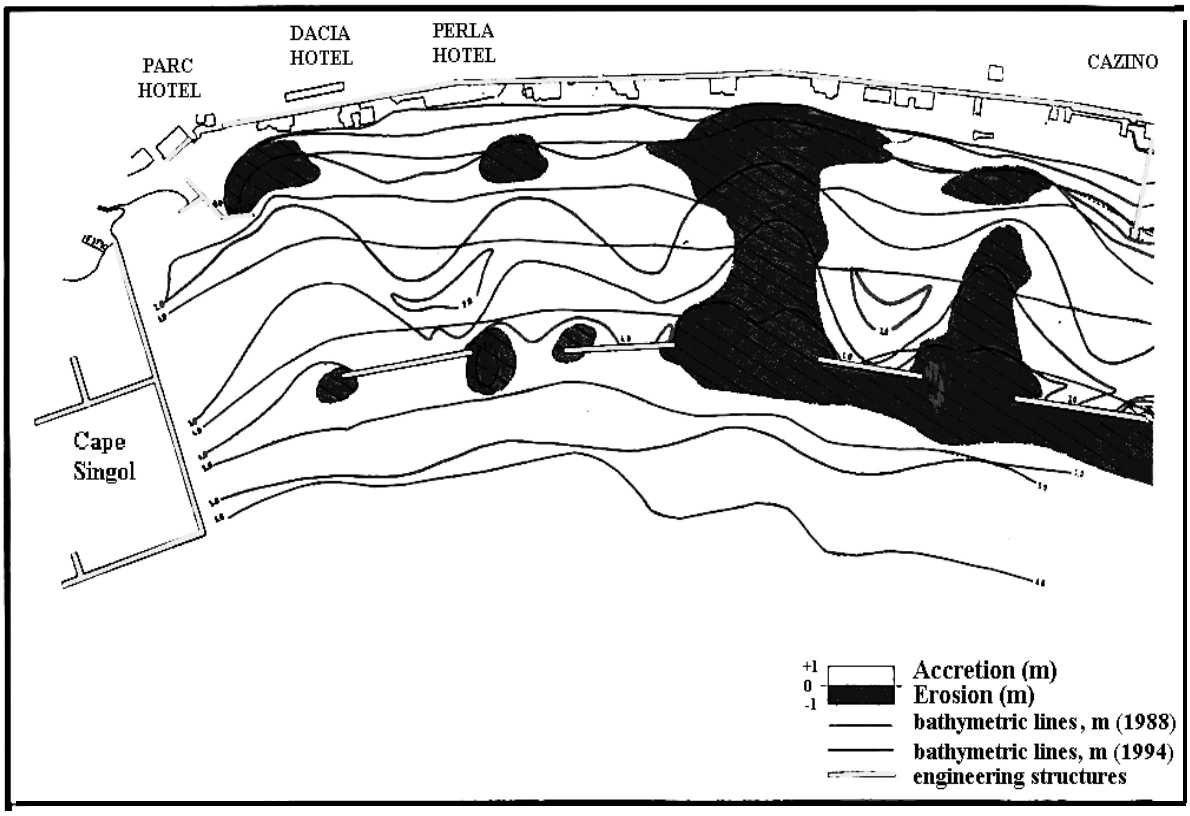

Fig.2 Sedimentary processes in the southern part of Mamaia beach (between 1988-1994) Scale 1:10000

The shoreline is sinuously shaped with crescent "*tombolo*" structures in the breakwaters shadow zone and landwards concavities between.

During a winter storm the nourishment material was dispersed northward in a very specific manner, according to the new hydrodynamic spectrum (fig. 3).

Throughout the area shown in fig. 2 (about 2,5 mil.m^2) there are slight depositions behind the breakwaters (10.000-22.500 m^3) and northward of the Cape Singol groin (95.500 m^3)' nevertheless, in the considered zone, a sedimentary budget deficit of 290.000 m^3 is recorded.

Comparing the pre-Midia harbour topography with the modern one, a sedimentary deficit of approximately 10-12 mil.m^3 is obtained for the entire area of Mamaia Bay until the 6-7 m depth.

These huge volumes of sediments might be supplied by – passing the sands trapped in the northern part of Midia harbour. In addition, we suggest to be achieved a hydrotechnical trap system consisting of:

- breakwaters (heavy structures already existing);
- new submerged crescent shape breakwaters types with the concavity shoreward, made up of geotextile bags, placed normally to the rip channels, at 2,5-3,0 m depth;
- submerged geotextile groins, from the backshore to the 2,5 m isobath.

The beach will be monitorised for the first year, and the hydrotehnical system will be corrected, depending on the induced hydrodynamic effects.

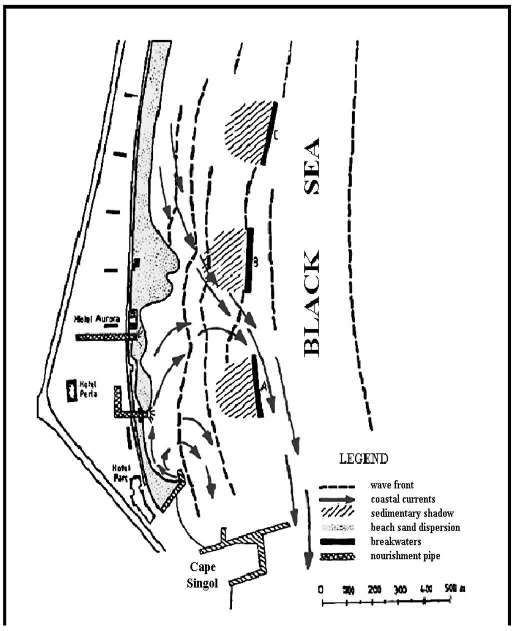

Fig.3 Coastal dynamics during a winter storm from 1989 in the southern part of Mamaia beach

4.Bibliography:

[1]Caraivan, G., *The sedimentological study of the beach and inner shelf deposits in front of the Romanian coast between Portitza and Cape Tuzla* 1982.

[2]Caraivan, G., *Upper Quaternary evolution of the Mamaia zone*. 1982, Pontica, 15, p. 15-3

[3]Caraivan, G., Hertz, N. and Noakes, J., *New proofs of the Black Sea rise during the Middle Würm interstadial.* 1986, D.S. Inst. Geol. Geofiz., vol. 70-71/5, p. 57-62

[4]Panin, N., *Danube Delta: genesis, evolution, sedimentology,* 1988 Rev. Roum Geol. Geophys., Geogr. Geographie, 33, p. 25-36.

Ovidius University Annals Series: Civil Engineering Volume 1, Number 5, 2003

Confinement of Concrete Cylinders with Fibre Reinforced Composite Jackets

Mihaela-Anca CIUPALA [a] Kypros PILAKOUTAS[a] Nicolae TARANU[a]

[a]*The University of Sheffield, Sheffield, UK*

Rezumat: Lucrarea prezintă rezultatele experimentale obținute din încercarea la compresiune pe cilindri din beton confinați cu materiale compozite din răşini epoxidice armate cu fibre din sticlă, carbon şi aramidice. Parametrii experimentali considerați au fost rezistența la compresiune a betonului şi tipul de material compozit folosit. Rezultatele experimentale au arătat faptul că utilizarea materialelor polimerice armate cu fibre la confinarea elementelor din beton conduce la creşteri semnificative ale rezistenței la compresiune şi ductilității acestora. Cedarea betonului confinat a fost dominată de ruperea materialului compozit şi pulverizarea betonului. Rezultatele experimentale sunt comparate cu cele date de câteva modele analitice existente în literatura de specialitate.

Abstract: This paper describes axial compression test results of concrete cylinders confined with carbon, glass and aramid fiber reinforced epoxy composite jackets. The experimental parameters include the plain concrete compressive strength and the type of the composite jacket. It was found that the fiber composite jacketing can significantly increase the compressive strength and ductility of concrete. The failure of the confined concrete was dominated by the rupture of the jacket and the concrete crushing. The test results are compared with some analytical models available in the literature.

Keywords: *:* fibre reinforced polymer (FRP), confinement, composite materials.

1.Introduction:

As civil infrastructure enters maturity or ages, rehabilitation and upgrading dominate construction activities. Repair or retrofitting of bridge decks, beams or columns in buildings, parking structures and others, due to ageing, environmentally induced degradation, poor initial design and/or construction, or to lack of maintenance, are now of great importance. At the same time, seismic strengthening demand is increasing due to the introduction of new codes and a better understanding of seismic risk.

One of today's state-of-the-art techniques for structural strengthening is the use of Fibre Reinforced Polymer (FRP) composites, which are currently viewed by structural engineers as highly promising materials due to their versatility. Currently, the primary structural strengthening applications for FRP include plate bonding, shear strengtehning and confinement for reinforced concrete (RC) elements. This paper will deal with the topic of confinement.

FRP composite materials are resistant to corrosion, have low weight, high tensile strength and good fatigue behaviour. They are also recognized for their ease of transportation, handling and low maintenance costs [1].

FRP materials have an elastic behaviour up to failure and therefore exert their confining action on concrete specimens under axial loading in a different way compared to steel. The amount of confining action depends on the lateral dilation of concrete, which in turn is affected by the Posson effect, the confining pressure and the state of the confined concrete. Confined concrete behaves in a more or less elastic manner at the initial stages with a Poisson's ratio of about 0.15-0.20. Once the lateral strain exceeds a certain value, volumetric expansion takes place, primarily due to the formation of internal cracking. If this expansion is not controlled by confinement, concrete fails in apparent compression very soon after. If confinement is prevented, compression failure is delayed and a significant increase in axial strain can be obtained.

ISSN-12223-7221

Thus, FRP-confined concrete models should account for the interaction between the laterally expanding concrete and the confining material [1].

Many experimental studies on concrete confined with FRP have been carried out [2-6] and confirm that the method is easy to apply and can give effective structural confinement. Analytical and numerical research has also been done [7-10] and several constitutive laws have been developed for FRP confined models.

However, it has been demonstated [11] that many of the proposed models were only calibrated on limited experimental data and, as such, are not able to predict the behaviour of concrete confined with all the different materials. A large experimental program is currently taking place at the University of Sheffield where experimental work is examining three different types of materials as well as different levels of lateral pre-tensioning of the jackets.

This paper presents a small part of the behaviour of concrete cylinders confined with one layer of carbon fibre reinforced polymer (CFRP), aramid fibre reinforced polymer (AFRP) and glass fibre reinforced polymer (GFRP) and concentrates on the experimental techniques.

2. Experimental program

The results from four concrete cylinders are presented: one plain concrete cylinder and three cylinders wrapped with one layer of CFRP, GFRP and AFRP.The diameter of all cylinders was D=150mm and the height of cylinders was H=300mm,Fig.1.

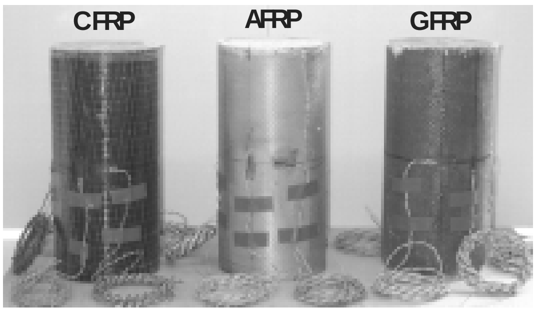

Fig. 1. Test specimens

The physical and mechanical properties of the fibre sheets used as confining jacket (j) are given in Table 1 (thickness t_j, modulus of elasticity E_j, tensile strength f_{ju}, ultimate elongation ε_{ju}).

Table 1. Fibre properties

Fibre type	t_j (mm)	E_j (N/mm^2)	f_{ju} (N/mm^2)	ε_{ju} (%)
CFRP	0.117	240000	3900	1.55
GFRP	0.068	65000	1700	2.8
AFRP	0.200	120000	2900	2.5

All cylinders were subjected to monotonic axial loading. Figure 2 shows the testing equipment and data acquisition system used.

Data acquisition system

Test-rig

“Amsler” control unit

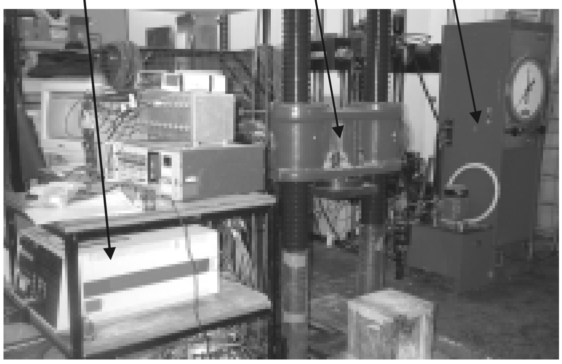

Fig. 2. Testing equipment and data acquisition system

Three horizontal (H1, H2, H3) and two vertical (V1,V2) strain gauges were attached to the composite jacket, as shown in Fig. 3a. In addition, three linear voltage displacement transducers (LVDTs) were used for the measurements at 120^0 apart around the circumference of the specimens.

They are fixed on two aluminium rings around the cylinder and are located at a distance of 73 mm apart, Fig. 3b.

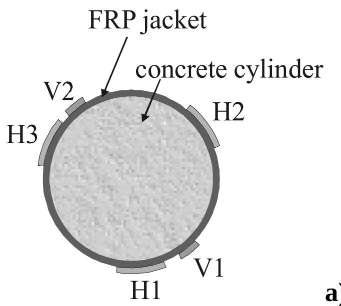

a)

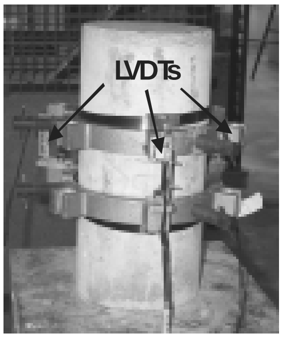

b)

Fig. 3. Strain gauges location (a)
and LVDTs location (b)

For all specimens an initial 200 kN cycling loading was applied to ensure that the loading is applied axially and that the instrumentation was working properly. After that, the loading was monotonically increased up to failure.

3. Experimental results

The first test was performed on the plain concrete specimen, Fig. 4. The concrete strength is $f_{cu} = 26.35\ N/mm^2$ (failure load $N_u = 480\ kN$) and the strain at failure is $\varepsilon_{cu} = 0.00216$.

The experimental test on CFRP confined concrete cylinder led to a failure load of $N_u = 860\ kN$ which corresponds to an ultimate axial strength of $f'_{cu} = 48.7\ N/mm^2$. The ultimate axial strain in the concrete, as measured from the jacket, is $\varepsilon_{cu,a} = 0.00795$ and the ultimate lateral strain is $\varepsilon_{cu,l} = 0.0134$. This final value shows that the CFRP confinement is almost fully utilised, considering that the ultimate elongation given by the material supplier for CFRP is $\varepsilon_{ju} = 1.55\%$.

Fig. 4. Plain concrete specimen

The results show that the lateral confinement with one layer of CFRP increases the strength by 80% and the ductility of plain concrete by 270%.

The failure was explosive due to the high strain energy stored in the FRP material. The failure of fibres in the lower part of the specimen (top as cast) led to the rapid debonding of the filaments near that location and failure, Fig. 5.

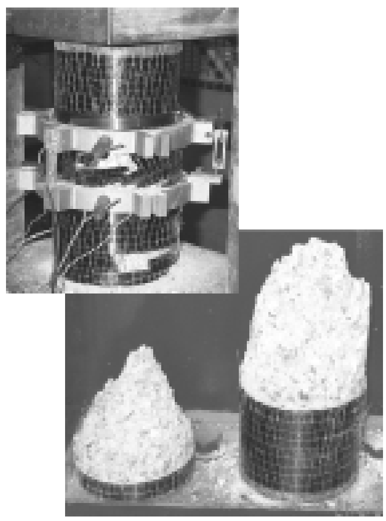

Fig. 5. Concrete cylinder confined with CFRP

In the case of AFRP confinement, the failure load is $N_u = 870\ kN$ which corresponds to an ultimate axial strength of confined concrete $f'_{cu} = 49.2\ N/mm^2$. The ultimate axial strain is

$\varepsilon_{cu,a} = 0.0147$ and the ultimate lateral strain is $\varepsilon_{cu,l} = 0.0271$. The ultimate elongation of the fibre guarantied by the material supplier is $\varepsilon_{ju} = 2.5\%$ which shows that AFRP confinement is also fully utilised.

The lateral confinement with one layer of AFRP increases the strength by 80% and by 580% the ductility of the plain concrete.

The failure was explosive, similar to the case of CFRP confinement, and it occured in the middle of the cylinder height, Fig. 6.

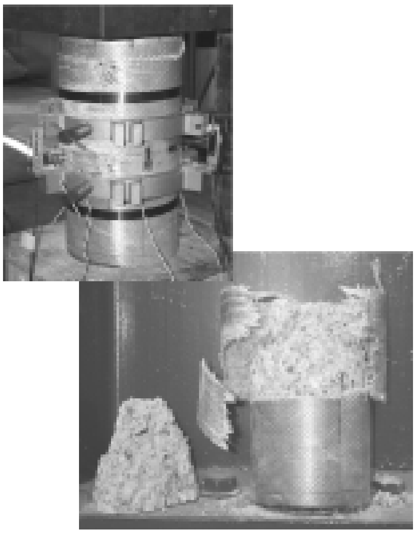

Fig. 6. Concrete cylinder confined with AFRP

In the case of the GFRP confined concrete cylinder, Fig. 7, the failure load is $N_u = 530\,kN$ which corresponds to an ultimate axial strength of confined concrete of $f'_{cu} = 30\ N/mm^2$.

The ultimate axial strain in the concrete is $\varepsilon_{cu,a} = 0.00502$. The ultimate lateral strain *in the jacket* is $\varepsilon_{cu,l} = 0.0175$ which represents about 60% of the ultimate elongation of the glass fibre guarantied by the supplier ($\varepsilon_{ju} = 2.8\%$). This shows that the GFRP confinement is not fully utilised. Further experimental work at the University of Sheffield [12] shows that to fully utilise such confinement, lateral pre-tensioning needs to be applied.

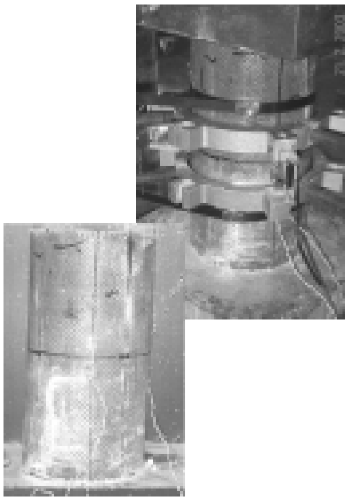

Fig. 7. Concrete cylinder confined with GFRP

The experimental results show that the lateral confinement with one layer of GFRP did not significantly increase the strength of confined concrete cylinder, but increased the ductility. In order to increase the strength of the confined cylinder, more then one GFRP layer is required. The failure of the GFRP confined specimen is presented in Fig. 7.

A comparison of lateral strains for the three FRP jackets is presented in Fig. 8.

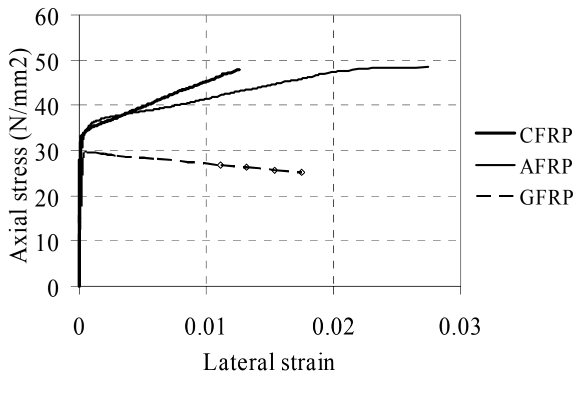

Fig. 8. Axial stress - lateral strain relationship: experimental results

It can be seen that the CFRP and AFRP confinement were fully utilised, while the failure of the

GFRP confined concrete was dominated by the rupture of the jacket at an average strain much smaller than the ultimate strain given by the FRP supplier (about 60%).

4. Analytical models

Several constitutive models can be found in the literature for FRP-confined circular columns.

In order to compare the experimental results with analytical predictions, some of these models have been considered: Samaan et al. [7], Miyauchi et al. [8], Spoelstra and Monti [9] and Lam and Teng [10].

Figure 9 shows the comparison between the experimental results and the analytical predictions.

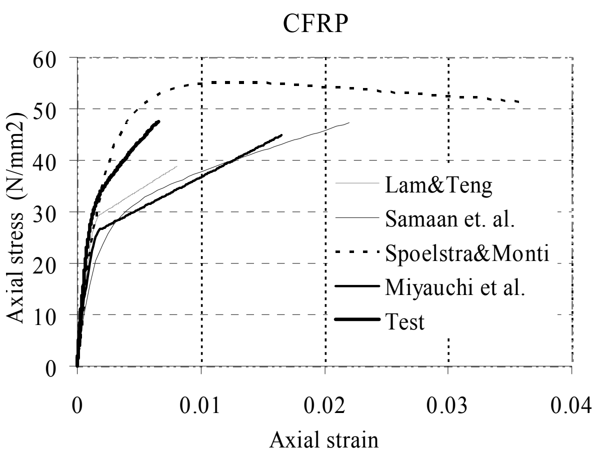

Fig. 9. Axial stress - axial strain relationship: Comparison between analytical models and experimental results for CFRP confinement

It can be noticed that the axial strength of confined concrete calculated using the Samaan et al. and Miyauchi et al. models is very close to the one obtained from the experimental tests. Nevertheless, these models overestimate the lateral strain more than twice compared to the experimental values.

Lam and Teng model provides conservative predictions for the axial strength of concrete, but the ultimate axial strain is almost the same with the test.

Spoelstra and Monti model overestimates both the axial strength and the ultimate axial strain of confined concrete.

5. Conclusions

Experimental results for concrete cylinders wrapped with composite materials are presented in this paper. The concrete is confined with one layer of carbon, aramid and glass fiber reinforced polymer composite jackets.

Significant increase in strength and ductility of concrete can be achieved by one layer of carbon and aramid fiber composite jacketing. In the case of GFRP jacket, more than one layer is needed in order to increase the strength and ductility of concrete, especially when dealing with large scale applications.

The ultimate condition of the confined concrete is determinated by the rupture of the composite jacket. In general, the average rupture strain of the jacket is smaller than the expected ultimate strain and, hence, this needs to be taken into account during design.

The test results are compared with some analytical models available in the literature. The difference between the experimental and analytical results shows some inadequacies of existing models for FRP concrete confinement. Hence, it can be concluded that improved constitutive models need to be developed.

6. Acknowledgements

This research has been supported by two Marie Curie Fellowships of the European Community programme Human Potential under contract number HPMF-CT-2001-01279 and HPMF-CT-2002-01553.

7. References

[*] m.a.ciupala@sheffield.ac.uk

[1] Federation International de Beton, *Externally bonded FRP reinforcement for RC structures*, 2001, *fib* Bulletin 14, Lausanne.

[2] Saadatmanesh H., Ehsani M. R. and Jin L., *Strength and Ductility of Concrete Columns Externally Reinforced with Fibre Composite Straps*, 1994, ACI Structural Journal, No. 4, Vol. 91, pp. 434-447.

[3] Seible F., Priestley M. J. N. and Innamorato D., *Earthquake retrofit of bridge columns with continuous*

fibre jackets. Design guidelines, Advanced composite technology transfer consortium, 1995, Report No. ACTT-95/08, University of California, San Diego, USA.

[4] Picher F., Rochette P. and Labossière P. *Confinement of concrete cylinders with CFRP*. 1996, Proceedings of 1st International Conference on Composite Infrastructures. Tucson, Arizona, USA, pp. 829-841.

[5] Matthys S., Taerwe L. and Audenaert K. *Tests on axially loaded concrete columns confined by FRP sheet wrapping*. 1999, Proceedings of the 4th International Symposium on FRP for Reinforced Concrete Structures. Baltimore, USA, pp. 217-228.

[6] Demers M. and Neale K.W., *Confinement of reinforced concrete columns with fibre-reinforced composite sheets – an experimental study*, 1999, Canadian Journal of Civil Engineering, No. 2, Vol. 26, pp. 226-241.

[7] Samaan M., Mirmiran A. and Shahawy M., *Model of concrete confined by fibre composite*, 1998, Journal of Structural Engineering, ASCE, No. 9, Vol. 124, pp. 1025-1031.

[8] Miyauchi K., Inoue S., Kuroda T. and Kobayashi A., *Strengthening effects of concrete columns with carbon fibre sheet*, 1999, Transactions of The Japan Concrete Institute, Vol. 21, pp. 143-150.

[9] Spoelstra M. and Monti G., *FRP-confined concrete model*, 1999, Journal of Composites for Construction, No. 3, Vol. 3, pp. 143-150.

[10] Teng J.G., Chen J.F. and Smith S.T., *FRP Strengthened RC Structures*, 2002, John Wiley & Sons Ltd, Chichester, UK.

[11] Mortazavi A.A., *Behaviour of confined concrete columns with and without lateral pre-tensioning*, 2003, PhD Thesis, University of Sheffield, UK.

[12] Mortazavi A.A., Pilakoutas K. and Ciupala M.A. *Lateral Prestressing of RC Columns with FRP Jackets*. 2003, 6th International Symposium on Fibre Reinforced Polymer (FRP) Reinforcement for Concrete Structures (FRPRCS-6). Singapore, 8-10 July (accepted for publication).

Aspects Concerning Water Supply Control and Distribution Systems Management

Gilda GAVRILAS[a] Vasile VASCU[a]

[a]*Technical University "Gh.Asachi" Iassy, Iassy, Romania*

Abstract: Each country applies different water supply control politicies depending on the existent economic and technology conditions.

A rational management of large water systems requires gathering and centralizing information, and then optimally controlling the system using automatic devices and equipments. On this basis the authors propose a management schedule for water utilities, meant to produce additional energy savings. This goal can be reached by through correlation between the study of water pumping plant, the model which simulates the optimal operation of the network and the consumer outflow forecast.

For the diagram described in this the modeling system must comprise three basic problems: network simulation and data analysis; short-term water consumption forecast ;pumps scheduling to achieve savings.

This paper describes the mathematical models used to solve these problems.

Keywords: management, optimal control.

1 Introduction

The management of water supply systems aims to accomplish an efficient functioning of the systems regardless of their complexity at high costs. In order to obtain the maximum benefits from the control and automatic systems there must be taken into consideration a global point of view that gathers all the different components of an integrate system.

The structure of the water supply systems can be presented as a configuration of subsystems, mainly interconnected through reservoirs and pumping stations. In the case of such systems, through an operative control, the production subsystems functioning is controlled and coordinated, in order to function as much as possible under the best technological rules, under the conditions of keeping up the required values, from a technological and economical point of view, as well as respecting the deadlines for water supply.

Considering the big production volume, any improvement in the system functioning will lead to important economical effects.

2. Optimum control scheme

In the field of water supply and distribution everything can be implemented in several ways and at different levels of complexity.

The accomplishment of a daily exploitation requires mainly centralized information, automatic processes and an optimum control.

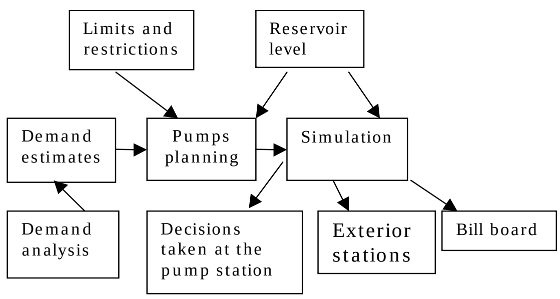

Fig. 1

Considering that the level of the automatic system in transport and water supply in our country is still low, there is presented a scheme for the management operations of a water supply system (Fig.1) which includes the following:

ISSN-12223-7221

- simulation of the network functioning in time and data analysis
- plan the pumps functioning in order to save energy
- water consumption estimate on a short term

These algorithms allow obtaining a decisive and shaping devise, both in the case of functioning survey with a dispatcher and in the case of a proper technological equipment, in real time. [1,2]

3. Case – study

The study of a distribution system functioning requires the knowledge of the network position, of section diameters and materials, of required or existent levels in the reservoirs, of functioning parameters of the pumping stations as well as of the water consumption in the junctions at the same time.

In order to give the basic information necessary for the consumption estimates in the case of water supply system there was used a model of Artificial Neural Networks. [1]

In figure 2 there is presented a water supply system with two reservoirs and an SP

On the network graph there are shown the pipes length and diameter as well as the land elevation in junctions.

The functioning parameters of the network are obtained using the network simulation for a certain consumption hour (Chart 1 and 2).

The obtained results include the following:
number of sections, water flow in the sections, water flows coming out of the reservoirs and of SP, change of charge, water speed, piezometer values and pressure in the junctions.

Chart 1

Junction	Section	Way	Diam.(mm)	Length (m)	Flow (l/s)	Losses (m)	Speed (m)
1	1	1 – 2	150	300	12,783	1,3197	0,7233
	2	1 – 5	200	200	20,217	0,4893	0,6435
	3	17 – 1	250	40	40,000	1,1654	0,8148
2	4	3 – 2	80	300	3,142	2,2268	0,6251
	5	2 – 6	125	200	6,925	0,6894	0,5642
3	6	4 – 3	200	300	20,312	0,7406	0,6465
	7	3 – 7	125	200	8,170	0,9455	0,6657
4	8	4 – 8	200	200	17,688	0,3789	0,5630
	9	18 – 4	250	300	45,000	1,0973	0,9167
5	10	5 – 6	100	300	4,671	1,5198	0,5947
	11	5 – 9	125	200	7,546	0,8123	0,6149
6	12	7 – 6	80	300	2,947	1,9706	0,5863
	13	6 – 10	100	200	4,543	0,9609	0,5784
7	14	8 – 7	125	300	7,829	1,3072	0,6379
	15	7 – 11	80	200	3,052	1,4042	0,6071
Junction	Section	Way	Diam.(mm)	Length (m)	Flow (l/s)	Losses (m)	Speed (m)
8	16	8 – 12	65	200	1,859	1,5761	0,5601
	17	9 – 10	65	300	1,546	1,6685	0,4660
9	17	11– 10	100	300	4,683	1,5274	0,5962
10	18	13-10	50	250	0,728	1,2742	0,3705
	19	12-11	150	300	11,818	1,1353	0,6687
11	20	14-11	65	250	1,313	1,0218	0,3957
	21	15-12	200	250	18,959	0,5409	0,6034
12	22	14-13	125	300	7,728	1,2750	0,6297
13	23	15-14	200	300	19,041	0,6544	0,6060
14	24	16-15	250	200	45,00	0,7315	0,9167
15	25	-	-	-	-	-	-
16	-	-	-	-	-	-	-
17	-	-	-	-	-	-	-
18	-	-	-	-	-	-	-

Chart 2

Junction	Consumption (l / s)	Piezometer value (m)	Land height (m)	Available Pressure (m)
1	7	191,035	165	26,035
2	9	189,715	167	22,715
3	9	191,942	170	21,942
4	7	192,683	173	19,683
5	8	190,546	170	20,546
6	10	189,026	172	17,026
7	10	190,996	174	16,996
8	8	192,304	175	17,304
9	8	189,733	174	15,733
10	14	188,065	175	13,065
11	14	189,592	177	12,592
12	9	190,727	180	10,727
13	7	189,399	178	11,399
14	10	190,614	182	8,614
15	7	191,268	185	6,268
16	- 45	192,000	190	2,000
17	- 40	192,000	160	32,200
18	- 45	193,780	180	13,780

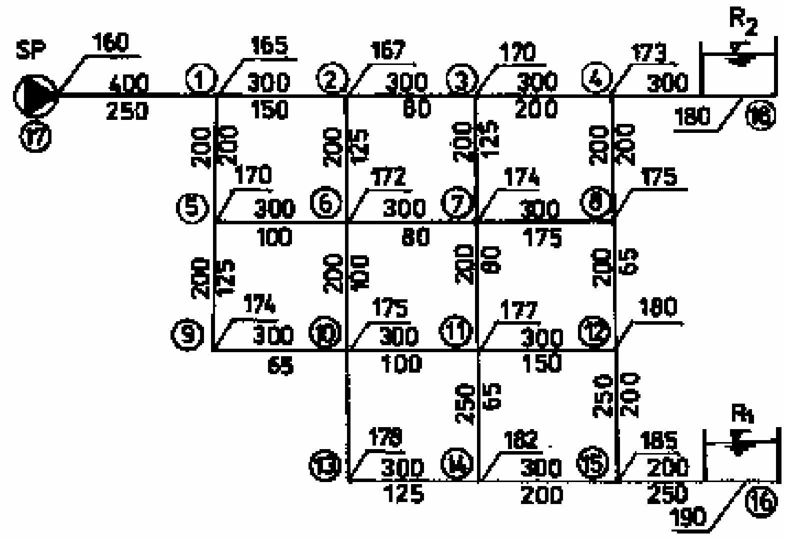

Fig.2

4.Conclusions:

In the water supply systems, the water flows vary during the day.

In order to accomplish an efficient management, the study of the pump stations must be correlated with the model of optimum functioning of the water supply system and with the consumption flows estimates in a decisive system.

The advantages of the optimum control lead to the following:

- indirect optimum flow during the night, on a one day basis, respecting the estimated water consumption
- direct optimum flow regulation in the case of a proper technical equipment

- best pump planning
- timed simulation of the future system functioning
- data storage on the water consumption in the network in order to make the demand and flow estimates
- evaluate the indirect results of the adopted control strategies.

Obtaining all these advantages is conditioned by the fact that the studied supply system function correctly and in a stable way, and that the data base used have correct values taken for the longest period possible.

Thus, the use of the optimum control of the water supply systems leads to the improvement in the system functioning and to the saving of energy ensuring an efficient management.

Bibliography:

[1] Gavrilas G, Hapurne T – *Aspects Concerning the Artificial Intelligence Application in the Water Feeding Control* – International Symposium on Water Management and Hydraulic Engineering, Dubrovnik, Croatia, 1998- page 169 – 178

[2] Gavrilas G, -*Hidraulica urbana (Urban Hydraulics)*, Gh Asachi Publishing House, Iasi, 1999

[3] Guran M, Filip F, -*Hierarchical Systems in Real Time, with Distributed Data Analysis*, Editura Tehnica,Bucuresti,1986

Construction Cost Estimating – General Aspects

Marilena GHITA[a] Raluca GRASU[a]

[a]*Technical University of Civil Engineering, Bucharest,7000 Romania*

Rezumat: Articolul trateaza principalele caracteristici ale evaluarii costurilor in domeniul industriei constructiilor. Sunt prezentate in lucrare tipurile de estimare folosite in mod uzual in domeniul estimarii costurilor lucrarilor de executie in constructii.

Abstract: The article deals with the main characteristics of the evaluation of costs in the field of construction works. There are shown in this article all the types of estimates used usually in the field of execution construction works.

Keywords: cost, evaluation, contractor, bid.

1. Generals

Estimating is one of the most important aspects of building contractor's business since success often depends on the contractors ability to make accurate estimates of total job costs. This holds true whether the builder bids competitively for his work on lump sum contracts, or obtains most of his work through negotiations with owners. Yet many contractors put little thought into their estimating activities and, therefore, have a inadequate estimating procedures. Because they don't understand the purpose of estimating, they only see it as a burden.

To understand estimating it is necessary to ask the question, what is a construction estimate and what is the objective of estimating?

To the estimator an estimate should be the probable cost of project as computed from the available plans and specifications. The objective of estimating is to provide an orderly, comprehensive and accurate estimation of the job costs. The estimator does not establish the cost of a project, he only prepares the closest possible approximation to the cost so that a bid may be determined. It is important then, that the contracting company have an established procedure for estimation that is both accurate and efficient.

There are several types of estimates available to the contractor; these are valuable tools as long as their limits are recognized. Estimates can be broken into three main categories as follows:

a. Order of magnitude estimates
b. Semi-detailed estimates
c. Detailed estimates

In preparing bids there is no substitute for complete, detailed material take off and pricing.

a. Order of magnitude estimates.

Order of magnitude, also called predesign estimates, provide a relatively low level of the accuracy and can seldom be counted on to be within 15% of actual costs. They can be a valuable tool for the contractor in quickly screening a large number of alternative designs. The most useful of these are based on end product units, ratios and physical dimensions. This type of estimate should never be used as a basis for a bid.

b. Semi-detailed estimates

Semi-detailed estimates, also called budget estimates, should be accurate to within about 10% of actual project cost. This level of accuracy is usually considered adequate for decisions on project feasibility. The accuracy of semi-detailed estimates is directly dependent on the amount and quality of information available at the time the estimate is made.

c. Detailed estimates

Detailed estimates, which should be accurate to within 5% of actual project costs, are prepared from complete specifications, drawings and site surveys. This type of estimate should be a "pre-determined

ISSN-12223-7221

truthful evaluation of the cost and time necessary for your company to accomplish a quantity of wok of construction, necessarily approximate, but presumably based upon visualization, experience, and judgement".

Detailed estimates, which are the subject of our study, are time-consuming and expensive to prepare; consequently, they should be made on projects that offer potentially good profit opportunities. The accuracy of detailed estimates will be dependent, to a large degree, upon the ability of the estimator and the adequacy of the contract documents.

There are many reasons for contractor failure; probably the most important of these is the inability of estimator to come up with realistic and accurate estimates of job cost.

2. The role of estimator in a construction company.

The estimator is one of the most important people in a construction company. It is his job to prepare the estimates that will either make or break the company. If the estimator's estimates are too high then the company will never get any projects; if his estimates are too low then the company will not be able to realize a reasonable profit. For these reasons it is required that an estimator have certain skills an qualifications.

To properly organize a bid, the estimator must first have an understanding of the building process. This means having the ability to read plans, understanding job conditions thoroughly and being able to visualize the assembly of construction materials into workable units. Compiling a bid requires several steps including the quantity surveys, determination of unit prices, taking subcontractors bids, determination of the contract price and finally submission of the bid at the bid opening. For the estimator to carry out all of these activities correctly, he must be knowledgeable in basic mathematics including geometry and trigonometry, he must be able to convert the construction operations involved into monetary figures. Above all the estimator has to be practical, organized and consistent.

Consistency and organization are very important. The estimator should always use the same basic methodology in preparing a bid and he should follow the defined format and procedures. Deviation from these can only serve to confuse the other members of the firm who must use and review the estimate. Th estimator should understand that the estimate will be used as a guide for cost control and scheduling throughout the life of the job and keep these two phases of the job control in mind when preparing the estimate.

Before any work is done on a project, the estimator will have to familiarize himself with the project documents. There is, however, the constraint that any time spent on a project be productive. The vehicle to overcome the restraint is Project Summary and Project Sheet. This sheet should be prepared by the estimator as soon as become familiar with the project while doing productive work, second, the summary serves as a check list of things to do during the bid period.

The summary should be in three parts, direct costs, indirect costs and the summary of alternates. The direct costs, generally taken from the technical specifications, will include labor, materials, and equipment charges, and the sub contracts for the physical items in job. Indirect costs will be these costs related to the project which can not be identified with one specific work item and other costs which are primarily found in the general conditions of the specifications.

As mentioned before, the direct costs of the job will include labor, materials and equipment. Labor costs will consist of basic wages paid to all field personnel for performance of field operations. Material costs will include the purchase price of the materials, parts or installed equipment that are supplied by yourself.

2.1. Estimating excavation

In estimating for ordinary excavation work, proper study should be made of the nature of the material to be removed, the general method of removal, special handling that may be necessary for top soil or plants, temporary storage of material for backfill, method of disposal of the excess material, distance to the dump, cost of dumping, equipment and trucking costs, permits, protection of side walks and pavements, temporary roads and runways, ramps, safeguards, lights, watchmen, foreman, labor, risks, weather conditions, breakdowns and rehandling.

In estimating for complex excavations, engineering skill is necessary and should be provided. Most excavations should be considered to be complex if they have rock or water to be cared for or if they are more than 10 feet deep or if there are adjoining structures in which the foundations do not extend down as for as the bottom level of the new excavation.

The estimator should visit the site so that he may ascertain the type of ground, whether it is hard or soft, wet or dry, etc. The labor cost varies according to these conditions. The general method of doing the work must also be given consideration at site- whether it shall be done by hand with picks and shovels, or by drag scrapers, bulldozer or power shovel, or some other means.

2.2. Estimating concrete

It is customary to estimate items of work in the order in which they are ordinarily done in a structure. Therefore, after completing the excavation, concrete formwork would be next in the order of work done. However, because the amount of formwork required is based on the area of concrete in contact with the forms, many estimators will list the concrete first.

In preparing the concrete estimate, each type of concrete needed for structure should be kept a separate heading. Sections or portions of the structure requiring the different types of concrete can then be listed under these headings.

After the amount of concrete needed under each division is determined, it is totaled. The total of each type of concrete is then determined and listed. The cost of concrete is determined by multiplying the cost per cubic meter times the number of cubic meters required.

The cost of concrete may be based on the price of ready-mix delivered to the job, or it may be based on the cost of concrete batched and mixed on the job. When job-mixed concrete is used, the estimator must consider the cost of aggregates, cement, water, equipment, labor to operate the equipment, and space for the mixing plant when determining the cost per cubic meter.

Labor required to place, consolidate, finish, and cure the concrete is estimated on the basis of the contractor's previous experience for similar type of work. Often this cost is based on time required to place a cubic meter of concrete. By determining the work hours necessary to complete a job, it is easy to adjust the cost on the estimate because of changing wage rates.

When determining labor costs on concrete work, care should be taken to avoid omission of any part of the work involved. The cost of placing, consolidating, finishing, and finally curing the concrete must be considered. Overtime is often necessary on large concrete jobs. Because of the added cost, the amount of overtime must be determined- and its cost allowed for.

Equipment needed on a reinforced concrete structure will vary with the type and size of the building. The estimator must determine the type, amount, and cost of all equipment required for the job.

Concrete work done in cold weather may require insulation on the formwork, temporary enclosures, and heaters to prevent freezing of the concrete before it sets. The cost of these items can be considerable. Therefore care must be taken to allow for it.

2.3. Estimating site work

The site work take-off is performed last so that the contractor has sufficient time to become familiar with the plans and the site work subcontractors that are available in the area. Most importantly the site work take-off requires a thorough site visit and any follow up visits that may be necessary. The site visit should help the contractor obtain information on a variety of conditions that may not be covered in the specifications.

Upon completion of site visit, the contractor should be fairly familiar with existing site conditions and have some ideas on how the site work will be approached. Information should also be gathered on the following:

a. Probable weather conditions.
b. Availability of temporary site utilities.
c. Access to the site.
d. Local ordinances and regulations concerning the use of public property.
e. Local building codes and their effect on the construction in question; requirements for special permits.
f. Conditions pertaining to adjacent property protection.

g. Site topography, drainage, and water-table conditions.
h. Soil conditions.
i. Underground obstructions and services.
j. Labor market conditions.
k. Rental of construction equipment.
l. Availability of local subcontractors
m. Wrecking, site clearing and tree cutting.
n. Other matters that pertain to the proposed construction.

It is important that the site visit be performed by an experienced member of the construction organization, especially in locations that are relatively new or strange. Overlooking any major items that affect the cost of the work can result in an unprofitable job.

3. Pricing site work

One of the major considerations in pricing site work will be the equipment used. Before pricing starts the estimator will have to determine which types of equipment are best suited for the job. If you determine that a particular piece of equipment is the best suited for the task based upon the amount of material to be moved, don't forget to consider other requirements such as site access, terrain, turn-around space and capability and availability of operators.

Remember also, when determining unit prices fro equipment use, that productivity of equipment will be affected by the age of the equipment, type of soil, experience of operators and use of equipment. If the equipment being used belongs to your firm then operator cost, fuel, oil and grease, equipment cost and maintenance should be considered in the determination of unit prices.

If the equipment used is leased and an operator comes with it, then the rental fee will have to be considered in the calculations of unit prices. Remember that the cost of keeping equipment on the site must be passed on to the client. Always consider that it costs money to move soil whether it was on the site or brought in. There should be charges in the estimate for both the cut and fill operations.

3.1. Job expenses, Overheads and Profits

In preparing an estimate of a construction project, the two most obvious expense items are for materials and labor. There are other expenses which must be included in the estimate that are directly connected to the cost to the cost of construction.

Among these are charges for equipment, job offices, utilities (water and electricity), temporary construction, rubbish removal and cleanup, and superintendents' and engineers' wages. Other items of job expense which must be allowed for are drafting costs, cost of signs and progress photographs and insurance.

Another type of expense which must be allowed for in preparing a cost estimate is overhead expense. Overhead takes in all the costs of running the construction company which cannot be charged directly to any one job. Salaries of management and office personnel and the general cost of maintaining and operating the company office are items which would be classed as 'Overhead'.

3.2. Job Expenses

The various costs which are incurred as a result of doing a job may be referred to as job expense. As has been already been stated, material and labor costs are the two most obvious job expenses. Other job expenses include:

3.2.1. Performance bonds

Performance bonds are a job expense which must be allowed for in the cost estimate. On a small job the cost will be comparatively small. On larger jobs, where the amount of bond is greater and the period of time for which the bond is required is longer, the cost may become a major item. Some contractors may elect to provide a certified check in place of a bond. The cost of putting the required amount of money aside should not be overlooked. It is at least equal to the amount lost by not being able to invest it, perhaps 4, 5, or 6 percent, or more, of the principal.

3.2.2. Insurance

Various types of insurances are required on a construction job. Workmen's compensation, unemployment compensation, and social security insurance are directly connected to wages or labor costs and may be figured as a part of the hourly rate which must be charged for labor. Regardless of how this cost is handled, it is important to make sure that it is included somewhere in the job cost.

Insurance carried by the contractor which adds to job costs is insurance for public liability, personal injury, fire and theft, storm damage, and property damage for property other than the new construction. The cost of such insurance can best be determined, after the major cost of the job is known, by obtaining the advice of the company's insurance and carriers. Again it is important, here as elsewhere in the estimate, not to overlook this item.

3.2.3. Temporary construction

Temporary job offices, tool houses, storage sheds, and other such conveniences are part of the expense of carrying on a job. Temporary fences, barricades, runways, bridge, stairways, and platforms are also to be considered as items of cost. The law demands that proper safeguards be constructed and maintained in good order to prevent accidents at open shafts, well holes, and other places that are likely to be locations of accidents if not so guarded. The law also demands temporary toilets, drinking water, and other conveniences for the health and comfort of the workmen. Trade unions also demand these and other things besides.

3.2.4. Utilities

Water and electricity are common requirements for construction projects, yet many estimators neglect to make provision enough in their estimates for these items. Water involves not only the water charges, but also the installation, maintenance, and removal of the temporary lines and the changing about of these lines when necessary; and, similarly, for temporary light and power there is the charge for current, the cost of maintaining the lines, and the cost of bulbs and fixtures.

To heat a construction job in winter is a costly undertaking. Some of the elements of this cost are the installation and first cost of the system or devices used for heating, the fuel cost, the additional temporary enclosure work required, the labor of attending to the heating, the repairing and rearranging of the equipment, the loss of time resulting from the men's working under these conditions, and the extra cost of supervising.

3.2.5. Special Equipment

Special equipment of various kinds may be required to complete a job. The cost of this equipment must be added to the job cost. This cost may be in the form of rental charges for rented equipment or prorated ownership costs based on the length of time the equipment is used in relation to its normal useful life. Ownership costs on equipment are often overlooked, and after a period of time when replacement becomes necessary, the contractor may find himself without sufficient funds for equipment replacement.

3.2.6. Services of persons not directly involved in production

Almost all construction jobs require the services of one or more persons who do not directly work on the production of structure. Among these persons are the job superintendent, structural engineers, surveyors, and watchmen. Because these men do not work on the actual construction, it is easy to overlook the cost of their services.

Nearly all jobs require a superintendent who will start the job and follow it through to completion. The superintendent will be on the job even on some days when no work is performed. The estimator must allow for the total number of days on which the job will require superintendence plus a contingent for delays which may be expected due to weather changes, material shortages, etc.

Where the services of an engineer are anticipated, the length and type of service should be indicated on the job expense form and the cost of that service entered. By entering the type, length, and cost of the service, it is easy for the contractor to check the estimate against the actual cost and charge the owner for extras if there are any.

Surveys are always required on a construction job. In addition to the initial survey, several surveys may be required during the course of construction. The estimator must check the specifications to see if any are required and make the proper allowances. In some cases additional surveys may not be required, but the contractor may do well to provide for them in the event he may have to prove that his project is constructed in the place called for by the plans and specifications.

Most large jobs and many smaller ones require night watchmen as well as day watchmen. The number of days and nights for which watchmen are required must be determined and the cost entered on the job cost sheet. By keeping this cost item separate on the job expense sheet it is easy to determine if the actual cost and estimated cost are in agreement.

Once in house take-offs have been completed, the estimator is ready to begin tabulating the final bid. It is at this point that the majority of subcontractor bids will start to be received. Subcontractor bids may be recorded quickly and efficiently.

The final bid should be tabulated, not later than the day before the bid opening. To do this the estimator should pull out the bid file and evaluate all sub bids. By now all in-house take-offs will have been entered in the summary, so evaluation of subcontractors' bids will be all that is left. In evaluating the bids, the estimator will find that the correct bid is not always the lowest. For this reason, a selection should not be made until the scope of each bid has been examined closely. A subcontractor's bid that appears to be low one may prove to be useless if certain items are missing. The beginner should therefore be cautious in selecting subcontractors' bids.

The bid form may be completed once the base bid and values for required alternatives have been determined. Many firms however will not complete the bid form until bid day since bid price changes can occur up to the time of the bid opening. The estimator has to be prepared to handle the volley of changes that may come in at the last minute and his ability to do so will determine to a large extent how successful a bidder he is.

Before submitting the bid, the estimator should be certain that the correct procedure have been followed in preparing the bid form. All the efforts could be wasted if a firm submits a proposal that does not confirm to the requirements in the specifications. The invitation to bid and instructions to bidders should be reviewed carefully to make sure that nothing has been missed. Above all, get to the bid opening on time. No matter how well prepared your bid is, it will not be acceptable if it is submitted late.

Bibliography

[1] W.P.Jackson, *Cost records for construction estimating.* 1984, Craftsman Book Company

[2] James M. Neil, *Construction Cost Estimating for Project Control,* 1982, Prentice-Hall, Inc.

[3] Vick Crespin, C. Dawson Zeigler, *Manual for Construction Cost Estimating,* 1985, Frank R. Walker Company

[4] George Cooper, Stanley Badzinski Jr., *Building Construction Estimating,* 1986, McGraw-Hill Book Company

[5] Sol A. Ward, Thornedike Litchfield, *Cost Control in Design and Construction,* 1987, McGraw-Hill Book Company

Fiber Reinforced Polymers in Concrete Structures

Maurizio GUADAGNINI[a] Mihaela-Anca CIUPALA[a] Kypros PILAKOUTAS[a]

[a]*The University of Sheffield, Sheffield,UK*

Rezumat: Lucrarea prezintă stadiul actual al utilizării materialelor compozite polimerice armate cu fibre, atât ca armatură internă a betonului cât şi ca armătură externă pentru consolidarea structurilor de construcţii. Deşi elaborarea de normative de proiectare care să includă folosirea acestor materiale la structurile din beton este într-o fază incipientă, importante studii teoretice şi experimentale au fost efectuate până în prezent în lume. Sunt prezentate numeroase aplicaţii practice în domeniul construcţiilor, fiind discutate şi alte posibile domenii de utilizare.

Abstract: The paper presents an overview on the use of Fiber Reinforced Polymer (FRP) reinforcement in the construction industry, both as internal concrete reinforcement and external bonded reinforcement. Although the development of codes of practice that incorporate the use of FRP reinforcement in reinforced concrete structures is still at an early stage, much research has been done worldwide. Several examples of applications in civil engineering are shown and possible applications in various fields are also discussed.

Keywords: fibre reinforced polymer (FRP), composite materials, reinforcement, rehabilitation.

1. Introduction

The use of steel reinforcement in concrete structures in adverse environments often leads to serious problems such as corrosion of the reinforcement and, hence, premature deterioration of the entire structure. In the attempt to increase structural durability, various solutions are currently used, all of which either add further costs or complicate construction. The latest effort to eliminate this problem is through the replacement of conventional steel reinforcement with Fiber Reinforced Polymers (FRP) reinforcement in Concrete Structures.

As a result of their peculiar mechanical and physical characteristics, such as high strength and light weight, these non-ferrous materials are suitable not only as concrete reinforcement in new constructions, but also in rehabilitation and prestressed concrete applications.

Firstly used in the late 1980’s by the Japanese for their non-magnetic characteristics, non-ferrous reinforcement started to be used more extensively in the mid 1990’s and many demonstration projects have been completed in Japan, North America and Europe [1].

Despite the relatively extensive use of FRP products, especially in repair and strengthening applications, the use of non-ferrous reinforcement in RC structures has been suffering from the lack of accepted standards for design.

This situation is currently being addressed by various national and international code committees that are scrutinising results arising from the enormous worldwide research effort being made in to the use of FRPs in construction.

In the past fifteen years various Scientific Committees were established in Japan, Canada and in the USA to deal with FRP reinforcement and in 1996 the International Federation for Structural Concrete (*fib*) established the first European Committee (Task Group 9.3), with the objective of developing design guidelines for the design of concrete structures, reinforced, prestressed or strengthened with advanced composites.

This paper will give an overview of the use of FRP reinforcement in concrete structures and the main features of FRP products and their applications will be discussed.

ISSN-12223-7221

2. Overview on FRP products

The mechanical characteristics of FRP reinforcement are different in many respects from conventional steel reinforcement and depend very much on the type of fibres and resins used.

FRP materials are manufactured in many forms such as rebars, sheets, grids and links, as for conventional steel reinforcement, Fig. 1.

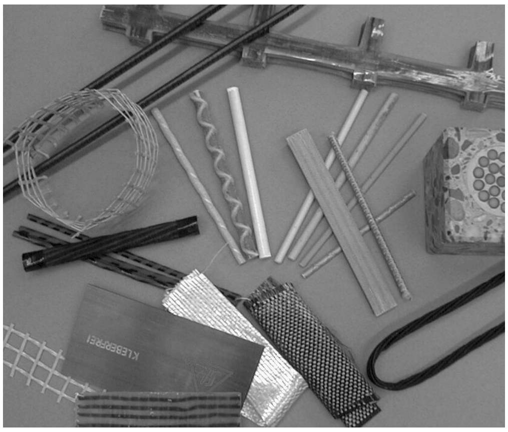

Fig. 1. Examples of various FRP reinforcements

The commonly used structural FRP materials comprise fibres of carbon, glass, aramid and other polymers impregnated with a resin matrix. Due to the non-structural importance of the resins, as well as their high cost, a minimum resin volume ratio is always desirable. However, the maximum fibre ratio that can be practically achieved is normally below 70% [2].

FRP materials can be manufactured by using many techniques such as pultrusion, filament winding, moulding, braiding and manual lay-up.

Composites can be engineered to meet the specific demands of each particular application and their overall performance and characteristics depend on the choice of materials (fibre and matrix), the volume fraction of fibre and matrix, fibre orientation, fabrication method. Furthermore, in order to enhance the bond characteristics of FRP reinforcing bars in concrete, several techniques are used including surface deformation, sand coating, over-moulding a new surface on the bar or a combination of processes.

The main advantages and disadvantages of these advanced composites versus steel are listed in Table 1.

Table 1. Advantages and disadvantages of FRP reinforcement

Advantages	Disadvantages
higher ratio of strength to self weight (10 to 15 times greater than steel)	higher raw material cost
carbon and aramid fibre reinforcement have excellent fatigue characteristics	lower elastic moduli (except some Carbon FRPs)
excellent corrosion resistance and electromagnetic neutrality	Glass FRP reinforcement suffers from stress corrosion
low axial coefficient of thermal expansion.	lack of ductility

High strength and low module of elasticity, together with the fact that FRP materials, unlike steel, do not offer plasticity, are the key properties of these materials that differentiate their performance in concrete structures.

3. Structural considerations

The mechanical properties of FRP reinforcement according to the type of fibres are shown in Fig. 2.

FRP products are characterized by a perfectly elastic behaviour up to failure and can develop higher tensile strength than conventional steel in the direction of the fibres. Their anisotropy affects the shear strength, which is very low, compared to the tensile strength and, again, depends on the properties of the matrix and orientation of the fibres. The elastic modulus of FRP materials used in construction generally varies between 20% of that of steel for glass fibres to 75% of that of steel for carbon fibres.

Although these materials, in general, have a low compressive strength, due to low buckling strength of the individual fibres, this is not usually a concern since, in the majority of civil engineering applications, these elements are essentially used only in tension.

Due to the particular mechanical properties of the reinforcement, and especially due to their lack of ductility, FRP RC structures are normally governed by brittle modes of failure, generally considered to be undesirable. Based on these considerations, it appears evident that both construction techniques and design philosophy need to be carefully reassessed [3].

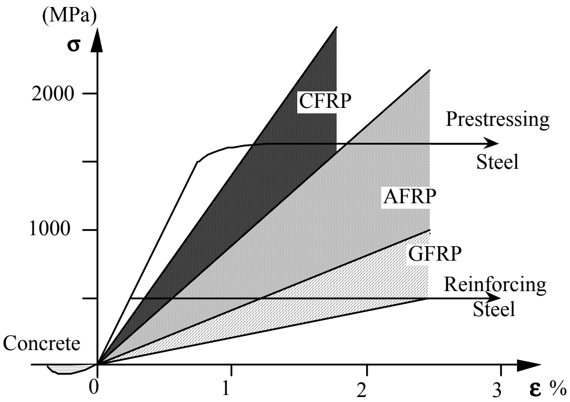

Fig. 2. Stress-strain characteristics for concrete and reinforcing materials

Although many pilot structures have been built using this new type of reinforcement, a mature code of practice that accounts for FRP material does not currently exist. Research undertaken by the Japan Society of Civil Engineers [4], the Canadian Standard Association [5] and ISIS Canada [6,7], the American Concrete Institute [8,9] and, in the Europe, by the EUROCRETE project [10,11] and *fib* Task Group 9.3 [12] has lead to design recommendations, which are based primarily on modifications of design guidelines that were originally developed for steel reinforced concrete.

4. Applications

FRP products have made a dramatic entry into the construction industry in the past few years and many demonstration projects, especially in Japan, were developed in the late eighties and early 90's. In 1996 the Eurocrete project installed the first totally FRP reinforced concrete footbridge in Europe [13], Fig. 3.

The number of applications in Europe has increased substantially during the last decade and this especially relates to externally bonded structures where the FRP reinforcement is used as an external reinforcement to strengthen and rehabilitate the structure [14].

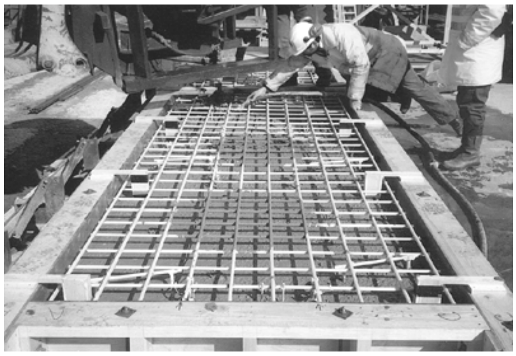

Fig. 3. Fidgett footbridge, Chalgrove - Oxfordshire (Courtesy EUROCRETE Project)

When specifying the use of FRP reinforcement in concrete structures, durability is usually the primary concern. Because of their relatively high cost, the use of advanced composites is therefore only likely to replace steel reinforcement in those applications where the superior corrosion resistance properties of the FRPs are required. For these special applications, FRPs can be highly competitive with other corrosion resistant products such as stainless steel and epoxy coated reinforcement, which currently only account for about 3-4 % of the total reinforcement market.

Based on the above considerations, many areas of application can be identified and are discussed in the following.

4.1. Durability

A large proportion of the expenditure on the repairing and maintenance of infrastructures is due to problems with concrete structures mostly related to the deterioration of the reinforcement. Steel reinforcement has the tendency to corrode and this process becomes relevant when concrete structures are exposed to the environment. When steel corrodes, additional stresses develop due to the additional volume of the iron oxides and accumulate in the concrete. These stresses are capable of splitting the concrete near the surface, allowing much faster ingress of water and chemicals and the reaction speeds up until the concrete cover is fully damaged and eventually spalls off.

FRP reinforcement represents a valid alternative for anti-corrosive purposes and it has many possible applications in structures in or near marine environments, Fig. 4, in or near the ground, in chemical and other industrial plants and in places where good quality concrete can not be achieved.

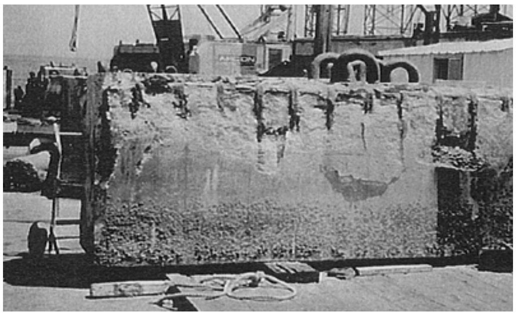

a)

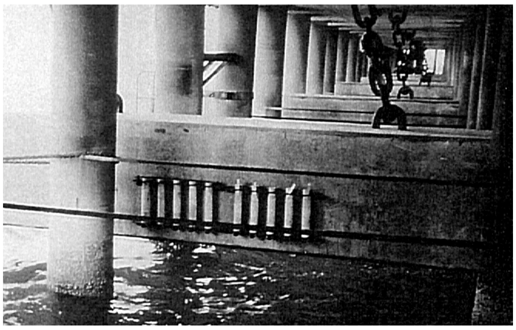

b)

Fig. 4. Corroded fender support beam (a) and FRP reinforced concrete replacement beam (b), Qatar (Courtesy EUROCRETE Project)

4.2. Electromagnetic neutrality

Steel reinforcement is usually avoided when magnetic neutrality is required and in many applications, especially for the mobile telecommunications industry and the defence industry, this can be a big concern. As an alternative to the more conventional steel reinforcement, FRP reinforcement can be used succesfully in structures situated in the vicinity of transmitting stations or receiving devices. For instance, concrete posts and fence panels reinforced with FRP reinforcement were used for this purpose during the Eurocrete Project, Fig. 5a. Other possible applications include the bases of large motors, magnetic scanning equipment and magnetic levitation systems such as the MAGLEV, Fig. 5b.

a)

b)

Fig. 5. FRP reinforced post and panel fencing around a transmitter (a), MAGLEV train in Japan (b)

4.3. High strength

One of the more important properties of FRPs is the very high strength that can be developed, allowing a reduction in the area of reinforcement needed in certain applications. However, since high strength in the reinforcement can only be developed when accompanied by high strains, this property can only be fully exploited in prestressed concrete elements, Fig. 6a. Furthermore, when FRP is adopted for prestressing, the high stresses developed in the reinforcement are also accompanied by lower losses than those associated with conventional steel tendons due to the lower elastic modulus of the FRP material. However, because of the stress corrosion that affects FRP materials, particularly glass fibre based products, only carbon and aramid are likely to be appropriate for applications in this field.

In addition, FRP cables can be used in cable stay bridges and in other anchoring applications such as ground anchors or rock bolts, Fig. 6b.

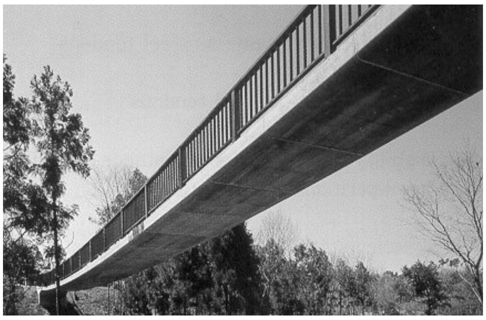

a)

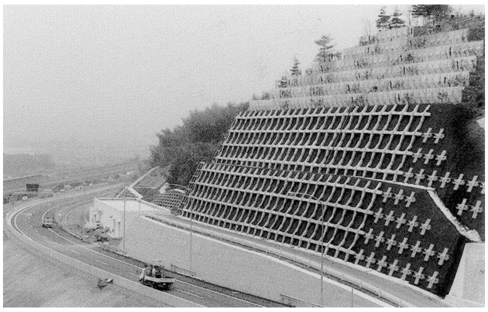

b)

Fig. 6. Prestressed FRP cables used in a ribbon bridge in Japan (a) and ground anchors (b)

4.4. Light weight

Despite the fact that the weight of steel reinforcement is normally insignificant compared to that of concrete, the light weight of FRP reinforcement can have some practical advantages in construction, especially in specific applications when work must be carried out in confined spaces and lightweight reinforcement can speed up construction. Again the light weight of FRPs becomes relevant when dealing with externally bonded reinforcement for repair purposes, Fig. 7. In this application the strength and compatibilities of

Fig. 7. Devonshire Place Bridge, Skipton, UK [14]

4.5. Mouldability

Strengthening columns against earthquakes or impact requires the reinforcement to go around an existing element. FRP fabrics have been proven to be a huge success in this respect and are rapidly replacing conventional jacketing techniques, Fig. 8.

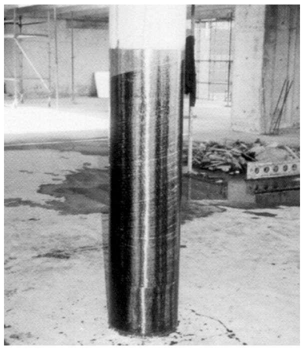

a)

b)

Fig. 8. Column strengthening with FRP sheets (a), retrofitting of chimney with automatic winding machine, Mitsubishi (b)

5. Conclusions

FRP materials offer an effective solution to the problem of steel durability in aggressive environments and where the magnetic or electrical properties of steel are undesirable. They also appear to be suitable for the manufacturing of non-structural pre-cast elements where the weight of the reinforcement and concrete required is a disadvantage. Using FRPs allows a drastic cut down of the overall weight of the elements and facilitates handling and installation procedures.

The aim of using FRP reinforcement is not to totally replace steel reinforcement from RC structures, but to identify areas in which steel can be successfully replaced. Examples of such applications have been discussed in this paper and others that can be identified include:

- non-structural elements
- deep structural elements
- elements that can safely be subjected to large deformations such as highway separators or parapets
- elements in which high damping is required
- elements in which good fatigue characteristics are required

Nevertheless, many aspects of advanced composite structural behaviour has to be addressed in detail before their full potential could be exploited in new constructions or for the structural repair of existing structures.

6. Acknowledgements

The authors wish to acknowledge the European Commission for funding the TMR Network „ConFibreCrete" and the Marie Curie Fellowship (Human Potential programme) under contract number HPMF-CT-2001-01279.

7. References

[*] m.a.ciupala@sheffield.ac.uk

[1] Japan Concrete Institute, *Proceedings of The Third International Symposium on Non-Metalic (FRP) Reinforcement For Concrete Structures*, October 1997, Tokyo.

[2] Taranu N. and Isopescu D., *Structures Made of Composite Materials*, 1996, Ed. Vesper, Iasi.

[3] Gdoutos E. E., Pilakoutas K. and Rodopoulos C. A., *Composites in Concrete Construction*, 2000, McGraw-Hill, London, pp. 449-497.

[4] Japan Society of Civil Engineers, *Recommendation for Design and Construction of Concrete Structures using Continuous Fibre Reinforcing Materials*, 1997, Concrete Engineering, Series 23.

[5] Canadian Standard Association, *Canadian Highway Bridge Design Code Section 16: Fibre Reinforced Structures*, 1996, Final Draft, CHBDC.

[6] ISIS Canada - Intelligent Sensing for Innovative Structures, *Reinforced Concrete Structures with Fibre Reinforced Polymers*, *Design manual No. 3*, 2001, ISIS Canada Corporation, Manitoba, Canada.

[7] ISIS Canada - Intelligent Sensing for Innovative Structures, *Strengthening Reinforced Concrete Structures with Externally-Bonded Fibre Reinforced Polymers*, *Design manual No. 4*, 2001, ISIS Canada Corporation, Manitoba, Canada.

[8] American Concrete Institute, *Guide for the Design and Construction of Concrete Reinforced with FRP Bars*, *ACI 440.1R-01*, 2001, ACI Committee 440, Farmington Hills, MI, USA.

[9] American Concrete Institute, *Guide for the Design and Construction of Externally Bonded FRP Systems for Strengthening Concrete Structures*, *ACI 440.2R-02, 2002*, ACI Committee 440, Farmington Hills, MI, USA.

[10] Clarke J. L., O'Regan D. P. and Thirugnanenedran C., *EUROCRETE Project, Modification of Design Rules to Incorporate Non-Ferrous Reinforcement*, 1996, EUROCRETE Project, Sir William Halcrow & Partners, London.

[11] The Institution of Civil Engineers, *Interim Guidance on the Design of Reinforced Concrete Structures Using Fibre Composite Reinforcement*, August 1999, SETO Ltd., London.

[12] Federation International du Beton, *Externally Bonded FRP Reinforcement for RC Structures, fib bulletin 14*, 2001, Lausanne.

[13] Clarke J. L. and Waldron P., *The Reinforcement of Concrete Structures with Advanced Composites*, 1996, The Structural Engineer, No. 17, Vol. 74, pp. 283-288.

[14] Leeming M., *EBR Reinforcement for Concrete Structures, Database*, January 2000, *fib* Task Group 9.3.

On Calculating the Apparent Sound Insulation According to EN12354 Acoustic Prediction Model

Grațiela HÎNCU[a] Rodica ROTBERG[a]

[a]*Universitatea Tehnică "Gh. Asachi" Iași , Iași, România*

Rezumat: Lucrarea prezintă rezultatele obținute, urmare a unui studiu privind transmisia zgomotului aerian şi de impact prin pereți, respectiv elemente de planşeu, în cazul unei clădiri de locuit de tip multi-familial, pe baza normelor europene EN12354. S-a analizat influența dispoziției încăperilor şi a caracteristicilor lor geometrice şi fizico-acustice asupra nivelului de izolare acustică la zgomot aerian şi din impact, în varianta în care pereții despărțitori de tip A şi planşeele tip F nu sunt/sunt tratate absorbant din punct de vedere acustic. S-a constatat că, prin dispunerea dublajelor pe planşee şi pe pereții despărțitori, se obține o reducere substanțială a nivelului de zgomot structural şi o îmbunătățire a indicelui ponderat de atenuare sonoră.

Abstract: This paper presents selected results from a study regarding the airborne and impact sound transmission through the partition walls and floors, respectively, in the case of a multi-family residential building, according to the EN12354 European Code. The influence of the rooms disposal and their geometrical and acoustic characteristics on the airborne insulation level and weighted normalized impact sound pressure level have been analyzed, when the partition walls and floor elements are not/are treated acoustically. By using floor coverings and wall linings, it has been observed that the impact noise level decreases substantially and the weighted sound reduction index increases.

Keywords: weighted normalized impact noise level, weighted sound reduction index.

1. Introduction:

The acoustic insulation of two enclosures is defined as the arithmetic difference between the sound level of the emitting room and that of the receiving one. Estimating acoustic insulation involves listing the ways of sound transmission and the evaluation of the amount of noise transmitted on each way.

All the walls that confine the emitting enclosure are subjected to vibration due to the noise. These vibrations will be transmitted to all the walls of the receiving room as a result of the junctions between them.

2. Estimation of airborne sound insulation when the flanking transmission is taking into account

The sound insulation between two enclosures depends on:

- sound reduction index of the partition wall;
- area of partition wall;
- transmission through lateral walls, sound reduction index and area of lateral walls considering the attenuations in the wall joints;
- volume of receiving room;
- acoustic characteristics (reverberation time) of receiving room.

The relation allowing to estimate the normalized sound insulation, D_n , is:

$$D_n = R + 10 \cdot log(\frac{0.16V}{T \cdot S}) \quad (1)$$

in which:

R is the sound reduction index of the partition wall, dB(A);
V – volume of the receiving room, m^3;

ISSN-12223-7221

S – area of the partition wall, m^2;
T – reverberation time of receiving room, s;
TL – insulation losses due to flanking transmissions.

2.1. Calculus method recommended by C125 Romanian Code

For homogeneous fastening elements in a layer, the curve of attenuation index $R_i(f)$ is plotted and then, the effect of sound transmission by collateral ways is introduced, by displacing the curve $R_i(f)$ with the value $\Delta R_C = -20\, log(\frac{Z_i}{Z_f} + 1)$ (dB),

where:
Z_i is mechanical impedance corresponding to the structural element under study (daNs/m);
Z_f – average mechanical impedance of the structural elements adjacent to the element under study (daNs/m).

2.2. European method recommended by CEN

The principle of the method consists in taking into account various potential noise transmission ways (generally, one direct way and 12 lateral ones) and calculating for each of these an apparent reduction index. The insulation is calculated for a number of composing elements equal to the radiation channels in the receiving room, each of these elements having an apparent reduction index.

The amount of noise transmitted through one of the lateral ways is a function of several parameters:

- sound reduction indexes of walls at emission and reception;
- sound attenuation at passing through the junction of the three walls (lateral emission/partition wall/lateral-reception);
- geometric characteristics.

The method recommends the calculus of the reduction index R_{ij} of transmission through the wall i in the emitting room and the wall j in the receiving room, using the relation :

$$R_{ij} = \frac{R_i}{2} + \frac{R_j}{2} + K_{ij} + 10\, log\,(\frac{S_z}{l_f}) \qquad (2)$$

where:

R_i is the reduction index of lateral wall i in the emitting room;
R_j – reduction index of lateral wall j in the receiving enclosure;
K_{ij} – reduction index of junction for ij way;
S_z – area of partition wall, m^2;
L_f – length of junction between the partition wall and the walls i and j, m.

One of the difficulties in applying this method is a good knowledge of the reduction index of junction K_{ij}. This represents the attenuation of the junction and the higher the value of the index is, the more important the attenuation is. Research is under way aiming at determining the calculus model for these indexes function of wall thickness, volumetric mass, Young's modulus and Poisson's coefficient for material, internal losses coefficient, etc. At the moment, experimental measurements are being made to determine the vibration level of the walls. In both cases (calculus and experimental tests), the objective is to create a data base on K_{ij} indexes for a sufficient large number of junctions, in order to solve all the existing cases.

The CEN Project proposes in one of its Appendices the calculus relations for K_{ij} function of the ratio of partition and lateral walls masses, for a number of simple current cases. After having considered $M = lg(m_2/m_1)$, where m_1 is the mass on surface of wall 1 and m_2 is the mass on surface of wall normal to wall 1 in the junction point, the Project CEN indicates the following:

- for cross rigid junction

$K_{11} = 8.7 + 17.1\, M + 5.7\, M^2$

$K_{12} = K_{21} = 8.7 + 5.7\, M^2$

- T rigid junction

$K_{11} = 5.7 + 14.1\, M + 5.7\, M^2$

$K_{12} = K_{21} = 5.7 + 5.7\, M^2$

- junction with a lightweight façade

$K_{11} = 5 + 10\ |M|$, with a minimum of 5 dB

$K_{12} = K_{21} = 10 + 10\ |M|$

- simple wall

$K_{11} = 10 - 20\ |M|$, with a minimum of 10 dB

$K_{12} = K_{21} = 10 + 10\ |M|$

$K_{22} = 2.5 + 14.1\,|M| + 5.7\ M^2$, if $m_2/m_1 > 3$

- junction of two lightweight double walls

$K_{11} = 10 - 20\ |M|$, with a minimum of 10 dB

$K_{12} = K_{21} = 10 + 10\,|M|$

If the contact between the lateral and the partition wall is inexistent or almost inexistent, the index K_{ij} is given by the expression:

$$K_{ij} = 10\ lg\ (l_f(1/S_i+1/S_j)) \qquad (3)$$

where:

- l_f is the length of junction and
- S_i and S_j are areas of walls i and j, respectively.

The total reduction index results from the logarithmic addition of the indexes of the partition wall and of the indexes $K_{ij.}$ Coverings, suspended ceilings can be placed on the walls of the basic structure. The additional walls shall be characterized acoustically by the reduction index ΔR. The effect of the additional wall is calculated separately. The method shall be applied to the basic structure to which the reduction index ΔR is added. In this case, the calculus relation of the reduction index R_{ij} has the form:

$$R_{ij} = \frac{R_i}{2} + \frac{R_j}{2} + \Delta R_{ij} + K_{ij} + 10\,log(\frac{Sz}{l_f}) \qquad (4)$$

in which:

$\Delta R_{ij} = \Delta R_i$ or ΔR_j , for a single covering layer;

$\Delta R_{ij} = \Delta R_i + \Delta R_j\ /2$ *or* $\Delta R_j + \Delta R_i\ /2$, for two covering layers.

3. Theoretical approach

The ISOVER program determines the level of airborne and structural sound insulation of various rooms in a dwelling. This program is interactive, the input data (specific weight and sound reduction index for the wall type elements, partition wall and floor, as well as the impact noise level for floors) being able to enter from a personalized data bank which can be up-dated.

From a data base with horizontal and vertical sections, one can select the module that suits the situation required by the case study (fig. 1). Specifications are provided for wall areas of type B, C, D and H, of partition walls of type A, of floors of type F, as well as of the height of the rooms. If openings are cut in the façade or interior walls (doors, windows), their surface shall be substracted from the area of the respective walls.

The program allows for the introduction of coverings disposed on any confining surface (walls or floors) chosen from the data base.

The ISOVER program uses the following acoustic values:

L_n – normalized impact sound pressure level, measured in laboratory, with suppressed flanking transmissions;

L_{nw} – the weighted normalized impact sound pressure level on the shifted rating curve, at 500Hz;

L'_{nw} – the apparent normalized impact sound pressure level, measured in real building, under the effect of direct and flanking sound transmission;

R – the sound reduction index, measured in laboratory conditions, with suppressed flanking transmissions;

R_w – the weighted sound reduction index on the rating curve, at 500Hz;

R' – the apparent sound reduction index.

As output data, the program enables the user L'_{nw} and the weighted standardized sound pressure level difference between the adjacent rooms, on the horizontal and on the vertical, respectively (1→2, 2→1, 1→3, 3→1).

Table 1. The acoustic and construction data

Surface denomination and its structure	Specific weight (Kg/m^2)	R_w dB(A)	L_{nw} dB(A)
A – partition wall, single layer, plastered light concrete wall, 13cm.	85	41	
B – plastered brick block, 22cm.	210	45.2	
C – plastered brick block, 22cm.	210	45.2	
D – plastered brick block, 22cm.	210	45.2	
H – plastered brick block, 22cm.	210	45.2	
F – reinforced concrete floor, 15cm.	360	54	76

4. Case study

The application considered rooms with the following geometric dimensions: L=4.00m, l=3.00m and h=2.60m. The physico-acoustic characteristics of the confining surfaces and of the partition walls are given in the table 1. window openings (S_w=1.10m^2). As far as coverings are concerned, there have been used:

- for floors, timber finish on glasswool plate of 5cm. on concrete layer;
- for the partition walls, mineral wool, 3dB(A) efficiency.

The type D walls are provided with door openings (S_d=1.90m^2) and the type H ones, with

The results of our research (Table 2) show that:

- the treatment with sound absorbing coverings of the partition wall leads to increases of 2…3 dB to 5…6 dB of the airborne sound insulation level;
- the placing of the parquet covering on glasswool plate on the floor leads to a reduction by approximative 40% of the impact noise level.

Table 2. D'_{nw} and L'_{nw} values, taking into account the direction of propagation

Room disposal D_{nw} (dB)	1	2	3	4	5	6	7
1 → 2	40(43)	41(45)	40(43)	45(47)	40(43)	40(45)	44(49)
2 → 1	40(43)	45(45)	40(43)	41(45)	40(43)	40(44)	45(49)
1 → 3	49(53)	49(54)	49(53)	49(53)	49(54)	48(54)	49(54)
3 → 1	49(53)	49(54)	49(53)	49(53)	49(54)	49(55)	49(55)
Ln (dB)	79(47)	79(47)	79(47)	79(47)	79(47)	77(47)	79(47)

The case study has not made an analysis of the possibility of sound protection for the exterior walls. This aspect makes the object of further research.

5. Conclusions

The ISOVER program is a fast and useful instrument in determining the airborne and impact sound level and it observes the European Codes of practice in the field. The program is provided with an open data base that can be up-dated by the user and has facilities in terms of positioning the functional units on level and orientation, while the latter can be selected from a bank of pictograms.

The advantages of this program reside in the fact that the airborne and impact insulation level results from a single running, while the noise insulation level can be calculated for two adjacent rooms, from the sound source to the receiver and the other way round.

6. Bibliography

[1] *** ISOVER - *Reference Manual*, 2003.

[2] Dimitriu-Vâlcea, E., *Indrumar de proiectare,* 1976, Ed. Tehnică, Bucureşti.

Experimental Research on Cracking Behaviour of Partially Prestressed Concrete Beams

Carmen NUȚIU[a] Traian ONEȚ[a]

[a]*Technical University of Cluj-Napoca, Cluj-Napoca, România*

Rezumat: În lucrare se prezintă cercetările experimentale efectuate asupra unor grinzi din beton parțial precomprimat, cu armătură preîntinsă, cu privire la fisurarea acestora. Programul experimental a cuprine trei serii a câte şase grinzi, analizându-se următorii parametri: gradul de precomprimare şi solicitarea (în regim static şi repetat). Rezultatele experimentale obținute oferă posibilitatea de apreciere a preciziei de evaluare a deschiderii fisurilor după prevederile din normele româneşti şi europene de calcul şi permit formularea unor propuneri de perfecționare a acestora..

Abstract: This work presents the experimental research made on cracking behaviour of partially prestressed concrete beams with pretensioned reinforcement. The experimental test was carried out in three stages (each involving six beams) towards the analysis of the following parameters: prestress level and strain (statically and cyclically applied loadings). The experimental results thus obtained allows for a correlation between prestress level and crack width at partially prestressed concrete members.

Keywords: pretensioned reinforcement, prestress level and strain, analysis, concrete beams

1.General

Ensuring high performance of a concrete structure, taking into consideration the environmental influences and specific response, involves equally the improvement of materials properties, proper design, neat execution, inspection measurements, maintenance and prevention of damage risks.

The cracks in the constituent elements of the concrete structure are brought about by dynamically, statically and cyclically applied loadings, temperature changes, creep and shrinkage of concrete, soil settlement, incorrect reinforcement anchorage and binding, deviations from the rules of section formation etc.

A method for calculation of crack width cannot be fully worked out only in theory, as the effect of some parameters which affects the cracking behaviour can only be determined on empirical bases. The whole process itself fluctuates so as different computational methods yield different values. It's obvious that every formula which is individually analysed agrees with the experimental data that generated it, but its accuracy declines when compared to other experimental results.

Experimental Research

Tests carried out abroad pointed out a very good resilience of partially prestressed concrete as the cracks that appeared as a result of applying loads closed to that of the collapse load became invisible at the moment of the unloading.

In 1946, upon carrying out tests on partially prestressed concrete beams with binding wires, Abeles P.W. noticed that the cracks completely closed at unloading, even if the load was close to that of the collapse load. Similar results was achieved over many years of study and trials and the partially prestressed concrete was thus accepted in England since 1948.

Later on, proffesor Campus F. carried out fatigue loading tests in Liege on partially prestressed concrete composite slabs with the following results:

-in one of the tests, after a cycle of one million loadings with the tensile unit stresses between 0.7 and 4.2 N/mm^2, the cracks became entirely invisible after unloading;

-another test showed that after a cycle of 3 million loadings with tensile unit stress reaching

ISSN-12223-7221

the value of 7 N/mm^2, only very fine cracks were visible.

The proceedings of IABSE Congress in 1956 made clear that cracks in monolithic beams with tensioned reinforcement and good concrete binding (pretensioned or post-tensioned reinforcement skillfully injected) are fine and safe. They fully close at unloading, when loading value reaches 80-90% of dead load value or doesn't exceed 2/3 of collapse load value. As for the tensioned reinforcement beams with no binding (post-tensioned uninjected reinforcement) the cracks are not fully closed at unloading. The reason is that in the first case the binding is damaged only near the crack, while in the second case the reinforcement elongates on its entire length and residual deformations might appear.

Tests carried out by Benett E.W. and Chandrasekar C.S on 20 partially prestressed concrete beams (post-tensioned rebars, strands or wires) 6.4 m long and cross-section of 152/304 mm showed that cracks closing and their opening at reloading occurred close to concrete release. An exception from this were the beams with reduced prestressing where the cracks stayed visible after unloading.

Prasada Rao A.S., Gandotra K. and Ramaswaaamy G.S. performed tests on double tees with injected post-tensioned reinforcement, at different levels of prestressing. All the cracks that appeared, even when the dead load was 75% of collapse load, fully closed at unloading as long as the prestressing level stayed above 0.4.

As per his research, professor Castelli Guidi claims that a reduced prestressing suffices for the closing of cracks when diminishing the applied loading values. This is not the case when the reinforcement are strained beyond their ultimate elastic limit and the cracks partially close due to appeareance of residual deformations.

A great deal of experimental research and studies was made in Romania on loading behaviour of the partially prestressed concrete members with pretensioned reinforcement made of cold-drawn steel wires with or without passive reinforcement.

These works pointed out that using the profiled passive reinforcement (small in diameter) interweaved with the pretensioned one led to a decrease of cracks openings both near pretensioned and non-pretensioned reinforcement. The tests made on members with mixed reinforcement showed minor differences between crack opening in long-term loading (M_{ld}^E) and limited loading (20-iteration cycle).Several maximum allowable local values for crack opening due to M_{ld}^E strain decreased after the loading was reiterated and the average opening of the cracks remained unchanged.

The laboratory of Reinforced and Prestressed Concrete within the Civil Engineering Faculty in Cluj-Napoca performed a research programme on the relationship between loading duration, cyclically applied loading (limited number of times) and cracks opening in partially prestressed concrete members [O.2].

It was noticed that the moment of crack opening (maximum allowable α_f = 0.01 mm) grows longer and longer with the increase of the prestressing level. α_f reaches its maximum of 0.1 mm after 1 year of applying the load. The cyclic loading in these conditions had no significant effect.

3. Experimental Programme

The experimental tests are grouped in three series: Series I, Series II and Series III.

Series I

The tests in this series focused on the cracking behaviour evolvement under working loads or cyclic loads applied on members with different ratios between pretensioned active reinforcement and complementary non-pretensioned reinforcement.

The test were carried out on secondary prestressed beams of 6 m span used on cement asbestos undulated roofings.

The following parameters were considered to elaborate the experimental programme:

- reinforcement and level of prestressing

GSP - 12 K = 1.320; 1 TBP 12 + 2 SBPA Φ 5
GSPP - 9 K = 0.685; 1 TBP 9 + 1Φ 10 PC 52
GSPP - 7.5 K = 0.485; 1 TBP 7.5 + 1Φ 12 PC 52

- loading: - statistically applied (I)
  - cyclically applied (II)

For each prestressing level two identical beams were made, one for testing under statically applied loads and the other one for testing under cyclically applied load. A total number of 6 beams were tested.

Cyclic loading was made in 20 loading/unloading cycles (5 oscillations per minute), the numerical results being shown in [N1].

Series II

The tests in this series focused on partially prestressed concrete beams (12 x 25 x 320 cm, 6 members) under monotonic and cyclic loads.

The tests were made on partially prestressed members (30-day old) under monotonic and cyclic loads.

The following parameters were examined:

- reinforcement and level of prestressing

K = 0.523 (0.325); 1 TBP 9 + 2 Φ 12 PC 52
K = 0.613 (0.450); 1 TBP 9 + 2 Φ 10 PC 52
K = 0.726 (0.750); 1 TBP 12 + 2 Φ 10 PC 52

- loading: - monotonic (I)
  - cyclic (II)

Testing was as follows:

-Monotonic and statically applied loading performed on one member for each prestressing level had three phases:

a) $M = 0$; $M = M^E$; $M = 0$
b) $M = 0$; $M = M^r$

Where M^E - working moment for maximum crack width $\alpha_f = 0.1$ mm;
M^r - collapse moment.

-Cyclic loading made on one element at a time for each prestressing level as specified in [N1].

Series III

The focus is mostly the same as in previous tests. The members that were tested had similar characteristics to those in series II, and were used in a more complex research programme on beam behaviour under different types of loadings.

The tests in this series were made on beams (12 x 25 x 320 cm, 6 members) with different prestressing levels under statically and cyclically applied loads.

The following parameters were examined:

- reinforcement and level of prestressing

K = 0.480; 1 TBP 9 + (3 Φ 14 + 1Φ 10) - PC 60
K = 0.587; 2 TBP 9 + 2 Φ 14 - PC 60
K = 0.668; 3 TBP 9 + 2 Φ 10 - PC 60

- loading: - statically applied (I)
  - cyclic (II)

Testing was as follows:

-Monotonic and statically applied loading performed on one member (28-year old) for each prestressing level had the following phases:

a) $M = 0$; $M = M_{0.01}$; $M = M_{crack\ closing}$
b) $M = M_{crack\ closing}$; $M = M_r$

Where M^r - collapse moment.

-Cyclic loading made on one element at a time for each prestressing level was as follows:

a) $M = 0$; $M = M_{0.01}$; $M = M_{crack\ closing}$
b) 1500 cycles ranging from 0.5 M^E to M^E (M^E - $M_{\alpha f}{}^{max} = 0.1$ mm).

Data output on cracking state due to statically and cyclically applied loadings is shown in the 27 annexes from [N 1].

4.Comparative Analysis of Theoretical and Experimental Results on Cracks Opening

Methods of calculations for crack opening are compared according to romanian design normatives (STAS 10107/0-90 [S 1]), MODEL CODE/FIB 1990 [C 1] and EUROCODE 2 1989 [E 1].

The necessary data concerning the geometry of the member cross-sections, quality of materials, active and passive reinforcement, prestressing force and level are shown in [N 1].

The experimental results are compared with the numerical values yielded by the above mentioned methods of calculations.

4.1 Statically Applied Loadings

Crack opening calculation results computed for each series of beams under statically applied loading are compared with the experimental results for same and shown in fig. 4.1.

Their analysis gives the following:

-ratio fluctuation between calculation and experimental results for crack opening can be considered reasonable for the range of ±50%, taking into account the inherent unsteadiness of cracking process and numerous parameters that affect it;

-an almost complete agreement is made when comparing the calculation results with the experimental results according to EUROCODE 2;

-calculation results given by romanian normatives are acceptable in agreement for 4 out of 9 situations, for the remaining 5 the calculation being way out;

-also, the normatives CEB/FIP gives major differences when comparing the calculation results with the experimental ones.

4.2 Cyclic Loading

Figure 4.3 shows the comparison between experimental results and calculation results computed for each series of beams under cyclically applied loadings.

Their analysis gives the same conclusions as above. The reiteration until 1500 cycles are reached does not affect significantly the values for crack openings.

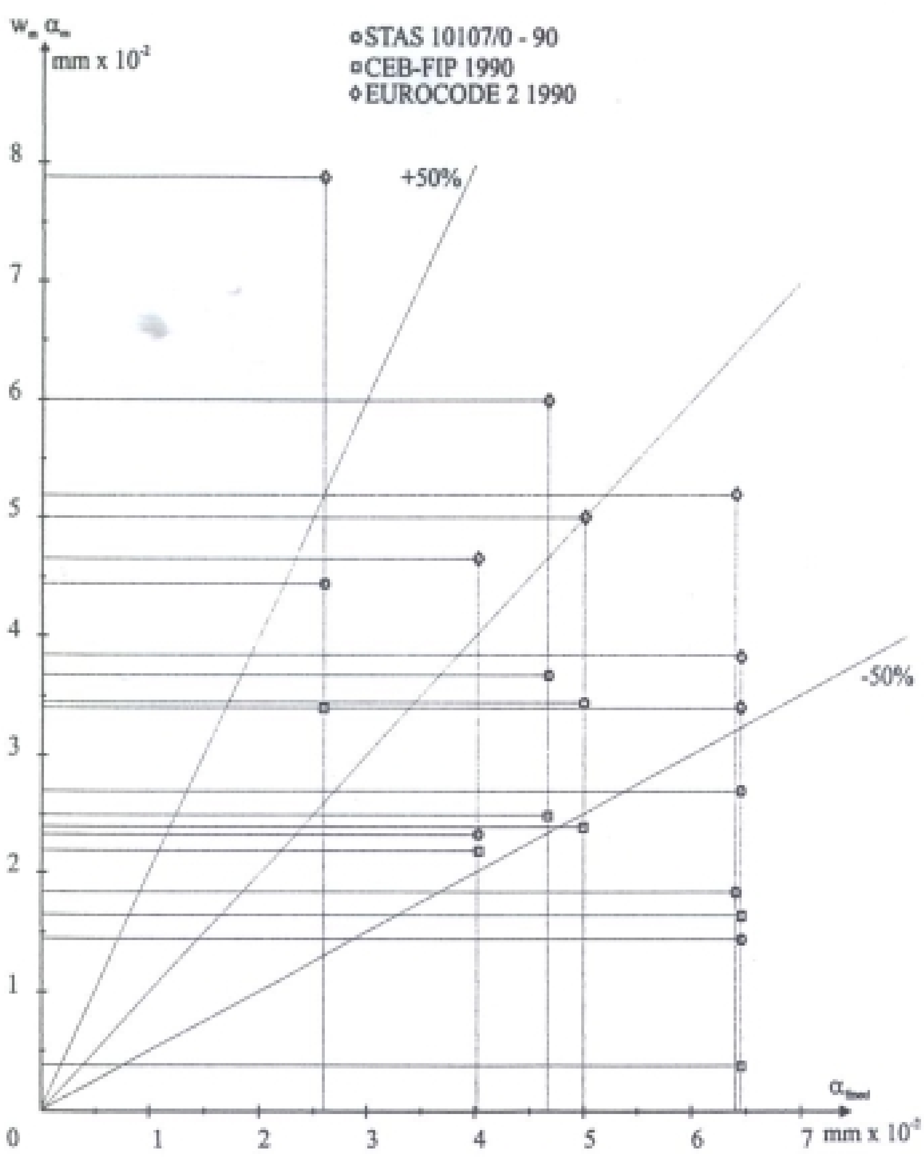

Fig. 4.1 Numerical values and experimental results for crack opening under statically applied loadings.

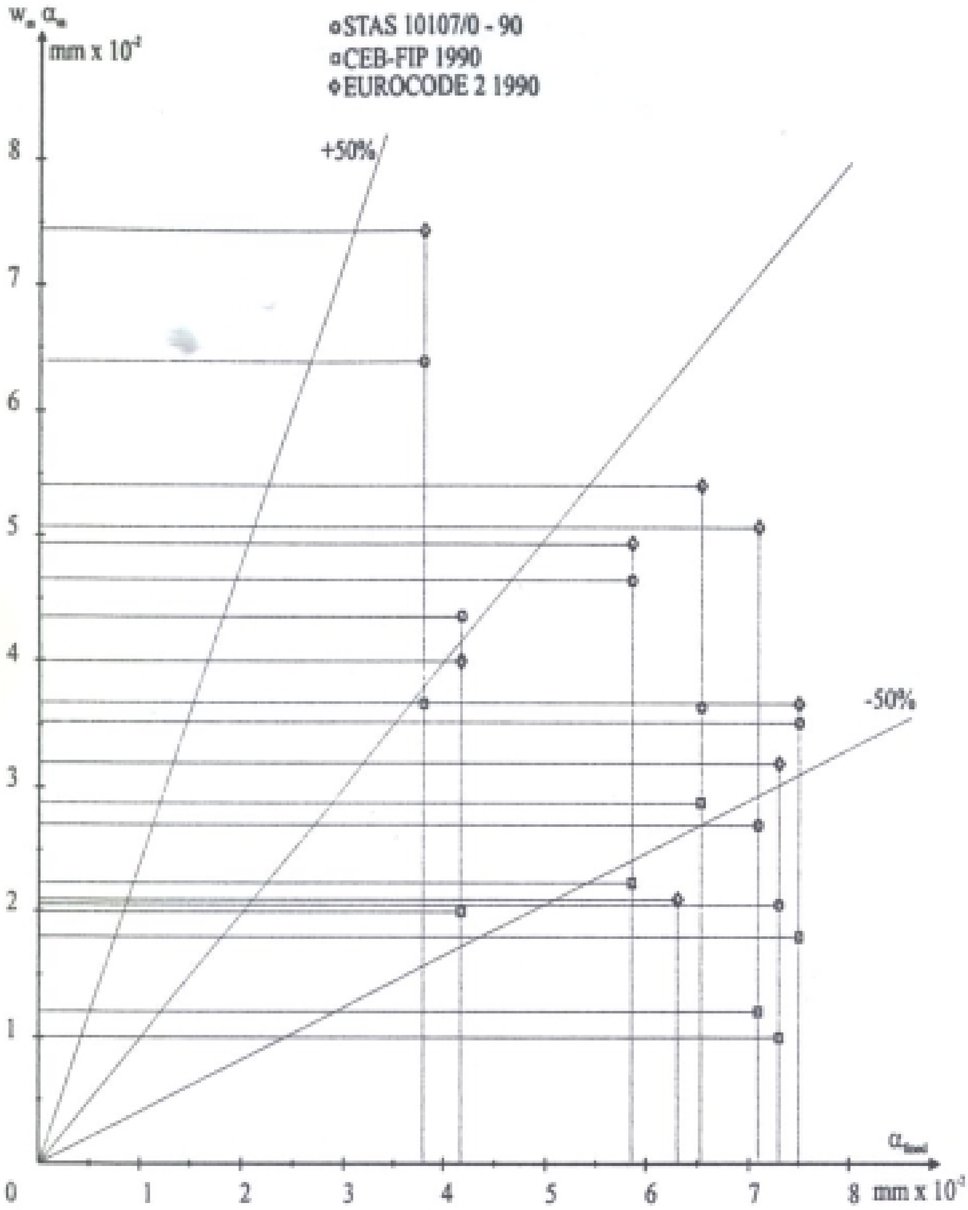

Fig. 4.2 Numerical values and experimental results for crack opening under cyclically applied loadings.

5. Conclusions

The analysis of the parameters that influence the crack openings shows that the most important one is the prestressing level K, as defined in [S 1].

As a result, the crack opening in partially prestressed concrete members can be predicted using the formulae:

$$\alpha_{fmediu} = 0.17 - 0.2K + 0.074K^2 \tag{5.1}$$

for statically applied loadings, and

$$\alpha_{fmediu} = 0.048 + 0.235K - 0.271K^2 \qquad (5.2)$$

for cyclically applied loadings.

It is deemed necessary that the revised draft of the romanian design normatives CR 2000 to additionally comprise provisions for cracking behaviour control by limiting the range for diameter and space between reinforcements, without making a direct calculation for all situations.

Bibliography

[1] C.1. CEB Model Code 1990. Final Draft, 1991.
[2] E.1. EUROCODE 2, Design of Concrete Structures. Part 1. General Rules and Rules for Buildings. Revise Final Draft. Dec. 1989.
[3] N.1. Nuțiu Carmen, Fisurabilitatea elementelor din beton parțial precomprimat, Teza de doctorat, Cluj-Napoca, 1998.
[4] O.1. Oneț T., Măgureanu Cornelia, Nuțiu Carmen, Flexural Cracking Behaviour of Partially Prestressed Pretensioned Beams. Construction 2000. International Symposium 15-16 Oct, 1993. Cluj-Napoca. Proceedings 1.
[5] O.2. Oneț T., Betonul parțial precomprimat. Editura Cărții de Știință, Cluj-Napoca, 1993.
[6] O.3. Oneț T., Nuțiu Carmen, The Cracking of Partially Prestressed Concrete Members. Jubileumi Tudomanyos Ulesszak, Pecs, 1995.
[7] S.1 XXX STAS 10107/0-90, Construcții civile şi industriale. Calculul şi alcătuirea elementelor din beton, beton armat şi beton precomprimat.

The Analysis of the Investment Decision in the Changing Environment

Dumitra STANCU[a]

[a] *Technical University of Civil Engeneering, Bucharest*

Rezumat: Analiza deciziei de investitii in mediul aleator se face in cadrul aceluiasi sistem de ipoteze (piata eficienta, anticipari omogene = simetrie de informatii, neutralitate fata de risc, mediu economic stabil = rata constanta a inflatiei etc.), dar cu o schimbare fundamentala pentru apropierea de realitatea economica. Se elimina ipoteza existentei unui mediu cert, determinist, prin integrarea in procesul analizei a unui mediu probabilistic. Se presupun cunoscute diferitele stari de conjunctura economica si probabilitatea de aparitie a acestora.

Abstract: The analysis of the investment decision in the changing environment is done within the same hypothesis system (efficient market, homogeneous expectation = information symmetry, risk neutrality, stable economic environment = constant inflation rate etc.), but with a fundamental change for approaching the economic reality. The hypothesis of a stable, determinist environment, is excluded, integrating in the analysis a likelihood environment.. Different economic circumstances and their likelihood are assumed to be known.

Keywords: likehood environement, sensitivity analysis, break-even point, Monte Carlo simulation, decision tree

1.Introduction

The analysis of competitive investments, in the changing environment, is based on four main techniques for calculating net present value: sensitivity analysis, break-even analysis, Monte Carlo simulation and decision tree. All of these take into account the Net Present Value criteria (NPV), based on a likelihood environment.

Sensitivity Analysis, is calculated on a net present value matrix of an investment for every direct factor and for every given environment. The factors are considered to be hypothetical independent, and the circumstances are equally-probable.

Break-Even Analysis, outlines the volume of sales (QPR) where NPV of the project is zero (NPV=0). For this volume of sales (Q_{PR}) the present value of inflows is equal with the present value of outflows for investments, for variable and fixed costs, for the income tax and NPV of the investment is zero.

Monte Carlo simulation is a more elaborated sensitivity analysis, calculating a sample (finite) of probable circumstances of the CFO_t factors, selected based on a generating process of random numbers. Simulation takes into account the different inter relations between CFO factors, linearly or nonlinearly, untemporarily, and/or temporarily.

Decision Tree, analyses the NPV of the investment based on a timely inter relation of annual cash-flows and the current opportunities: investment extension, waiting or abandoning. Net Present Value of the investment project (NPV) will be the sum of NPV of potential cash-flows (without real options) and present value of real options (extension = CALL and abandonment = PUT).

2. Sensitivity analysis

Sensitivity Analysis, is done on different NPV for the same investment project for which possible changes were simulated over the main factors for calculating future cash-flows. The initial costs of investments (I_0) and discount rate (k) are the only constant. The other NPV components (CFD_t; VR_n; n) can vary according to each direct factor.

In sensitivity analysis we underline the most important variable NPV, respectively over the available cash-flows (CFD) during the operating years of investment. The analysis is done in two steps: 1.

ISSN-12223-7221

identifying direct factors of CFD (it is desirable not to be any correlation between these factors, but to be independent, to remove redundant effects) and 2. simulating different potential measures of each direct factor, keeping unchanged the other factors and calculating NPV for each case.

NPV sample for each simulated factor outlines the project sensitivity (of NPV criteria) related to the changes of the analyzed factor. Observations are more of warning over the vulnerability points of the proposed investment project and adjusting the certainty of a NPV (positive one) with a likelihood of a negative NPV.

As for example, a 60 billion lei investment takes into account the extension of manufacturing capacity of a company for the product: "air-conditioning equipment ". The interest rate without risk is of 10%, and the service life of the equipment is 3 years (it is assumed that after 3 years, multi-post airconditioning equipments will be adopted, replacing the mono-post ones). The future cash flows forecasted in a stable environment are the followings: 24; 26 and 26, and the residual value of equipment (VR_3) will be 12.

The two steps of the sensitivity analysis will be:

a. Analytical model for calculating CFD_t could be the following:

$$CFD_t = \left[Q_t(p-v) - F - \frac{I_0}{n}\right](1-\tau) + \frac{I_0}{n} - (Q_t - Q_{t-1}) \cdot p \cdot \frac{D_{ACRnet}}{360} = [Q_t(p-v) - F](1-\tau) + \frac{I_0}{n}\tau - (Q_t - Q_{t-1}) \cdot p \cdot \frac{D_{ACRnet}}{360} \quad (1)$$

where:

Q_t = quantity of products going to be sold in year t;

p = unit selling price/product;

v = unit variable cosUprOOuct;

F = fixed operating costs of the project (others than amortization);

τ = share of the income tax;

I_0 = initial investment cost in fixed assets (10) with linear amortization and without additional investments in the future ($\Delta Imo_t = Amo_t$);

n = service life of the project;

D_{ACRnet} = no. of rotating days of net current assets.

From the model we can underline four direct **factors** (unfortunately, non independent) of CFD_t: Q; p; v and F. At this turn, these factors derived also from the external environment factors determining sensitivity variances of their measures and of CFD_t. So, Q factor is calculated internally:

$$Q = S_i + Q_f - S_f, \text{ with } Q_r = \text{Cap. prod.} \cdot \text{IDC etc.} \quad (2)$$

where:

$Si(S_f)$ = finished products at the beginning (respectively, at the end) of the year;

Q_r = manufactured quantity depending on the production capacity and the index of production capacity use (IUC).

and an external arithmetic relation:

$$Q = \text{Market} \cdot \% \text{ Company} \quad (3)$$

where:

Market = domestic demand of airconditioning equipments (and foreign one in case of export sales);

% Company = market share of the company (in percentages).

Practically, the production (output) which can be sold by the company (Q_{int}) can not exceed the one accepted by the market (Q_{ext}): $Q_{int} \leq Q_{ext}$

P factor is computed externally, according to the ratio demand (Market)/offer (competitive manufacturers), by the market share of the company offering a monopoly or oligopoly position, as well as by the purchasing power of the product consumers, and by inflation, etc.

v factor has generally speaking, an internal way of computing, regarding the specific material consumption and manual labor, but also an external one of the acquisition price for the materials and some parts of the salary men/hour (as a consequence of some social regulations regarding the work in shifts and/or at the end of the week, regarding the index-link to inflation etc.).

Besides the complexity of computing these factors we can outline in the same time their inter conditioning related to certain macro factors: an increased demand for products means an increase in sales, but also an increase of the selling prices, an increase in sales means also an increase in supplies and so the prices for materials and manual labor etc. Inflation causes a range of effects of the selling price, and also of the acquisition ones etc.

Consequently, the simulations over the potential evolution of these factors must start from the measures estimated by experts knowing very well these inter correlations, and also the sample of reasonable solutions (p > 0, v > 0 and not so high, 0 < Q < Total demand and the others). We can notice that the sensitivity analysis, as an evaluation technique of investments, pays a big tribute to the inherent subjectivism of these experts.

b. Generally speaking, estimations are done for the following economic circumstances: favorable, (optimistic), neuter and unfavorable (pessimistic) and for each factor.

For our example these estimations can be as follows:

Factor	Favour-able	Neuter	Unfavour-able
Market (unit.)	110.000	100.000	90.000
% Company	15%	10%	5%
p (ths. lei)	9,12	9	8,4 (8,2)
v (ths. lei)	4	4,5	5,4
F (ths. lei) *	10	15	20

$\tau = 0,4$
DACRnet = 8 days
* only expenses with amortisation

For these potential measures of the CFD_t, direct factors, we can get the following Net Present Value (NPV):

Factor	Favorable	Neuter	Unfavorable
Market	18,5	11,9	5,0
% Company	45,3	11,9	-21,6
p	13,6	11,9	2,9 (-0,05)
v	19,3	11,9	-1,6
F	19,3	11,9	4,4

Besides describing the five significant factors of CPO, the sensitivity analysis underlines the volatility of NPV to the potential changes of the factors. In our example, the project is vulnerable to the changes of the market share of the company.

High and unstable competition, especially of the foreign producers as a consequence of varying fiscal and custom policies, causes significant changes of the company on this market, and in this unfavorable case of the company, the project has a NPV of 3 times smaller than in the normal case and, obviously, a negative one [NPV (%Company = 5%) = - 21,6].

Investment project is *in the same time subject to the changes of the variable costs. An increase of 20% (uncorrelated with the increase of selling prices) will cause a negative NPV* [NPV (v = 5,4) = - 1,6].

Sensitivity Analysis, is calculated on a net present value matrix of an investment for every direct factor and for every given environment. The factors are considered to be hypothetical independent, and the circumstances are equally-probable.

Monte Carlo simulation is a more elaborated sensitivity analysis, calculating a sample (finite) of probable circumstances of the CFD_t factors, selected based on a generating process of random numbers. Simulation takes into account the different inter relations between CFD factors, linearly or nonlinearly, untemporarily, and/or temporarily.

3. Break-even analisys

An investment project can be accepted, when NPV = 0. This project can not increase the company value, and not decrease it, but maintain it. This acceptance break (or rejection) of a project, called also the break-even point, can be used as a limit of company exposal to the risk of the investment. Consequently, the direct factors outlined in the sensitivity analysis can be used also for calculating the break-even point for NPV = O. Besides this break-even point NPV will have negative values. We noticed previously that only decreasing the selling price under 8,2 ths. lei/unit, NPV < 0.

Most frequent managers describe the break-even analysis related to the "selling factor = Q", derived by the total demand (Market) and the market share of the company (%Company). The simplified arithmetic relation, is the following[1]:

[1] This relation derives from the equality $V_0 = I_0$ for which $NPV = V_0 - I_0$ is zero and for CFD_t are constant in operating period n of the investment. CFD_t constant allows to use the "a" annuity factor and simplifying the break-even relation.

$$Q_{PR} = \frac{F + \frac{I_0}{1-\tau}\left(\frac{1}{a} - \frac{\tau}{n}\right)}{p - v} \quad \text{or}$$

$$Q_{PR} = \frac{F + \frac{I_0}{n \cdot a} \cdot \frac{n - a \cdot \tau}{1-\tau}}{p - v} \qquad (4)$$

Under the hypothesis of the simplified model of the break-even analysis, the minimum volume of sales where the project has a nonnegative is NPV is[2]*:*

$$Q_{PR} = \frac{15 + \frac{60}{3 \cdot 2{,}48685} \cdot \frac{3 - 2{,}48685 \cdot 0{,}4}{1 - 0{,}4}}{9 - 4{,}5} = 9{,}3$$

ths. units

NPV (Q = 9,3 thousand units) = [(9,3 · 4,5 - 15) · - 0,6 + 20 · 0,4] · 2,48685 - 60 = 0

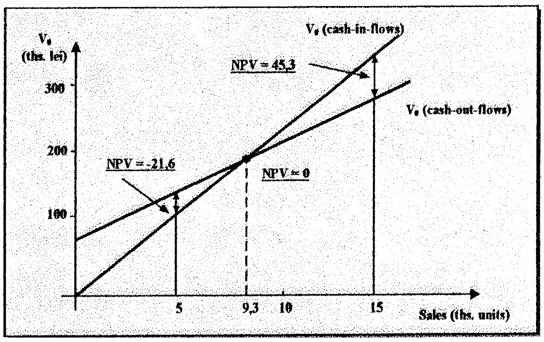

Fig. 1. Graphic representation of the breakeven point for NPV of investment

Consequently, for the company to have at this project NPV $\geq$ *0, it has to sell at least 9,300 units. For a volume of sales equal to the breakeven point* (Q_{PR})*, the present value of cash-in flows from selling the products of the investment* ($Q_{PR.P}$) *is equal with the present value of the cash-out-flows for investments* I_0*, for variable costs* ($Q_{PR} \cdot v$)*, and fixed ones (F) and for the tax income (Imp):*

V_0 (cash-inflows) = 9,3 · 9 · 2,48685 = 208,15

V_0 (cash-outflows) = 60 (I_0) + 9,3· 4,5 2,48685 ($Q_{PR} \cdot v$) + 15 · 2,48685 (F) + [9,3(9 - 4,5) – 15 - - 60/3] ·0,4 · 2,48685 (Imp) = 208,19

Consequently, NPV for Q_{PR} = 9,3 *thousand units is zero:* NPV = V_0 (cash-inflows) – V_0 (cashoutflows) = 0. *It was noticed, that a decrease with* 5 *points in the market share* (% Company= 10 - 5 = 5%), *respectively for a volume of sales of 5.000 units. The project has* NPV = - 21,6 billion lei. *At this volume of sales, the present value of the cash-in-flows is* 5 · 9 · 2,48685 = 112 billion lei, *and the present value of cash-out-jlows is* 133,6, *so* NPV contrary, *favorable case is where the volume of sales 15.000 units,* V_0 *(cash-in-jlows)* = 335,7, *and* V_0 *(cash-out-flows) = 290,4, so* NPV (Q = 15) = 335,7 - 290,4 = 45,3 billion lei. *On these additional data we can draw the break-even point using present values of the investment cash-j1ows (see figure no. 1).*

Practically, break-even point is very frequently used in accounting terms as a result of accounting data availability, as well as due to its simple arithmetic relation:

$$Q'_{PR} = \frac{F + \frac{I_0}{n}}{p - v} \qquad (5)$$

Working hypothesis are the same: CFD_t=constant; linear amortization.

Under these circumstances, the level of sales for which the accounting profit (both gross and net profit) is zero is the following:

$$Q'_{PR} = \frac{15 + \frac{60}{3}}{9 - 4{,}5} = 6{,}667 \quad \textit{thousand units}$$

The accounting break-even point is considerable decreased as a result of not taking into account the opportunity cost of the initial invesunent of 60 billion. Linear amortization is recorded in accounting annually,

[2] During 3 years of the investment and at a discount rate of 10%, the annuity factor $a = \frac{1 - \frac{1}{1{,}1^3}}{0{,}1} = 2{,}48685$

20 billion for depredation, while the present value of the cash-flows takes into account also to reinvest this amount at a discount rate of 10%. Consequently, yearly equivalent cost (CAE) of the initial investment (as a present value) on a 3 years period at a discount rate of 10% is 24,13 billion lei:

$$CAE \cdot a = I_0 \Rightarrow CAE = \frac{60}{2{,}486825} = 24{,}13 \text{ billion lei} \quad (6)$$

Under these circumstances, the company with an accounting break-even point (6,667 ths. units in our example) will record a negative NPV to the investment project, as a consequence of losing the opportunity cost of the cash-flows reinvestment[3]. So, a considerable error will be to consider as minimum sales, the accounting break-even point.

At this level of sales, the net present value, in our example is -17, 7 *billion lei:*

$$\left[(6{,}667 \cdot 4{,}5 - 15) \cdot 0{,}6 + \frac{60}{3} \cdot 0{,}4\right] \cdot 2{,}486825 - 60 = \\ = -17{,}7 \ \textit{billion lei}$$

Starting form this ($Q'_{PR} < Q_{PR}$), we "explore", below, the informative power of the break-even point (financially = Q_{PR}). This gives the possibility of measuring the operational economic risk of the investment project by calculating the elasticity coefficient (operating leverage = e):

$$e = \frac{Q_0}{Q_0 - Q'_{PR}} = \frac{10}{10 - 9{,}3} = 14{,}2857 \quad (7)$$

where:
Q_0 = initial volume of sales (normal in our case).

In other words, if the volume of sales is changing by one percent, the net present value of the investment project is changing with 14,3%. Our project is considered to be risky, confirming its vulnerability to the changes of the market share of the sales. The closer the break-even point is to the estimated volume of sales, the more risky the project is.

In our example, a 10% variance in the volume of sales (from 10 ths. units to 11 ths. units) causes a 143% *variance in measuring the NPV of the investment project.*

NPV(Q=10) = [10 · 4,5 – 15) · 0,6 + 20 · 0,4] · 2,48685 – 60 = 4,66

NPV(Q=11) = [11 · 4,5 – 15) · 0,6 + 20 · 0,4] · 2,48685 – 60 = 11,37

$$\Delta NPV\% = \frac{11{,}37 - 4{,}66}{4{,}66} \cdot 100 = 144\% \cong 143\%$$

(consequently to the estimations).

It is obvious that a decrease of 10% from the volume of sales will cause a 143% *of NPV and even to negative values:* NPV(Q=9) = -2; ΔNPV% = [4,66 - (-2)] · 100/4,66 = 144% ≅ 143%.

The main sensitivity factor outlined by the break-even point is the size of the fixed costs (F). Consequently, projects with significant fixed costs from the total costs will have a break-even point higher and subsequently a higher coefficient of elasticity.

If the company analyses an investment project similar to the one studied so far, with the same NPV(Q=10) = 4,66, *but with higher fixed costs* (F = 30) *and smaller variable costs* (v = 3), *subsequently to an increase in the automating rate, the break-even point will be:*

$$Q_{PR} = \frac{30 + \frac{60}{3 \cdot 2{,}48685} \cdot \frac{3 - 2{,}48685 \cdot 0{,}4}{1 - 0{,}4}}{9 - 3} = 9{,}48$$

with:

VAN(Q_{PR}) = {[9,48 · (9 - 3) - 30] · 0,6 + 20 · 0,4}· · 2,48685 – 60 = 0

$$e = \frac{10}{10 - 9{,}48} = 19{,}23 > 14{,}3$$

[3] Reinhardt E.U decribes this entrapment in his article "Break--Even Analysis for Lockheed's trlstar: An Application of Financial Theory", Journal Finance, 28, 1973, p. 821-838.

The coefficient of elasticity (e = 19,23) *describes a higher risk of the competitive project, placing it in a superior class of risk with a higher bank rate (interest rate without risk* + *corresponding risk bonus).*

Bibliografie References

[1] BREALEY AND MYERS, *Principles of Corporate Finance,* fifth edition, The McGraw-Hill Companies Inc., 1996, ch. 10

[2] FAMA E., *Discounting Under Uncertainity,* Journal of Business, 69, No.4 (1996), pg. 415 - 428

[3] MAGEE J., *How to Use Decision Analisys in Capital Investment Problems,* Sloan Management Review, 17 (Winter 1976), pg. 19 - 48

[4] REINHARDT U.E., *Break-Even Analysis for Lookheed's Tristar: An Application of Financial Theory,* Journal of Finance, 28, 1973, pg. 821 – 838

Cost – Duration Relation

Madalina STOIAN[a] Nicolae ENE[a] Dumitra STANCU[a]

[a]*Technical University of Civil Engineering, Bucharest,7000 Romania*

Rezumat: La stabilirea programului de executie al unui proiect se iau in considerare criterii ca minimizarea volumelor de lucrari, minimizarea costului de baze tehnologice, minimizarea duratei de executie si maximizarea productivitatii muncii. Relatia beneficiar-ofertant in economia de piata impune insa o analiza minutioasa atat in ceea ce priveste valoarea ofertei in vederea realizarii proiectului, cat si durata de executie a acestuia, aceste doua criterii functionand ca elemente de baza printre criteriile de eligibilitate in vederea obtinerii adjudecarii proiectelor.

Abstract: When the construction schedule of a project is established, the following criteria are taken into consideration: minimizing the work volumes, minimizing cost by technological means, minimizing the work duration, minimizing work productivit. The investor-bidder relation is based on a minutios analysis regarding both the value of the bid for project and the duration of the project, those two criteria being basic elements among the eligibility criteria for the project adjudication.

Keywords: project, cost, duration.

1. Introduction

When the construction schedule of a project is established, the following criteria are taken into consideration:

- *minimizing the work volumes*
- *minimizing cost by technological means*
- *minimizing the work duration*
- *minimizing work productivity*

The investor-bidder relation is based on a minutios analysis regarding both the value of the bid for project and the duration of the project, those two criteria being basic elements among the eligibility criteria for the project adjudication.

After contracting, the bidder becomes contractor and he must work to respect the planned work duration for all the work processes and to reduce as much as possible the production expenditures, in order to achieve proposed profit. Consequently, the curt-duration relation becomes an indispensable instrument of the project planning and monitoring.

The big value and significant duration of the road projects, the finance sources which are public and the important social impact of them must determine the contractors working in the road domain to comprehensively know and to use practically the methodology of analyse.

The project analysing on cost-duration basis, the technical solutions have been analysed during the designing phase and the best construction variants have been selected, taking account the dimensions, the exploitation and the maintenance of the constructions during their life time.

Using the cost-duration relation in project planning involves a very good knowledge of the contractor conditions, regarding production capacity, the equipment, the level of calcification and the professional structure of the staff and the level of expenditures.

All the marketing informations must be available, regarding the procurement, supply of equipment, plant and transportation.

2. Cost structure

Construction production cost is the sum of all the expenditures made by the contractor for achieving the production.

ISSN-12223-7221

The production expenditures could be classified in accordance with:

- ❖ the distribution of the expenditures
- ❖ the volume of the production
- ❖ the nature of the element which produces the expenditures.

By the distribution of the expenditures we can define:

- direct expenditures
- general expenditures

The direct expenditures are the funds consumed strictly for production activity, consisting in the expenditures for the materials, labour, equipment, plant and transportation means.

General expenditures cannot be directly allocated to the production processes. They consist in expenditures for the contractor's management and administration, legal fees, taxes and excises, amortizing fix production means of general interest, health and safety, security, remediation and supplements of the product at delivery, advertising and development, bank interests, fines and damages, etc.

By the production volume, the expenditures could be:

- fixes expenditures;
- variables expenditures

The fix expenditures are expenditures which have the same value, not depending on the executed production volume. The total fix expenditures are constant, not depending on the fiscal volume of production, decreasing of the product unit when the volume of production grows and increasing on the product unit when the production increases.

The variable expenditures are varying with the physical volume of the executed production. They are usually proportional with the production volume variation, but they can be also progressive or regressive.

When the variable expenditures are proportional, the expenditures per product unit are constant.

When the volume of production is not correlated with the production capacity, the per product unit will grow, therefore the variable expenditures will be progressive.

The regressive expenditures appear when the total expenditures grow in a proportion smaller than the growth of the physical volume of the production. The regressive nature of the variable expenditures can be determinated by the increase of the work experience, the improvement of the technology and organizatoric parameters.

Dependent of the elements which determine the expenditures they can be structured in:

- raw materials, prefabricated, fuel, energy, etc
- salaries
- amortizing fix production means
- interests and damages.

Analysing the cost structure we find out that, generally, they are dependent on time, regarding the duration of the production processes. They can be growing expenditures usually the general expenditures and decreasing, usually the indirect expenditures.

Taking into account that the total sum of the direct and general expenditures gives the value of the production cost and this thing, represented by a cost-time axes system, the optimum duration of the completion of the project can be determined.

The decreasing evolution of the direct expenditures in accordance with the growth of the execution duration is justified by using a reduced number of workers being able to achieve a high level of work productivity.

The general expenditures which are distributed in a global way for the whole year, are increasing in accordance with the duration of the execution and they can be expressed using a linear function

The construction duration of a construction object can be analysed from various points of vue:

- normed duration
- optimal duration
- minimal technological duration.

The cost of the construction production evolving in different ways, in accordance with them.

Thus, when the optimal duration taken into consideration by the contractor is at the level of the normated duration, the expenditures necessary for the construction product are at the level of those included in the estimate.

When this duration is below the normated duration the production expenditures are also lower, especially because of the reduction of the general expenditures – wages for the supervising and auxiliary staff, land taxes for technologic facilities and site organizing, equipment rents, etc. When a reduction of the construction duration is below the optimal duration is wanted, the costs will have again growing tendencies mainly because of additional resources of all kinds, human, material and equipment. This trend has negative effect on the economic efficiency of the construction contractor but can have however feavorable effects on the investor's activity when he is interested in giving the contractor a bonus for earlier completion of the project.

When the construction duration is longer that the normated one, the production costs are also growing because of the increase of the indirect expenditures and/or because of immobilizing the circulant production means.

Those production costs can grow very much and they can strongly affect the economic efficiency of constructor contractor if the construction contract includes damages clauses regarding excending the contracted project duration.

The optimal completion time is determined using the Critical Path Analysis Methods or classic methods.

From the construction contractor point of view, the effect of economical efficiency obtained by reducing the construction duration is directly materialised when a firm contract or an indexable contract exists and the indexation is made in accordance with the global index of price increase for the discount period.

The effect of the optimal execution duration disappears completely if the contract does not include clauses regarding time compliance.

Increasing the degree of exigency regarding the compliance with the contracted times cannot have anything else then benefic effects over the investor-contractor relation and also over spending the public funds for the roads projects.

In case of reducing the construction duration, diminishing of the production expenditures by decreasing the general expenditures included in the estimate, can be calculated by the next formula:

$$E_1=M*g-M\ (q_1+q_2*T_1/T)$$

With:
E_1 – saving from the production expenditures
M – the amount of the direct construction expenditures
g – the value of the general expenditures expressed in percentage
g_1 – the value of the general expenditures expressed in percentage which do not depend on the execution duration (about 10% of g)
g_2 – the value of the general expenditures expressed in percentage which depend on the execution duration (about 60% of g)
T- normated execution duration (contracted duration)
T_1 – reduced execution duration

When the normated construction duration respected the value of the general expenditures in percentage will be:

$$g=g_{1+}g_2$$

and it is applied to the total of the direct production expenditures, respectively to the sum of the expenditures for materials, labour and plant from the Chapter A of the estimate.

For $T_1<T_2$, de ratio is below first and:

$$g^{'} = g_1+g_2 *T_1/T_2 < g$$

The bigger the difference between T_1 and T_2 ($T_1<T_2$), the smaller the percentage of the general expenditures which are depended on the execution duration consequently the production expenditures will decrease.

For $T_1>T_2$, when normated contracted execution duration is overrun, the ration T_1/T will be over first, therefore the percentage of the general expenditures depend on the construction duration will grow:

$$g^{'} = g_1+g_2 *T_1/T_2 > g$$

In this case, the fall of the production expenditures is determined by the folowing relation:

$$P_1= M\ (g1+g_2\ \mathbf{T_1/T_2)} - \mathbf{M}*g$$

But the level of production is influenced also by the change in time of the direct expenditures, for all materials, labour and plant. Even if in the case of a stabile economy without growth in prices, the unfavourable effect of the increase of the execution duration is felt. The level of expenditures grows as a result of the losses due of some materials because of prolonged storing, due to ineffective, inadequate and incomplete use of the labour and plant.

In what we have presented so far, the economical efficieng has been analysed, from the construction contractor point of view. In a free market economy, based on real competition the contractor can take part in a public project competitive bidding, with an estimated bid value of for the optional execution duration. Therefore a price up to 5% below the estimate price for the normated execution duration.

Such an offer, beside the reduction pf the investment expenditures, has the advantage of a shorter completion time of the construction object.

But the execution duration is strongly influenced by the constructive variant chosen in the design. Consequently, for deciding the constructive solution , the designer must take into account not only the functional conditions required for the construction object, but also the introduction of advance technologies, without waiting a period of time which will lead to the increase of the construction duration.

Another modality of reducing the construction duration is the use with priority of a reduced number of sorts, types and dimensions of raw materials, with a high degree of repeatability. For instance in the situation of concrete reinforcement works using some type of steel barr for a structure leads to a reduction of the labour and duration, even if unjustified reinforcement could occur.

Obviously, in every case, the solution must be selected in an accordance with the economical result which are influenced by the construction – life exploitation and maintenance expenditures.

In conclusion, we must underline the fact that for any investment, the execution technologies must be selected on the grounds of a scientific and rigorous analysis regarding the construction duration in the compliance with the functional parameters included in the technical project and within the quality limits from the tasks book.

Delays in the delivery of the construction objective, especially the productive ones lead to effects which are difficult to quantify, therefore practically unretriereble, even when the contracts includes damages.

Bibliografie:

[1] Phillip F. Ostwald – "*Cost estimating for engineering and management*" – Prentince Hall International;

[2] Edward W. Merrow, Stephen W. Chapel, Christopher Worthing – "*A Review of Cost Estimation in New technologies*" – Rand Corporation;

[3] King Royer – "*The Construction Manager*" - Prentince Hall International

The Analyses of Work in Different Cultures

Mihail TOMA[a] Marina STOIAN[a]

[a]*Technical University of Civil Engineering, Bucharest,7000 Romania*

Rezumat: Această lucrare analizează deschiderea multiculturală în contextul globalizării afacerilor. Sunt evidențiate avantajele cunoaşterii caracteristicilor modelului cultural al ţării în care urmează să-şi desfăşoare activitatea managerul. Această cunoaştere determină prosperitatea afacerilor.

Abstract: This work presents the opening many-cultural in the totally context business. There are praising the advantages of knowledge typical cultural model of country which follow unfurls activity manager. This knowledge determines the flowering business.

Keywords: monocronical cultural model, policronical cultural model, the Japanese paternistical management

1. Introduction

In our days business became aggregate. The firms unfurl their activity not only in the country in which they born, but also in other country, the managers confronting with different cultural models.

The misunderstanding of cultures differences make the business negotiation to fail.

Example: The investigation show that 16-40% from the managers that are charging to unfurl their activity in one country with a new and different culture than theirs, are forced to come back before the term, because they have a inferior activity, or they don't succeed in adapting at the local culture. All of this hide how difficult could be to create business relations from one culture to another.

2. The bases of the analyses of work in different cultures

The key of business success is to learn as much as possible about the country in which follows to unfurl our activity:

- traditions of social medium like history effect;
- outlooks regarding one's own obligations and responsibilities;
- the attitudes face given to change, to engage at effort, at work;
- the population psychological climate (or agreement as regards at a problem, or scission);
- the rapport face given to value and norms (how we report at work, morality, harmony, aesthetic, social life);
- how we report at institutions (family, church, the state institutions).

The biggest companies send their employees that supposed to unfurl their activity in foreign countries to courses of culture investigation, that include discussion about history, values, customs, work morality.

Example of culture brief center:

- Council business of International Understanding (BCIU) from Washington, Columbia District;
- American University from Washington, Columbia District;
- -Monterey Institute for International Studies from Monterey, California.

An unprepared person could destroy in few days any kind of business good relation, previous settled between the two countries.

So, is the case that every companies have in view seriously, the necessity of employees instruction on cultural plan, even they will not live in a foreign country, only just they will travel frequently.

ISSN-12223-7221

The work is different estimate from country to country. The attitudes watching work, changing, the engage to effort are different.

In the figure 1 do not misunderstand: the fact that Germany and Great Britain are in the forehead of the pyramid, doesn't means that their don't like the work.

But although, the work is an important element in their life, they also grant attention to personal time, social time and cultural time.

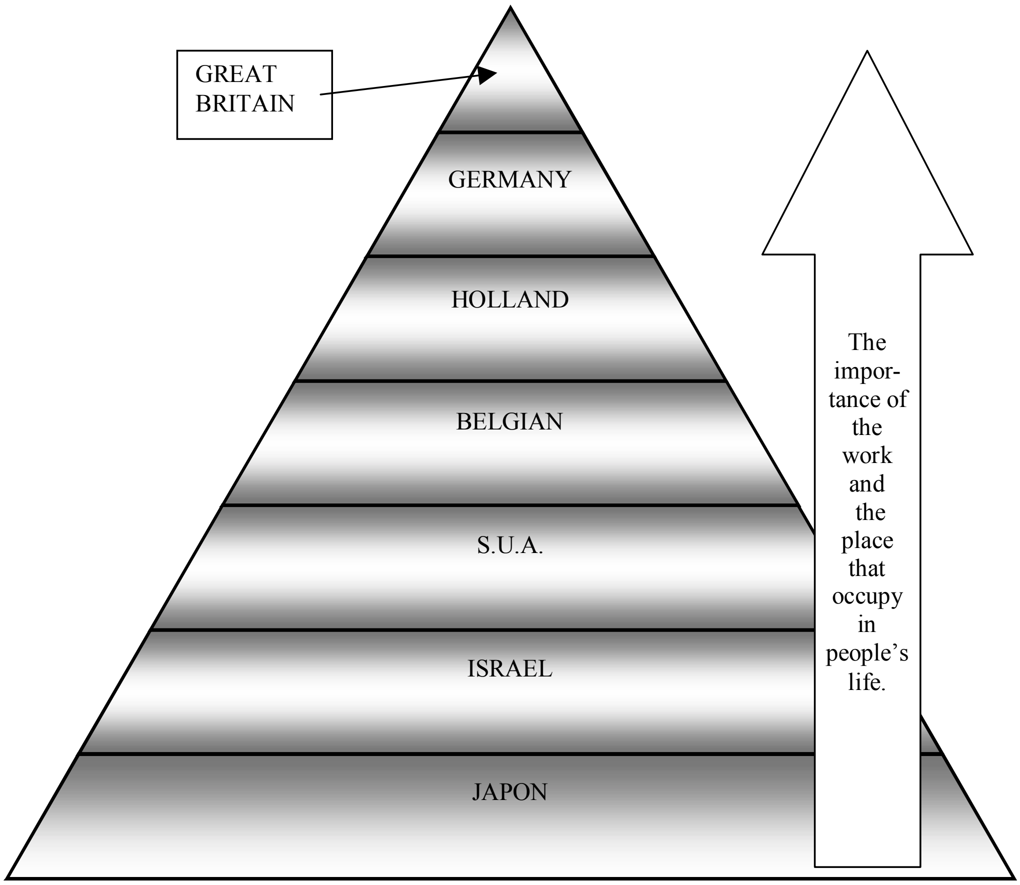

Fig. 1 The importance of the work

They love work, but they also love the life near the nature, the satisfaction of their hobby (skin, navigation…), the time spends together the family, friend etc. They are not like japanese, for which spending the time with mates or clients for late in night is a natural thing.

Example:

- A British manager, after he settled in his post from Japan, head that the japans managers work, usually, too much after program and they spend the time near the mates or clients until the midnight.
- The Japanese manager, after he settled in his post from Great Britain, hear that British manager don't work usually after program and if they spend the evening in a restaurant, this is not the adequate place to continue the business discussions.
- In France, the managers like that in the morning they take the breakfast and to read the newspaper in

silence, while american managers like to solve the business at breakfast.

So, a French manager who received a post in S.U.A., is disturbed by meetings at breakfast.

Example of managerial errors:

- for Mexicans, to live and to enjoy of like is one of their main worth.

The growth salary of one group of Mexican workers makes them to work fewer hours and not more. The explication is that Mexicans considered that now they could earn enough money in the same time like before or less, so they could enjoy their life.

- The promotion of one japanese employee make decrease his performance, because the japaneses need harmony, to harmonize with their workmates. The promotion (a individual reward) separated the japanese employee from his workmates, depressed him and finally decreased the motivation for work.

One of the frequent mistakes made by numerous foreign firms, is the trial to use a importation-man list, like a possibility of achieve a first contact. The japaneses prefer to make business with someone only in case that partners have been introduce oneself adequate and they have a personal contact with them. The introduce made by an interloper, serve for guarantee and loyalty of both parts.

This method help to the lost of restraint Japanese side. Sources of recommendation for interlopers could be another japaneses firms, another company that have success in our business in Japan, the banks, the commercial association, trade rooms, the embassy of Romania at Tokyo, JETRO.

In individualistic society (like SUA, Canada, Great Britain, Australia) the people tend to estimate the individual initiative, intimacy and self protect. Here is about the monocronic cultural model.

Example:

Two cultural models from standpoint of work importance.

Monocronical or Germanic cultural model (only a thing at one moment):

- one thing at once;
- give exclusive priority to the load;
- difficult to interrupt;
- is punctual (is very important when it starts and when it finishes);
- methodically;
- he guides in time by a rigorous plan.

Policronical or Romanian cultural model:

- has the tendency to begin many things at once;
- has, in the same time, more priority (give priority to the duty, but also to the family, friends and clients);
- -is easy to interrupt;
- -is seldom punctual when it starts and when it finishes;
- is eager to make quickly;
- it's changing often the plan.

Japanese cultural model:

- a tradition of long work;
- ability to intense and prolong effort (in 1997 the average of holidays from all the Japanese economy was 7,5 days. The rest of the days they worked not because it must, but they wanted, although they have 20 days of holiday).

This Japanese tradition of long work, it owing to the territory depriving by own resource. From here, the idea that every good, product, it the result of a long effort which impose respect. The export is the only alternative of Japanese life. They import the resource and export the product.

This long work is explained through discipline and modesty.

- spirit of initiative and big tenaciousness in achievement (until he make a thing he doesn't let go);
- a superior level of culture and education;
- traditional relation of subordinating. A very long stability of a hierarchical structures. Each is on certain step. All of them, must to respect this rule.
- very strictly morality principles;
- a high sense of honor and dignity;
- the spirit of family very advanced, the attachment for the family. This spirit transferred from family to firm (the paternistic japanese conception);
- centralization on man, not on money like Americans.

(In Romanian cultural model, the bread is the cultural value – the bread mustn't be throwed, it is a saint thing.

This cultural value resulted from the fact that in absence of machines, it has deposited big efforts to obtain wheat.

In our days this cultural value disappeared.)

The Japan economy is the second like size in the world, with a PIB of 3783 million $ in 1998 (about 17% from gross world product).

There were admired the Japanese performance, they achieving in their economical sectors, in confrontation with international competition, remarkable results.

Comparatively with us, japonese firm doesn't hase such financial dependence on exterior.

The Japanese paternistical management:

The firm is like a family. It ask from every employee one thing: to put all his resource: psychical, intellectual and ethical available to the firm (that is to be totally subordinate to the firm's objectives).

The firm offer instead:

- a stable place of work, on life;
- the promotion;
- the access to firm's social ensurance;
- the periodical increasing of salary at once with the firm's profit growth;
- -the priority engagement of the family members;
- -the retired at the firm.

The paternist system from Japanese economy include 25% from the wage-earner's number of big companies. The rest, 75% from wage-earner's number, are employees who knows the unemployment and the poor working conditions. The paternist make that in a big company the changing of work place to be impossible.

So, there are advantages and disadvantages.

It says that in the first part of life we hoard information, in the middle of life begin to understand the world, and when you could makesomething real with all of these, you are estrange or retired.

The japaneses understand that, and they place in the front of enterprise on the post of boss or president advisor, people with age over 70.

In our country this wasn't understand and so, experience people and professional good prepared don't succeed to final a work place and that only because of age.

It lose the employees that have hoard a lot of precious knowledge for firm's flowering, and at the same time it lose time with those are in the beginning of road.

The most offer of work place is for the people under 35 years old.

Conclusion:

The quality of man is reflect in the quality of the product, service and affair as a rule.

If the cultural models is unfit, the product anal the service are identically.

The cultural model establish the behaviour of the people in society.

"The road of freedom break through culture."

Bibliography:

[1] Gary Johns , "*Comportament organizațional*", 1996, Ed. Economică, București.

[2] Letitia Baldrice – *"Codul manierelor in afaceri"*, 1985, Ed. Ştiinţă & Tehnică S.A.

[3] Meryem Le Saget – "*Managerul intuitiv*", 1999, Ed. Economică.

Ovidius University Annals Series: Civil Engineering Volume 1, Number 5, 2003

The Improvement of Water Supply for Swimming Pools

Vasile VASCU[a] Gilda GAVRILAS[a]

[a]*Technical University "Gh.Asachi" Iassy, Iassy, Romania*

Rezumat: Noile norme europene şi exigenţele în materie de securitate privind piscinele publice impun analiza şi îmbunătăţirea sistemelor de funcţionare ale acestora .La bazinele de înot apa uzată este continuu evacuată, tratată şi reintrodusă, purificarea având loc prin diluţii.

În acest sens se prezintă un model hidraulic şi matematic de poluare şi evacuare a poluanţilor din bazinul de înot.

Abstract: The new European standards and security demands with regard to public piscines require the analysis and improvement of the way they function. Treating the water in the pools is a delicate, difficult operation. In the swimming pools with a closed circuit the used water is continuously evacuated, treated and re-introduced, its purification being performed by dilution. The concentration of the initial components is diluted due to the new water added. This fact leads to the idea of examining the pollution reduction laws of the water in the swimming pools, by continuous dilution with re circulated water. The research and investiation for establishing the lawes of the reduction of water pollution ware done on hydrauliv and mathematical models.

Keywords: piscines, the pollution reduction

1.Introduction

A public swimming pool is an establishment in open air or covered, formed of one or several pools and annexes.

The construction of a modern swimming pool requires a judicious team work of the architect talent, technicians competence and hygiene experts demands, as well as the trainers and trainees wishes, without leaving aside the economical considerations.

The water in the swimming pools must have an irreproachable quality. For the common people, it must be clear, without any smell or taste.

What does this mean for a specialist?

How can there be preserved the quality of drinking water of the swimming pool waters?

The degree of usage of the swimming pools may be the reason of the different effects/illnesses of the swimmers.

Thus, the maintenance of the water quality in the swimming pools is the main concern of many specialists.

The new European norms and exigencies as regards the security measures for the public swimming pools demand the analysis and improvement of the functioning systems.

2.Study – Water circulation in the swimming pools

Treating the water in a swimming pool is a delicate operation. Even though the treatment problems are relatively known, the new usage conditions of the swimming pools raise difficulties specific to every case.

The water circulation in the swimming pools, the supply and evacuation methods are controversial issues.

In the case of swimming pools with a close circuit, the used water is continuously evacuated, treated and re-supplied, the treatment being made through continuous dilutions.

ISSN-12223-7221

The concentration of the initial components diminishes due to the dilution with fresh water.

Following this idea there have been studied different methods for the reduction of the swimming pool water pollution through continuous dilutions with re-circulating waters.

This study was made on a reduced scale model after an existent swimming pool.

The comparative parameter used is the pollution concentration variation in time, which helps to check on the water supply and evacuation methods used for the swimming pools, as well as the disinfecting methods.

There was used sodium chlorate in order to obtain the initial concentration of the water (artificial pollution) and then the model was supplied with clean water, with the usual concentration and there was analyzed the concentration variation in several representative areas.

The mixture concentration in different areas of the basin was determined using the new formula proposed by A. Vilssert [2]>

$$C = \frac{k}{r} = k \cdot \delta (mg/l) \qquad (1)$$

Where k – transformation coefficient with a constant value

R – electric resistance in Ω cm

$$R = \frac{1}{\delta} \qquad (2)$$

δ - electric conductivity (m s)

the water and the electric conductivity. Thus, the concentration has been calculated by measuring the electric conductivity in the studied areas.

This formula expresses the linear dependence between the global contents of solved substances in

The mathematical model was studied starting from the balance equation as an integral of the mass of polluting substance in a volume V, thus obtaining the equation of the pool:

$$V = \frac{dc}{dt} + Q_e \cdot C = Q_{mp} + C_a \cdot Q_a$$

where:

Qe = Qe (t) – water flow of the water evacuated from the pool (de/s)

Qmp = Qmp (t) – polluting substance mass water flow produced by the swimmers (de/s)

Qa =Qa (t) – fresh water flow

Ca = Ca (t) – concentration of the polluting substance in the water to be refreshed

Finally there was established a calculation program that solves the problem mathematically.

Presentation of results

After the study made on the model on a reduced scale and after the mathematical formula there were obtained the results presented in Table 1

The analysis of the presented data shows that there is a difference between the results of the hydraulic and mathematical model between 0,1% and 3,3%. This fact shows that the mathematical solution of the phenomenon can be counted on.

Table 1

Time (minutes)	0	18	28	38	48	64	75,6
Average concentration measured on the model	9,6	8,6	8,12	7,8	7,35	7,01	6,70
Average concentration determined through mathematical formula	9,6	8,56	8,101	7,69	7,34	6,87	6,56
Percentage of evacuated polluting substance							
Time (minutes)	0	18	28	38	48	64	75,6
- measured on the hydraulic model %	-	21	31	39	49	56	63
- measured on mathematical model %	-	22	32,6	41,5	49,1	59,3	66
Percentage differences between the results from the hydraulic and mathematical model	-	1	1,6	2,5	0,1	3,3	3

4.Conclusions

For the study of the water circulation in the pool there was made a research on a model on reduced scale and there was also established the mathematical solution of the phenomenon.

The results obtained on the model can be applied on prototypes under the conditions of respecting the similitude criteria- Reech Fronde.

The mathematical solution is the equation of the pool which solves the following problems:

-it calculates the concentration of the polluting substance in the pool at fixed periods of time

-it calculates the necessary period of time to obtain the imposed concentration

-it calculates the water supply - evacuation flow necessary to maintain the concentration of imposed polluting substance function of the pollution given by the swimmers.

The solving program of the equation allows establishing the parameters for the automatization of the recycling pumps and of the cleaning station.

5. Bibliography:

[1] Vascu, V, Thesis- *Contributions on the water supplies for the swimming pools,* Iasi, 1992

[2].Boule, P, Castex, L, - *Le mélange des eaux à l'intérieur d'un réservoir circulaire*, TSM 6-73

Change in the Construction Process Organization

Marian Silviu Ionescu Vlasceanu [a]

[a]*Technical University of Civil Engineering, Bucharest,7000 Romania*

Rezumat: Lucrarea de fata prezinta pe scurt modificarile ce trebuie aduse organizarii activitatii in constructii. Organizarea traditionala avand dezavantaje din toate punctele de vedere: al clientului, al competitiei si al executiei se adopta o noua abordare a organizarii activitatii in constructii ce va fi stabilita in mod individual pentru fiecare proiect conform tipului si naturii constructiei, sistemul si practici de procurement, know-how-ului partilor implicate si altor aspecte, fiind posibile mai multe alternative. Se prezinta ideea si principiul "luarii deciziilor pe faze intermediare tinand cont de dorintele clientului" care permite beneficiarului sa prezinte optiuni pe parcursul derularii proiectului, solutiile detaliate fiind lasate pentru fazele ulterioare mai favorabile luarii deciziilor corespunzatoare, precum si ideea diferentierii dintre structura si inchideri pe de o parte si interiorul cladirii pe de alta parte.

Abstract: This work makes a brief presentation of the necessary change and evolution of the organization of the construction process. The traditional process organization involves weaknesses regarding the client's viewpoint, the competition's viewpoint and the production viewpoint . In the new approach, the organization of the construction activity will be decided individually for each project in accordance with the type and nature of the buildings, the procurement system and practice, the parties' know-how and other aspects , more alternatives being possible. The material presents the idea or the principle of "consumer- oriented phased and focused decision making of the building process" which allow individual customers to make late choices, detailed solutions being left for a later stage of the process when condition for decision making are more favourable and also the idea of the distinction between the shell and the interior of de building.

Keywords: organizational change, client's viewpoint, the competition's viewpoint, the production viewpoint, consumer- oriented phased and focused decision making

1. Introduction

This material presents the change in the building process organization derived from the existing production philosophies and their organizational impacts or demands. It first introduces the overall change as a whole (sec. 2.). Then, this change is examined more closely by dealing separately with its first component principle (sec. 3).

The initial introduction of organizational change describes, primarily, the change in the division of labour within the construction process and industry in general. The presentation is made in relation to the present prevalent modes of action. Detailed description and the argumentation can be found from the outlines of the partial principles elsewhere. The principles are, again, classified from three viewpoints to give perspective and, above all, to provide the reader with an easy and hierarchical presentation.

The principle-based outline contains a compact description of the bases of and problems related to present practice, a description of the actual change that sheds light on the new operational method and its effects as well as a general outline of relationships with other parallel principles. It should be mentioned here that problems as well as benefits are generally linked to several principles and that presenting them in connection with, traditional contracting, including separate design and competitive bidding based on price, work-specific labour-only-subcontractors implementing the building through intensive on-site work, etc. (Fig. 1). The industry's know-how and

ISSN-12223-7221

division of labour also conform to it generally, though a single, although the key principle of change, is mainly introductory.

It is also essential to keep in mind that we are here observing only organizational changes in keeping with the goals of the research. However, some principles were so closely connected to the description of the basic structure that leaving them out seemed impractical and were thus included. In addition, in connection with the analyzed philosophies other different principles were also presented (eg. technical). These suggestions for improvement should not be forgotten in further development work nor the practical application of changes as they are closely connected with the comprehensive development of construction together with the more general organizational principles.

2. Overview Of Organizational Change:

The building process involves many kinds of activities and tasks required to erect a building and maintain it. These tasks are alternatives to some degree or at least vary according to the mode of implementing the building. On the other hand, the concrete aim of the research was to produce a vision of the division of labour between firms engaged in the future building construction project, hence allocating performers for these tasks which have to be done and providing a mechanism for their coordination. To bring some order to this amount of information, a schematic map was created as a basis for the presentation (Fig.1 and 2).

The presentation of conclusions about changes is made in relation to the present prevalent organization or, in practice, procurement methodthere are also many other procurement methods meaning that the coordinating mechanism varies.

Correspondingly, the focus is primarily on the recommendations that are independent of procurement systems and contractual relationships etc. which vary according to the type of project and its goals and constraints. This means that the division of labour, mainly on an inter-enterprise level of functioning, is the result proper and hierarchy and authority are somewhat less definite. From this viewpoint the basic structure of the future building process organisation is presented in Fig.2.

Basically, the figures present main lines, how future's building process organization differs from the traditional one. The figures are oversimplified. For instance, the several tasks assigned to a party may have to be implemented by various departments or they may even be tasks of different firms closely resembling traditional practice. In such cases, however, close and continuous cooperation is pursued which makes it possible to draw them as a single entity.

Further, the marked areas that define the tasks of a party represent often several parties engaged in parallel tasks. This is clear when considering the numerous manufacturers, suppliers and subcontractors normally hired for a project. The separate contracts system may lead to this also in 'higher level implementation'. On the other hand, there are normally a few consultants representing different professions, who do the technical design of the building. Consultants may be used already in the programming and requirements planning phase in addition to the architect. However, from the overall organizational viewpoint they can be defined as a single type according to the nature and positioning of their tasks, although, in practice, they form a 'suborganization' by themselves.

3. Organizational Change Inlight Of Core Principles:Client's Viewpoint

3.1. Consumer-oriented phased and focussed decision making:

In traditional building the individual needs of various customers occupying various spaces of the building cannot be taken into account well enough, since the plans have been fixed already at the initial stage of the project -even as to details - whether the end users are not known or not. Standard quality for all is not, however, the solution when clients are capable of paying for having their wishes implemented. This is especially true when building dwelling blocks, but similar problems apply in the case of, for example, offices, where conditions affect the effectiveness of the activity.

Even if the users are known at the start of planning, the channelling of the wishes of various users and details about their use experiences via that

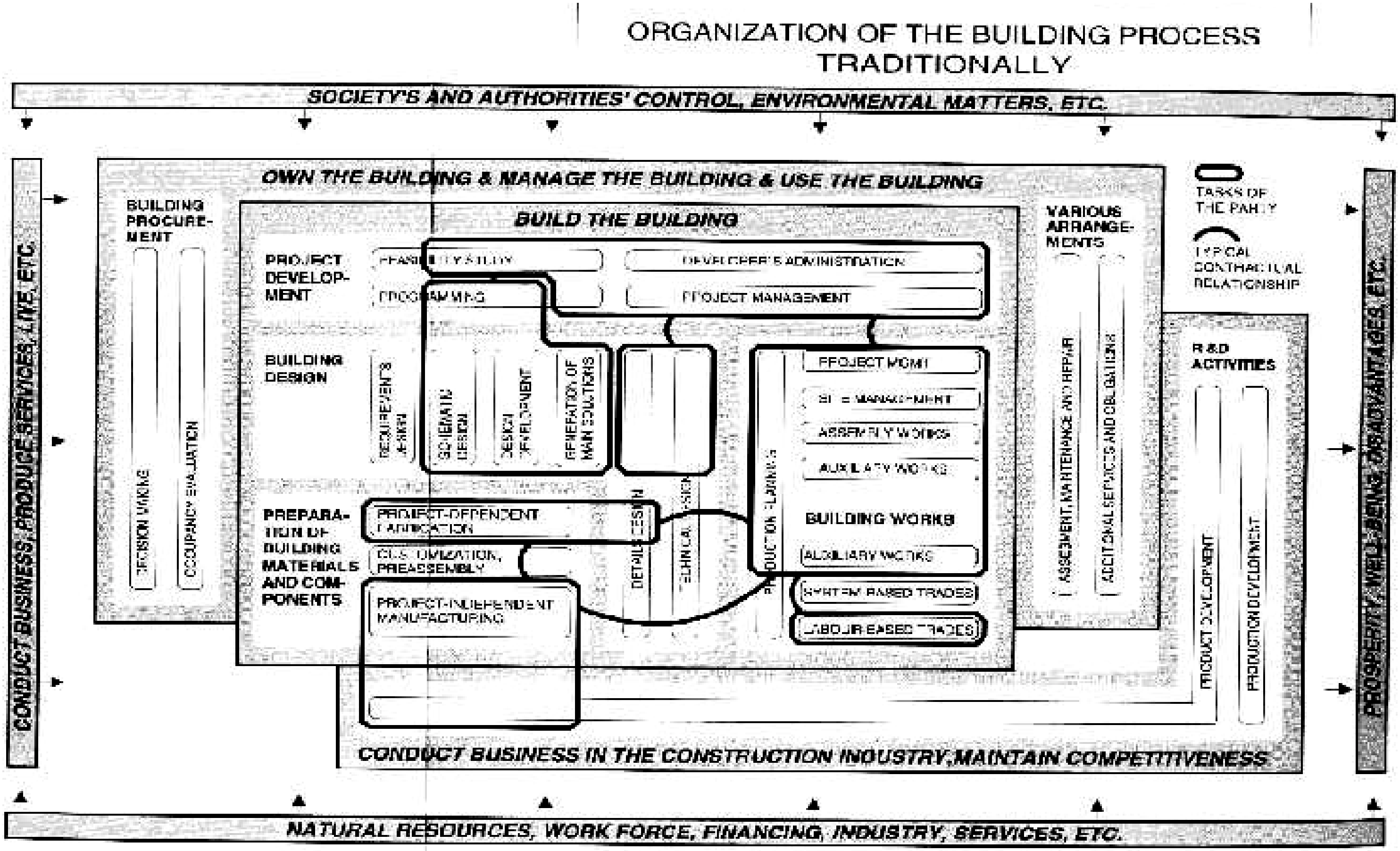

Fig. 1 A rough illustration of the basic structure of the organization of the traditional building process and industry. The weaknesses of this kind of building practice, which is based on separate design and competitive bidding, on-site building and breakdown of tasks into impractical activities are widely recognized. In addition, the changes in demand due to increasing individuality and speed of change as well as tightening competition and new technology, have forced builders around the world to invest in the creation of new and effective operational principles (cf. Fig. 2).

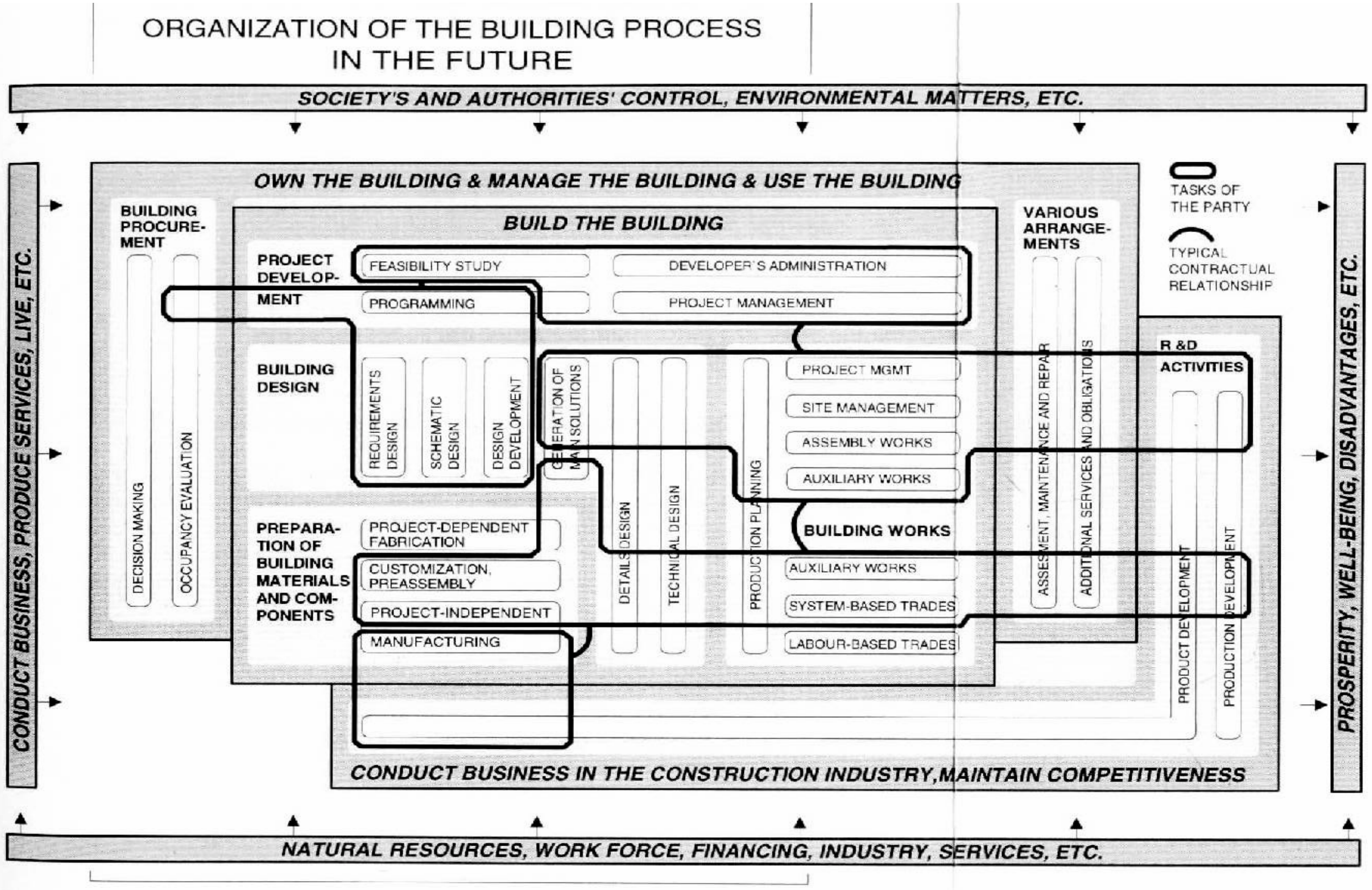

Fig. 2 . A rough illustration of the basic structure of the organization of the building process and industry in the future when the characteristics of the suggested overall change have been fully introduced (cf. Fig. 1). The organization of the building process will be decided individually for each project. The organization form is affected by the type and nature of the building, the procurement system and practice, the parties' know-how and other goals of the firms and the project. Several alternatives adhering to the main outline are possible.

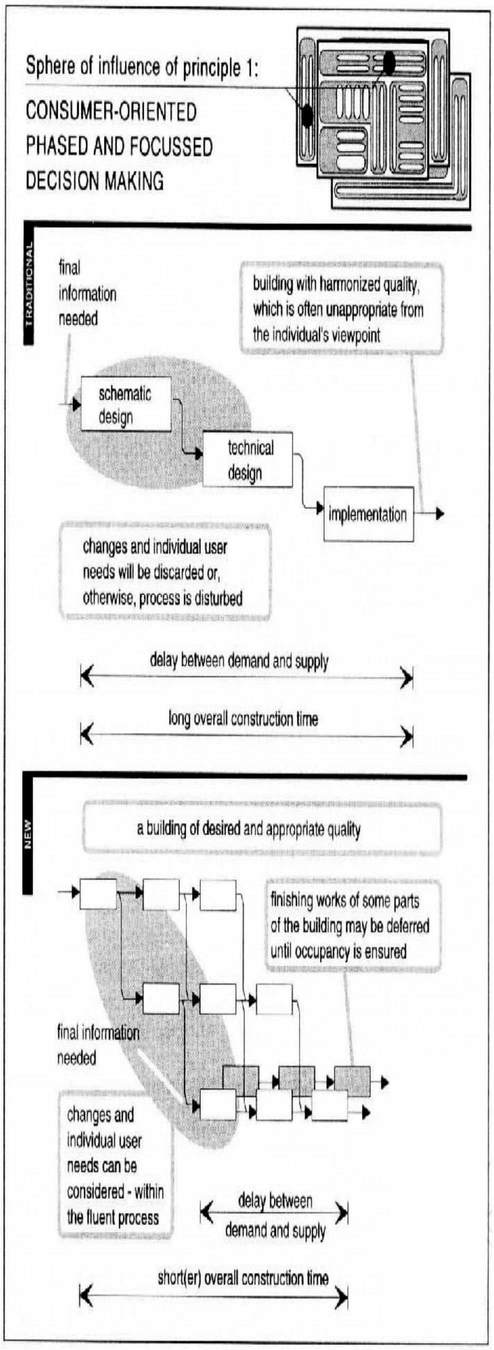

Fig. 3. An abstraction of the principal influences of 'Consumer-oriented phased and focussed decision making' on the building process. Change is introduced by illustrating both the traditional process (top) and the new one (bottom).

phase is not necessarily sensible since the procedure tends to extend overall duration of the project while the risk concerning changes in plans during construction related to the traditional process remains, resulting in significant additional costs and disputes.

The major point is that the resources could be used to build a building more suitable for the customers needs if he were listened to. The change from a seller's to a buyer's market and general individualization as well as increasing speed of change have to be considered in the building process.

Change principle 1 (Fig. 3)

The opinion of the customer (and various groups) is incorporated through decision-making at various levels and phases. Thus, decisions about the internal systems, for example, will be individually taken by the actual customer, the immediate user, at a late phase of the process. Alternatives are offered and visualized to the customer in question and each of them can make his choice from a reasonable number of available solutions. The procedure provides solutions that meet the customer's individual needs while the phasing of planning and its overlapping with production enables a shorter project implementation time.

A changed process yields better readiness to meet the ever increasing diversity in demand which results in buildings with better performance in relation to the client's functions carried out in the completed building. This is important when considering that operational costs are often significantly higher than investment, maintenance and repair costs. From the builder's viewpoint it is also important that change orders which could now be taken into account easier, arc partly avoided. In addition, a single point of responsibility is a sign of a client-oriented building process.

The idea of allowing individual customers to make late choices is becoming practical now that the industry is developing its system products, whose standard components can easily be assembled into unique buildings. The supplier and the product system are selected and the pricing bases defined sometimes at a very early stage of the process, but the detailed solution is left for a later stage when the conditions for decision making are more favourable (updated information, visualization).

This way, capital is also not tied up unnecessarily in internal systems before income is fully secured. This applies to all construction, in principle, but is highly important in speculative building where some parts of the building are taken into use considerably later than other spaces. Thus, the decision making process supports scattered technical systems which are increasing along with intelligent buildings. In practice, phased decision making means also the overlapping of planning and implementation and, also, shorter construction time (fast track) while also requiring the use of system products.

3.2. Distinction between the shell and interior of the building

The changes in the needs of users during the life cycle of a building, and changing users, have been poorly considered in construction. Project-specific design and building from raw materials and small components favour on-site construction and yield buildings with integrated structures and systems as a result of ad hoc site applications and short-sightedness. In the production stage, practice impedes the development of construction production techniques and proper sharing of liability. The life-cycle economics of the building also suffer as future changes and renovation can be expected to be unnecessarily expensive due to the large amount of heavy construction that needs to be done.

The generally increasing pace of societal change and the emphasis on individuality demand much higher modifiability and uniqueness of the building. Therefore, systems with long and short life cycles must be differentiated technically. The diverse clientele and production technological reasons necessitate also organizational changes in the building process.

Change principle 2

Technical differentiation between the shell and the interior of the building is necessary primarily to better take into account individuality and to gain needed modifiability. It results in different entities from the viewpoint of production technology. The production technology and know-how for them can best be developed in separate organizations based on clearly defined tasks. Also, since the shell and interior often have different clients, the first's client being a larger entity and the second's a smaller subgroup or individual, their implementation is differentiated also organizationally and, to some extent, timewise.

4. Bibliography:

Reorganizing the Building Process - The holistic approach

Pertti LAHDENPARÄ

VTT – Technical Research Centre Of Finland - Building Technology ESPOO 1995.